

Path Integral Methods

in Quantum Statistics, Quantum Field Theory, and Membrane Physics

Michael Bachmann



im

**Fachbereich Physik der Freien Universität Berlin
eingereichte Dissertation**

Berlin, 14. Mai 2001

Erstgutachter: Prof. Dr. H. Kleinert
Zweitgutachter: Prof. Dr. B. Hamprecht

Disputation: 25. Juni 2001

Contents

Preface	7
1 Introduction	9
1.1 Path Integrals	9
1.2 Perturbative and Non-Perturbative Methods for the Calculation of Path Integrals	10
1.3 Contents of This Thesis	10
Part I: The Path Integral from a Perturbative Perspective	13
2 Perturbatively Defined Path Integral in Phase Space	15
2.1 Introduction	15
2.2 Perturbative Definition of the Path Integral for Density Matrices	16
2.3 Restricted Partition Function and Two-Point Correlations	16
2.4 Perturbative Expansion for the Effective Classical Hamiltonian	18
2.5 Effective Classical Hamiltonian of Harmonic Oscillator	19
2.6 High-Temperature Versus Weak-Coupling Expansion	21
2.7 Free-Particle Smearing Formula	22
3 Smearing Formulas for Fluctuation Effects	25
3.1 Generalized Euclidean Action in Phase Space	25
3.2 Density Matrix with External Sources	27
3.2.1 Calculation of the Phase Space Path Integral	27
3.2.2 Example: Density Matrix of the One-Dimensional Harmonic Oscillator with Sources	30
3.2.3 Expectation Values and Correlation Functions	33
3.3 Smearing Formula for Density Matrices	35
3.3.1 Perturbative Expansion for the Density Matrix of a System with Interaction	35
3.3.2 Smearing Formula for Gaussian Fluctuations	36
3.4 Generalized Wick Rules and Feynman Diagrams	38
3.4.1 Ordinary Wick Rules	39
3.4.2 Generalized Wick Rule	40
3.4.3 New Feynman-Like Rules for Nonpolynomial Interactions	41
3.5 Particle Density in the Presence of External Sources	44
3.6 Partition Function with Currents	45
3.6.1 Partition Function in the Presence of External Sources	46
3.6.2 The Harmonic Oscillator Revisited	46
3.7 Perturbative Expansion for the Free Energy	48
3A Algebraic Properties of Block Matrices	50
3B Generalized Correlation Functions	51

4	Effective Classical Theory for Quantum Systems	53
4.1	The Zero-Mode Problem	53
4.1.1	Harmonic Fluctuation Width for Periodic Paths	53
4.1.2	Fluctuation Width for Fixed Ends	55
4.2	Restricted Partition Function and Effective Classical Hamiltonian	57
 Part II: Graphical Recursion Relations for Feynman Diagrams		63
5	Quantum Statistics	65
5.1	Introduction	65
5.2	Systematic Construction of Feynman Diagrams for the Quartic Oscillator Free Energy	66
5.2.1	Basic Graphical Operations	67
5.2.2	Perturbation Theory	74
5.2.3	Functional Differential Equation for $W = \ln Z$	76
5.2.4	Recursion Relation and Graphical Solution	77
6	Quantum Field Theory	81
6.1	Introduction	81
6.2	Generating Functional without Particle Sources	82
6.2.1	Partition Function of QED	82
6.2.2	Generalized Action	82
6.3	Perturbation Theory	84
6.3.1	Functional Derivatives	85
6.3.2	Vacuum Energy as Generating Functional	88
6.4	Graphical Recursion Relation for Connected Vacuum Diagrams	89
6.4.1	Functional Differential Equation for $W = \ln Z$	89
6.4.2	Recursion Relation	90
6.4.3	Graphical Solution	91
6.5	Scattering Between Electrons and Photons	92
6.5.1	Self Interactions	93
6.5.2	Scattering Processes	94
6.5.3	Three-Point Vertex Function	95
6.6	Scattering of Electrons and Photons in the Presence of an External Electromagnetic Field	95
6.6.1	Recursion Relation for the Vacuum Energy with External Source	96
6.6.2	Scattering of Electrons and Photons in the Presence of an External Source	99
 Part III: Variational Perturbation Theory in Quantum Statistics		101
7	Introduction	103
7.1	Variational Approach via Jensen-Peierls Inequality	105
7.2	Variational Perturbation Theory to Any Order	107
8	Variational Perturbation Theory for Density Matrices	109
8.1	Introduction	109
8.2	General Features	109
8.3	Variational Perturbation Theory	111
8.4	Smearing Formula for Density Matrices	112
8.5	First-Order Variational Results	114
8.5.1	Alternative Formula for First-Order Smearing	114
8.5.2	Classical Limit of Effective Classical Potential	116
8.5.3	Zero-Temperature Limit	117
8.6	Smearing Formula in Higher Spatial Dimensions	118
8.6.1	Isotropic Approximation	118

8.6.2	Anisotropic Approximation	119
8.7	Applications	119
8.7.1	The Double Well	119
8.7.2	Distribution Function for the Electron in the Hydrogen Atom	125
9	Variational Approach to Hydrogen Atom in Uniform Magnetic Field	129
9.1	Introduction	129
9.2	Effective Classical Representations for the Quantum Statistical Partition Function . . .	130
9.2.1	Effective Classical Potential	130
9.2.2	Effective Classical Hamiltonian	131
9.2.3	Exact Effective Classical Hamiltonian for an Electron in a Constant Magnetic Field	132
9.3	Hydrogen Atom in Constant Magnetic Field	135
9.3.1	Generalized Variational Perturbation Theory	135
9.3.2	First-Order Effective Classical Potential	137
9.3.3	Application to the Hydrogen Atom in a Magnetic Field	138
9.4	Results	139
9.4.1	Effective Classical Potential for Different Temperatures and Magnetic Field Strengths	140
9.4.2	Ground-State Energy of the Hydrogen Atom in Uniform Magnetic Field	140
9A	Generating Functional for Particle in Magnetic Field and Harmonic Oscillator Potential	146
9B	Properties of Green Functions	150
9B.1	General Properties	150
9B.2	Derivatives of Green Functions	150
9C	Generating Functional for Position- and Momentum-Dependent Correlation Functions .	152
Part IV: Strong-Coupling Theory for Membranes		159
10	Fluctuating Membranes	161
10.1	Introduction	161
10.2	Differential Geometry for Curves and Surfaces	162
10.2.1	Local Curvature of Curves	162
10.2.2	Local Curvature of Surfaces	164
11	Strong-Coupling Calculation of Fluctuation Pressure of a Membrane	171
11.1	Membrane Between Walls	171
11.2	Smooth Potential Model of Membrane Between Walls	172
11.2.1	Smooth Potential Adapting Walls	172
11.2.2	Perturbation Expansion for Free Energy	173
11.3	Evaluation of the Fluctuation Pressure up to Four-Loop Order	175
11.4	Extrapolation Towards the Exact Constant	178
11.5	Comparison with the Renormalization Group Approach	179
12	Fluctuation Pressure of a Stack of Membranes	181
12.1	Introduction	181
12.2	Stack of Strings	182
12.2.1	Free Fermion Model	182
12.2.2	Perturbative Approach	182
12.3	Stack of Membranes	187
12A	Evaluation of the Sunset Diagram	191
Concluding Remarks		195
13	Summary	197

Acknowledgments	199
Bibliography	201
Zusammenfassung	207
Curriculum Vitae	209

Preface

Introduction

In this thesis, some new aspects in dealing with path integrals are discussed, in particular the perturbatively defined quantum statistical path integral and the application of methods known from quantum field theory such as generating functionals in phase space. The expectation values appearing in perturbative expansions of path integrals are usually pictured by Feynman diagrams. We derive a graphical recursion relation to systematically construct topologically different Feynman diagrams with their correct multiplicities for the anharmonic oscillator as a quantum statistical example and for scattering processes in quantum electrodynamics, which illustrates the power of this method for quantum field theoretic problems. Generalizations and extensions of variational perturbation theory are used to calculate statistical properties of quantum systems and membranes.

1.1 Path Integrals

It was in 1948 when R.P. Feynman introduced the quantum mechanical path integral to calculate the transition amplitude for a charged particle in electromagnetic field [1]. With the path integral, the reinterpretation of the classically known notions “paths” and “orbits” became possible. Not only the paths which make the action extremal but also all other ways the particle may follow contribute to the transition amplitude with a phase factor which relates the action of a path to Planck’s constant \hbar . In its Euclidean form, the statistical path integral is built up from Boltzmann factors indeed indicating the probability of a certain path of the particle [2–4].

The exact calculation of path integrals is only possible for systems whose action is quadratic in the canonical variables, for example position $x(\tau)$ and momentum $p(\tau)$. In quantum mechanics, the path integrals for the transition amplitudes of the free particle and the harmonic oscillator are exactly calculated by time-slicing. Explicitly evaluating the path integral for a system with a more complicated potential is impossible, if it cannot be brought into the necessary Gaussian form. This is, however, possible for a class of systems, where the path integral can be transformed to be of oscillator type, e.g. for the hydrogen atom by applying the Duru-Kleinert transformation [4]. In non-interacting quantum field theories, e.g. for Klein-Gordon or Dirac fields, the Lagrangian density is usually quadratic in the fields and their derivatives. Thus such path integrals are of Gaussian type and can easily be calculated. If quantum fields interact, functional integrals cannot be evaluated analytically in almost all cases.

1.2 Perturbative and Non-Perturbative Methods for the Calculation of Path Integrals

Nevertheless, the interest in functional integrals has grown rapidly. Path integrals for a physical system with weakly coupled interaction allow for a simple perturbation expansion, where the correlation functions can be graphically pictured by Feynman diagrams. The most famous example is the interaction of charged relativistic particles with an electromagnetic field, as described by quantum electrodynamics, where the coupling constant is $\alpha \approx 1/137$. For strong-coupling systems, path integrals are used for the development of nonperturbative methods. Strong-coupling theories are necessary for calculating critical exponents of a system near a phase transition [5], for describing confinement between quarks in quantum chromodynamics [6], or for the investigation of interacting strings [7]. Path integral Monte Carlo methods on a lattice were developed to combine the selective probability picture of path integrals with the great numerical power of supercomputers. Analytic non-perturbative methods for strongly coupled systems are usually used to perform resummations of perturbative expansions as, for example, by Padé or Borel methods. Alternatively, Feynman and Kleinert [8] as well as Giachetti and Tognetti [9] developed a variational approach to approximatively calculate path integrals for *arbitrarily* coupled quantum mechanical systems. Within the last decade, the precision has been strongly improved by extending it to higher-order variational perturbation theory [4, Chap. 5]. Additionally, considerable progress was achieved in applying it to calculate critical exponents from strong-coupling series of the Ginzburg-Landau theory of critical phenomena [5,10,11].

1.3 Contents of This Thesis

This thesis is divided into four parts. In **Part I**, a perturbative definition of the quantum statistical phase space integral is introduced. Conventional time-slicing methods for calculating path integrals yield integration measures, which are not well defined since these are infinite in the continuum limit. Moreover, it is difficult to prove reparametrization invariance of the path integral under coordinate transformations, in particular in curved spaces. A perturbative expansion of any phase space path integral, where the complete Hamiltonian is treated as perturbation, does not possess these problems, since the exactly solvable contribution has a regular measure and is trivially reduced to products of δ functions. It is interesting that this procedure leads directly to a high-temperature expansion for the partition function. We prove the applicability of this method by calculating the effective classical potential for the harmonic oscillator.

Since it is necessary to calculate expectation values of products of Hamiltonians, it is useful to introduce Feynman rules, which can also be applied, if the Hamiltonian contains nonpolynomial terms. This requires to generalize Wick's rule, too. Furthermore, the calculation of mixed position-momentum correlations must be considered. As examples, we study harmonic expectation values whose treatment is necessary for the harmonic variational perturbation theory. In the case of nonpolynomial perturbations, so-called smearing formulas replace the ordinary Wick decompositions of polynomial correlations into products of two-point correlation functions. We also discuss the role of zero-mode fluctuations for paths with periodic and fixed boundary conditions.

In high orders of perturbation theory, it becomes often difficult to determine all topologically different Feynman diagrams and their multiplicities. Usually this problem is attacked with the help of combinatorial considerations. A powerful alternative is presented in **Part II**. We derive recursion relations from which all Feynman diagrams in any order are systematically generated without introducing artificial currents. These relations can be completely expressed in a graphical way. This means that the Feynman diagrams of a certain theory in any order are generated by cutting, removing, and glueing operations on diagrams of previous orders of perturbation. We present recursion relations for the quantum mechanical anharmonic oscillator and investigate the applicability to quantum field theories, where we specialize to quantum electrodynamics.

The resummation of divergent perturbative series with harmonic variational perturbation theory is the central aspect of **Part III**. After a short introduction of variational perturbation theory, we first

generalize this theory to density matrices and calculate the particle densities for the double well and the pair distribution function of hydrogen for different temperatures. Another interesting system is the hydrogen atom in a uniform external magnetic field, since it destroys the isotropy of the Coulomb interaction between electron and proton. The calculation of the effective classical potential, which governs the quantum statistics of this system, is followed by a detailed treatment of the ground-state energy. This quantity has a power expansion for weak strengths of the magnetic field, but a complicated logarithmic behavior for strong magnetic fields. We use the variational approach to find an expression for the ground-state energy as a function of the magnetic field strength, which is valid for all strengths of the magnetic field although the asymptotic behavior is so extremely different. The results are in good agreement with known values from numerical calculations. Considering the strong-field asymptotics in detail, we go analytically beyond an estimate presented by Landau.

Another example, where variational perturbation theory yields very good results, is the strong-coupling calculation of the fluctuation pressure of a membrane between walls. This shall be discussed in **Part IV**. A fluid membrane is tensionless, and its shape is governed by the curvature energy. By thermal fluctuations, the membrane exerts a pressure upon the walls. The pressure law is ideal-gas-like and contains a dimensionless pressure constant, whose value is not exactly known. From our strong-coupling calculation we obtain a very precise value that lies well in the error bounds of former Monte Carlo simulations. We also evaluate the pressure constants for a stack of membranes, where our strong-coupling approach is applicable for any number of membranes. Compared with Monte Carlo simulations, where only constants for low numbers of membranes were computed, our results are in very good agreement.

Part I

The Path Integral from a Perturbative Perspective

Perturbatively Defined Path Integral in Phase Space

As an alternative to Feynman's time-sliced definition, we introduce a perturbative definition of path integrals in phase space [12]. This will be shown to lead naturally to a high-temperature expansion for the effective classical Hamiltonian of quantum statistical systems. In this definition, the unperturbed system is trivial and the calculation of Feynman diagrams is simple. As an application, we shall apply this formalism to find the effective classical Hamiltonian for the harmonic oscillator.

2.1 Introduction

The definition of path integrals by time-slicing [4] becomes ambiguous for physical systems with non-trivial metric, where operator quantum mechanics has an ordering problem and reparametrization invariance has been a problem for many years [13]. It was solved recently by a perturbative definition of path integrals in *configuration space* [14] using dimensional regularization methods, which successfully guarantees gauge invariance in the quantum theory of non-Abelian gauge fields [15]. Ultimately, rules were found for calculating integrals over products of distributions, which establish a unique procedure for a perturbative calculation of path integrals, which fully respects reparametrization invariance [16]. The path integral of any system is expanded around that of a free particle in powers of the coupling constant of the potential.

Here we extend the definition to path integrals in *phase space* and derive a short-time expansion of the Hamiltonian quantum mechanical time evolution amplitude. In Euclidean space, the density matrix is obtained as a high-temperature expansion. By a simple resummation, this series can be turned into an expansion in powers of the coupling constant of the potential described above. In the expansion to be derived the solution for an exactly known nontrivial path integral such as that of a free particle is *not* required. The perturbative definition presented here is completely general. The usual expansion around the free-particle system can always be reproduced by simply changing the order of summations.

In a first step, the method is used to calculate the *effective classical Hamiltonian* of the harmonic oscillator $H_{\omega,\text{eff}}(p_0, x_0)$ by exactly summing up the perturbation series. In terms of $H_{\omega,\text{eff}}(p_0, x_0)$, the quantum statistical partition function is given by the classically looking phase space integral

$$Z_\omega = \int \frac{dx_0 dp_0}{2\pi\hbar} \exp\{-\beta H_{\omega,\text{eff}}(p_0, x_0)\}, \quad (2.1)$$

where $\beta = 1/k_B T$ is the inverse thermal energy.

2.2 Perturbative Definition of the Path Integral for Density Matrices

Slicing the interval $[0, \hbar\beta]$ into $N + 1$ pieces of width $\varepsilon = \hbar\beta/(N + 1)$, the unnormalized density matrix can be expressed by the continuum limit of a product of integrals as [4]

$$\tilde{q}(x_b, x_a) = \lim_{N \rightarrow \infty} \prod_{n=1}^N \left[\int_{-\infty}^{\infty} dx_n \right] \prod_{n=1}^{N+1} \left[\int_{-\infty}^{\infty} \frac{dp_n}{2\pi\hbar} e^{ip_n(x_n - x_{n-1})/\hbar} \right] \exp \left\{ -\varepsilon \sum_{n=1}^{N+1} H(p_n, x_n)/\hbar \right\}, \quad (2.2)$$

where $x_a = x_0$ and $x_b = x_{N+1}$ are the fixed end points of the path. Upon expanding the last exponential in powers of ε/\hbar , we recognize that the zeroth-order contribution to the density matrix (2.2) is an *infinite product of δ functions* due to the identity

$$\int_{-\infty}^{\infty} \frac{dp_n}{2\pi\hbar} e^{ip_n(x_n - x_{n-1})/\hbar} = \delta(x_n - x_{n-1}). \quad (2.3)$$

This infinite product simply reduces to

$$\lim_{N \rightarrow \infty} \int_{-\infty}^{\infty} dx_N \cdots dx_1 \delta(x_{N+1} - x_N) \cdots \delta(x_2 - x_1) \delta(x_1 - x_0) = \delta(x_b - x_a), \quad (2.4)$$

which is the unperturbed contribution to the unnormalized density matrix (2.2) obtained here from a trivial path integral. Thus, the phase space path integral for the unnormalized density matrix (2.2) can be perturbatively defined as

$$\begin{aligned} \tilde{q}(x_b, x_a) &= \delta(x_b - x_a) + \sum_{n=1}^{\infty} \frac{(-1)^n}{\hbar^n n!} \int_0^{\hbar\beta} d\tau_1 \cdots \int_0^{\hbar\beta} d\tau_n \\ &\quad \times \langle H(p(\tau_1), x(\tau_1)) \cdots H(p(\tau_n), x(\tau_n)) \rangle_0^{x_b, x_a}, \end{aligned} \quad (2.5)$$

with expectation values

$$\langle \cdots \rangle_0^{x_b, x_a} = \lim_{N \rightarrow \infty} \prod_{n=1}^N \left[\int_{-\infty}^{\infty} dx_n \right] \prod_{n=1}^{N+1} \left[\int_{-\infty}^{\infty} \frac{dp_n}{2\pi\hbar} \cdots e^{ip_n(x_n - x_{n-1})/\hbar} \right]. \quad (2.6)$$

These expectation values may be pictured by Feynman diagrams. This is possible for polynomial as well as nonpolynomial functions of momentum and position [17]. We show this in detail in Section 3.4. Note that the exponent on the right-hand side of Eq. (2.6) is the time-sliced version of the eikonal $S = -i \int d\tau p(\tau) dx(\tau)/d\tau$.

2.3 Restricted Partition Function and Two-Point Correlations

The trace over the unnormalized density matrix (2.5) of our unperturbed system with vanishing Hamiltonian $H(p, x) = 0$ yields the partition function, which diverges with the phase space volume. This divergence is the same as in the classical partition function. The regularization of these divergences is possible by excluding from the phase space path integral the zero-frequency fluctuations x_0 and p_0 of the Fourier decomposition of the periodic path $x(\tau)$ and momentum $p(\tau)$, respectively [4,18,19]. At the end, we may calculate the quantum statistical partition function from the classical phase space integral

$$Z = \int \frac{dx_0 dp_0}{2\pi\hbar} Z^{p_0, x_0}. \quad (2.7)$$

The restricted partition function in the integrand contains the Boltzmann factor of the effective classical Hamiltonian defined by the path integral

$$\begin{aligned} Z^{p_0 x_0} &\equiv \exp\{-\beta H_{\text{eff}}(p_0, x_0)\} = 2\pi\hbar \oint \mathcal{D}x\mathcal{D}p \delta(x_0 - \bar{x})\delta(p_0 - \bar{p}) \\ &\times \exp\left(-\frac{1}{\hbar} \int_0^{\hbar\beta} d\tau \left\{ -i[p(\tau) - p_0] \frac{d}{d\tau}[x(\tau) - x_0] + H(p(\tau), x(\tau)) \right\}\right), \end{aligned} \quad (2.8)$$

with the measure

$$\oint \mathcal{D}x\mathcal{D}p = \lim_{N \rightarrow \infty} \prod_{n=1}^{N+1} \left[\int_{-\infty}^{\infty} \frac{dx_n dp_n}{2\pi\hbar} \right]. \quad (2.9)$$

The quantities \bar{x} and \bar{p} are the temporal mean values $\bar{x} = \int_0^{\hbar\beta} d\tau x(\tau)/\hbar\beta$ and $\bar{p} = \int_0^{\hbar\beta} d\tau p(\tau)/\hbar\beta$.

As illustrated in the preceding section, the unperturbed system can be assumed to have a vanishing Hamiltonian. The calculation of the restricted partition function $Z^{p_0 x_0}$ of this system, denoted by $Z_0^{p_0 x_0}$, is then as trivial as for its unnormalized density matrix in (2.4). A cancellation of δ functions yields $Z_0^{p_0 x_0} = 1$.

In what follows, we want to find the correlation functions of position- and momentum-dependent quantities. For this purpose it is convenient to introduce the generating functional

$$\begin{aligned} Z_0^{p_0 x_0}[j, v] &= 2\pi\hbar \oint \mathcal{D}x\mathcal{D}p \delta(x_0 - \bar{x})\delta(p_0 - \bar{p}) \\ &\times \exp\left\{-\frac{1}{\hbar} \int_0^{\hbar\beta} d\tau \left[-i[p(\tau) - p_0] \frac{d}{d\tau}[x(\tau) - x_0] + j(\tau)[x(\tau) - x_0] + v(\tau)[p(\tau) - p_0] \right]\right\}, \end{aligned} \quad (2.10)$$

with currents $j(\tau)$ and $v(\tau)$. The action in the exponent contains only the trivial Euclidean eikonal $S = -i \int d\tau (p - p_0)d(x - x_0)/d\tau$. The calculation yields

$$Z_0^{p_0 x_0}[j, v] = \exp\left\{\frac{1}{\hbar^2} \int_0^{\hbar\beta} d\tau \int_0^{\hbar\beta} d\tau' j(\tau) G^{p_0 x_0}(\tau, \tau') v(\tau')\right\}, \quad (2.11)$$

where the periodic Green function has the Fourier representation

$$G^{p_0 x_0}(\tau, \tau') = \frac{2i}{\beta} \sum_{m=1}^{\infty} \frac{\sin \omega_m(\tau - \tau')}{\omega_m} \quad (2.12)$$

with Matsubara frequencies

$$\omega_m = \frac{2\pi m}{\hbar\beta}, \quad (2.13)$$

omitting the zero-mode. Evaluating the sum in Eq. (2.12) yields

$$G^{p_0 x_0}(\tau, \tau') = -\frac{i}{2\beta} \{2(\tau - \tau') - \hbar\beta [\Theta(\tau - \tau') - \Theta(\tau' - \tau)]\}. \quad (2.14)$$

Observe the antisymmetry $G^{p_0 x_0}(\tau, \tau') = -G^{p_0 x_0}(\tau', \tau)$. As a consequence of reparametrization invariance of the eikonal $S = -i \int d\tau (p - p_0)d(x - x_0)/d\tau$, the Green function depends only on the reduced variables

$$\bar{\tau} \equiv \frac{\tau}{\beta} \quad (2.15)$$

and can thus be written as

$$G^{p_0 x_0}(\bar{\tau}, \bar{\tau}') = -\frac{i}{2} \{2(\bar{\tau} - \bar{\tau}') - \hbar [\Theta(\bar{\tau} - \bar{\tau}') - \Theta(\bar{\tau}' - \bar{\tau})]\}. \quad (2.16)$$

Introducing expectation values as

$$\langle \dots \rangle_0^{p_0, x_0} = 2\pi\hbar \oint \mathcal{D}x \mathcal{D}p \delta(x_0 - \bar{x}) \delta(p_0 - \bar{p}) \cdots \exp \left\{ \frac{1}{\hbar} \int_0^{\hbar\beta} d\tau i [p(\tau) - p_0] \frac{d}{d\tau} [x(\tau) - x_0] \right\}, \quad (2.17)$$

the two-point functions are obtained from the generating functional (2.10) by performing appropriate functional derivatives with respect to $j(\tau)$ and $v(\tau)$, respectively:

$$\langle \tilde{x}(\tau) \tilde{x}(\tau') \rangle_0^{p_0, x_0} = 0, \quad (2.18)$$

$$\langle \tilde{x}(\tau) \tilde{p}(\tau') \rangle_0^{p_0, x_0} = G^{p_0, x_0}(\tau, \tau'), \quad (2.19)$$

$$\langle \tilde{p}(\tau) \tilde{p}(\tau') \rangle_0^{p_0, x_0} = 0. \quad (2.20)$$

The off-diagonal nature of the trivial action in (2.17) entails that only *mixed* position-momentum correlations do not vanish.

2.4 Perturbative Expansion for the Effective Classical Hamiltonian

Expanding the restricted partition function (2.8) in powers of the Hamiltonian,

$$Z^{p_0, x_0} = 1 + \sum_{n=1}^{\infty} \frac{(-1)^n}{\hbar^n n!} \int_0^{\hbar\beta} d\tau_1 \cdots \int_0^{\hbar\beta} d\tau_n \langle H(p(\tau_1), x(\tau_1)) \cdots H(p(\tau_n), x(\tau_n)) \rangle_0^{p_0, x_0}, \quad (2.21)$$

rewriting this into a cumulant expansion, and utilizing the relation (2.8) between restricted partition function and effective classical Hamiltonian, we obtain

$$H_{\text{eff}}(p_0, x_0) = \frac{1}{\beta} \sum_{n=1}^{\infty} \frac{(-1)^{n+1}}{\hbar^n n!} \int_0^{\hbar\beta} d\tau_1 \cdots \int_0^{\hbar\beta} d\tau_n \langle H(p(\tau_1), x(\tau_1)) \cdots H(p(\tau_n), x(\tau_n)) \rangle_{0,c}^{p_0, x_0}. \quad (2.22)$$

Using Wick's rule, all correlation functions can be expressed in terms of products of two-point functions. Since only mixed two-point functions (2.14) can lead to nonvanishing contributions to the effective classical Hamiltonian, we use the rescaled version (2.16) of the Green function. The scaling transformation gives a factor β from each of the n integral measures. Thus the expansion (2.22) is a *high-temperature* expansion of the effective classical Hamiltonian:

$$H_{\text{eff}}(p_0, x_0) = \sum_{n=1}^{\infty} \beta^{n-1} \frac{(-1)^{n+1}}{\hbar^n n!} \int_0^{\hbar} d\bar{\tau}_1 \cdots \int_0^{\hbar} d\bar{\tau}_n \langle H(p(\bar{\tau}_1), x(\bar{\tau}_1)) \cdots H(p(\bar{\tau}_n), x(\bar{\tau}_n)) \rangle_{0,c}^{p_0, x_0}. \quad (2.23)$$

For the following considerations it is useful to assume the Hamilton function to be of standard form

$$H(p(\bar{\tau}), x(\bar{\tau})) = \frac{p^2(\bar{\tau})}{2M} + gV(x(\bar{\tau})), \quad (2.24)$$

where we have introduced the coupling constant g of the potential. Defining the functionals

$$a[p] = \int_0^{\hbar} d\bar{\tau} \frac{p^2(\bar{\tau})}{2M}, \quad b[x] = \int_0^{\hbar} d\bar{\tau} V(x(\bar{\tau})), \quad (2.25)$$

the high-temperature expansion (2.23) is expressed as

$$H_{\text{eff}}(p_0, x_0) = \sum_{n=1}^{\infty} \beta^{n-1} \frac{(-1)^{n+1}}{n! \hbar^n} \sum_{k=0}^n g^k \binom{n}{k} \langle a^{n-k}[p] b^k[x] \rangle_{0,c}^{p_0, x_0}. \quad (2.26)$$

Before pointing out how this high-temperature expansion is connected with an expansion in powers of the coupling constant g of the potential, we calculate the exact effective classical Hamiltonian of the harmonic oscillator.

2.5 Effective Classical Hamiltonian of Harmonic Oscillator

In this section, we calculate the effective classical Hamiltonian for the harmonic oscillator

$$H_\omega(p, x) = \frac{p^2}{2M} + \frac{1}{2}M\omega^2 x^2 \quad (2.27)$$

by an exact resummation of the high-temperature expansion (2.26). For systematically expressing the terms of this expansion, it is useful to introduce the following Feynman rules:

$$\bar{\tau}_1 \text{ --- } \bar{\tau}_2 \equiv \langle p(\bar{\tau}_1)p(\bar{\tau}_2) \rangle_0^{p_0 x_0} = p_0^2, \quad (2.28)$$

$$\bar{\tau}_1 \text{ --- } \bar{\tau}_2 \equiv \langle x(\bar{\tau}_1)x(\bar{\tau}_2) \rangle_0^{p_0 x_0} = x_0^2, \quad (2.29)$$

$$\bar{\tau}_1 \text{ --- } \bar{\tau}_2 \equiv \langle x(\bar{\tau}_1)p(\bar{\tau}_2) \rangle_0^{p_0 x_0} = G^{p_0 x_0}(\bar{\tau}_1, \bar{\tau}_2) + x_0 p_0, \quad (2.30)$$

$$\bar{\tau}_1 \text{ --- } \bar{\tau}_2 \equiv \langle p(\bar{\tau}_1)x(\bar{\tau}_2) \rangle_0^{p_0 x_0} = -G^{p_0 x_0}(\bar{\tau}_1, \bar{\tau}_2) + p_0 x_0, \quad (2.31)$$

$$\bar{\tau} \text{ --- } \star \equiv \langle p(\bar{\tau}) \rangle_0^{p_0 x_0} = p_0, \quad (2.32)$$

$$\bar{\tau} \text{ --- } \star \equiv \langle x(\bar{\tau}) \rangle_0^{p_0 x_0} = x_0, \quad (2.33)$$

$$\bullet \equiv \int_0^{\hbar} d\bar{\tau}, \quad (2.34)$$

where the current-like expectations in (2.32) and (2.33) arise from $\langle \tilde{p}(\bar{\tau}) \rangle_0^{p_0 x_0} = 0$ and $\langle \tilde{x}(\bar{\tau}) \rangle_0^{p_0 x_0} = 0$, respectively. In order to simplify the calculation of the expectation values in the high-temperature expansion of the effective classical Hamiltonian (2.26), we also define operational subgraphs

$$\text{---} \equiv \frac{1}{2M\hbar} \int_0^{\hbar} d\bar{\tau} p^2(\bar{\tau}), \quad (2.35)$$

$$\text{---} \equiv \frac{1}{2\hbar} M\omega^2 \int_0^{\hbar} d\bar{\tau} x^2(\bar{\tau}), \quad (2.36)$$

which are useful for the systematic construction of the Feynman diagrams. These diagrams are composed by attaching the legs of such subgraphs to one another or by connecting legs with suitable currents. Note that only combinations of different types of subgraphs lead to nonvanishing contributions, since the connection of subgraphs of same type,

$$\text{---} \text{---}, \quad \text{---} \text{---}, \quad (2.37)$$

leads to a new subgraph, which contains a propagator (2.28) or (2.29), respectively. These propagators are, however, independent of $\bar{\tau}$, such that the $\bar{\tau}$ -integrals related to the vertices in these subgraphs are trivial. Thus, there does not really exist a connection between these vertices and the propagators (2.28) and (2.29) can be expressed by the currents (2.32) and (2.33):

$$\bar{\tau}_1 \text{ --- } \bar{\tau}_2 = \bar{\tau}_1 \text{ --- } \star \star \text{ --- } \bar{\tau}_2, \quad (2.38)$$

$$\bar{\tau}_1 \text{ --- } \bar{\tau}_2 = \bar{\tau}_1 \text{ --- } \star \star \text{ --- } \bar{\tau}_2. \quad (2.39)$$

As a consequence, connected diagrams for $n > 1$ containing propagators of type (2.28) or (2.29) *must* break up into disconnected parts. Analytically, this is seen by considering for example

$$\langle x(\bar{\tau}_1)x(\bar{\tau}_2) \rangle_0^{p_0 x_0} = \langle \tilde{x}(\bar{\tau}_1)\tilde{x}(\bar{\tau}_2) \rangle_0^{p_0 x_0} + \langle x(\bar{\tau}_1) \rangle_0^{p_0 x_0} \langle x(\bar{\tau}_2) \rangle_0^{p_0 x_0}. \quad (2.40)$$

The first term on the right-hand side vanishes due to Eq. (2.18), while the second simply yields x_0^2 , which proves Eq. (2.29). This means that only Feynman diagrams, which consist of a mixture of subgraphs (2.35) and (2.36) contribute to the effective classical Hamiltonian. To illustrate this, we discuss the first and second order of expansion (2.23) in more detail.

The Feynman diagrams of the first-order contribution to the effective classical Hamiltonian are simply constructed from the subgraphs

$$H_{\omega, \text{eff}}^{(1)}(p_0, x_0) \propto \text{---} + \text{---}$$

$$\begin{aligned}
&= \frac{1}{2M\hbar} \text{cloud} + \frac{1}{2\hbar} M\omega^2 \text{circle} = \frac{1}{2M\hbar} \text{wavy} + \frac{1}{2\hbar} M\omega^2 \text{dotted} \\
&= \frac{p_0^2}{2M} + \frac{1}{2} M\omega^2 x_0^2,
\end{aligned} \tag{2.41}$$

where we have used the identities (2.38) and (2.39) in the second expression of the second line. Note that the first-order term (2.41) obviously reproduces the classical Hamiltonian. This is the consequence of the high-temperature expansion (2.26), since only the first-order contribution is nonzero in the limit $\beta = 1/k_B T \rightarrow 0$. The second-order contribution reads

$$\begin{aligned}
H_{\omega,\text{eff}}^{(2)}(p_0, x_0) &\propto (\text{wavy} + \text{dotted}) (\text{wavy} + \text{dotted}) \\
&= -\frac{\omega^2}{8\hbar^2\beta} \left(8 \text{chain} + 4 \text{loop} \right).
\end{aligned} \tag{2.42}$$

The chain diagram is zero, while the loop diagram has the value $-\hbar^4\zeta(2)/2\pi^2$, where

$$\zeta(z) = \sum_{n=1}^{\infty} \frac{1}{n^z} \tag{2.43}$$

is the Riemann ζ function. Thus we obtain

$$H_{\omega,\text{eff}}^{(2)}(p_0, x_0) = \beta\hbar^2\omega^2\zeta(2)/4\pi^2. \tag{2.44}$$

This second-order contribution (2.42) shows the characteristic types of Feynman diagrams appearing in each order $n > 1$ of the expansion (2.23) for the harmonic oscillator: chain and loop diagrams. In order to calculate the n th-order contribution, we must evaluate these diagrams more general. By constructing Feynman diagrams from the product of n sums of subgraphs,

$$H_{\omega,\text{eff}}^{(n)}(p_0, x_0) \propto \underbrace{(\text{wavy} + \text{dotted}) (\text{wavy} + \text{dotted}) \cdots (\text{wavy} + \text{dotted})}_{n \text{ times}}, \tag{2.45}$$

it turns out that only following chain and loop diagrams contribute:

$$\begin{aligned}
&\text{wavy} \text{---} \text{dotted} \text{---} \text{dotted} \text{---} \text{wavy}, \\
&\text{dotted} \text{---} \text{wavy} \text{---} \text{wavy} \text{---} \text{dotted}, \\
&\text{dotted} \text{---} \text{dotted} \text{---} \text{wavy} \text{---} \text{wavy}, \\
&\text{circle}
\end{aligned} \tag{2.46}$$

The evaluation of the chain diagrams is easily done and yields zero. An explicit calculation in Fourier space shows that there occur Kronecker symbols δ_{m0} . Since the Matsubara sum of the Green function (2.12) does not contain the zero mode $m = 0$, all chain diagrams are zero.

Determining the values of loop diagrams is more involved. It is obvious that loop diagrams can only be constructed in *even* order ($n = 2, 4, 6, \dots$), since for a loop diagram with mixed propagators (2.30) or (2.31) pairs of different subgraphs (2.35) and (2.36) are necessary. Thus we have found the result that *odd* orders of expansion (2.26) *vanish*, and only loop diagrams for $n \in \{2, 4, 6, \dots\}$ must be calculated. Evaluating loop diagrams of n th order in Fourier space is straightforward and entails

$$\text{circle} = 2(-1)^k \left(\frac{\hbar^2}{2\pi} \right)^{2k} \zeta(2k), \tag{2.47}$$

where $k = n/2$. The multiplicity of such a diagram with $2k$ vertices is easily determined, yielding

$$\mu_k = \frac{2^{2k} (2k)!}{2k}. \tag{2.48}$$

Thus the high-temperature expansion for the effective Hamiltonian of the harmonic oscillator can be written as

$$H_{\omega,\text{eff}}(p_0, x_0) = \frac{p_0^2}{2M} + \frac{1}{2}M\omega^2 x_0^2 + \sum_{k=1}^{\infty} \beta^{2k-1} \frac{(-1)^{k+1}}{k} \left(\frac{\hbar\omega}{2\pi}\right)^{2k} \zeta(2k). \quad (2.49)$$

Substituting the ζ function by its definition (2.43) and exchanging the summations, the last term in Eq. (2.49) can be expressed as a logarithm

$$\sum_{k=1}^{\infty} \beta^{2k-1} \frac{(-1)^{k+1}}{k} \left(\frac{\hbar\omega}{2\pi}\right)^{2k} \zeta(2k) = \frac{1}{\beta} \ln \left(\prod_{n=1}^{\infty} \left[1 + \frac{\hbar^2 \beta^2 \omega^2}{4\pi^2 n^2} \right] \right). \quad (2.50)$$

Applying the relation

$$\frac{1}{z} \sinh z = \prod_{n=1}^{\infty} \left(1 + \frac{z^2}{n^2 \pi^2} \right), \quad (2.51)$$

we find the more familiar form of the effective classical Hamiltonian for a harmonic oscillator

$$H_{\omega,\text{eff}}(p_0, x_0) = \frac{p_0^2}{2M} + \frac{1}{2}M\omega^2 x_0^2 - \frac{1}{\beta} \ln \frac{\hbar\omega\beta}{2 \sinh \hbar\omega\beta/2}. \quad (2.52)$$

Performing the x_0 - and p_0 -integrations in Eq. (2.1), we obtain the well-known form of the partition function of the harmonic oscillator $Z_{\omega} = 1/2 \sinh \hbar\omega\beta/2$.

2.6 High-Temperature Versus Weak-Coupling Expansion

In Section 2.4 we have shown that the perturbative expansion around a vanishing Hamiltonian leads to a perturbative series in powers of the inverse temperature in a natural manner. Now we elaborate its relation to more customary perturbative expansions in powers of the coupling constant g of the potential. Changing the order of summation in Eq. (2.26), we obtain

$$H_{\text{eff}}(p_0, x_0) = \sum_{k=0}^{\infty} g^k \sum_{n=0}^{\infty} \beta^{n+k-1} \binom{n+k}{k} \frac{(-1)^{n+k+1}}{(n+k)! \hbar^{n+k}} \langle a^n [p] b^k [x] \rangle_{0,c}^{p_0, x_0} + \frac{1}{\beta}, \quad (2.53)$$

which is rewritten, after explicitly evaluating the $(n=0)$ - and $(k=0)$ -contributions, as

$$\begin{aligned} H_{\text{eff}}(p_0, x_0) &= \frac{p_0^2}{2M} + gV(x_0) + \frac{1}{\beta} \sum_{k=1}^{\infty} g^k \sum_{n=1}^{\infty} \frac{(-1)^{n+k+1}}{n! k! \hbar^{n+k} (2M)^n} \\ &\times \int_0^{\hbar\beta} d\tau_1 \cdots \int_0^{\hbar\beta} d\tau_k \int_0^{\hbar\beta} d\tau_{k+1} \cdots \int_0^{\hbar\beta} d\tau_{k+n} \\ &\times \langle V(x(\tau_1)) \cdots V(x(\tau_k)) p^2(\tau_{k+1}) \cdots p^2(\tau_{k+n}) \rangle_{0,c}^{p_0, x_0}. \end{aligned} \quad (2.54)$$

In this expression, we have inverted the scaling transformation in Eq. (2.15), and used the expectation values

$$\int_0^{\hbar\beta} d\tau \langle p^2(\tau) \rangle_{0,c}^{p_0, x_0} = \hbar\beta p_0^2, \quad \int_0^{\hbar\beta} d\tau \langle V(x(\tau)) \rangle_{0,c}^{p_0, x_0} = \hbar\beta V(x_0). \quad (2.55)$$

All higher-order expectations of functions, which only depend on x or p are zero, due to the vanishing of expectations of functions of \tilde{x} or \tilde{p} in a Wick expansion into products of two-point functions (2.18) and (2.20). All other possible contributions are disconnected.

We now observe that the expansion (2.54) is equal to a perturbation expansion around a free-particle theory

$$H_{\text{eff}}(p_0, x_0) = \frac{p_0^2}{2M} + gV(x_0) + \frac{1}{\beta} \sum_{k=1}^{\infty} g^k \frac{(-1)^{k+1}}{k! \hbar^k} \int_0^{\hbar\beta} d\tau_1 \cdots \int_0^{\hbar\beta} d\tau_k$$

$$\times \langle V(x(\tau_1)) \cdots V(x(\tau_k)) \rangle_{\text{free}, c}^{x_0}, \quad (2.56)$$

in which cumulants are formed from position-dependent expectation values

$$\begin{aligned} \langle \cdots \rangle_{\text{free}}^{x_0} &= 2\pi\hbar e^{\beta p_0^2/2M} \oint \mathcal{D}x \mathcal{D}p \delta(x_0 - \bar{x}) \delta(p_0 - \bar{p}) \cdots \\ &\times \exp \left\{ -\frac{1}{\hbar} \int_0^{\hbar\beta} d\tau \left[-i(p(\tau) - p_0) \frac{\partial}{\partial \tau} (x(\tau) - x_0) + \frac{1}{2M} p^2(\tau) \right] \right\}. \end{aligned} \quad (2.57)$$

This expression is identical with

$$\langle \cdots \rangle_{\text{free}}^{x_0} = \sqrt{\frac{2\pi\hbar^2\beta}{M}} \oint \mathcal{D}'x \delta(x_0 - \bar{x}) \cdots \exp \left\{ -\frac{M}{2\hbar} \int_0^{\hbar\beta} d\tau \dot{x}^2(\tau) \right\}, \quad (2.58)$$

with the dot denoting the derivative with respect to τ . The new measure is

$$\oint \mathcal{D}'x = \lim_{N \rightarrow \infty} \prod_{n=1}^{N+1} \left[\int_{-\infty}^{\infty} \frac{dx_n}{\sqrt{2\pi\hbar\varepsilon/M}} \right]. \quad (2.59)$$

In the following section we will consider how the expectation values appearing in the high-temperature expansion (2.54) of the effective classical Hamiltonian go over into the cumulants in the weak-coupling expansion (2.56). We thus study the relation between both expansions and we are led to the so-called *smearing formula* for arbitrary expectation values of functions depending on position or/and momentum. Being a Gaussian convolution of these functions, its application will be in particular useful for calculating expectation values of nonpolynomial expressions.

2.7 Free-Particle Smearing Formula

Consider a general correlation function appearing in the expansion (2.54) of the effective classical Hamiltonian, which can be written as

$$M_{kn} = \prod_{m=1}^{k+n} \left[\int_0^{\hbar\beta} d\tau_m \right] \left\langle \prod_{l=1}^k [V(x(\tau_l))] \prod_{s=1}^n [p^2(\tau_{k+s})] \right\rangle_0^{p_0 x_0}. \quad (2.60)$$

In order to reduce the expectation value to an expression, which has already been calculated we split off the time dependencies by Fourier transformations. This yields

$$\begin{aligned} M_{kn} &= \prod_{m=1}^{k+n} \left[\int_0^{\hbar\beta} d\tau_m \right] \prod_{l=1}^k \left[\int_{-\infty}^{\infty} \frac{d\kappa_l}{2\pi} V(\kappa_l) e^{i\kappa_l x_0} \right] \prod_{s=1}^n \left[\int_{-\infty}^{\infty} \frac{d\bar{p}_s}{2\pi\hbar} \bar{p}_s^2 \int_{-\infty}^{\infty} d\xi_s e^{i(\bar{p}_s - p_0)\xi_s/\hbar} \right] \\ &\times \left\langle \exp \left\{ i \sum_{l=1}^k \kappa_l [x(\tau_l) - x_0] - \frac{i}{\hbar} \sum_{s=1}^n \xi_s [p(\tau_{k+s}) - p_0] \right\} \right\rangle_0^{p_0 x_0}. \end{aligned} \quad (2.61)$$

By introducing currents

$$j(\tau) = -i\hbar \sum_{l=1}^k \delta(\tau - \tau_l) \kappa_l, \quad v(\tau) = i \sum_{s=1}^n \delta(\tau - \tau_{k+s}) \xi_s, \quad (2.62)$$

the expectation value in Eq. (2.61) can be rewritten as the generating functional (2.10) with the result (2.11). We reinsert now the expressions (2.62) for the currents into the functional (2.11) and perform the τ -integrations. This leads to

$$Z_0^{p_0 x_0}[\kappa, \xi] = \exp \left[\frac{1}{\hbar} \sum_{l=1}^k \sum_{s=1}^n \kappa_l G^{p_0 x_0}(\tau_l, \tau_{k+s}) \xi_s \right]. \quad (2.63)$$

Using this result in Eq. (2.61), the ξ_s -integration can be done and yields

$$\int_{-\infty}^{\infty} \frac{d\xi_s}{2\pi\hbar} \exp \left\{ \frac{i}{\hbar} \left[\bar{p}_s - p_0 - i \sum_{l=1}^k \kappa_l G^{p_0 x_0}(\tau_l, \tau_{k+s}) \right] \xi_s \right\} = \delta \left(\bar{p}_s - p_0 - i \sum_{l=1}^k \kappa_l G^{p_0 x_0}(\tau_l, \tau_{k+s}) \right), \quad (2.64)$$

leaving us with

$$M_{kn} = \prod_{l=1}^k \left[\int_0^{\hbar\beta} d\tau_l \int_{-\infty}^{\infty} \frac{d\kappa_l}{2\pi} V(\kappa_l) e^{i\kappa_l x_0} \right] \prod_{s=1}^n \left[\int_0^{\hbar\beta} d\tau_{k+s} \left(p_0 + i \sum_{l=1}^k \kappa_l G^{p_0 x_0}(\tau_l, \tau_{k+s}) \right)^2 \right]. \quad (2.65)$$

After expanding the squared parentheses, terms like

$$\int_0^{\hbar\beta} d\tau_{P(k+1)} p_0^2 \int_0^{\hbar\beta} d\tau_{P(k+2)} \cdots \int_0^{\hbar\beta} d\tau_{P(k+s)} f_1(\tau_{P(k+2)}, \dots, \tau_{P(k+s)}) \quad (2.66)$$

and

$$\int_0^{\hbar\beta} d\tau_{P(k+1)} G^{p_0 x_0}(\tau_{P(k+1)}, \tau_l) \int_0^{\hbar\beta} d\tau_{P(k+2)} \cdots \int_0^{\hbar\beta} d\tau_{P(k+s)} f_2(\tau_{P(k+2)}, \dots, \tau_{P(k+s)}) \quad (2.67)$$

occur, where $f_1(\tau_{P(k+2)}, \dots, \tau_{P(k+s)})$ and $f_2(\tau_{P(k+2)}, \dots, \tau_{P(k+s)})$ are functions independent of τ_{k+1} . Due to the separate time integration, expressions of the form (2.66) correspond to disconnected diagrams and may be omitted in the following. Since $\int_0^{\hbar\beta} d\tau G^{p_0, x_0}(\tau, \tau')$ vanishes, terms like (2.67) do not contribute. The permutation operator P exhibits that this is also right for any permutation of the τ_i 's ($i \in \{1, \dots, s\}$). Since we shall omit disconnected contributions (2.66), we are left with the cumulant

$$M_{c, kn} = \prod_{l=1}^k \left[\int_0^{\hbar\beta} d\tau_l \int_{-\infty}^{\infty} \frac{d\kappa_l}{2\pi} V(\kappa_l) e^{i\kappa_l x_0} \right] \times \prod_{s=1}^n \left[(-1) \sum_{l_1, l_2=1}^k \kappa_{l_1} \kappa_{l_2} \int_0^{\hbar\beta} d\tau_{k+s} G^{p_0 x_0}(\tau_{l_1}, \tau_{k+s}) G^{p_0 x_0}(\tau_{k+s}, \tau_{l_2}) \right]. \quad (2.68)$$

Using the Fourier decomposition of the Green function (2.12) with Matsubara frequencies (2.13), the time integration in the second product is easily done yielding

$$\begin{aligned} \int_0^{\hbar\beta} d\tau_{k+s} G^{p_0 x_0}(\tau_{l_1}, \tau_{k+s}) G^{p_0 x_0}(\tau_{k+s}, \tau_{l_2}) &= -\frac{2\hbar}{\beta} \sum_{m=1}^{\infty} \frac{1}{\omega_m^2} \cos \omega_m (\tau_{l_1} - \tau_{l_2}) \\ &= -\frac{M}{\hbar} G_{\text{free}}^{p_0 x_0}(\tau_{l_1}, \tau_{l_2}), \end{aligned} \quad (2.69)$$

where

$$G_{\text{free}}^{p_0 x_0}(\tau, \tau') = \frac{1}{2M\beta} \left(|\tau - \tau'|^2 - \hbar\beta|\tau - \tau'| + \frac{1}{6}\hbar^2\beta^2 \right) \quad (2.70)$$

is the Green function for a free particle with periodic boundary conditions and the zero-frequency mode excluded. It satisfies the equation of motion

$$\frac{M}{2\hbar} \frac{\partial^2}{\partial \tau^2} G_{\text{free}}^{p_0 x_0}(\tau, \tau') = \delta(\tau - \tau'), \quad \tau, \tau' \in [0, \hbar\beta]. \quad (2.71)$$

with periodic boundary conditions $G_{\text{free}}^{p_0 x_0}(\tau, \tau') \equiv G_{\text{free}}^{p_0 x_0}(\tau - \tau') = G_{\text{free}}^{p_0 x_0}(\tau - \tau' + \hbar\beta)$. Thus the cumulant (2.68) can be written as

$$M_{c, kn} = \prod_{l=1}^k \left[\int_0^{\hbar\beta} d\tau_l \int_{-\infty}^{\infty} \frac{d\kappa_l}{2\pi} V(\kappa_l) e^{i\kappa_l x_0} \right] \left[\frac{M}{\hbar} \sum_{l_1, l_2=1}^k \kappa_{l_1} G_{\text{free}}^{p_0 x_0}(\tau_{l_1}, \tau_{l_2}) \kappa_{l_2} \right]^n. \quad (2.72)$$

The expansion (2.54) can now be expressed as

$$H_{\text{eff}}(p_0, x_0) = \frac{p_0^2}{2M} + gV(x_0) + \frac{1}{\beta} \sum_{k=1}^{\infty} g^k \frac{(-1)^{k+1}}{k! \hbar^k} \sum_{n=1}^{\infty} \frac{(-1)^n}{2^n n!} M_{c, kn}. \quad (2.73)$$

It is useful to move the classical potential term $gV(x_0)$ into the last sum. This is done by extending the second sum in (2.73) by the $n = 0$ -term:

$$\begin{aligned} \sum_{k=1}^{\infty} g^k \frac{(-1)^{k+1}}{k! \hbar^k} \prod_{l=1}^k \left[\int_0^{\hbar\beta} d\tau_l \int_{-\infty}^{\infty} \frac{d\kappa_l}{2\pi} V(\kappa_l) e^{i\kappa_l x_0} \right] \\ = \sum_{k=1}^{\infty} g^k \frac{(-1)^{k+1}}{k! \hbar^k} \int_0^{\hbar\beta} d\tau_1 \dots \int_0^{\hbar\beta} d\tau_k [V(x_0)]^k = gV(x_0). \end{aligned} \quad (2.74)$$

In the second expression we have utilized that terms with $k > 1$ lead to disconnected contributions, which do not appear in $M_{c, kn}$. Thus expansion (2.73) reads

$$\begin{aligned} H_{\text{eff}}(p_0, x_0) = \frac{p_0^2}{2M} + \frac{1}{\beta} \sum_{k=1}^{\infty} g^k \frac{(-1)^{k+1}}{k! \hbar^k} \prod_{l=1}^k \left[\int_0^{\hbar\beta} d\tau_l \int_{-\infty}^{\infty} dx_l V(x_l) \int_{-\infty}^{\infty} \frac{d\kappa_l}{2\pi} \right] \\ \times \exp \left\{ i\boldsymbol{\kappa}(\mathbf{x}_0 - \mathbf{x}) - \frac{1}{2} \boldsymbol{\kappa}^T \mathbf{G}_{\text{free}}^{p_0 x_0} \boldsymbol{\kappa} \right\}, \end{aligned} \quad (2.75)$$

where we have introduced the n -dimensional vectors $\boldsymbol{\kappa} = (\kappa_1, \dots, \kappa_n)$ and the symmetric $n \times n$ matrix of Green functions

$$\mathbf{G}_{\text{free}}^{p_0 x_0} = \begin{pmatrix} G_{\text{free}}^{p_0 x_0}(\tau_1, \tau_1) & \dots & G_{\text{free}}^{p_0 x_0}(\tau_1, \tau_n) \\ \vdots & \ddots & \vdots \\ G_{\text{free}}^{p_0 x_0}(\tau_1, \tau_n) & \dots & G_{\text{free}}^{p_0 x_0}(\tau_n, \tau_n) \end{pmatrix}. \quad (2.76)$$

After diagonalizing this matrix, the κ_l -integrals in Eq. (2.75) are easily calculated. The effective classical Hamiltonian can then be expressed with the help of a Gaussian convolution integral, which smears out products of the potential $V(x)$:

$$\begin{aligned} H_{\text{eff}}(p_0, x_0) = \frac{p_0^2}{2M} + \frac{1}{\beta} \sum_{k=1}^{\infty} g^k \frac{(-1)^{k+1}}{k! \hbar^k} \prod_{l=1}^k \left[\int_0^{\hbar\beta} d\tau_l \int_{-\infty}^{\infty} dx_l V(x_l) \right] \\ \times \frac{1}{\sqrt{2\pi \det \mathbf{G}_{\text{free}}^{p_0 x_0}}} \exp \left\{ -\frac{1}{2} \sum_{l_1, l_2=1}^k (x_{l_1} - x_0) [G_{\text{free}}^{p_0 x_0}(\tau_{l_1}, \tau_{l_2})]^{-1} (x_{l_2} - x_0) \right\}. \end{aligned} \quad (2.77)$$

The extension of this result to higher spatial dimensions is straightforward.

Smearing Formulas for Fluctuation Effects

It is well known from perturbative expansions of interacting quantum fields and quantum mechanical systems with polynomial interactions that correlation functions appearing in a certain perturbative order can be decomposed into sums of products of two-point correlation functions by applying Wick's rule [4, Chap. 3]. When the potential of a physical system is nonpolynomial, the correlation functions are more complicated, and Wick's rule fails. This case can only be treated with a so-called smearing formula, which simply turns out to be a Gaussian convolution of the original classical potential. The width of the Gaussian distribution is governed by the two-point correlation functions or Green functions of the unperturbed system. A special example was the perturbative expansion for the effective classical Hamiltonian (2.77), which will now be generalized to arbitrary Gaussian systems.

3.1 Generalized Euclidean Action in Phase Space

The most general Euclidean quadratic action in flat $2d$ -dimensional phase space reads

$$\begin{aligned} \mathcal{A}_0[\mathbf{p}, \mathbf{x}; \mathbf{j}, \mathbf{v}] = & \frac{\hbar}{2} \int_0^{\hbar\beta} d\tau \int_0^{\hbar\beta} d\tau' [\mathbf{x}^T(\tau) D_{\mathbf{x}\mathbf{x}}(\tau, \tau') \mathbf{x}(\tau') + \mathbf{x}^T(\tau) D_{\mathbf{x}\mathbf{p}}(\tau, \tau') \mathbf{p}(\tau') \\ & + \mathbf{p}^T(\tau) D_{\mathbf{p}\mathbf{x}}(\tau, \tau') \mathbf{x}(\tau') + \mathbf{p}^T(\tau) D_{\mathbf{p}\mathbf{p}}(\tau, \tau') \mathbf{p}(\tau')] + \int_0^{\hbar\beta} d\tau [\mathbf{j}^T(\tau) \mathbf{x}(\tau) + \mathbf{v}^T(\tau) \mathbf{p}(\tau)], \end{aligned} \quad (3.1)$$

where $\mathbf{j}(\tau)$ and $\mathbf{v}(\tau)$ are external currents coupled linearly to the respective d -dimensional phase space coordinate $\mathbf{x}(\tau)$ or $\mathbf{p}(\tau)$. The superscript T denotes the transpose with respect to the phase space coordinates. The $d \times d$ matrices $D_{\mathbf{x}\mathbf{x}}(\tau, \tau')$, $D_{\mathbf{x}\mathbf{p}}(\tau, \tau')$, $D_{\mathbf{p}\mathbf{x}}(\tau, \tau')$, and $D_{\mathbf{p}\mathbf{p}}(\tau, \tau')$ are arbitrary at the moment.

Integrating $\exp\{-\mathcal{A}_0[\mathbf{p}, \mathbf{x}; \mathbf{j}, \mathbf{v}]/\hbar\}$ over all possible configurations satisfying periodic boundary conditions in phase space yields the partition function of the system with external sources

$$Z_0[\mathbf{j}, \mathbf{v}] = \oint \mathcal{D}^d x \mathcal{D}^d p e^{-\mathcal{A}_0[\mathbf{p}, \mathbf{x}; \mathbf{j}, \mathbf{v}]/\hbar}. \quad (3.2)$$

This serves as the generating functional for all correlation functions. The path integral measure is

defined by slicing:

$$\oint \mathcal{D}^d x \mathcal{D}^d p = \lim_{N \rightarrow \infty} \prod_{n=1}^{N+1} \left[\int \frac{d^d x_n d^d p_n}{(2\pi\hbar)^d} \right]. \quad (3.3)$$

The partition function can also be written as an integral over the unnormalized particle density $\tilde{\varrho}_0(\mathbf{x})[\mathbf{j}, \mathbf{v}]$,

$$Z_0[\mathbf{j}, \mathbf{v}] = \int d^d x \tilde{\varrho}_0(\mathbf{x})[\mathbf{j}, \mathbf{v}]. \quad (3.4)$$

The unnormalized particle density $\tilde{\varrho}_0(\mathbf{x})[\mathbf{j}, \mathbf{v}]$ is the diagonal element of the unnormalized density matrix

$$\tilde{\varrho}_0(\mathbf{x}_b, \mathbf{x}_a)[\mathbf{j}, \mathbf{v}] = \int \mathcal{D}'^d x \mathcal{D}^d p e^{-\mathcal{A}_0[\mathbf{p}, \mathbf{x}; \mathbf{j}, \mathbf{v}]/\hbar} \quad (3.5)$$

with the sliced measure

$$\int \mathcal{D}'^d x \mathcal{D}^d p = \lim_{N \rightarrow \infty} \prod_{n=1}^N \left[\int d^d x_n \right] \prod_{n=1}^{N+1} \left[\int \frac{d^d p_n}{(2\pi\hbar)^d} \right]. \quad (3.6)$$

The density matrix is normalized by the partition function (3.2):

$$\varrho_0(\mathbf{x}_b, \mathbf{x}_a)[\mathbf{j}, \mathbf{v}] = \frac{\tilde{\varrho}_0(\mathbf{x}_b, \mathbf{x}_a)[\mathbf{j}, \mathbf{v}]}{Z_0[\mathbf{j}, \mathbf{v}]}. \quad (3.7)$$

For the calculation of the density matrix in the presence of external sources (3.5), it is useful to introduce natural units with $\hbar = \beta = M = 1$, where M is the particle mass. Thus, positions are measured in units of $\sqrt{\hbar^2 \beta / M}$, and the Euclidean time is given as a multiple of $\hbar \beta$.

The action (3.1) can be written in the $2d \times 2d$ matrix form

$$\mathcal{A}_0[\mathbf{p}, \mathbf{x}; \mathbf{j}, \mathbf{v}] = \frac{1}{2} \int_0^1 d\tau \int_0^1 d\tau' \mathbf{w}^T(\tau) S(\tau, \tau') \mathbf{w}(\tau') + \int_0^1 d\tau \mathbf{C}^T(\tau) \mathbf{w}(\tau), \quad (3.8)$$

with $2d$ phase space vectors $\mathbf{w}^T(\tau) = (\mathbf{x}^T(\tau), \mathbf{p}^T(\tau))$ and currents $\mathbf{C}^T(\tau) = (\mathbf{j}^T(\tau), \mathbf{v}^T(\tau))$. The $2d \times 2d$ matrix $S(\tau, \tau')$ is composed as follows:

$$S(\tau, \tau') = \begin{pmatrix} D_{\mathbf{xx}}(\tau, \tau') & D_{\mathbf{xp}}(\tau, \tau') \\ D_{\mathbf{px}}(\tau, \tau') & D_{\mathbf{pp}}(\tau, \tau') \end{pmatrix}. \quad (3.9)$$

Utilizing the invariance of the first term of the action (3.8) under transposing and interchanging τ and τ' , we introduce a symmetrized matrix

$$S^s(\tau, \tau') = \begin{pmatrix} D_{\mathbf{xx}}^s(\tau, \tau') & D_{\mathbf{xp}}^s(\tau, \tau') \\ D_{\mathbf{px}}^s(\tau, \tau') & D_{\mathbf{pp}}^s(\tau, \tau') \end{pmatrix}, \quad (3.10)$$

where the superscript ‘‘s’’ denotes the symmetry $S^s(\tau, \tau') = S^{sT}(\tau', \tau)$. The symmetrized kernels are

$$D_{\mathbf{xx}}^s(\tau, \tau') = \frac{1}{2} [D_{\mathbf{xx}}(\tau, \tau') + D_{\mathbf{xx}}^T(\tau', \tau)], \quad D_{\mathbf{pp}}^s(\tau, \tau') = \frac{1}{2} [D_{\mathbf{pp}}(\tau, \tau') + D_{\mathbf{pp}}^T(\tau', \tau)] \quad (3.11)$$

and satisfy

$$D_{\mathbf{xx}}^s(\tau, \tau') = D_{\mathbf{xx}}^{sT}(\tau', \tau), \quad D_{\mathbf{pp}}^s(\tau, \tau') = D_{\mathbf{pp}}^{sT}(\tau', \tau). \quad (3.12)$$

For the mixed kernels, we have

$$D_{\mathbf{xp}}^s(\tau, \tau') = \frac{1}{2} [D_{\mathbf{xp}}(\tau, \tau') + D_{\mathbf{px}}^T(\tau', \tau)], \quad D_{\mathbf{px}}^s(\tau, \tau') = \frac{1}{2} [D_{\mathbf{px}}(\tau, \tau') + D_{\mathbf{xp}}^T(\tau', \tau)], \quad (3.13)$$

which implies the symmetry

$$D_{\mathbf{px}}^s(\tau, \tau') = D_{\mathbf{xp}}^{sT}(\tau', \tau). \quad (3.14)$$

We will only use the symmetrized kernels in the following sections, where we calculate the path integrals for the unnormalized density matrix (3.5) and the partition function (3.2) in the presence of external sources. For simplicity, we omit the superscript “s” for the symmetrized matrices in the sequel.

By varying the symmetrized action without external sources,

$$\delta \mathcal{A}_0[\mathbf{p}, \mathbf{x}; 0, 0] = 0, \quad (3.15)$$

we find the general Hamiltonian equations of motion

$$\int_0^1 d\tau' [D_{\mathbf{x}\mathbf{x}}(\tau, \tau') \mathbf{x}_{\text{cl}}(\tau') + D_{\mathbf{x}\mathbf{p}}(\tau, \tau') \mathbf{p}_{\text{cl}}(\tau')] = 0, \quad (3.16)$$

$$\int_0^1 d\tau' [D_{\mathbf{p}\mathbf{p}}(\tau, \tau') \mathbf{p}_{\text{cl}}(\tau') + D_{\mathbf{p}\mathbf{x}}(\tau, \tau') \mathbf{x}_{\text{cl}}(\tau')] = 0 \quad (3.17)$$

for the classical paths in phase space $\mathbf{x}_{\text{cl}}(\tau)$ and $\mathbf{p}_{\text{cl}}(\tau)$.

3.2 Density Matrix with External Sources

We now calculate the general path integral (3.5) by a time-slicing procedure and find in particular the generating functional and the two-point correlation functions for the one-dimensional harmonic oscillator.

3.2.1 Calculation of the Phase Space Path Integral

By dividing the time interval $[0, 1]$ into $N + 1$ pieces of length ε , the unnormalized density matrix in the presence of external sources (3.5) can be written as

$$\begin{aligned} \tilde{\varrho}_0(\mathbf{x}_b, \mathbf{x}_a) \mathbf{j}, \mathbf{v} &= \lim_{N \rightarrow \infty} \prod_{n=1}^N \left[\int d^d x_n \right] \prod_{n=1}^{N+1} \left[\int \frac{d^d p_n}{(2\pi)^d} \right] \exp \left[- \sum_{n=1}^N (\mathbf{x}_n \mathbf{j}_n + \mathbf{p}_n \mathbf{v}_n) \right] \\ &\times \exp \left[- \frac{1}{2} \sum_{n,m=1}^{N+1} (\mathbf{x}_n [D_{\mathbf{x}\mathbf{x}}]_{nm} \mathbf{x}_m + 2 \mathbf{x}_n [D_{\mathbf{x}\mathbf{p}}]_{nm} \mathbf{p}_m + \mathbf{p}_n [D_{\mathbf{p}\mathbf{p}}]_{nm} \mathbf{p}_m) \right], \end{aligned} \quad (3.18)$$

where we have absorbed the lattice constant ε in the discrete matrices and currents, respectively. The calculation of the momentum integrals is easily done after quadratic completion and rotation into the diagonal basis of $D_{\mathbf{p}\mathbf{p}}$. In continuum representation, we obtain

$$\begin{aligned} \tilde{\varrho}_0(\mathbf{x}_b, \mathbf{x}_a) \mathbf{j}, \mathbf{v} &= \frac{1}{\sqrt{(2\pi)^d \det D_{\mathbf{p}\mathbf{p}}}} \exp \left[- \frac{1}{2} \int_0^1 d\tau \int_0^1 d\tau' \mathbf{v}^T(\tau) D_{\mathbf{p}\mathbf{p}}^{-1}(\tau, \tau') \mathbf{v}(\tau') \right] \\ &\times \int_{\mathbf{x}(0)=\mathbf{x}_a}^{\mathbf{x}(1)=\mathbf{x}_b} \mathcal{D}_{\text{cs}}^d x \exp \left[- \frac{1}{2} \int_0^1 d\tau \int_0^1 d\tau' \mathbf{x}^T(\tau) G_{\mathbf{x}\mathbf{x}}^{\text{D}}^{-1}(\tau, \tau') \mathbf{x}(\tau') - \int_0^1 d\tau \mathbf{J}^T(\tau) \mathbf{x}(\tau) \right], \end{aligned} \quad (3.19)$$

where the path integral measure in configuration space is

$$\int \mathcal{D}_{\text{cs}}^d x = \lim_{N \rightarrow \infty} \prod_{n=1}^N \left[\int \frac{d^d x_n}{(2\pi)^{d/2}} \right]. \quad (3.20)$$

The expression (3.19) possesses the remarkable property that the current

$$\mathbf{J}(\tau) = \mathbf{j}(\tau) - \int_0^1 d\tau_1 \int_0^1 d\tau_2 D_{\mathbf{x}\mathbf{p}}(\tau, \tau_1) D_{\mathbf{p}\mathbf{p}}^{-1}(\tau_1, \tau_2) \mathbf{v}(\tau_2), \quad (3.21)$$

which linearly couples to the coordinate $\mathbf{x}(\tau)$, contains a term with $\mathbf{v}(\tau)$ originally being coupled to the momentum. It is a general property of such functionals that currents coupling to momenta can always be considered as new currents, which couple to positions [17].

The other new quantity, which has been introduced in Eq. (3.19), is

$$G_{\mathbf{xx}}^{\mathbf{D}^{-1}}(\tau, \tau') = D_{\mathbf{xx}}(\tau, \tau') - \int_0^1 d\tau_1 \int_0^1 d\tau_2 D_{\mathbf{xp}}(\tau, \tau_1) D_{\mathbf{pp}}^{-1}(\tau_1, \tau_2) D_{\mathbf{px}}(\tau_2, \tau'). \quad (3.22)$$

Enclosed by coordinates $\mathbf{x}(\tau)$ in the configuration space path integral appearing in Eq. (3.19), the quantity $G_{\mathbf{xx}}^{\mathbf{D}^{-1}}(\tau, \tau')$ is interpreted as a new kernel. It maps the Green function $G_{x_i x_j}^{\mathbf{D}}(\tau, \tau')$ to a δ function:

$$\sum_{j=1}^d \int_0^1 d\tau G_{x_i x_j}^{\mathbf{D}^{-1}}(\tau_1, \tau) G_{x_j x_k}^{\mathbf{D}}(\tau, \tau_2) = \delta_{ik} \delta(\tau_1 - \tau_2), \quad (3.23)$$

where the Kronecker symbol δ_{ij} is defined as

$$\delta_{ij} = \begin{cases} 1, & i = j, \\ 0, & i \neq j. \end{cases} \quad (3.24)$$

The δ function has the property

$$\int_0^1 d\tau f(\tau) \delta(\tau - \tau') = f(\tau'), \quad \tau' \in (0, 1), \quad (3.25)$$

for any smooth test function $f(\tau)$. With Eqs. (3.22) and (3.23), we write the matrix of Green functions as

$$G_{\mathbf{xx}}^{\mathbf{D}}(\tau, \tau') = \left[D_{\mathbf{xx}}(\tau, \tau') - \int_0^1 d\tau_1 \int_0^1 d\tau_2 D_{\mathbf{xp}}(\tau, \tau_1) D_{\mathbf{pp}}^{-1}(\tau_1, \tau_2) D_{\mathbf{px}}(\tau_2, \tau') \right]^{-1}. \quad (3.26)$$

Since the end points of the paths are fixed, $\mathbf{x}(0) = \mathbf{x}_a$ and $\mathbf{x}(1) = \mathbf{x}_b$, fluctuations are vanishing at these edges, and the Green function $G_{x_i x_j}^{\mathbf{D}}(\tau, \tau')$ must obey Dirichlet boundary conditions:

$$G_{x_i x_j}^{\mathbf{D}}(0, \tau') = G_{x_i x_j}^{\mathbf{D}}(1, \tau') = 0, \quad G_{x_i x_j}^{\mathbf{D}}(\tau, 0) = G_{x_i x_j}^{\mathbf{D}}(\tau, 1) = 0. \quad (3.27)$$

The calculation of the configuration space path integral in Eq. (3.19),

$$\langle \mathbf{x}_b | 1 | \mathbf{x}_a 0 \rangle [\mathbf{J}] = \int_{\mathbf{x}(0)=\mathbf{x}_a}^{\mathbf{x}(1)=\mathbf{x}_b} \mathcal{D}_{\text{cs}}^d e^{-\mathcal{A}_{\text{cs}}[\mathbf{x}; \mathbf{J}]/\hbar}, \quad (3.28)$$

with the action in configuration space

$$\mathcal{A}_{\text{cs}}[\mathbf{x}; \mathbf{J}] = \frac{\hbar}{2} \int_0^1 d\tau \int_0^1 d\tau' \mathbf{x}^T(\tau) G_{\mathbf{xx}}^{\mathbf{D}^{-1}}(\tau, \tau') \mathbf{x}(\tau') + \int_0^1 d\tau \mathbf{J}^T(\tau) \mathbf{x}(\tau), \quad (3.29)$$

is done on usual footing. We decompose the path $\mathbf{x}(\tau)$ into a classical part $\mathbf{x}_{\text{cl}}(\tau)$ and the fluctuation term $\delta\mathbf{x}(\tau)$,

$$\mathbf{x}(\tau) = \mathbf{x}_{\text{cl}}(\tau) + \delta\mathbf{x}(\tau), \quad (3.30)$$

where the fluctuations may vanish at the boundaries, $\delta\mathbf{x}(0) = \delta\mathbf{x}(1) = 0$. The variation of the action (3.29) in the absence of the external current $\mathbf{J}(\tau)$ vanishes for the classical path. Performing this variation, we obtain a relation, which we need for the following considerations:

$$\begin{aligned} \delta\mathcal{A}_{\text{cs}}[\mathbf{x}_{\text{cl}}; \mathbf{0}] &= \frac{1}{2} \int_0^1 d\tau \int_0^1 d\tau' \left[\delta\mathbf{x}^T(\tau) G_{\mathbf{xx}}^{\mathbf{D}^{-1}}(\tau, \tau') \mathbf{x}_{\text{cl}}(\tau') + \mathbf{x}_{\text{cl}}^T(\tau) G_{\mathbf{xx}}^{\mathbf{D}^{-1}}(\tau, \tau') \delta\mathbf{x}(\tau') \right] \\ &= \int_0^1 d\tau \int_0^1 d\tau' \delta\mathbf{x}^T(\tau) G_{\mathbf{xx}}^{\mathbf{D}^{-1}}(\tau, \tau') \mathbf{x}_{\text{cl}}(\tau') = 0. \end{aligned} \quad (3.31)$$

Here we have utilized in the last line the symmetry of $G_{\mathbf{xx}}^{\mathbf{D}^{-1}}(\tau, \tau')$, which is obvious from the definition (3.22) and the properties (3.12) and (3.14). From (3.31), we read off the Euler–Lagrange equations of motion

$$\int_0^1 d\tau' G_{\mathbf{xx}}^{\mathbf{D}^{-1}}(\tau, \tau') \mathbf{x}_{\text{cl}}(\tau') = 0. \quad (3.32)$$

Inserting now the decomposition (3.30) into the action (3.29), considering the vanishing of the coupling of fluctuations and classical path from the last line in (3.31), and acknowledging that the measure is invariant under the translation (3.30), $\mathcal{D}_{\text{cs}}^d x = \mathcal{D}_{\text{cs}}^d \delta x$, the functional (3.28) can be expressed as

$$\begin{aligned} (\mathbf{x}_b | \mathbf{x}_a 0) [\mathbf{J}] &= \exp \left\{ \frac{1}{2} \int_0^1 d\tau \int_0^1 d\tau' \left[\mathbf{J}^T(\tau) G_{\mathbf{xx}}^{\mathbf{D}}(\tau, \tau') \mathbf{J}(\tau') - \mathbf{x}_{\text{cl}}^T(\tau) G_{\mathbf{xx}}^{\mathbf{D}^{-1}}(\tau, \tau') \mathbf{x}_{\text{cl}}(\tau') \right] \right\} \\ &\times \exp \left\{ - \int_0^1 d\tau \mathbf{J}^T(\tau) \mathbf{x}_{\text{cl}}(\tau) \right\} \int_{\delta \mathbf{x}(0)=0}^{\delta \mathbf{x}(1)=0} \mathcal{D}_{\text{cs}}^d \delta x \exp \left\{ - \frac{1}{2} \int_0^1 d\tau \int_0^1 d\tau' \right. \\ &\times \left. \left[\delta \mathbf{x}^T(\tau) + \int_0^1 d\tau_1 \mathbf{J}^T(\tau_1) G_{\mathbf{xx}}^{\mathbf{D}}(\tau_1, \tau) \right] G_{\mathbf{xx}}^{\mathbf{D}^{-1}}(\tau, \tau') \left[\delta \mathbf{x}(\tau') + \int_0^1 d\tau_2 G_{\mathbf{xx}}^{\mathbf{D}}(\tau', \tau_2) \mathbf{J}(\tau_2) \right] \right\}. \end{aligned} \quad (3.33)$$

The path integral over the fluctuations is a constant, since it is independent of the end points \mathbf{x}_a and \mathbf{x}_b . For convenience, we introduce the new variable

$$\mathbf{y}(\tau) = \delta \mathbf{x}(\tau) + \int_0^1 d\tau' G_{\mathbf{xx}}^{\mathbf{D}}(\tau, \tau') \mathbf{J}(\tau'), \quad (3.34)$$

which also vanishes at the boundary, $\mathbf{y}(0) = \mathbf{y}(1) = 0$, since the Green functions $G_{\mathbf{xx}}^{\mathbf{D}}(\tau, \tau')$ satisfy the Dirichlet boundary conditions (3.27). The measure of the path integral over the fluctuations remains unchanged, $\mathcal{D}_{\text{cs}}^d y = \mathcal{D}_{\text{cs}}^d \delta x$, and the calculation of this path integral is simply done, e.g. in discrete space, yielding

$$\int_{\mathbf{y}(0)=0}^{\mathbf{y}(1)=0} \mathcal{D}_{\text{cs}}^d y \exp \left[- \frac{1}{2} \int_0^1 d\tau \int_0^1 d\tau' \mathbf{y}^T(\tau) G_{\mathbf{xx}}^{\mathbf{D}^{-1}}(\tau, \tau') \mathbf{y}(\tau') \right] = \frac{1}{\sqrt{\det G_{\mathbf{xx}}^{\mathbf{D}^{-1}}}}. \quad (3.35)$$

Combining the results (3.19), (3.33), and (3.35), we obtain the density matrix in the presence of external sources

$$\begin{aligned} \tilde{\varrho}_0(\mathbf{x}_b, \mathbf{x}_a) [\mathbf{j}, \mathbf{v}] &= \left(\frac{M}{2\pi\hbar^2\beta} \right)^{d/2} \frac{1}{\sqrt{\det D_{\mathbf{pp}} \det G_{\mathbf{xx}}^{\mathbf{D}^{-1}}}} \exp \left\{ - \frac{1}{\hbar} \int_0^{\hbar\beta} d\tau [\mathbf{j}^T(\tau) \mathbf{x}_{\text{cl}}(\tau) + \mathbf{v}^T(\tau) \mathbf{p}_{\text{cl}}(\tau)] \right\} \\ &\times \exp \left[- \frac{1}{2} \int_0^{\hbar\beta} d\tau \int_0^{\hbar\beta} d\tau' \mathbf{x}_{\text{cl}}^T(\tau) G_{\mathbf{xx}}^{\mathbf{D}^{-1}}(\tau, \tau') \mathbf{x}_{\text{cl}}(\tau') \right] \\ &\times \exp \left\{ \frac{1}{2\hbar^2} \int_0^{\hbar\beta} d\tau \int_0^{\hbar\beta} d\tau' \left[\mathbf{j}^T(\tau) G_{\mathbf{xx}}^{\mathbf{D}}(\tau, \tau') \mathbf{j}(\tau') + \mathbf{j}^T(\tau) G_{\mathbf{xp}}^{\mathbf{D}}(\tau, \tau') \mathbf{v}(\tau') \right. \right. \\ &\left. \left. + \mathbf{v}^T(\tau) G_{\mathbf{px}}^{\mathbf{D}}(\tau, \tau') \mathbf{j}(\tau') + \mathbf{v}^T(\tau) G_{\mathbf{pp}}^{\mathbf{D}}(\tau, \tau') \mathbf{v}(\tau') \right] \right\}, \end{aligned} \quad (3.36)$$

where we have reused the standard units. In order to prevent complications, the determinants shall be treated as dimensionless quantities here. For this reason, we have already extracted the dimension-carrying prefactor $(M/\hbar^2\beta)^{d/2}$. As a rule, the determinants are calculated with $\hbar = \beta = M = 1$. At the end, powers of \hbar , β , and M are multiplied to the determinant to make it dimensionless.

In (3.36), we further utilized the relation

$$\mathbf{p}_{\text{cl}}(\tau) = - \int_0^{\hbar\beta} d\tau_1 \int_0^{\hbar\beta} d\tau_2 D_{\mathbf{pp}}^{-1}(\tau, \tau_1) D_{\mathbf{px}}(\tau_1, \tau_2) \mathbf{x}_{\text{cl}}(\tau_2), \quad (3.37)$$

which is a direct consequence of the Hamiltonian equation of motion (3.17), when solved with respect to $\mathbf{p}_{\text{cl}}(\tau)$.

Additionally to $G_{\mathbf{xx}}^{\text{D}}(\tau, \tau')$, defined by (3.26), we have introduced the $d \times d$ matrices

$$G_{\mathbf{xp}}^{\text{D}}(\tau, \tau') = - \int_0^{\hbar\beta} d\tau_1 \int_0^{\hbar\beta} d\tau_2 G_{\mathbf{xx}}^{\text{D}}(\tau, \tau_1) D_{\mathbf{xp}}(\tau_1, \tau_2) D_{\mathbf{pp}}^{-1}(\tau_2, \tau'), \quad (3.38)$$

$$\begin{aligned} G_{\mathbf{px}}^{\text{D}}(\tau, \tau') &= [G_{\mathbf{xp}}^{\text{D}}]^T(\tau', \tau) \\ &= - \int_0^{\hbar\beta} d\tau_1 \int_0^{\hbar\beta} d\tau_2 D_{\mathbf{pp}}^{-1}(\tau, \tau_1) D_{\mathbf{px}}(\tau_1, \tau_2) G_{\mathbf{xx}}^{\text{D}}(\tau_2, \tau'), \end{aligned} \quad (3.39)$$

$$\begin{aligned} G_{\mathbf{pp}}^{\text{D}}(\tau, \tau') &= D_{\mathbf{pp}}^{-1}(\tau, \tau') + \int_0^{\hbar\beta} d\tau_1 \cdots \int_0^{\hbar\beta} d\tau_4 \\ &\quad \times D_{\mathbf{pp}}^{-1}(\tau, \tau_1) D_{\mathbf{px}}(\tau_1, \tau_2) G_{\mathbf{xp}}^{\text{D}}(\tau_2, \tau_3) D_{\mathbf{xp}}(\tau_3, \tau_4) D_{\mathbf{pp}}^{-1}(\tau_4, \tau'). \end{aligned} \quad (3.40)$$

These expressions are equivalent to position- and/or momentum-dependent two-point correlation functions, as we show in Section 3.2.3. Before embarking to this, however, we will first check the density matrix functional (3.36) for a simple example, the one-dimensional harmonic oscillator.

3.2.2 Example: Density Matrix of the One-Dimensional Harmonic Oscillator with Sources

The harmonic oscillator is usually a pretty good system for checking a general theory, since its exact quantum statistical properties are well known. Due to the Gaussian type of the Boltzmann factor, the path integrals for density matrix and partition function are simply solved. Additionally, this system is nontrivial in a sense that it possesses a nonvanishing interaction.

In what follows, we calculate the density matrix functional for the one-dimensional case, since it already contains the interesting properties that we would like to point out, e.g. the two-point correlation functions. The action of this system in the presence of external sources $j(\tau)$ and $v(\tau)$ reads

$$\mathcal{A}_\omega[p, x; j, v] = \int_0^{\hbar\beta} d\tau \left\{ -ip(\tau) \frac{d}{d\tau} x(\tau) + \frac{1}{2} \left[\frac{p^2(\tau)}{M} + M\omega^2 x^2(\tau) \right] + j(\tau)x(\tau) + v(\tau)p(\tau) \right\}. \quad (3.41)$$

By comparing this action with the general one introduced in Eq. (3.1), we identify

$$\begin{aligned} D_{xx}(\tau, \tau') &= \frac{M}{\hbar} \omega^2 \delta(\tau, \tau'), \quad D_{pp}(\tau, \tau') = \frac{1}{\hbar M} \delta(\tau, \tau'), \quad D_{xp}(\tau, \tau') = \frac{i}{\hbar} \frac{\partial}{\partial \tau} \delta(\tau, \tau'), \\ D_{px}(\tau, \tau') &= -\frac{i}{\hbar} \frac{\partial}{\partial \tau} \delta(\tau, \tau') + \frac{i}{\hbar} \delta(\tau, \tau') [\delta(\hbar\beta, \tau) - \delta(\tau, 0)]. \end{aligned} \quad (3.42)$$

The δ functions with two arguments act as the usual δ function with the exception of time translational invariance. It is a consequence of the Dirichlet boundary conditions the paths must satisfy due to the fixing of the end points. This will become clear after expanding the fluctuations into a complete set of orthonormal functions and is shown later on.

The symmetric splitting of the first term in the action (3.41) is necessary to ensure the symmetry of the matrix $S(\tau, \tau')$, defined in Eq. (3.9). This requires that the nondiagonal elements D_{xp} and D_{px} of S must be transposed to one another.¹ It is a nice problem to show what the transpose of the operator $i\partial/\partial\tau$ is. It is well known from quantum mechanics that the operator

$$\hat{H} \rightarrow i \frac{\partial}{\partial \tau} \quad (3.43)$$

¹The second and third terms of $D_{px}(\tau, \tau')$ appear since operators with derivatives yield boundary terms: $\int_0^{\hbar\beta} d\tau f(\tau) \dot{g}(\tau) = f(\tau)g(\tau)|_{\tau=0}^{\tau=\hbar\beta} - \int_0^{\hbar\beta} d\tau \dot{g}(\tau)f(\tau)$. If $f(\tau)$ and $g(\tau)$ have periodic or Dirichlet boundary conditions, these additional terms vanish, and $D_{px}(\tau, \tau')$ is exactly the transpose of $D_{xp}(\tau, \tau')$.

is Hermitian, $\hat{H} = \hat{H}^\dagger$. This means that any representation of this operator is identical to its transpose with complex conjugated elements. With (3.43), we obtain

$$i\frac{\partial}{\partial\tau} = \left(i\frac{\partial}{\partial\tau}\right)^\dagger = \left[\left(i\frac{\partial}{\partial\tau}\right)^*\right]^T = -i\left(\frac{\partial}{\partial\tau}\right)^T \implies \left(\frac{\partial}{\partial\tau}\right)^T = -\frac{\partial}{\partial\tau}. \quad (3.44)$$

This explains the different signs of D_{xp} and the first term of D_{px} in (3.42).

The first quantity we shall calculate is $G_{xx,\omega}^{\text{D}-1}(\tau, \tau')$, defined in Eq. (3.22). Inserting the identifications from (3.42) into (3.22) yields

$$G_{xx,\omega}^{\text{D}-1}(\tau, \tau') = \frac{M}{\hbar} [\delta(\hbar\beta - \tau) - \delta(\tau)] \frac{\partial}{\partial\tau} \delta(\tau - \tau') - \frac{M}{\hbar} \left(\frac{\partial^2}{\partial\tau^2} - \omega^2\right) \delta(\tau - \tau'). \quad (3.45)$$

Thus, calculating the classical action of the density matrix (3.36) for the one-dimensional harmonic oscillator gives the known result (without external currents):

$$\begin{aligned} \mathcal{A}_{\omega,\text{cl}}[x] &= \frac{\hbar}{2} \int_0^{\hbar\beta} d\tau \int_0^{\hbar\beta} d\tau' x_{\text{cl}}(\tau) G_{xx,\omega}^{\text{D}-1}(\tau, \tau') x_{\text{cl}}(\tau') \\ &= \frac{M}{2} \left[x_{\text{cl}}(\hbar\beta) \dot{x}_{\text{cl}}(\hbar\beta) - x_{\text{cl}}(0) \dot{x}_{\text{cl}}(0) - \int_0^{\hbar\beta} d\tau x_{\text{cl}}(\tau) \left(\frac{\partial^2}{\partial\tau^2} - \omega^2\right) x_{\text{cl}}(\tau) \right] \\ &= \int_0^{\hbar\beta} d\tau \left[\frac{1}{2} M \dot{x}_{\text{cl}}^2(\tau) + \frac{1}{2} M \omega^2 x_{\text{cl}}^2(\tau) \right]. \end{aligned} \quad (3.46)$$

Since the classical path for the harmonic oscillator is known to be [4, Chap. 2]

$$x_{\text{cl}}(\tau) = \frac{1}{\sinh \hbar\beta\omega} [x_b \sinh \omega\tau + x_a \sinh \omega(\hbar\beta - \tau)], \quad (3.47)$$

the classical action (3.46) becomes the usual one

$$\mathcal{A}_{\omega,\text{cl}}(x_b, x_a) = \frac{M\omega}{2 \sinh \hbar\beta\omega} [(x_a^2 + x_b^2) \cosh \hbar\beta\omega - 2x_a x_b]. \quad (3.48)$$

Now we consider the Green function $G_{xx,\omega}^{\text{D}}(\tau, \tau')$ given by Eq. (3.26). Due to the vanishing of the fluctuations $\delta x(\tau)$ at the fixed end points of the path, this Green function is required to satisfy Dirichlet boundary conditions (3.27). The fluctuations can be expanded into a complete set of orthonormal functions [4, Chap. 3],

$$\delta x_n(\tau) = \frac{1}{\sqrt{\hbar\beta}} \sin \nu_n \tau, \quad (3.49)$$

with

$$\nu_n = \frac{\pi n}{\hbar\beta} \quad (3.50)$$

being half the Matsubara frequencies defined in Eq. (2.13).

The completeness relation is then

$$\delta(\tau, \tau') = \sum_{n=-\infty}^{\infty} \delta x_n(\tau) \delta x_n(\tau') = \frac{1}{\hbar\beta} \sum_{n=-\infty}^{\infty} \sin \nu_n \tau \sin \nu_n \tau' = \frac{2}{\hbar\beta} \sum_{n=1}^{\infty} \sin \nu_n \tau \sin \nu_n \tau'. \quad (3.51)$$

Here we see the necessity to introduce the δ function with two arguments, since the expression on the right-hand side is not invariant under time translations. Substituting the δ functions in expression (3.45) by the completeness relation (3.51), it turns out that the boundary terms vanish. Thus we obtain the decomposition

$$G_{xx,\omega}^{\text{D}-1}(\tau, \tau') = \frac{2}{\hbar\beta} \sum_{n=1}^{\infty} \frac{M}{\hbar} (\omega^2 + \nu_n^2) \sin \nu_n \tau \sin \nu_n \tau'. \quad (3.52)$$

Inverting the kernel yields the Green function in Fourier space

$$G_{xx,\omega}^D(\nu_n) = \frac{\hbar}{M} \frac{1}{\omega^2 + \nu_n^2}. \quad (3.53)$$

After performing the Fourier back transformation, we obtain the Green function for the harmonic oscillator with fixed end points

$$G_{xx,\omega}^D(\tau, \tau') = \frac{\hbar}{2M\omega \sinh \hbar\beta\omega} [\cosh \omega(|\tau - \tau'| - \hbar\beta) - \cosh \omega(\tau + \tau' - \hbar\beta)]. \quad (3.54)$$

The calculation of the two-point functions (3.38)–(3.40) is straightforward, since these can be derived from $G_{xx,\omega}^D(\tau, \tau')$. Inserting (3.42) into (3.38) leads to

$$\begin{aligned} G_{xp,\omega}^D(\tau, \tau') &= - \int_0^{\hbar\beta} d\tau_1 \int_0^{\hbar\beta} d\tau_2 G_{xx,\omega}^D(\tau, \tau_1) \frac{i}{\hbar} \frac{\partial}{\partial \tau_1} \delta(\tau_1, \tau_2) \hbar M \delta(\tau_2, \tau') \\ &= -iM \int_0^{\hbar\beta} d\tau_1 G_{xx,\omega}^D(\tau, \tau_1) \frac{\partial}{\partial \tau_1} \delta(\tau_1, \tau') = iM \frac{\partial}{\partial \tau'} G_{xx,\omega}^D(\tau, \tau'). \end{aligned} \quad (3.55)$$

In the last line we have carried out a partial integration, where the boundary term vanishes due to the Dirichlet boundary conditions (3.27). The derivative with respect to the second argument of the Green function (3.54) is easily performed and yields

$$\begin{aligned} G_{xp,\omega}^D(\tau, \tau') &= -\frac{i\hbar}{2 \sinh \hbar\beta\omega} \frac{1}{\hbar} [\Theta(\tau - \tau') \sinh \omega(\tau - \tau' - \hbar\beta) - \Theta(\tau' - \tau) \sinh \omega(\tau' - \tau - \hbar\beta) \\ &\quad + \sinh \omega(\tau + \tau' - \hbar\beta)]. \end{aligned} \quad (3.56)$$

As the explicit calculation of (3.39) shows, it is

$$G_{px,\omega}^D(\tau, \tau') = iM \frac{\partial}{\partial \tau} G_{xx,\omega}^D(\tau, \tau'). \quad (3.57)$$

The difference between (3.55) and (3.57) is that the derivative now acts on the first argument of the Green function $G_{xx,\omega}^D(\tau, \tau')$. Thus, we obtain

$$\begin{aligned} G_{px,\omega}^D(\tau, \tau') &= \frac{i\hbar}{2 \sinh \hbar\beta\omega} \frac{1}{\hbar} [\Theta(\tau - \tau') \sinh \omega(\tau - \tau' - \hbar\beta) - \Theta(\tau' - \tau) \sinh \omega(\tau' - \tau - \hbar\beta) \\ &\quad - \sinh \omega(\tau + \tau' - \hbar\beta)] = G_{xp,\omega}^D(\tau', \tau). \end{aligned} \quad (3.58)$$

Calculating (3.40) exposes no new aspects and yields

$$\begin{aligned} G_{pp,\omega}^D(\tau, \tau') &= \hbar M \delta(\tau, \tau') - M^2 \frac{\partial^2}{\partial \tau \partial \tau'} G_{xx,\omega}^D(\tau, \tau') \\ &= \frac{M\hbar\omega}{2 \sinh \hbar\beta\omega} [\cosh \omega(|\tau - \tau'| - \hbar\beta) + \cosh \omega(\tau + \tau' - \hbar\beta)]. \end{aligned} \quad (3.59)$$

The sole task remaining to be done to specify the density matrix functional (3.36) for the one-dimensional harmonic oscillator is the calculation of the determinants. Since we know that the prefactor $\sqrt{M/\hbar^2\beta}$ carries the complete physical dimension of the density matrix, it is useful, for evaluating the determinants, to return to dimensionless natural variables by setting $M = \hbar = \beta = 1$. Determining the determinant of D_{pp} is quite simple and yields $\det D_{pp} = 1$. This is a simple consequence that D_{pp} is unity in Fourier space and an infinite product of unity yields again unity. The calculation of the other determinant is much more involved and shall be presented in detail in the following. With the Fourier representation (3.52) of $G_{xx,\omega}^{D-1}$, the appropriate fluctuation factor of (3.36) can be written as

$$\left[\det G_{xx,\omega}^{D-1} \right]^{-1/2} = \exp \left(-\frac{1}{2} \text{Tr} \ln G_{xx,\omega}^{D-1} \right) = \exp \left[-\frac{1}{2} \int_0^1 d\tau \, 2 \sum_{n=1}^{\infty} \ln(\omega^2 + \nu_n^2) \sin^2 \nu_n \tau \right]. \quad (3.60)$$

The integration of the sine-squared over τ is easily done, $\int_0^1 d\tau \sin^2 \nu_m \tau = 1/2$, and Eq. (3.60) becomes

$$\left[\det G_{xx,\omega}^{\text{D}-1} \right]^{-1/2} = \exp \left\{ -\frac{1}{2} \ln \prod_{n=1}^{\infty} [\omega^2 + (\pi n)^2] \right\}. \quad (3.61)$$

Obviously, the product diverges, but this divergence is not physical. A lattice calculation would have proved the finiteness of the determinant [4, Chap. 2]. By regularizing the expression within the product with respect to the free-particle Green function, we obtain

$$\prod_{n=1}^{\infty} [\omega^2 + (\pi n)^2] \implies \prod_{n=1}^{\infty} \left[\frac{\omega^2 + (\pi n)^2}{(\pi n)^2} \right] = \prod_{n=1}^{\infty} \left[1 + \frac{\omega^2}{(\pi n)^2} \right] = \frac{1}{\omega} \sinh \omega. \quad (3.62)$$

Inserting this result into (3.61), we eventually find

$$\left[\det G_{xx,\omega}^{\text{D}-1} \right]^{-1/2} = \sqrt{\frac{\hbar\beta\omega}{\sinh \hbar\beta\omega}}, \quad (3.63)$$

with physical units.

Thus we have calculated the density matrix of the one-dimensional harmonic oscillator in the presence of external sources, with the result [17]

$$\begin{aligned} \tilde{\varrho}_\omega(x_b, x_a)[j, v] &= \sqrt{\frac{M\omega}{2\pi\hbar \sinh \hbar\beta\omega}} \exp \left\{ -\frac{M\omega}{2\hbar \sinh \hbar\beta\omega} [(x_a^2 + x_b^2) \cosh \hbar\beta\omega - 2x_a x_b] \right\} \\ &\times \exp \left\{ -\frac{1}{\hbar \sinh \hbar\beta\omega} \int_0^{\hbar\beta} d\tau \left[j(\tau) + iMv(\tau) \frac{\partial}{\partial \tau} \right] [x_b \sinh \omega \tau + x_a \sinh \omega (\hbar\beta - \tau)] \right\} \\ &\times \exp \left\{ \frac{1}{2\hbar^2} \int_0^{\hbar\beta} d\tau \int_0^{\hbar\beta} d\tau' \left[j(\tau) G_{xx,\omega}^{\text{D}}(\tau, \tau') j(\tau') + j(\tau) G_{xp,\omega}^{\text{D}}(\tau, \tau') v(\tau') \right. \right. \\ &\left. \left. + v(\tau) G_{px,\omega}^{\text{D}}(\tau, \tau') j(\tau') + v(\tau) G_{pp,\omega}^{\text{D}}(\tau, \tau') v(\tau') \right] \right\}, \quad (3.64) \end{aligned}$$

where the two-point functions are given by (3.54), (3.56), (3.58), and (3.59). For $j(\tau) = v(\tau) = 0$, Eq. (3.64) reduces to the well-known expression for the density matrix of the one-dimensional harmonic oscillator.

3.2.3 Expectation Values and Correlation Functions

We usually define expectation values as

$$\langle \dots \rangle^{\mathbf{x}_b, \mathbf{x}_a} = \tilde{\varrho}_0^{-1}(\mathbf{x}_b, \mathbf{x}_a) \int \mathcal{D}'^d x \mathcal{D}^d p \dots e^{-\mathcal{A}_0[\mathbf{p}, \mathbf{x}]/\hbar}, \quad (3.65)$$

with the action (3.1) but vanishing currents,

$$\mathcal{A}_0[\mathbf{p}, \mathbf{x}] \equiv \mathcal{A}_0[\mathbf{p}, \mathbf{x}; 0, 0]. \quad (3.66)$$

The expectation values are normalized with respect to the density matrix (3.36) with vanishing currents,

$$\tilde{\varrho}_0(\mathbf{x}_b, \mathbf{x}_a) \equiv \tilde{\varrho}_0(\mathbf{x}_b, \mathbf{x}_a)[0, 0], \quad (3.67)$$

which ensures $\langle 1 \rangle^{\mathbf{x}_b, \mathbf{x}_a} = 1$. For the following consideration, however, it is useful to reintroduce the currents as artificial quantities. If the expectation value of a polynomial function consisting of powers

of x and p shall be evaluated, one can apply functional derivatives with respect to these currents. Such derivatives act as follows:

$$\frac{\delta}{\delta z(\tau)} \int d\tau' f(z(\tau'), u(\tau')) = \int d\tau' \frac{\partial f(z(\tau'), u(\tau'))}{\partial z(\tau')} \delta(\tau - \tau') = \frac{\partial f(z(\tau), u(\tau))}{\partial z(\tau)}. \quad (3.68)$$

Applying, for example, to the action (3.1) a functional derivative with respect to $\mathbf{j}(\tau)$ yields:

$$\frac{\delta}{\delta \mathbf{j}^T(\tau)} \mathcal{A}_0[\mathbf{p}, \mathbf{x}; \mathbf{j}, \mathbf{v}] = \mathbf{x}(\tau). \quad (3.69)$$

Analogously, one obtains when differentiating with respect to $\mathbf{v}(\tau)$:

$$\frac{\delta}{\delta \mathbf{v}^T(\tau)} \mathcal{A}_0[\mathbf{p}, \mathbf{x}; \mathbf{j}, \mathbf{v}] = \mathbf{p}(\tau). \quad (3.70)$$

We can use this recovery of \mathbf{x} and \mathbf{p} to formulate a redefinition of expectation values for polynomial quantities, e.g.

$$\langle x_k^n(\tau) p_l^m(\tau') \rangle^{\mathbf{x}_b, \mathbf{x}_a} = \tilde{\varrho}_0^{-1}(\mathbf{x}_b, \mathbf{x}_a) (-\hbar)^{n+m} \prod_{i=1}^n \left[\frac{\delta}{\delta j_k(\tau)} \right] \prod_{i=1}^m \left[\frac{\delta}{\delta v_l(\tau')} \right] \tilde{\varrho}_0(\mathbf{x}_b, \mathbf{x}_a) [\mathbf{j}, \mathbf{v}] \Big|_{\mathbf{j}=\mathbf{v}=0}. \quad (3.71)$$

In the following, we specify some values for (n, m) , where n denotes the overall power of x and m that of p , to obtain the lowest-order correlations. For $(1, 0)$, we obtain the expectation value of $\mathbf{x}(\tau)$ by applying to the density matrix functional (3.36) a single functional derivative with respect to $\mathbf{j}(\tau)$ and setting the currents to zero thereafter:

$$\langle \mathbf{x}(\tau) \rangle^{\mathbf{x}_b, \mathbf{x}_a} = -\hbar \tilde{\varrho}_0^{-1}(\mathbf{x}_b, \mathbf{x}_a) \frac{\delta}{\delta \mathbf{j}^T(\tau)} \tilde{\varrho}_0(\mathbf{x}_b, \mathbf{x}_a) [\mathbf{j}, \mathbf{v}] \Big|_{\mathbf{j}=\mathbf{v}=0} = \mathbf{x}_{\text{cl}}(\tau). \quad (3.72)$$

Thus, the expectation value of $\mathbf{x}(\tau)$ is simply identical with the classical path. Evaluating the case $(0, 1)$, we obtain the expectation value of the momentum $\mathbf{p}(\tau)$:

$$\langle \mathbf{p}(\tau) \rangle^{\mathbf{x}_b, \mathbf{x}_a} = -\hbar \tilde{\varrho}_0^{-1}(\mathbf{x}_b, \mathbf{x}_a) \frac{\delta}{\delta \mathbf{v}^T(\tau)} \tilde{\varrho}_0(\mathbf{x}_b, \mathbf{x}_a) [\mathbf{j}, \mathbf{v}] \Big|_{\mathbf{j}=\mathbf{v}=0} = \mathbf{p}_{\text{cl}}(\tau). \quad (3.73)$$

Calculating $(2, 0)$, $(0, 2)$, and $(1, 1)$ yields the two-point correlation functions

$$\begin{aligned} \langle x_k(\tau) x_l(\tau') \rangle^{\mathbf{x}_b, \mathbf{x}_a} &= \hbar^2 \tilde{\varrho}_0^{-1}(\mathbf{x}_b, \mathbf{x}_a) \frac{\delta^2}{\delta j_k(\tau) \delta j_l(\tau')} \tilde{\varrho}_0(\mathbf{x}_b, \mathbf{x}_a) [\mathbf{j}, \mathbf{v}] \Big|_{\mathbf{j}=\mathbf{v}=0} \\ &= G_{x_k x_l}^{\text{D}}(\tau, \tau') + x_{\text{cl},k}(\tau) x_{\text{cl},l}(\tau'), \end{aligned} \quad (3.74)$$

$$\begin{aligned} \langle p_k(\tau) p_l(\tau') \rangle^{\mathbf{x}_b, \mathbf{x}_a} &= \hbar^2 \tilde{\varrho}_0^{-1}(\mathbf{x}_b, \mathbf{x}_a) \frac{\delta^2}{\delta v_k(\tau) \delta v_l(\tau')} \tilde{\varrho}_0(\mathbf{x}_b, \mathbf{x}_a) [\mathbf{j}, \mathbf{v}] \Big|_{\mathbf{j}=\mathbf{v}=0} \\ &= G_{p_k p_l}^{\text{D}}(\tau, \tau') + p_{\text{cl},k}(\tau) p_{\text{cl},l}(\tau'), \end{aligned}$$

$$\begin{aligned} \langle x_k(\tau) p_l(\tau') \rangle^{\mathbf{x}_b, \mathbf{x}_a} &= \hbar^2 \tilde{\varrho}_0^{-1}(\mathbf{x}_b, \mathbf{x}_a) \frac{\delta^2}{\delta j_k(\tau) \delta v_l(\tau')} \tilde{\varrho}_0(\mathbf{x}_b, \mathbf{x}_a) [\mathbf{j}, \mathbf{v}] \Big|_{\mathbf{j}=\mathbf{v}=0} \\ &= G_{x_k p_l}^{\text{D}}(\tau, \tau') + x_{\text{cl},k}(\tau) p_{\text{cl},l}(\tau'). \end{aligned} \quad (3.75)$$

From Eq. (3.39) follows that the latter expectation value can be used to identify

$$\begin{aligned} \langle p_k(\tau) x_l(\tau') \rangle^{\mathbf{x}_b, \mathbf{x}_a} &= \hbar^2 \tilde{\varrho}_0^{-1}(\mathbf{x}_b, \mathbf{x}_a) \frac{\delta^2}{\delta v_k(\tau) \delta j_l(\tau')} \tilde{\varrho}_0(\mathbf{x}_b, \mathbf{x}_a) [\mathbf{j}, \mathbf{v}] \Big|_{\mathbf{j}=\mathbf{v}=0} \\ &= G_{p_k x_l}^{\text{D}}(\tau, \tau') + p_{\text{cl},k}(\tau) x_{\text{cl},l}(\tau'). \end{aligned} \quad (3.76)$$

Re-expressing the two-point functions with the help of Eqs. (3.72) and (3.73), we obtain

$$\begin{aligned} G_{x_k x_l}^{\text{D}}(\tau, \tau') &= \langle \tilde{x}_k(\tau) \tilde{x}_l(\tau') \rangle^{\mathbf{x}_b, \mathbf{x}_a}, & G_{p_k p_l}^{\text{D}}(\tau, \tau') &= \langle \tilde{p}_k(\tau) \tilde{p}_l(\tau') \rangle^{\mathbf{x}_b, \mathbf{x}_a}, \\ G_{x_k p_l}^{\text{D}}(\tau, \tau') &= \langle \tilde{x}_k(\tau) \tilde{p}_l(\tau') \rangle^{\mathbf{x}_b, \mathbf{x}_a}, & G_{p_k x_l}^{\text{D}}(\tau, \tau') &= \langle \tilde{p}_k(\tau) \tilde{x}_l(\tau') \rangle^{\mathbf{x}_b, \mathbf{x}_a}, \end{aligned} \quad (3.77)$$

with abbreviations

$$\tilde{\mathbf{x}}(\tau) = \mathbf{x}(\tau) - \mathbf{x}_{\text{cl}}(\tau), \quad \tilde{\mathbf{p}}(\tau) = \mathbf{p}(\tau) - \mathbf{p}_{\text{cl}}(\tau). \quad (3.78)$$

Thus, we have identified the elements of the $d \times d$ matrices $G_{\mathbf{x}\mathbf{x}}^{\text{D}}(\tau, \tau')$, $G_{\mathbf{x}\mathbf{p}}^{\text{D}}(\tau, \tau')$, $G_{\mathbf{p}\mathbf{x}}^{\text{D}}(\tau, \tau')$, and $G_{\mathbf{p}\mathbf{p}}^{\text{D}}(\tau, \tau')$, introduced in Eq. (3.36), with appropriate two-point correlation functions.

3.3 Smearing Formula for Density Matrices

In the previous sections we have investigated the exactly solvable density matrix for systems governed by a Gaussian action (3.1) with external sources. We will now use the results to set up a perturbative treatment of density matrices for systems with nontrivial interaction. In order to calculate the expectation values, which appear in the perturbation expansion, we derive the *smearing formula*, which is useful, in particular, for nonpolynomial potentials.

3.3.1 Perturbative Expansion for the Density Matrix of a System with Interaction

The exact calculation of the density matrix

$$\tilde{\varrho}(\mathbf{x}_b, \mathbf{x}_a) = \int_{\mathbf{x}(0)=\mathbf{x}_a}^{\mathbf{x}(\hbar\beta)=\mathbf{x}_b} \mathcal{D}^d x \mathcal{D}^d p e^{-\mathcal{A}[\mathbf{p}, \mathbf{x}]/\hbar} \quad (3.79)$$

with an action which contains a potential,

$$\mathcal{A}[\mathbf{p}, \mathbf{x}] = \mathcal{A}_0[\mathbf{p}, \mathbf{x}] + \int_0^{\hbar\beta} d\tau V(\mathbf{p}(\tau), \mathbf{x}(\tau)), \quad (3.80)$$

is impossible for most systems. The potential $V(\mathbf{p}(\tau), \mathbf{x}(\tau))$ shall be as general as possible, and thus it may depend on momentum and position. The potential is considered as a perturbation of the exactly calculable system with the action (3.66). A Taylor expansion of the exponential in (3.79) with respect to V yields a perturbation expansion around the density matrix $\tilde{\varrho}_0(x_b, x_a)$ of the unperturbed system, defined in (3.67):

$$\begin{aligned} \tilde{\varrho}(\mathbf{x}_b, \mathbf{x}_a) &= \int_{\mathbf{x}(0)=\mathbf{x}_a}^{\mathbf{x}(\hbar\beta)=\mathbf{x}_b} \mathcal{D}^d x \mathcal{D}^d p e^{-\mathcal{A}_0[\mathbf{p}, \mathbf{x}]/\hbar} \left[1 - \frac{1}{\hbar} \int_0^{\hbar\beta} d\tau V(\mathbf{p}(\tau), \mathbf{x}(\tau)) \right. \\ &\quad \left. + \frac{1}{2! \hbar^2} \int_0^{\hbar\beta} d\tau_1 \int_0^{\hbar\beta} d\tau_2 V(\mathbf{p}(\tau_1), \mathbf{x}(\tau_1)) V(\mathbf{p}(\tau_2), \mathbf{x}(\tau_2)) - \dots \right]. \end{aligned} \quad (3.81)$$

Using the definition (3.65) of the expectation values, the perturbation expansion can be written as

$$\tilde{\varrho}(\mathbf{x}_b, \mathbf{x}_a) = \tilde{\varrho}_0(\mathbf{x}_b, \mathbf{x}_a) \left[1 + \sum_{n=1}^{\infty} \frac{(-1)^n}{n! \hbar^n} \int_0^{\hbar\beta} d\tau_1 \cdots \int_0^{\hbar\beta} d\tau_n \langle V(\mathbf{p}(\tau_1), \mathbf{x}(\tau_1)) \cdots V(\mathbf{p}(\tau_n), \mathbf{x}(\tau_n)) \rangle^{\mathbf{x}_b, \mathbf{x}_a} \right]. \quad (3.82)$$

The introduction of cumulants, where the first two are given by

$$\begin{aligned} \langle V(\mathbf{p}(\tau_1), \mathbf{x}(\tau_1)) \rangle_c^{\mathbf{x}_b, \mathbf{x}_a} &= \langle V(\mathbf{p}(\tau_1), \mathbf{x}(\tau_1)) \rangle^{\mathbf{x}_b, \mathbf{x}_a}, \\ \langle V(\mathbf{p}(\tau_1), \mathbf{x}(\tau_1)) V(\mathbf{p}(\tau_2), \mathbf{x}(\tau_2)) \rangle_c^{\mathbf{x}_b, \mathbf{x}_a} &= \langle V(\mathbf{p}(\tau_1), \mathbf{x}(\tau_1)) V(\mathbf{p}(\tau_2), \mathbf{x}(\tau_2)) \rangle^{\mathbf{x}_b, \mathbf{x}_a} \end{aligned}$$

$$- \langle V(\mathbf{p}(\tau_1), \mathbf{x}(\tau_1)) \rangle^{\mathbf{x}_b, \mathbf{x}_a} \langle V(\mathbf{p}(\tau_2), \mathbf{x}(\tau_2)) \rangle^{\mathbf{x}_b, \mathbf{x}_a},$$

enables us to re-express the right-hand side of Eq. (3.82) by

$$\tilde{\varrho}(\mathbf{x}_b, \mathbf{x}_a) = \left(\frac{M}{2\pi\hbar^2\beta} \right)^{d/2} \exp[-\beta V_{\text{eff,cl}}(\mathbf{x}_b, \mathbf{x}_a)]. \quad (3.83)$$

Here, we have used that, written in the form of a classical particle density

$$\tilde{\varrho}_{\text{cl}}(\mathbf{x}) = \left(\frac{M}{2\pi\hbar^2\beta} \right)^{d/2} \exp[-\beta V(\mathbf{x})], \quad (3.84)$$

the quantum statistical density matrix is governed by the *effective classical potential*

$$\begin{aligned} V_{\text{eff,cl}}(\mathbf{x}_b, \mathbf{x}_a) &= -\frac{1}{\beta} \ln \left[\lambda_{\text{th}}^{d/2} \tilde{\varrho}_0(\mathbf{x}_b, \mathbf{x}_a) \right] - \frac{1}{\beta} \sum_{n=1}^{\infty} \frac{(-1)^n}{n! \hbar^n} \int_0^{\hbar\beta} d\tau_1 \cdots \int_0^{\hbar\beta} d\tau_n \\ &\quad \times \langle V(\mathbf{p}(\tau_1), \mathbf{x}(\tau_1)) \cdots V(\mathbf{p}(\tau_n), \mathbf{x}(\tau_n)) \rangle_c^{\mathbf{x}_b, \mathbf{x}_a}, \end{aligned} \quad (3.85)$$

with the thermal wavelength

$$\lambda_{\text{th}} = \sqrt{\frac{2\pi\hbar^2\beta}{M}}. \quad (3.86)$$

The calculation of the density matrix for any system reduces to the calculation of the effective classical potential (3.85) and thus to an evaluation of the respective cumulants.

3.3.2 Smearing Formula for Gaussian Fluctuations

As a first application of the generating functional (3.36) we derive a general rule for calculating correlation functions of polynomial or nonpolynomial functions of $\mathbf{x}(\tau)$ and $\mathbf{p}(\tau)$ [17]. The result will be expressed in the form of a *smearing formula*. This formula will represent an essential tool for calculating perturbation expansions with nonpolynomial interactions.

Consider the correlation functions of a product of local functions

$$\begin{aligned} &\langle F_1(\mathbf{x}(\tau_1)) F_2(\mathbf{x}(\tau_2)) \cdots F_N(\mathbf{x}(\tau_N)) F_{N+1}(\mathbf{p}(\tau_{N+1})) F_{N+2}(\mathbf{p}(\tau_{N+2})) \cdots F_{N+M}(\mathbf{x}(\tau_{N+M})) \rangle^{\mathbf{x}_b, \mathbf{x}_a} \\ &= \tilde{\varrho}_0^{-1}(\mathbf{x}_b, \mathbf{x}_a) \int_{\mathbf{x}(0)=\mathbf{x}_a}^{\mathbf{x}(\hbar\beta)=\mathbf{x}_b} \mathcal{D}'^d x \mathcal{D}^d p \prod_{n=1}^N [F_n(\mathbf{x}(\tau_n))] \prod_{m=1}^M [F_{N+m}(\mathbf{p}(\tau_{N+m}))] e^{-\mathcal{A}_0[\mathbf{p}, \mathbf{x}]/\hbar}. \end{aligned} \quad (3.87)$$

By Fourier transforming the functions $F_n(\mathbf{x}(\tau_n))$ and $F_{N+m}(\mathbf{p}(\tau_{N+m}))$ according to

$$F_n(\mathbf{x}(\tau_n)) = \int d^d x_n F_n(\mathbf{x}_n) \delta(\mathbf{x}_n - \mathbf{x}(\tau_n)) = \int d^d x_n F_n(\mathbf{x}_n) \int \frac{d^d \xi_n}{(2\pi)^d} \exp\{i\xi_n(\mathbf{x}_n - \mathbf{x}(\tau_n))\} \quad (3.88)$$

and

$$\begin{aligned} F_{N+m}(\mathbf{p}(\tau_{N+m})) &= \int \frac{d^d p_m}{(2\pi\hbar)^d} F_{N+m}(\mathbf{p}_m) \delta(\mathbf{p}_m - \mathbf{p}(\tau_{N+m})) \\ &= \int \frac{d^d p_m}{(2\pi\hbar)^d} F_{N+m}(\mathbf{p}_m) \int d^d \kappa_m \exp\left\{-\frac{i}{\hbar} \kappa_m(\mathbf{p}_m - \mathbf{p}(\tau_{N+m}))\right\}, \end{aligned} \quad (3.89)$$

the correlation functions (3.87) may be re-expressed as

$$\langle F_1(\mathbf{x}(\tau_1)) \cdots F_{N+M}(\mathbf{p}(\tau_{N+M})) \rangle^{\mathbf{x}_b, \mathbf{x}_a} = \tilde{\varrho}_0^{-1}(\mathbf{x}_b, \mathbf{x}_a) \prod_{n=1}^N \left[\int d^d x_n F_n(\mathbf{x}_n) \int \frac{d^d \xi_n}{(2\pi)^d} \exp(i\xi_n \mathbf{x}_n) \right]$$

$$\times \prod_{m=1}^M \left[\int \frac{d^d p_m}{(2\pi\hbar)^d} F_{N+m}(\mathbf{p}_m) \int d^d \kappa_m \exp\left(-\frac{i}{\hbar} \kappa_m \mathbf{p}_m\right) \right] \tilde{\varrho}_0(\mathbf{x}_b, \mathbf{x}_a)[\mathbf{j}, \mathbf{v}], \quad (3.90)$$

where the generating functional is given by (3.36). The currents $\mathbf{j}(\tau)$ and $\mathbf{v}(\tau)$ are specialized to

$$\mathbf{j}(\tau) = i\hbar \sum_{n=1}^N \boldsymbol{\xi}_n \delta(\tau - \tau_n), \quad \mathbf{v}(\tau) = -i \sum_{m=1}^M \boldsymbol{\kappa}_m \delta(\tau - \tau_{N+m}). \quad (3.91)$$

Inserting these equations into the action of the functional (3.36) and the Green functions (3.26) and (3.38)–(3.40), we find the Fourier decomposition of the generating functional (3.36), so that the correlation functions (3.90) become

$$\begin{aligned} \langle F_1(\mathbf{x}(\tau_1)) \dots F_{N+M}(\mathbf{p}(\tau_{N+M})) \rangle^{\mathbf{x}_b, \mathbf{x}_a} &= \prod_{n=1}^N \left[\int d^d x_n F_n(\mathbf{x}_n) \int \frac{d^d \xi_n}{(2\pi)^d} \exp\{i \boldsymbol{\xi}_n [\mathbf{x}_n - \mathbf{x}_{cl}(\tau_n)]\} \right] \\ &\times \prod_{m=1}^M \left[\int \frac{d^d p_m}{(2\pi\hbar)^d} F_{N+m}(\mathbf{p}_m) \int d^d \kappa_m \exp\left\{-\frac{i}{\hbar} \boldsymbol{\kappa}_m [\mathbf{p}_m - \mathbf{p}_{cl}(\tau_{N+m})]\right\} \right] \\ &\times \exp\left\{-\frac{1}{2} \sum_{n, n'=1}^N \boldsymbol{\xi}_n G_{\mathbf{xx}}^{nn'} \boldsymbol{\xi}_{n'} + \frac{1}{\hbar} \sum_{n=1}^N \sum_{m=1}^M \boldsymbol{\xi}_n G_{\mathbf{xp}}^{nm} \boldsymbol{\kappa}_m - \frac{1}{2\hbar^2} \sum_{m, m'=1}^M \boldsymbol{\kappa}_m G_{\mathbf{pp}}^{mm'} \boldsymbol{\kappa}_{m'}\right\}, \end{aligned} \quad (3.92)$$

where we used the abbreviations

$$G_{\mathbf{xx}}^{nn'} = G_{\mathbf{xx}}^{\mathbf{D}}(\tau_n, \tau_{n'}), \quad G_{\mathbf{xp}}^{nm} = G_{\mathbf{xp}}^{\mathbf{D}}(\tau_n, \tau_{N+m}), \quad G_{\mathbf{pp}}^{mm'} = G_{\mathbf{pp}}^{\mathbf{D}}(\tau_{N+m}, \tau_{N+m'}). \quad (3.93)$$

To proceed, it is more convenient to write expression (3.92) as a convolution integral

$$\begin{aligned} \langle F_1(\mathbf{x}(\tau_1)) \dots F_{N+M}(\mathbf{p}(\tau_{N+M})) \rangle^{\mathbf{x}_b, \mathbf{x}_a} &= \prod_{n=1}^N \left[\int d^d x_n F_n(\mathbf{x}_n) \right] \prod_{m=1}^M \left[\frac{d^d p_m}{(2\pi\hbar)^d} F_{N+m}(\mathbf{p}_m) \right] \\ &\times \hbar^{Md} P(\mathbf{x}_1, \dots, \mathbf{x}_N, \mathbf{p}_1, \dots, \mathbf{p}_M) \end{aligned} \quad (3.94)$$

involving the Gaussian distribution

$$P(\mathbf{x}_1, \dots, \mathbf{p}_M) \equiv \frac{1}{(2\pi)^N} \int d^{N+M} w_1 \exp\left\{i \mathbf{w}_1^T \mathbf{w}_2 - \frac{1}{2} \mathbf{w}_1^T G \mathbf{w}_1\right\}. \quad (3.95)$$

The vectors \mathbf{w}_1 and \mathbf{w}_2 have $(N+M)d$ components and are defined as

$$\mathbf{w}_1^T = \left(\boldsymbol{\xi}_1, \dots, \boldsymbol{\xi}_N, \frac{1}{\hbar} \boldsymbol{\kappa}_1, \dots, \frac{1}{\hbar} \boldsymbol{\kappa}_M \right) \quad (3.96)$$

and

$$\mathbf{w}_2^T = (\mathbf{x}_1 - \mathbf{x}_{cl}(\tau_1), \dots, \mathbf{x}_N - \mathbf{x}_{cl}(\tau_N), -\mathbf{p}_1 + \mathbf{p}_{cl}(\tau_{N+1}), \dots, -\mathbf{p}_M + \mathbf{p}_{cl}(\tau_{N+M})). \quad (3.97)$$

The $(N+M)d \times (N+M)d$ -matrix of Green functions

$$G = \begin{pmatrix} A & B \\ B^T & C \end{pmatrix} \quad (3.98)$$

can be decomposed into block matrices A , B , and C . The $Nd \times Nd$ -matrix A and the $Md \times Md$ -matrix C are defined by

$$A = \begin{pmatrix} G_{\mathbf{xx}}^{11} & G_{\mathbf{xx}}^{12} & \dots & G_{\mathbf{xx}}^{1N} \\ G_{\mathbf{xx}}^{12} & G_{\mathbf{xx}}^{11} & \dots & G_{\mathbf{xx}}^{2N} \\ \vdots & \vdots & \ddots & \vdots \\ G_{\mathbf{xx}}^{1N} & G_{\mathbf{xx}}^{2N} & \dots & G_{\mathbf{xx}}^{11} \end{pmatrix}, \quad C = \begin{pmatrix} G_{\mathbf{pp}}^{11} & G_{\mathbf{pp}}^{12} & \dots & G_{\mathbf{pp}}^{1M} \\ G_{\mathbf{pp}}^{12} & G_{\mathbf{pp}}^{11} & \dots & G_{\mathbf{pp}}^{2M} \\ \vdots & \vdots & \ddots & \vdots \\ G_{\mathbf{pp}}^{1M} & G_{\mathbf{pp}}^{2M} & \dots & G_{\mathbf{pp}}^{11} \end{pmatrix} \quad (3.99)$$

and yield quadratic forms of the position and momentum variables, respectively. The $Nd \times Md$ -matrix

$$B = \begin{pmatrix} -G_{\mathbf{x}\mathbf{p}}^{11} & -G_{\mathbf{x}\mathbf{p}}^{12} & \cdots & -G_{\mathbf{x}\mathbf{p}}^{1M} \\ -G_{\mathbf{x}\mathbf{p}}^{21} & -G_{\mathbf{x}\mathbf{p}}^{22} & \cdots & -G_{\mathbf{x}\mathbf{p}}^{2M} \\ \vdots & \vdots & \ddots & \vdots \\ -G_{\mathbf{x}\mathbf{p}}^{N1} & -G_{\mathbf{x}\mathbf{p}}^{N2} & \cdots & -G_{\mathbf{x}\mathbf{p}}^{NM} \end{pmatrix} \quad (3.100)$$

gives rise to quadratic terms, which are linear in both position and momentum variables. The multidimensional integral in (3.95) is of Gaussian type and can easily be done, yielding an explicit expression for the Gaussian distribution (3.95)

$$P(\mathbf{x}_1, \dots, \mathbf{x}_N, \mathbf{p}_1, \dots, \mathbf{p}_M) = \frac{1}{\sqrt{(2\pi)^{(N-M)d} \det G}} \exp \left\{ -\frac{1}{2} \mathbf{w}_2^T G^{-1} \mathbf{w}_2 \right\}, \quad (3.101)$$

where G^{-1} represents the matrix inverse of (3.98) whose block form is [see Appendix 3A for a direct derivation]

$$G^{-1} = \begin{pmatrix} X^{-1} & -X^{-1}BC^{-1} \\ -C^{-1}B^T X^{-1} & C^{-1} + C^{-1}B^T X^{-1}BC^{-1} \end{pmatrix} \quad (3.102)$$

with the abbreviation

$$X = A - BC^{-1}B^T. \quad (3.103)$$

The calculation of the determinant is presented in Appendix 3A and yields

$$\det G = \det C \det X, \quad (3.104)$$

when the matrix C is regular. For singular matrix C but A regular, we obtain

$$\det G = \det \tilde{X} \det A, \quad (3.105)$$

with $\tilde{X} = C - B^T A^{-1} B$.

With the Gaussian distribution (3.101), our result (3.94) constitutes a *smearing formula*, which describes the effect of harmonic fluctuations upon arbitrary products of functions of space and momentum variables at different times.

3.4 Generalized Wick Rules and Feynman Diagrams

In applications, there often occur correlation functions for mixtures of nonpolynomial functions $F(\tilde{x}_k)$ or $F(\tilde{p}_k)$ and powers according to

$$\begin{aligned} \langle F(\tilde{x}_k(\tau_1)) \tilde{x}_l^n(\tau_2) \rangle^{\mathbf{x}_b, \mathbf{x}_a}, & \quad \langle F(\tilde{x}_k(\tau_1)) \tilde{p}_l^n(\tau_2) \rangle^{\mathbf{x}_b, \mathbf{x}_a}, \\ \langle F(\tilde{p}_k(\tau_1)) \tilde{x}_l^n(\tau_2) \rangle^{\mathbf{x}_b, \mathbf{x}_a}, & \quad \langle F(\tilde{p}_k(\tau_1)) \tilde{p}_l^n(\tau_2) \rangle^{\mathbf{x}_b, \mathbf{x}_a}, \end{aligned} \quad (3.106)$$

where we consider functions of the shifted phase space coordinates (3.78). In order to evaluate such correlation functions, we derive in this section generalized Wick rules and Feynman diagrams on the basis of the smearing formula (3.94). For simplicity, we restrict ourselves to the calculation in one dimension, since it already involves the interesting features, which we want to discuss in the following.

3.4.1 Ordinary Wick Rules

It is well known that if one has to calculate expectation values of polynomials with even power, Wick's rule can be written as the sum over all possible permutations of products of two-point functions. We shortly recall to this expansion by considering the case of a position-dependent n -point correlation function in one dimension, n even, defined as

$$G^{(n)}(\tau_1, \dots, \tau_n) = \langle \tilde{x}(\tau_1) \cdots \tilde{x}(\tau_n) \rangle^{x_b, x_a}. \quad (3.107)$$

Note that it will be sufficient to study only the correlation functions involving the deviations from the classical path, respectively. This expectation value can be decomposed with the help of Wick's expansion

$$G^{(n)}(\tau_1, \dots, \tau_n) = \sum_{\text{pairs}} G^{(2)}(\tau_{P(1)}, \tau_{P(2)}) \cdots G^{(2)}(\tau_{P(n-1)}, \tau_{P(n)}), \quad (3.108)$$

where P denotes the operation of pairwise index permutation. Note that Eq. (3.108) may be considered as a consequence of a simple derivative rule

$$\langle F(\tilde{x}(\tau_1)) \tilde{x}(\tau_2) \rangle^{x_b, x_a} = \langle \tilde{x}(\tau_1) \tilde{x}(\tau_2) \rangle^{x_b, x_a} \langle F'(\tilde{x}(\tau_1)) \rangle^{x_b, x_a} \quad (3.109)$$

with $F'(\tilde{x}) = \partial F(\tilde{x})/\partial x$. By applying this recursively, one eventually obtains (3.108). And conversely, the derivative rule (3.109) can be proved for *polynomial* functions $F(\tilde{x}(\tau))$, following directly from Wick's theorem (3.108).

The two-point Green function $G^{(2)}(\tau_1, \tau_2)$, occurring in (3.108), can be considered as a Wick contraction, which we introduce as follows:

$$\underbrace{\tilde{x}(\tau_1) \tilde{x}(\tau_2)} = \langle \tilde{x}(\tau_1) \tilde{x}(\tau_2) \rangle^{x_b, x_a} = G_{xx}^D(\tau_1, \tau_2), \quad (3.110)$$

$$\underbrace{\tilde{x}(\tau_1) \tilde{p}(\tau_2)} = \langle \tilde{x}(\tau_1) \tilde{p}(\tau_2) \rangle^{x_b, x_a} = G_{xp}^D(\tau_1, \tau_2), \quad (3.111)$$

$$\underbrace{\tilde{p}(\tau_1) \tilde{x}(\tau_2)} = \langle \tilde{p}(\tau_1) \tilde{x}(\tau_2) \rangle^{x_b, x_a} = G_{px}^D(\tau_1, \tau_2) = G_{xp}^D(\tau_2, \tau_1), \quad (3.112)$$

$$\underbrace{\tilde{p}(\tau_1) \tilde{p}(\tau_2)} = \langle \tilde{p}(\tau_1) \tilde{p}(\tau_2) \rangle^{x_b, x_a} = G_{pp}^D(\tau_1, \tau_2). \quad (3.113)$$

Decomposing polynomial correlations of $\tilde{x}(\tau)$ and $\tilde{p}(\tau)$ with the help of these contractions corresponding to Eq. (3.108) or successively applying the derivative rule (3.109) leads to following results

$$\langle \tilde{x}^n(\tau_1) \tilde{x}^m(\tau_2) \rangle^{x_b, x_a} = \sum_{\substack{l=\alpha, \alpha+2, \\ \alpha+4, \dots}}^{\min(n, m)} c_l [G_{xx}^D(\tau_1, \tau_1)]^{(n-l)/2} [G_{xx}^D(\tau_1, \tau_2)]^l [G_{xx}^D(\tau_2, \tau_2)]^{(m-l)/2}, \quad (3.114)$$

$$\langle \tilde{x}^n(\tau_1) \tilde{p}^m(\tau_2) \rangle^{x_b, x_a} = \sum_{\substack{l=\alpha, \alpha+2, \\ \alpha+4, \dots}}^{\min(n, m)} c_l [G_{xx}^D(\tau_1, \tau_1)]^{(n-l)/2} [G_{xp}^D(\tau_1, \tau_2)]^l [G_{pp}^D(\tau_2, \tau_2)]^{(m-l)/2}, \quad (3.115)$$

$$\langle \tilde{p}^n(\tau_1) \tilde{x}^m(\tau_2) \rangle^{x_b, x_a} = \sum_{\substack{l=\alpha, \alpha+2, \\ \alpha+4, \dots}}^{\min(n, m)} c_l [G_{pp}^D(\tau_1, \tau_1)]^{(n-l)/2} [G_{xp}^D(\tau_2, \tau_1)]^l [G_{xx}^D(\tau_2, \tau_2)]^{(m-l)/2}, \quad (3.116)$$

$$\langle \tilde{p}^n(\tau_1) \tilde{p}^m(\tau_2) \rangle^{x_b, x_a} = \sum_{\substack{l=\alpha, \alpha+2, \\ \alpha+4, \dots}}^{\min(n, m)} c_l [G_{pp}^D(\tau_1, \tau_1)]^{(n-l)/2} [G_{pp}^D(\tau_1, \tau_2)]^l [G_{pp}^D(\tau_2, \tau_2)]^{(m-l)/2}, \quad (3.117)$$

with the multiplicity factor

$$c_l = \frac{(n-l-1)!! (m-l-1)!! n! m!}{l! (n-l)! (m-l)!}. \quad (3.118)$$

Note, that $(-k)!! \equiv 1$ for any positive integer k . For nonvanishing correlation, the sum $n+m$ must be even so that the regulation parameter α is defined as follows:

$$\alpha = \begin{cases} 0, & n, m \text{ even,} \\ 1, & n, m \text{ odd.} \end{cases} \quad (3.119)$$

The contractions defined in (3.110)–(3.113) can be used to treat Taylor-expandable functions $F(\tilde{x}(\tau))$ and $F(\tilde{p}(\tau))$ only. The desired derivative rules for such correlations read

$$\langle F(\tilde{x}(\tau_1)) \tilde{x}^n(\tau_2) \rangle^{x_b, x_a} =$$

$$\sum_{l=\alpha, \alpha+2, \alpha+4, \dots}^n \frac{n!}{(n-l)!! l!} [G_{xx}^D(\tau_2, \tau_2)]^{(n-l)/2} [G_{xx}^D(\tau_1, \tau_2)]^l \langle F^{(l)}(\tilde{x}(\tau_1)) \rangle^{x_b, x_a}, \quad (3.120)$$

$$\langle F(\tilde{x}(\tau_1)) \tilde{p}^n(\tau_2) \rangle^{x_b, x_a} = \sum_{l=\alpha, \alpha+2, \alpha+4, \dots}^n \frac{n!}{(n-l)!! l!} [G_{pp}^D(\tau_2, \tau_2)]^{(n-l)/2} [G_{xp}^D(\tau_1, \tau_2)]^l \langle F^{(l)}(\tilde{x}(\tau_1)) \rangle^{x_b, x_a}, \quad (3.121)$$

$$\langle F(\tilde{p}(\tau_1)) \tilde{p}^n(\tau_2) \rangle^{x_b, x_a} = \sum_{l=\alpha, \alpha+2, \alpha+4, \dots}^n \frac{n!}{(n-l)!! l!} [G_{pp}^D(\tau_2, \tau_2)]^{(n-l)/2} [G_{pp}^D(\tau_1, \tau_2)]^l \langle F^{(l)}(\tilde{p}(\tau_1)) \rangle^{x_b, x_a}, \quad (3.122)$$

$$\langle F(\tilde{p}(\tau_1)) \tilde{x}^n(\tau_2) \rangle^{x_b, x_a} = \sum_{l=\alpha, \alpha+2, \alpha+4, \dots}^n \frac{n!}{(n-l)!! l!} [G_{xx}^D(\tau_2, \tau_2)]^{(n-l)/2} [G_{xp}^D(\tau_2, \tau_1)]^l \langle F^{(l)}(\tilde{p}(\tau_1)) \rangle^{x_b, x_a}. \quad (3.123)$$

The parameter α distinguishes between even and odd power n :

$$\alpha = \begin{cases} 0, & n \text{ even,} \\ 1, & n \text{ odd,} \end{cases} \quad (3.124)$$

since even (odd) powers of n lead to even (odd) derivatives of the function $F(\tilde{x}(\tau_1))$. The l th derivative $F^{(l)}(\tilde{x}(\tau_1))$ is formed with respect to $x(\tau_1)$, and $F^{(l)}(\tilde{p}(\tau_1))$ is the l th derivative with respect to $p(\tau_1)$. Note, that in (3.123) the Green function G_{xp}^D appears with exchanged time arguments, which in this case happens to be inessential due to the symmetry $G_{xp}^D(\tau_2, \tau_1) = G_{px}^D(\tau_1, \tau_2)$.

3.4.2 Generalized Wick Rule

According to their derivation, the contractions (3.120)–(3.123) are only applicable to functions $F(\tilde{x}(\tau))$ and $F(\tilde{p}(\tau))$ which can be Taylor-expanded. In the following, we will show with the help of the smearing formula (3.94) that these derivative rules remain valid for functions $F(\tilde{x}(\tau))$ and $F(\tilde{p}(\tau))$ with Laurent expansions. Expectations of this type appear in variational perturbation theory (see Ref. [20] for position-position coupling). Since the proceeding is similar in all the cases (3.120)–(3.123), we shall only discuss the expectation value

$$\langle F(\tilde{x}(\tau_1)) \tilde{p}^n(\tau_2) \rangle^{x_b, x_a} \quad (3.125)$$

in detail. For this we consider the generating functional of all such expectation values following from (3.94)

$$\begin{aligned} \langle F(\tilde{x}(\tau_1)) e^{j\tilde{p}(\tau_2)} \rangle^{x_b, x_a} &= \frac{\hbar}{\sqrt{\det G}} \int_{-\infty}^{+\infty} dx F(x) \int_{-\infty}^{+\infty} \frac{dp}{2\pi\hbar} e^{jp} \\ &\times \exp \left\{ -\frac{1}{2 \det G} [G_{pp}^D(\tau_2, \tau_2) x^2 - 2G_{xp}^D(\tau_1, \tau_2) xp + G_{xx}^D(\tau_1, \tau_1) p^2] \right\}. \end{aligned} \quad (3.126)$$

The p -integration can easily be done, leading to

$$\begin{aligned} \langle F(\tilde{x}(\tau_1)) e^{j\tilde{p}(\tau_2)} \rangle^{x_b, x_a} &= e^{G_{pp}^D(t_2, t_2) j^2 / 2} \int_{-\infty}^{+\infty} \frac{dx}{\sqrt{2\pi G_{xx}^D(t_1, t_1)}} F(x + j G_{xp}^D(t_1, t_2)) e^{-x^2 / 2G_{xx}^D(t_1, t_1)} \\ &= e^{G_{pp}^D(t_2, t_2) j^2 / 2} \sum_{l=0}^{\infty} \frac{1}{l!} [j G_{xp}^D(t_1, t_2)]^l \langle F^{(l)}(\tilde{x}(t_1)) \rangle^{x_b, x_a}. \end{aligned} \quad (3.127)$$

The correlation of two functions at different times has been reduced to a single-time expectation value of the l th derivative of the function $F(\tilde{x}(\tau_1))$ with respect to $x(\tau_1)$, denoted by $F^{(l)}(\tilde{x}(\tau_1))$, with Green

functions describing the dependence on the second time. Expanding both sides in powers of j , we re-obtain (3.121).

Now we demonstrate that the derivative rules (3.120)–(3.123) for Laurent-expandable functions $F(\tilde{x}(\tau))$ and $F(\tilde{p}(\tau))$ also follow from generalized Wick rules. Without restriction of universality, we only consider the expectation value

$$\langle F(\tilde{x}(\tau_1)) \tilde{x}^n(\tau_2) \rangle^{x_b, x_a}. \quad (3.128)$$

The proceeding to reduce the power of the polynomial at the expense of the function $F(\tilde{x}(\tau_1))$ is as follows:

1a. If possible ($n \geq 2$), contract $\tilde{x}(\tau_2) \tilde{x}(\tau_2)$ with multiplicity $(n - 1)$, giving

$$(n - 1) \underbrace{\tilde{x}(\tau_2) \tilde{x}(\tau_2)} \langle F(\tilde{x}(\tau_1)) \tilde{x}^{n-2}(\tau_2) \rangle^{x_b, x_a}, \quad (3.129)$$

else jump to 1b. directly.

1b. Contract $F(\tilde{x}(\tau_1)) \tilde{x}(\tau_2)$ and let the remaining polynomial invariant. We define this contraction by the symbol

$$F(\tilde{x}(\tau_1)) \underbrace{\tilde{x}(\tau_2)} \tilde{x}^{n-1}(\tau_2) = \underbrace{\tilde{x}(\tau_1) \tilde{x}(\tau_2)} \langle F'(\tilde{x}(\tau_1)) \tilde{x}^{n-1}(\tau_2) \rangle^{x_b, x_a}. \quad (3.130)$$

1c. Add the terms 1a. and 1b.

2. Repeat steps 1a.-1c. until only expectation values of $F(\tilde{x})$ or expectations of its derivatives remain. Summarizing, we can express the first power reduction by the generalized Wick rule ($n \geq 2$)

$$\begin{aligned} \langle F(\tilde{x}(\tau_1)) \tilde{x}^n(\tau_2) \rangle^{x_b, x_a} &= (n - 1) \underbrace{\tilde{x}(\tau_2) \tilde{x}(\tau_2)} \langle F(\tilde{x}(\tau_1)) \tilde{x}^{n-2}(\tau_2) \rangle^{x_b, x_a} \\ &\quad + \underbrace{F(\tilde{x}(\tau_1)) \tilde{x}(\tau_2)} \tilde{x}^{n-1}(\tau_2) \end{aligned} \quad (3.131)$$

with the contraction rules defined in (3.110) and (3.130). For $n = 1$, we obtain

$$\langle F(\tilde{x}(\tau_1)) \tilde{x}(\tau_2) \rangle^{x_b, x_a} = \underbrace{\tilde{x}(\tau_1) \tilde{x}(\tau_2)} \langle F'(x(\tau_1)) \rangle^{x_b, x_a}, \quad (3.132)$$

which is valid for *any* function $F(\tilde{x}(\tau))$ generalizing the rule (3.109) that was proved for polynomial functions only. Recursively applying this power reduction, we finally end up with the derivative rule (3.120). Note that the generalization of Wick's rule for mixed position-momentum or pure momentum couplings is done along similar lines, leading to the derivative rules (3.121)–(3.123).

3.4.3 New Feynman-Like Rules for Nonpolynomial Interactions

Higher-order perturbation expressions become usually complicated. For simple polynomial interactions, Feynman diagrams are a useful tool to classify perturbative contributions with the help of graphical rules. Here, we are going to set up analogous diagrammatic rules for perturbation expansions for nonpolynomial interactions $V(x(\tau), p(\tau))$, whose contributions may be expressed as expectations values

$$\int_0^{\hbar\beta} d\tau_1 \cdots \int_0^{\hbar\beta} d\tau_n \langle V(x(\tau_1), p(\tau_1)) \cdots V(x(\tau_n), p(\tau_n)) \rangle^{x_b, x_a}. \quad (3.133)$$

From (3.110)–(3.113) follows that we have four basic propagators whose graphical representation may be defined as (setting $\hbar = M = \beta = 1$ from now on)

$$\begin{aligned} \tau_1 \text{ --- } \tau_2 &\equiv \langle \tilde{x}(\tau_1) \tilde{x}(\tau_2) \rangle^{x_b, x_a} = G_{xx}^D(\tau_1, \tau_2), \\ \tau_1 \text{ ~~~~~ } \tau_2 &\equiv \langle \tilde{p}(\tau_1) \tilde{p}(\tau_2) \rangle^{x_b, x_a} = G_{pp}^D(\tau_1, \tau_2), \\ \tau_1 \text{ - - } \tau_2 &\equiv \langle \tilde{x}(\tau_1) \tilde{p}(\tau_2) \rangle^{x_b, x_a} = G_{xp}^D(\tau_1, \tau_2), \end{aligned}$$

$$\tau_1 \text{ --- } \blacktriangleright \text{ --- } \tau_2 \quad \equiv \quad \langle \tilde{p}(\tau_1) \tilde{x}(\tau_2) \rangle^{x_b, x_a} = G_{px}^D(\tau_1, \tau_2) = G_{xp}^D(\tau_2, \tau_1).$$

A vertex is represented as usual by a small dot. The time variable is integrated over at a vertex in a perturbation expansion,

$$\bullet \quad \equiv \quad \int_0^1 d\tau.$$

We now introduce the diagrammatic representations of the expectation value of arbitrary functions $F(\tilde{x}(\tau))$ or $F(\tilde{p}(\tau))$ and their derivatives as

$$\begin{array}{ll} \star & \equiv \int_0^1 d\tau \langle F(\tilde{x}(\tau)) \rangle^{x_b, x_a}, & \star & \equiv \int_0^1 d\tau \langle F(\tilde{p}(\tau)) \rangle^{x_b, x_a}, \\ \star \diagup & \equiv \int_0^1 d\tau \langle F'(\tilde{x}(\tau)) \rangle^{x_b, x_a}, & \star \text{ wavy} & \equiv \int_0^1 d\tau \langle F'(\tilde{p}(\tau)) \rangle^{x_b, x_a}, \\ \star \diagdown & \equiv \int_0^1 d\tau \langle F''(\tilde{x}(\tau)) \rangle^{x_b, x_a}, & \star \text{ wavy} & \equiv \int_0^1 d\tau \langle F''(\tilde{p}(\tau)) \rangle^{x_b, x_a}, \\ \vdots & & \vdots & . \end{array}$$

With these elements, we can compose Feynman graphs for two-point correlation functions of the type (3.106) for arbitrary n by successively applying the generalized Wick rule (3.131) or directly using the derivative relations (3.120)–(3.123). The general results become obvious by giving explicitly a graphical representation of the following four correlation functions

$$\int_0^1 d\tau_1 \int_0^1 d\tau_2 \langle F(\tilde{x}(\tau_1)) \tilde{x}(\tau_2) \rangle^{x_b, x_a} = \int_0^1 d\tau_1 \int_0^1 d\tau_2 G_{xx}^D(\tau_1, \tau_2) \langle F'(\tilde{x}(\tau_1)) \rangle^{x_b, x_a} \quad (3.134)$$

$$\equiv \star \longrightarrow \bullet,$$

$$\begin{aligned} \int_0^1 d\tau_1 \int_0^1 d\tau_2 \langle F(\tilde{x}(\tau_1)) \tilde{x}^2(\tau_2) \rangle^{x_b, x_a} &= \int_0^1 d\tau_1 \int_0^1 d\tau_2 \left\{ G_{xx}^D(\tau_2, \tau_2) \langle F(\tilde{x}(\tau_1)) \rangle^{x_b, x_a} \right. \\ &\quad \left. + [G_{xx}^D(\tau_1, \tau_2)]^2 \langle F''(\tilde{x}(\tau_1)) \rangle^{x_b, x_a} \right\} \end{aligned} \quad (3.135)$$

$$\equiv \star \circlearrowleft + \star \circlearrowright,$$

$$\begin{aligned} \int_0^1 d\tau_1 \int_0^1 d\tau_2 \langle F(\tilde{x}(\tau_1)) \tilde{x}^3(\tau_2) \rangle^{x_b, x_a} &= \int_0^1 d\tau_1 \int_0^1 d\tau_2 \left\{ 3 G_{xx}^D(\tau_1, \tau_2) G_{xx}^D(\tau_2, \tau_2) \langle F'(\tilde{x}(\tau_1)) \rangle^{x_b, x_a} \right. \\ &\quad \left. + [G_{xx}^D(\tau_1, \tau_2)]^3 \langle F'''(\tilde{x}(\tau_1)) \rangle^{x_b, x_a} \right\} \end{aligned} \quad (3.136)$$

$$\equiv 3 \star \circlearrowleft \circlearrowleft + \star \circlearrowright \circlearrowright,$$

$$\begin{aligned} \int_0^1 d\tau_1 \int_0^1 d\tau_2 \langle F(\tilde{x}(\tau_1)) \tilde{x}^4(\tau_2) \rangle^{x_b, x_a} &= \int_0^1 d\tau_1 \int_0^1 d\tau_2 \left\{ [G_{xx}^D(\tau_2, \tau_2)]^2 \langle F(\tilde{x}(\tau_1)) \rangle^{x_b, x_a} \right. \\ &\quad + 6 [G_{xx}^D(\tau_1, \tau_2)]^2 G_{xx}^D(\tau_2, \tau_2) \langle F''(\tilde{x}(\tau_1)) \rangle^{x_b, x_a} \\ &\quad \left. + [G_{xx}^D(\tau_1, \tau_2)]^4 \langle F^{(4)}(\tilde{x}(\tau_1)) \rangle^{x_b, x_a} \right\} \end{aligned} \quad (3.137)$$

$$\equiv \star \circlearrowleft \circlearrowleft \circlearrowleft + 6 \star \circlearrowleft \circlearrowright + \star \circlearrowright \circlearrowright \circlearrowright.$$

Mixed position-momentum and momentum-momentum correlations and their graphical representations are given in Appendix 3B.

The consideration of higher-order correlations with more than one function $F(\tilde{x}(\tau))$ or $F(\tilde{p}(\tau))$ can be reduced to the results (3.114)–(3.117) or (3.120)–(3.123) by expanding them with respect to the classical path or momentum, respectively. By expanding both functions in the expectation value, one obtains for example

$$\langle F_1(\tilde{x}(\tau_1)) F_2(\tilde{x}(\tau_2)) \rangle^{x_b, x_a} = \sum_{m=0}^{\infty} \sum_{n=0}^{\infty} \frac{1}{m! n!} f_{1,m} f_{2,n} \langle \tilde{x}^m(\tau_1) \tilde{x}^n(\tau_2) \rangle^{x_b, x_a} \quad (3.138)$$

with

$$f_{i,m} = F_i^{(m)}(0), \quad i = 1, 2. \quad (3.139)$$

But constructing graphical rules for such general correlations is more involved due to the various summations over products of powers of propagators $G_{xx}^D(\tau_i, \tau_j)$ with $i, j = 1, 2$.

Finally, we apply the diagrammatic rules to the anharmonic oscillator with \tilde{x}^4 -interaction, which is a powerful system being discussed in detail by the help of a perturbation expansion [4, Chap. 3]. With the Green functions given by (3.26) and (3.38)–(3.40), the two-point-correlation for the anharmonic system can then be expressed graphically, yielding the known decomposition for the second-order perturbative contribution

$$\int_0^1 d\tau_1 \int_0^1 d\tau_2 \langle \tilde{x}^4(\tau_1) \tilde{x}^4(\tau_2) \rangle_c^{x_b, x_a} \equiv 72 \text{ (two circles)} + 24 \text{ (two circles with two internal lines)}, \quad (3.140)$$

with subscript c indicating that we restrict ourselves to connected graphs only. Beyond this, our theory allows to describe nonstandard systems with polynomial interactions (3.133) depending on both, position and momentum, to higher order. Finally, we want to give the graphs for a four-interaction $\tilde{x}^2 \tilde{p}^2$ to second order to see the variations of possible graphs in comparison with (3.140):

$$\begin{aligned} \int_0^1 d\tau_1 \int_0^1 d\tau_2 \langle \tilde{x}^2(\tau_1) \tilde{p}^2(\tau_1) \tilde{x}^2(\tau_2) \tilde{p}^2(\tau_2) \rangle_c^{x_b, x_a} \equiv & 2 \text{ (two circles with wavy lines)} + 16 \text{ (two circles with dashed lines)} \\ & + 16 \text{ (two circles with solid lines)} + 2 \text{ (two circles with wavy and dashed lines)} + 4 \text{ (two circles with solid and dashed lines)} + 16 \text{ (two circles with solid and wavy lines)} \\ & + 16 \text{ (two circles with dashed and wavy lines)} + 4 \text{ (two circles with dashed and solid lines)} + 16 \text{ (two circles with solid and dashed lines)} + 4 \text{ (two circles with solid and wavy lines)}. \end{aligned} \quad (3.141)$$

We see, that we have the same class of graphs already occurring in (3.140), however, with different propagators connecting the vertices. Thus, both classes decay into subclasses with different multiplicities, but the total numbers remain 72 and 24 for each type of class, respectively. Furthermore, all graphs are vacuum-like graphs. Eventually, it is easy to construct the Feynman graphs for polynomial correlations higher than second order by applying Wick's rule or the Feynman rules given in this section.

Due to its universality, the theory should serve as a basis for investigating physical systems with nonstandard Hamiltonian via perturbation theory and its variational extension.

3.5 Particle Density in the Presence of External Sources

The particle density for a quantum statistical system is given by the diagonal elements of the density matrix. This means, for an explicitly given system, that the knowledge of the density matrix implies

the particle density and is obtained by

$$\varrho(\mathbf{x})[\mathbf{j}, \mathbf{v}] \equiv \frac{\tilde{\varrho}(\mathbf{x}, \mathbf{x})[\mathbf{j}, \mathbf{v}]}{\text{Tr} \tilde{\varrho}(\mathbf{x}_b, \mathbf{x}_a)[\mathbf{j}, \mathbf{v}]}.$$
 (3.142)

The normalization ensures

$$\int d^d x \varrho(\mathbf{x})[\mathbf{j}, \mathbf{v}] = \frac{\text{Tr} \tilde{\varrho}(\mathbf{x}, \mathbf{x})[\mathbf{j}, \mathbf{v}]}{\text{Tr} \tilde{\varrho}(\mathbf{x}_b, \mathbf{x}_a)[\mathbf{j}, \mathbf{v}]} = 1.$$
 (3.143)

In order to calculate the particle density for the general action (3.1), we follow, however, a different way, since extracting the diagonal elements of expression (3.36) requires the knowledge of the classical path with periodic boundary conditions $\mathbf{x}(0) = \mathbf{x}_a = \mathbf{x}(\hbar\beta) = \mathbf{x}_b \equiv \mathbf{x}$, which is determined by the solution (we assume that there is only one) of the general Hamiltonian equations (3.16) and (3.17). Rather, we utilize that the unnormalized particle density $\tilde{\varrho}(\mathbf{x})$ can also be obtained from a path integral over all periodic paths with an inserted δ function $\delta(\mathbf{x}(\tau') - \mathbf{x})$, which restricts the end points of the periodic paths to \mathbf{x} . This position is any point of the loop-like path $\mathbf{x}(\tau)$ at the time τ' , but it is the same position in space for all loops we integrate over. Thus all periodic paths touch each other in this point. The unnormalized particle density for a system with an action (3.1) reads

$$\tilde{\varrho}_0(\mathbf{x})[\mathbf{j}, \mathbf{v}] = \oint \mathcal{D}^d x \mathcal{D}^d p \delta(\mathbf{x}(\tau') - \mathbf{x}) e^{-\mathcal{A}_0[\mathbf{p}, \mathbf{x}; \mathbf{j}, \mathbf{v}]/\hbar},$$
 (3.144)

where the path integral measure is given by (3.3). Without any restriction of universality and as a consequence of the time-translation invariance of actions of periodic paths, one could also have chosen, for example, the points $\mathbf{x}(0) = \mathbf{x}_a$ or $\mathbf{x}(\hbar\beta) = \mathbf{x}_b$.

Similarly to (3.91), we rewrite the δ function in Eq. (3.144) as

$$\delta(\mathbf{x}(\tau') - \mathbf{x}) = \int \frac{d^d k}{(2\pi)^d} \exp \left[i\mathbf{k}^T \mathbf{x} - \frac{1}{\hbar} \int_0^{\hbar\beta} d\tau \mathbf{j}_0^T(\tau) \mathbf{x}(\tau) \right],$$
 (3.145)

with the artificial current

$$\mathbf{j}_0(\tau) = i\hbar \mathbf{k} \delta(\tau - \tau').$$
 (3.146)

After adding the second term in the brackets of the expression (3.145) to the action in the path integral of Eq. (3.144), the Gaussian phase space path integral is easily solved. Introducing $2d$ -dimensional phase space coordinates and currents

$$\mathbf{w}^T(\tau) = (\mathbf{x}^T(\tau), \mathbf{p}^T(\tau)), \quad \boldsymbol{\eta}^T = (\mathbf{j}^T(\tau) + \mathbf{j}_0(\tau), \mathbf{v}^T(\tau)),$$
 (3.147)

and using the symmetric $2d \times 2d$ -matrix (3.10), expression (3.144) can be written as

$$\begin{aligned} \tilde{\varrho}_0(\mathbf{x})[\mathbf{j}, \mathbf{v}] &= \int \frac{d^d k}{(2\pi)^d} e^{i\mathbf{k}^T \mathbf{x}} \oint \mathcal{D}^{2d} w \\ &\times \exp \left[-\frac{1}{2} \int_0^{\hbar\beta} d\tau_1 \int_0^{\hbar\beta} d\tau_2 \mathbf{w}^T(\tau_1) S(\tau_1, \tau_2) \mathbf{w}(\tau_2) - \frac{1}{\hbar} \int_0^{\hbar\beta} d\tau \boldsymbol{\eta}^T(\tau) \mathbf{w}(\tau) \right]. \end{aligned}$$
 (3.148)

The calculation is straightforward. After a quadratic completion and a rotation of the phase space vectors which makes S diagonal, the $2d$ -dimensional path integral reduces to a $2d$ -fold product of a single one. This yields

$$\tilde{\varrho}_0(\mathbf{x})[\mathbf{j}, \mathbf{v}] = \frac{1}{\sqrt{\det S}} \int \frac{d^d k}{(2\pi)^d} e^{i\mathbf{k}^T \mathbf{x}} \exp \left[\frac{1}{2\hbar^2} \int_0^{\hbar\beta} d\tau_1 \int_0^{\hbar\beta} d\tau_2 \boldsymbol{\eta}^T(\tau_1) S^{-1}(\tau_1, \tau_2) \boldsymbol{\eta}(\tau_2) \right].$$
 (3.149)

For further proceeding, it is practical to rewrite this expression with the help of the submatrices of S as defined in (3.10), (3.11), and (3.13). The calculation of the inverse of S and its determinant is done in Appendix 3A. We insert into Eq. (3.149) the components of

$$S^{-1}(\tau, \tau') = \begin{pmatrix} G_{\mathbf{xx}}^{\mathbf{p}}(\tau, \tau') & G_{\mathbf{xp}}^{\mathbf{p}}(\tau, \tau') \\ G_{\mathbf{px}}^{\mathbf{p}}(\tau, \tau') & G_{\mathbf{pp}}^{\mathbf{p}}(\tau, \tau') \end{pmatrix},$$
 (3.150)

which are two-point functions satisfying periodic boundary conditions,

$$G_{\mathbf{rs}}^{\mathbf{p}}(\tau, 0) = G_{\mathbf{rs}}^{\mathbf{p}}(\tau, \hbar\beta), \quad G_{\mathbf{rs}}^{\mathbf{p}}(0, \tau') = G_{\mathbf{rs}}^{\mathbf{p}}(\hbar\beta, \tau'), \quad \mathbf{r}, \mathbf{s} \in (\mathbf{x}, \mathbf{p}). \quad (3.151)$$

These two-point functions have the same shape as those for Dirichlet boundary conditions defined in Eqs. (3.26) and (3.38)–(3.40). We will discuss the properties of Green functions with periodic boundary conditions later on. To proceed, we substitute $\mathbf{j}_0(\tau)$ by the right-hand side of Eq. (3.146), which enables us to perform the Fourier integral over k . This finally yields the general expression for the particle density:

$$\begin{aligned} \tilde{\rho}_0(\mathbf{x})[\mathbf{j}, \mathbf{v}] &= \left(\frac{M}{2\pi\hbar^2\beta} \right)^{d/2} \frac{1}{\sqrt{\det D_{\mathbf{pp}} \det G_{\mathbf{xx}}^{\mathbf{p}-1} \det_s G_{\mathbf{xx}}^{\mathbf{p}}(\tau', \tau')}} \exp \left\{ -\frac{1}{2} \mathbf{x}^T G_{\mathbf{xx}}^{\mathbf{p}-1}(\tau', \tau') \mathbf{x} \right\} \\ &\times \exp \left\{ -\frac{1}{\hbar} \int_0^{\hbar\beta} d\tau \mathbf{J}^T(\tau) G_{\mathbf{xx}}^{\mathbf{p}-1}(\tau', \tau') \mathbf{x} + \frac{1}{2\hbar^2} \int_0^{\hbar\beta} d\tau_1 \int_0^{\hbar\beta} d\tau_2 \left[\mathbf{j}^T(\tau_1) G_{\mathbf{xx}}^{\mathbf{p}}(\tau_1, \tau_2) \mathbf{j}(\tau_2) \right. \right. \\ &\left. \left. + 2\mathbf{j}^T(\tau_1) G_{\mathbf{xp}}^{\mathbf{p}}(\tau_1, \tau_2) \mathbf{v}(\tau_2) + \mathbf{v}^T(\tau_1) G_{\mathbf{pp}}^{\mathbf{p}}(\tau_1, \tau_2) \mathbf{v}(\tau_2) \right] \right\}, \end{aligned} \quad (3.152)$$

where we have used the abbreviation

$$\mathbf{J}^T(\tau) = \mathbf{j}^T(\tau) G_{\mathbf{xx}}^{\mathbf{p}}(\tau, \tau') - \mathbf{v}^T(\tau) \int_0^{\hbar\beta} d\tau_1 \int_0^{\hbar\beta} d\tau_2 G_{\mathbf{pp}}^{\mathbf{p}}(\tau, \tau_1) D_{\mathbf{px}}(\tau_1, \tau_2) G_{\mathbf{xx}}^{\mathbf{p}}(\tau_2, \tau'). \quad (3.153)$$

It is necessary to remark that, after discretizing the Euclidean time interval $[0, \hbar\beta]$ into $N + 1$ pieces, the dimension of the matrix $G_{\mathbf{xx}}^{\mathbf{p}}(\tau', \tau')$ remains $d \times d$, since τ' is a fixed point of time within this interval. Thus, its determinant is calculated only over the space components. The determinant of the $(N + 1)d \times (N + 1)d$ matrices $G_{\mathbf{xx}}^{\mathbf{p}-1}$ and $D_{\mathbf{pp}}$ must be calculated, however, over all space-time components. We have marked the difference by attaching the subscript “s” to the determinant in the first case. For the evaluation of the determinants, it is useful to take into account, once more, the rules regarding the physical dimension given after Eq. (3.36).

3.6 Partition Function with Currents

The partition function is, beside the density matrix, another fundamental quantity of statistics. In the canonical ensemble of a closed thermodynamic system, it is related to the free energy F via

$$Z = e^{-\beta F}. \quad (3.154)$$

It is the free energy that we will devote considerable attention throughout this thesis. In a subsequent part, we are going to discuss its properties at finite and zero temperature, and in a different form, the role as effective classical potential.

Additionally, the partition function in the presence of external sources can also be used as a generating functional of the correlation functions, similar to the proceeding in Section 3.2.3.

3.6.1 Partition Function in the Presence of External Sources

The quantum statistical partition function is defined as the trace over the unnormalized density matrix. For a system governed by the action (3.1), this is the space integral of (3.152):

$$\begin{aligned} Z_0[\mathbf{j}, \mathbf{v}] &= \text{Tr} \tilde{\rho}_0(\mathbf{x})[\mathbf{j}, \mathbf{v}] = \int d^d x \tilde{\rho}_0(\mathbf{x})[\mathbf{j}, \mathbf{v}] \\ &= \frac{1}{\sqrt{\det S}} \exp \left[\frac{1}{2\hbar^2} \int_0^{\hbar\beta} d\tau \int_0^{\hbar\beta} d\tau' \mathbf{C}^T(\tau) S^{-1}(\tau, \tau') \mathbf{C}(\tau') \right], \end{aligned} \quad (3.155)$$

with $\mathbf{C}^T(\tau) = (\mathbf{j}^T(\tau), \mathbf{v}^T(\tau))$. Written in components of the matrix $S^{-1}(\tau, \tau')$, the functional (3.155) reads

$$Z_0[\mathbf{j}, \mathbf{v}] = \frac{1}{\sqrt{\det D_{\mathbf{pp}} \det G_{\mathbf{xx}}^{\mathbf{p-1}}}} \exp \left\{ \frac{1}{2\hbar^2} \int_0^{\hbar\beta} d\tau_1 \int_0^{\hbar\beta} d\tau_2 \left[\mathbf{j}^T(\tau_1) G_{\mathbf{xx}}^{\mathbf{p}}(\tau_1, \tau_2) \mathbf{j}(\tau_2) \right. \right. \\ \left. \left. + \mathbf{j}^T(\tau_1) G_{\mathbf{xp}}^{\mathbf{p}}(\tau_1, \tau_2) \mathbf{v}(\tau_2) + \mathbf{v}^T(\tau_1) G_{\mathbf{px}}^{\mathbf{p}}(\tau_1, \tau_2) \mathbf{j}(\tau_2) + \mathbf{v}^T(\tau_1) G_{\mathbf{pp}}^{\mathbf{p}}(\tau_1, \tau_2) \mathbf{v}(\tau_2) \right] \right\}. \quad (3.156)$$

The Green functions are obtained as the elements of the inverse matrix S^{-1} , which we investigate in detail in Appendix 3A. They look similar to those obeying Dirichlet boundary conditions defined in Eqs. (3.26) and (3.38)–(3.40), but they must satisfy periodic boundary conditions (3.151) now:

$$G_{\mathbf{xx}}^{\mathbf{p}}(\tau, \tau') = \left[D_{\mathbf{xx}}(\tau, \tau') - \int_0^{\hbar\beta} d\tau_1 \int_0^{\hbar\beta} d\tau_2 D_{\mathbf{xp}}(\tau, \tau_1) D_{\mathbf{pp}}^{-1}(\tau_1, \tau_2) D_{\mathbf{px}}(\tau_2, \tau') \right]^{-1}, \quad (3.157)$$

$$G_{\mathbf{xp}}^{\mathbf{p}}(\tau, \tau') = - \int_0^{\hbar\beta} d\tau_1 \int_0^{\hbar\beta} d\tau_2 G_{\mathbf{xx}}^{\mathbf{p}}(\tau, \tau_1) D_{\mathbf{xp}}(\tau_1, \tau_2) D_{\mathbf{pp}}^{-1}(\tau_2, \tau'), \quad (3.158)$$

$$G_{\mathbf{px}}^{\mathbf{p}}(\tau, \tau') = [G_{\mathbf{xp}}^{\mathbf{p}}]^T(\tau', \tau) = - \int_0^{\hbar\beta} d\tau_1 \int_0^{\hbar\beta} d\tau_2 D_{\mathbf{pp}}^{-1}(\tau, \tau_1) D_{\mathbf{px}}(\tau_1, \tau_2) G_{\mathbf{xx}}^{\mathbf{p}}(\tau_2, \tau'), \quad (3.159)$$

$$G_{\mathbf{pp}}^{\mathbf{p}}(\tau, \tau') = D_{\mathbf{pp}}^{-1}(\tau, \tau') + \int_0^{\hbar\beta} d\tau_1 \cdots \int_0^{\hbar\beta} d\tau_4 \\ \times D_{\mathbf{pp}}^{-1}(\tau, \tau_1) D_{\mathbf{px}}(\tau_1, \tau_2) G_{\mathbf{xp}}^{\mathbf{p}}(\tau_2, \tau_3) D_{\mathbf{xp}}(\tau_3, \tau_4) D_{\mathbf{pp}}^{-1}(\tau_4, \tau'). \quad (3.160)$$

In the following, we specify these Green functions in the example of the one-dimensional harmonic oscillator.

3.6.2 The Harmonic Oscillator Revisited

As an illustration, we calculate the partition function and the periodic Green functions of the one-dimensional harmonic oscillator in the presence of external sources \mathbf{j} and \mathbf{v} (3.41). With the definitions (3.42), where we now omit the boundary terms for $D_{px}(\tau, \tau')$ due to the periodicity of the paths to be considered, the matrix S reads

$$S(\tau, \tau') = \frac{1}{\hbar} \begin{pmatrix} M\omega^2 & i\partial_\tau \\ -i\partial_\tau & M^{-1} \end{pmatrix} \delta(\tau - \tau'), \quad (3.161)$$

where $\partial_\tau \equiv \partial/\partial\tau$. Since only periodic paths must be considered, it is useful to transform the system to Fourier space. The completeness relation for the periodic eigenfunctions is

$$\delta(\tau - \tau') = \frac{1}{\hbar\beta} \sum_{m=-\infty}^{\infty} e^{-i\omega_m(\tau - \tau')}, \quad (3.162)$$

with Matsubara frequencies $\omega_m = 2\pi m/\hbar\beta$. Inserting this into (3.161), the Fourier representation of the matrix $S(\tau, \tau')$ becomes

$$S(\tau, \tau') = \frac{1}{\hbar\beta} \sum_{m=-\infty}^{\infty} S(\omega_m) e^{-i\omega_m(\tau - \tau')}, \quad (3.163)$$

where

$$S(\omega_m) = \begin{pmatrix} D_{xx} & D_{xp}(\omega_m) \\ D_{px}(\omega_m) & D_{pp} \end{pmatrix}. \quad (3.164)$$

Thus, the elements of this matrix are

$$D_{xx} = \frac{M\omega^2}{\hbar}, \quad D_{xp}(\omega_m) = \frac{\omega_m}{\hbar} = -D_{px}(\omega_m), \quad D_{pp} = \frac{1}{M\hbar}. \quad (3.165)$$

Combining these components according to the expressions (3.157)–(3.160), we obtain the periodic two-point correlation functions of the one-dimensional harmonic oscillator in Fourier space. Then, the back transformation in time space yields

$$G_{xx,\omega}^p(\tau, \tau') = \frac{1}{\hbar\beta} \sum_{m=-\infty}^{\infty} \frac{\hbar}{M} \frac{1}{\omega_m^2 + \omega^2} e^{-i\omega_m(\tau-\tau')} = \frac{\hbar}{2M\omega} \frac{\cosh \omega(|\tau - \tau'| - \hbar\beta/2)}{\sinh \hbar\beta\omega/2}, \quad (3.166)$$

$$\begin{aligned} G_{xp,\omega}^p(\tau, \tau') &= -\frac{1}{\hbar\beta} \sum_{m=-\infty}^{\infty} \frac{\hbar\omega_m}{\omega_m^2 + \omega^2} e^{-i\omega_m(\tau-\tau')} = -iM \frac{\partial}{\partial \tau} G_{xx,\omega}^p(\tau, \tau') \\ &= -\frac{i\hbar}{2} \left[\Theta(\tau - \tau') \frac{\sinh \omega(\tau - \tau' - \hbar\beta/2)}{\sinh \hbar\beta\omega/2} - \Theta(\tau' - \tau) \frac{\sinh \omega(\tau' - \tau - \hbar\beta/2)}{\sinh \hbar\beta\omega/2} \right] \end{aligned} \quad (3.167)$$

$$= -G_{px,\omega}^p(\tau, \tau') = G_{px,\omega}^p(\tau', \tau), \quad (3.168)$$

$$\begin{aligned} G_{pp,\omega}^p(\tau, \tau') &= \frac{1}{\hbar\beta} \sum_{m=-\infty}^{\infty} \frac{\hbar M \omega^2}{\omega_m^2 + \omega^2} e^{-i\omega_m(\tau-\tau')} = M^2 \omega^2 G_{xx,\omega}^p(\tau, \tau') \\ &= \frac{1}{2} \hbar\omega M \frac{\cosh \omega(|\tau - \tau'| - \hbar\beta/2)}{\sinh \hbar\beta\omega/2}. \end{aligned} \quad (3.169)$$

For the calculation of the prefactor in (3.155), we use the eigenvalue representation of the determinant of S

$$\begin{aligned} [\det S]^{-1/2} &= \left[\prod_{m=-\infty}^{\infty} \prod_{k=+,-} \lambda_k(\omega_m) \right]^{-1/2} = \exp \left(-\frac{1}{2} \text{Tr} \ln S \right) \\ &= \exp \left\{ -\frac{1}{2} \sum_{m=-\infty}^{\infty} [\ln \lambda_+(\omega_m) + \ln \lambda_-(\omega_m)] \right\}. \end{aligned} \quad (3.170)$$

The eigenvalues of $S(\omega_m)$ are determined from Eqs. (3.164) and (3.165). According to our rule to calculate determinants in units with $\hbar = \beta = M = 1$, this leads to

$$\lambda_{\pm}(\omega_m) = \frac{1}{2} (\omega^2 + 1) \pm \sqrt{\frac{1}{4} (\omega^2 + 1) - (\omega^2 + \omega_m^2)}. \quad (3.171)$$

In (3.170), we have also utilized the definition of the logarithm of matrices via the diagonal representation of $S(\omega_m)$,

$$\ln S_{\text{diag}}(\omega_m) = \begin{pmatrix} \ln \lambda_+(\omega_m) & 0 \\ 0 & \ln \lambda_-(\omega_m) \end{pmatrix}. \quad (3.172)$$

The use of the diagonal representation is possible, since the trace appearing in (3.170) is independent of the representation of S .

Inserting the eigenvalues (3.171) in (3.170), we find

$$[\det S]^{-1/2} = \exp \left\{ -\frac{1}{2} \ln \prod_{m=-\infty}^{\infty} [\omega^2 + \omega_m^2] \right\} = \exp \left\{ -\ln \omega - \ln \prod_{m=1}^{\infty} [\omega^2 + \omega_m^2] \right\}. \quad (3.173)$$

The product in the latter expression diverges, and we regularize it, similar to (3.62), with respect to the free particle. Thus, we obtain

$$[\det S]^{-1/2} = \frac{1}{\omega} \frac{\omega/2}{\sinh \omega/2}. \quad (3.174)$$

For vanishing currents, $j = v = 0$, this is just the partition function of the one-dimensional oscillator,

$$Z_{\omega} = Z_{\omega}[0, 0] = [\det S]^{-1/2} = \frac{1}{2 \sinh \hbar\beta\omega/2}, \quad (3.175)$$

where we have chosen again physical units by demanding that the argument of sinh and the partition function itself must be dimensionless. Combining this result with the exponential containing the currents in Eq. (3.156), we obtain

$$Z_\omega[j, v] = \frac{1}{2 \sinh \hbar\beta\omega/2} \exp \left\{ \frac{1}{2\hbar^2} \int_0^{\hbar\beta} d\tau \int_0^{\hbar\beta} d\tau' \left[j(\tau) G_{xx,\omega}^p(\tau, \tau') j(\tau') + j(\tau) G_{xp,\omega}^p(\tau, \tau') v(\tau') \right. \right. \\ \left. \left. + v(\tau) G_{px,\omega}^p(\tau, \tau') j(\tau') + v(\tau) G_{pp,\omega}^p(\tau, \tau') v(\tau') \right] \right\}, \quad (3.176)$$

where the periodic Green functions of the harmonic oscillator are given in Eqs. (3.166)–(3.169).

3.7 Perturbative Expansion for the Free Energy

The free energy of a quantum statistical system is obtained as the logarithm of the partition function

$$F = -\frac{1}{\beta} \ln Z. \quad (3.177)$$

If we assume that the action of the system has the form (3.80), the partition function is given by the phase space path integral

$$Z = \oint \mathcal{D}^d p \mathcal{D}^d x e^{-A[\mathbf{p}, \mathbf{x}]/\hbar}, \quad (3.178)$$

and cannot exactly be solved in general. Considering the decomposition of the action ratio (3.80) into an unperturbed term and the interaction, and expanding the Boltzmann factor with respect to the potential $V(\mathbf{p}(\tau), \mathbf{x}(\tau))$ into a Taylor series, we obtain the perturbative expansion

$$Z = Z_0 + \sum_{n=1}^{\infty} \frac{(-1)^n}{n! \hbar^n} \int_0^{\hbar\beta} d\tau_1 \cdots \int_0^{\hbar\beta} d\tau_n \langle V(\mathbf{p}(\tau_1), \mathbf{x}(\tau_1)) \cdots V(\mathbf{p}(\tau_n), \mathbf{x}(\tau_n)) \rangle_0. \quad (3.179)$$

The expectation values are defined with the help of the unperturbed path integral

$$\langle \cdots \rangle_0 = Z_0^{-1} \oint \mathcal{D}^d p \mathcal{D}^d x \cdots e^{-A_0[\mathbf{p}, \mathbf{x}]/\hbar}, \quad (3.180)$$

where

$$Z_0 = Z_0[0, 0] = \oint \mathcal{D}^d p \mathcal{D}^d x e^{-A_0[\mathbf{p}, \mathbf{x}]/\hbar} \quad (3.181)$$

is the partition function of the unperturbed system and its solution for vanishing currents is given by (3.156) with $\mathbf{j} = \mathbf{v} = 0$. With the definition of the expectation values (3.180), the periodic Green functions (3.157)–(3.160) can be expressed by the two-point correlation functions

$$G_{x_k, x_l}^p(\tau, \tau') = \langle x_k(\tau) x_l(\tau') \rangle_0, \quad (3.182)$$

$$G_{x_k, p_l}^p(\tau, \tau') = \langle x_k(\tau) p_l(\tau') \rangle_0, \quad (3.183)$$

$$G_{p_k, x_l}^p(\tau, \tau') = \langle p_k(\tau) x_l(\tau') \rangle_0, \quad (3.184)$$

$$G_{p_k, p_l}^p(\tau, \tau') = \langle p_k(\tau) p_l(\tau') \rangle_0. \quad (3.185)$$

We introduce cumulants, where the first two are

$$\langle V(\mathbf{p}(\tau_1), \mathbf{x}(\tau_1)) \rangle_{0,c} = \langle V(\mathbf{p}(\tau_1), \mathbf{x}(\tau_1)) \rangle_0, \quad (3.186)$$

$$\langle V(\mathbf{p}(\tau_1), \mathbf{x}(\tau_1)) V(\mathbf{p}(\tau_2), \mathbf{x}(\tau_2)) \rangle_{0,c} = \langle V(\mathbf{p}(\tau_1), \mathbf{x}(\tau_1)) V(\mathbf{p}(\tau_2), \mathbf{x}(\tau_2)) \rangle_0 \\ - \langle V(\mathbf{p}(\tau_1), \mathbf{x}(\tau_1)) \rangle_0 \langle V(\mathbf{p}(\tau_2), \mathbf{x}(\tau_2)) \rangle_0, \quad (3.187)$$

which enable us to find a suitable expression for the free energy from (3.179) by using (3.177). Thus, the perturbative expansion for the free energy reads

$$F = F_0 - \frac{1}{\beta} \sum_{n=1}^{\infty} \frac{(-1)^n}{n! \hbar^n} \int_0^{\hbar\beta} d\tau_1 \cdots \int_0^{\hbar\beta} d\tau_n \langle V(\mathbf{p}(\tau_1), \mathbf{x}(\tau_1)) \cdots V(\mathbf{p}(\tau_n), \mathbf{x}(\tau_n)) \rangle_{0,c}, \quad (3.188)$$

with the free energy of the unperturbed system

$$F_0 = -\frac{1}{\beta} \ln Z_0. \quad (3.189)$$

The free energy is the energy, which is available for a canonical thermodynamic system in a heat bath with volume V at temperature T to perform mechanical work. Thus, it is the portion of energy, which remains when the inner system energy U is reduced by the entropic energy TS . Assuming the system to be closed ($T = \text{const.}$, $V = \text{const.}$), the entropy S ensures that the number of possible configurations of the system, expressed by the partition function Z , is maximal at equilibrium for a certain temperature T . Since Z is at maximum for an equilibrated system, the free energy is minimum. This is what Eq. (3.177) states. Thus, it is plausible that thermodynamics requires the relation

$$F = U - TS. \quad (3.190)$$

Since the inner energy U is identical with the entire system energy E , and the system goes over into its ground state for zero temperature, the quantum mechanical limit $T \rightarrow 0$ ($\beta \rightarrow \infty$) of the free energy is equal to the ground-state energy $E^{(0)}$ of the system:

$$\lim_{\beta \rightarrow \infty} F = E^{(0)}. \quad (3.191)$$

This is easily seen for the example of the harmonic oscillator, whose free energy is $F_\omega = (1/\beta) \ln 2 \sinh \hbar\beta\omega/2$. For $\beta \rightarrow \infty$, $\sinh \hbar\beta\omega/2$ has the asymptotics $\exp(\hbar\beta\omega/2)/2$. Inserting this into the free energy yields $\lim_{\beta \rightarrow \infty} F_\omega = \hbar\omega/2 \equiv E_\omega^{(0)}$, which is the ground-state energy of the harmonic oscillator with one degree of freedom.

3A Algebraic Properties of Block Matrices

Consider a symmetric matrix consisting of block matrices A , B , and C ,

$$S = \begin{pmatrix} A & B \\ B^T & C \end{pmatrix} = S^T, \quad (3A.1)$$

where A and C are also symmetric matrices. In what follows we calculate the inverse of S . In a first step, we decompose the matrix into a product of triangular matrices. For regular matrix C , this means that C^{-1} exists, we choose

$$S = S_1 S_2, \quad S_1 = \begin{pmatrix} I_A & B \\ 0 & C \end{pmatrix}, \quad S_2 = \begin{pmatrix} X & 0 \\ C^{-1}B^T & I_C \end{pmatrix}, \quad (3A.2)$$

with the abbreviation

$$X = A - BC^{-1}B^T. \quad (3A.3)$$

In (3A.2), we have also introduced the identity matrices I_A and I_C , which act in the same space as A and C , respectively. The inverse of S is determined by

$$S^{-1} = (S_1 S_2)^{-1} = S_2^{-1} S_1^{-1}. \quad (3A.4)$$

Since $S_i S_i^{-1} = I_S$, $i = 1, 2$, we have to calculate

$$S_1 \begin{pmatrix} a_1 & b_1 \\ c_1 & d_1 \end{pmatrix} = I_S, \quad S_2 \begin{pmatrix} a_2 & b_2 \\ c_2 & d_2 \end{pmatrix} = I_S. \quad (3A.5)$$

The identity matrix

$$I_S = \begin{pmatrix} I_A & 0 \\ 0 & I_C \end{pmatrix} \quad (3A.6)$$

is composed of the identity matrices I_A and I_C . Thus, the determination of the elements of the inverse matrices S_1^{-1} and S_2^{-1} becomes simple and we obtain

$$S_1^{-1} = \begin{pmatrix} a_1 & b_1 \\ c_1 & d_1 \end{pmatrix} = \begin{pmatrix} X^{-1} & 0 \\ -C^{-1}B^T X^{-1} & I_C \end{pmatrix}, \quad S_2^{-1} = \begin{pmatrix} a_2 & b_2 \\ c_2 & d_2 \end{pmatrix} = \begin{pmatrix} I_A & -BC^{-1} \\ 0 & C^{-1} \end{pmatrix}. \quad (3A.7)$$

Multiplying both in the order given in Eq. (3A.4) yields the desired inverse of S

$$S^{-1} = \begin{pmatrix} X^{-1} & -X^{-1}BC^{-1} \\ -C^{-1}B^T X^{-1} & C^{-1} + C^{-1}B^T X^{-1}BC^{-1} \end{pmatrix}. \quad (3A.8)$$

For the calculation of the determinant of S , we use again the decomposition (3A.2). Then, the determinant of S is given by the product rule for matrices

$$\det S = \det S_1 \det S_2 = \det C \det X. \quad (3A.9)$$

If C is singular but A regular, we can make use of another decomposition than (3A.2):

$$S = \begin{pmatrix} I_A & 0 \\ B^T A^{-1} & \tilde{X} \end{pmatrix} \begin{pmatrix} A & B \\ 0 & I_C \end{pmatrix}, \quad (3A.10)$$

with

$$\tilde{X} = C - B^T A^{-1} B. \quad (3A.11)$$

Then, the inverse of S turns out to be

$$S^{-1} = \begin{pmatrix} A^{-1} + A^{-1} B \tilde{X}^{-1} B^T A^{-1} & -A^{-1} B \tilde{X}^{-1} \\ -\tilde{X}^{-1} B^T A^{-1} & -\tilde{X}^{-1} \end{pmatrix} \quad (3A.12)$$

and the determinant is

$$\det S = \det \tilde{X} \det A. \quad (3A.13)$$

3B Generalized Correlation Functions

In this appendix we give the expectations for the correlation between a general position or momentum dependent function and a polynomial up to order $n = 4$:

Position-Momentum-Coupling:

$$\int_0^1 d\tau_1 \int_0^1 d\tau_2 \langle F(\tilde{x}(\tau_1)) \tilde{p}(\tau_2) \rangle^{x_b, x_a} = \int_0^1 d\tau_1 \int_0^1 d\tau_2 G_{xp}^D(\tau_1, \tau_2) \langle F'(\tilde{x}(\tau_1)) \rangle^{x_b, x_a} \quad (3B.1)$$

$$\equiv \star \dashrightarrow \bullet ,$$

$$\int_0^1 d\tau_1 \int_0^1 d\tau_2 \langle F(\tilde{x}(\tau_1)) \tilde{p}^2(\tau_2) \rangle^{x_b, x_a} = \int_0^1 d\tau_1 \int_0^1 d\tau_2 \left\{ G_{pp}^D(\tau_2, \tau_2) \langle F(\tilde{x}(\tau_1)) \rangle^{x_b, x_a} + [G_{xp}^D(\tau_1, \tau_2)]^2 \langle F''(\tilde{x}(\tau_1)) \rangle^{x_b, x_a} \right\} \quad (3B.2)$$

$$\equiv \star \text{ (circle) } + \star \text{ (loop) } ,$$

$$\int_0^1 d\tau_1 \int_0^1 d\tau_2 \langle F(\tilde{x}(\tau_1)) \tilde{p}^3(\tau_2) \rangle^{x_b, x_a} = \int_0^1 d\tau_1 \int_0^1 d\tau_2 \left\{ 3 G_{xp}^D(\tau_1, \tau_2) G_{pp}^D(\tau_2, \tau_2) \langle F'(\tilde{x}(\tau_1)) \rangle^{x_b, x_a} + [G_{xp}^D(\tau_1, \tau_2)]^3 \langle F'''(\tilde{x}(\tau_1)) \rangle^{x_b, x_a} \right\} \quad (3B.3)$$

$$\equiv 3 \star \text{ (circle) } + \star \text{ (loop) } ,$$

$$\int_0^1 d\tau_1 \int_0^1 d\tau_2 \langle F(\tilde{x}(\tau_1)) \tilde{p}^4(\tau_2) \rangle^{x_b, x_a} = \int_0^1 d\tau_1 \int_0^1 d\tau_2 \left\{ [G_{pp}^D(\tau_2, \tau_2)]^2 \langle F(\tilde{x}(\tau_1)) \rangle^{x_b, x_a} + 6 [G_{xp}^D(\tau_1, \tau_2)]^2 G_{pp}^D(\tau_2, \tau_2) \langle F''(\tilde{x}(\tau_1)) \rangle^{x_b, x_a} + [G_{xp}^D(\tau_1, \tau_2)]^4 \langle F^{(4)}(\tilde{x}(\tau_1)) \rangle^{x_b, x_a} \right\} \quad (3B.4)$$

$$\equiv \star \text{ (two circles) } + 6 \star \text{ (loop) } + \star \text{ (loop) } ;$$

Momentum-Position-Coupling:

$$\int_0^1 d\tau_1 \int_0^1 d\tau_2 \langle F(\tilde{p}(\tau_1)) \tilde{x}(\tau_2) \rangle^{x_b, x_a} = \int_0^1 d\tau_1 \int_0^1 d\tau_2 G_{px}^D(\tau_1, \tau_2) \langle F'(\tilde{p}(\tau_1)) \rangle^{x_b, x_a} \quad (3B.5)$$

$$\equiv \star \dashrightarrow \bullet ,$$

$$\int_0^1 d\tau_1 \int_0^1 d\tau_2 \langle F(\tilde{p}(\tau_1)) \tilde{x}^2(\tau_2) \rangle^{x_b, x_a} = \int_0^1 d\tau_1 \int_0^1 d\tau_2 \left\{ G_{xx}^D(\tau_2, \tau_2) \langle F(\tilde{p}(\tau_1)) \rangle^{x_b, x_a} + [G_{px}^D(\tau_1, \tau_2)]^2 \langle F''(\tilde{p}(\tau_1)) \rangle^{x_b, x_a} \right\} \quad (3B.6)$$

$$\equiv \star \text{ (circle) } + \star \text{ (loop) } ,$$

$$\int_0^1 d\tau_1 \int_0^1 d\tau_2 \langle F(\tilde{p}(\tau_1)) \tilde{x}^3(\tau_2) \rangle^{x_b, x_a} = \int_0^1 d\tau_1 \int_0^1 d\tau_2 \left\{ 3 G_{px}^D(\tau_1, \tau_2) G_{xx}^D(\tau_2, \tau_2) \langle F'(\tilde{p}(\tau_1)) \rangle^{x_b, x_a} + [G_{px}^D(\tau_1, \tau_2)]^3 \langle F'''(\tilde{p}(\tau_1)) \rangle^{x_b, x_a} \right\} \quad (3B.7)$$

$$\equiv 3 \quad \star \text{---} \bullet \text{---} \bigcirc + \quad \star \text{---} \bullet \text{---} \bigcirc \text{---} \bullet \text{---} \star ,$$

$$\int_0^1 d\tau_1 \int_0^1 d\tau_2 \langle F(\tilde{p}(\tau_1)) \tilde{x}^4(\tau_2) \rangle^{x_b, x_a} = \int_0^1 d\tau_1 \int_0^1 d\tau_2 \left\{ [G_{xx}^D(\tau_2, \tau_2)]^2 \langle F(\tilde{p}(\tau_1)) \rangle^{x_b, x_a} + 6 [G_{px}^D(\tau_1, \tau_2)]^2 G_{xx}^D(\tau_2, \tau_2) \langle F''(\tilde{p}(\tau_1)) \rangle^{x_b, x_a} + [G_{px}^D(\tau_1, \tau_2)]^4 \langle F^{(4)}(\tilde{p}(\tau_1)) \rangle^{x_b, x_a} \right\} \quad (3B.8)$$

$$\equiv \star \quad \bigcirc \text{---} \bigcirc + 6 \quad \star \text{---} \bullet \text{---} \bigcirc \text{---} \bullet \text{---} \star + \quad \star \text{---} \bullet \text{---} \bigcirc \text{---} \bullet \text{---} \star ;$$

Momentum-Momentum-Coupling:

$$\int_0^1 d\tau_1 \int_0^1 d\tau_2 \langle F(\tilde{p}(\tau_1)) \tilde{p}(\tau_2) \rangle^{x_b, x_a} = \int_0^1 d\tau_1 \int_0^1 d\tau_2 G_{pp}^D(\tau_1, \tau_2) \langle F'(\tilde{p}(\tau_1)) \rangle^{x_b, x_a} \quad (3B.9)$$

$$\equiv \star \text{---} \bullet \text{---} \text{---} \bullet ,$$

$$\int_0^1 d\tau_1 \int_0^1 d\tau_2 \langle F(\tilde{p}(\tau_1)) \tilde{p}^2(\tau_2) \rangle^{x_b, x_a} = \int_0^1 d\tau_1 \int_0^1 d\tau_2 \left\{ G_{pp}^D(\tau_2, \tau_2) \langle F(\tilde{p}(\tau_1)) \rangle^{x_b, x_a} + [G_{pp}^D(\tau_1, \tau_2)]^2 \langle F''(\tilde{p}(\tau_1)) \rangle^{x_b, x_a} \right\} \quad (3B.10)$$

$$\equiv \star \quad \bullet \text{---} \text{---} \bullet + \quad \star \text{---} \bullet \text{---} \text{---} \bullet ,$$

$$\int_0^1 d\tau_1 \int_0^1 d\tau_2 \langle F(\tilde{p}(\tau_1)) \tilde{p}^3(\tau_2) \rangle^{x_b, x_a} = \int_0^1 d\tau_1 \int_0^1 d\tau_2 \left\{ 3 G_{pp}^D(\tau_1, \tau_2) G_{pp}^D(\tau_2, \tau_2) \langle F'(\tilde{p}(\tau_1)) \rangle^{x_b, x_a} + [G_{pp}^D(\tau_1, \tau_2)]^3 \langle F'''(\tilde{p}(\tau_1)) \rangle^{x_b, x_a} \right\} \quad (3B.11)$$

$$\equiv 3 \quad \star \text{---} \bullet \text{---} \text{---} \bullet + \quad \star \text{---} \bullet \text{---} \text{---} \bullet \text{---} \bullet ,$$

$$\int_0^1 d\tau_1 \int_0^1 d\tau_2 \langle F(\tilde{p}(\tau_1)) \tilde{p}^4(\tau_2) \rangle^{x_b, x_a} = \int_0^1 d\tau_1 \int_0^1 d\tau_2 \left\{ [G_{pp}^D(\tau_2, \tau_2)]^2 \langle F(\tilde{p}(\tau_1)) \rangle^{x_b, x_a} + 6 [G_{pp}^D(\tau_1, \tau_2)]^2 G_{pp}^D(\tau_2, \tau_2) \langle F''(\tilde{p}(\tau_1)) \rangle^{x_b, x_a} + [G_{pp}^D(\tau_1, \tau_2)]^4 \langle F^{(4)}(\tilde{p}(\tau_1)) \rangle^{x_b, x_a} \right\} \quad (3B.12)$$

$$\equiv \star \quad \bullet \text{---} \text{---} \bullet \text{---} \text{---} \bullet + 6 \quad \star \text{---} \bullet \text{---} \text{---} \bullet \text{---} \bullet + \quad \star \text{---} \bullet \text{---} \text{---} \bullet \text{---} \bullet \text{---} \bullet .$$

The case of position-position-coupling has already been calculated in Section 3.4.3.

Effective Classical Theory for Quantum Systems

We have shown in Section 3.3.1 that the quantum statistical density matrix can be expressed with the help of a bilocal potential $V_{\text{eff,cl}}(\mathbf{x}_b, \mathbf{x}_a)$, which makes the density matrix classically looking (3.83). In the following we will develop a similar formalism for the quantum statistical partition function and the free energy. Since the path integral counts all paths in phase space, which satisfy periodic boundary conditions $\mathbf{x}(0) = \mathbf{x}(\hbar\beta)$, we first investigate the Fourier decomposition of such paths, and the influence of the zero modes on the Green functions (3.157)–(3.160) [4,20]. Then, we consider the fluctuations of paths with fixed end points.

After having separated the zero-frequency Fourier modes, which lead to diverging correlations in the classical limit of high temperatures $\beta \equiv 1/k_B T \rightarrow 0$, we finally turn to the derivation of the smearing formula for restricted partition functions.

4.1 The Zero-Mode Problem

In order to illustrate the relation between zero-mode fluctuations and classical statistical properties more obviously, we consider, once more, the example of the harmonic oscillator with the action

$$\mathcal{A}_\omega[x] = \int_0^{\hbar\beta} d\tau \left[\frac{M}{2} \dot{x}^2(\tau) + \frac{1}{2} M \omega^2 x^2(\tau) \right], \quad (4.1)$$

where the dot means differentiation with respect to τ .

4.1.1 Harmonic Fluctuation Width for Periodic Paths

According to Eq. (3.175), the partition function of the harmonic oscillator with the action (4.1) is given by

$$Z_\omega = \oint \mathcal{D}x e^{-\mathcal{A}_\omega[x]/\hbar} = \frac{1}{2 \sinh \hbar\beta\omega/2}. \quad (4.2)$$

Correlation functions of local quantities $O_1(x(\tau_1))O_2(x(\tau_2))\cdots$ are then defined as

$$\langle O_1(x(\tau_1))O_2(x(\tau_2))\cdots \rangle_\omega = Z_\omega^{-1} \oint \mathcal{D}x O_1(x(\tau_1))O_2(x(\tau_2))\cdots e^{-\mathcal{A}_\omega[x]/\hbar}. \quad (4.3)$$

The path $x(\tau)$ shall be periodic: $x(0) = x(\hbar\beta)$. Thus, it can be expanded into the Fourier series

$$x(\tau) = x_0 + \sum_{m=1}^{\infty} (x_m e^{-i\omega_m \tau} + x_m^* e^{i\omega_m \tau}). \quad (4.4)$$

Here, we have separated the zero frequency component x_0 from the sum. Since the quantities $x(\tau)$, x_0 , and the fluctuations must be real, there is the constraint $x_m^* = x_{-m}$. The Matsubara frequencies are as usual $\omega_m = 2\pi m/\hbar\beta$.

Now, we integrate (4.4) over τ and divide the result by $\hbar\beta$. This entails

$$\overline{x(\tau)} \equiv \frac{1}{\hbar\beta} \int_0^{\hbar\beta} d\tau x(\tau) = x_0, \quad (4.5)$$

where the contribution of the fluctuations around x_0 vanishes as a consequence of the orthogonality relation

$$\delta_{nm} = \frac{1}{\hbar\beta} \int_0^{\hbar\beta} d\tau e^{i(\omega_n - \omega_m)\tau}. \quad (4.6)$$

From Eq. (4.5), we conclude that the temporal mean value of the path is identical with the zero-frequency component x_0 . In the following, we investigate the violence of these zero-mode fluctuations. First we calculate the particle distribution of the harmonic oscillator at a certain position $x = x(\tau)$. This yields

$$P(x) = \langle \delta(x - x(\tau)) \rangle_{\omega} = \frac{1}{\sqrt{2\pi a^2}} \exp\left(-\frac{x^2}{2a^2}\right), \quad (4.7)$$

where a is the Gaussian fluctuation width and is related to the Green function (3.166) for equal times:

$$a^2 = G_{xx}^p(\tau, \tau) = \frac{\hbar}{2M\omega} \coth \frac{\hbar\beta\omega}{2}. \quad (4.8)$$

At zero temperature, this is equal to the square of the ground-state wave function of the harmonic oscillator, whose width is

$$a_0^2 = \frac{\hbar}{2M\omega}. \quad (4.9)$$

In the limit $\hbar \rightarrow 0$, from Eqs. (4.7) and (4.8) we obtain the classical distribution

$$P_{\text{cl}}(x) = \frac{1}{\sqrt{2\pi a_{\text{cl}}^2}} \exp\left(-\frac{x^2}{2a_{\text{cl}}^2}\right), \quad (4.10)$$

with

$$a_{\text{cl}}^2 = \frac{1}{\beta M \omega^2}. \quad (4.11)$$

The linear growth of this classical width is the origin of the famous Dulong-Petit law for the specific heat of a harmonic system. The classical fluctuations are governed by the integral over the Boltzmann factor

$$e^{-\beta M \omega^2 x^2 / 2} \quad (4.12)$$

in the classical partition function

$$Z_{\text{cl}} = \int_{-\infty}^{\infty} \frac{dx}{\sqrt{2\pi\hbar^2\beta/M}} e^{-\beta M \omega^2 x^2 / 2}. \quad (4.13)$$

From this we obtain the classical distribution (4.10) as the expectation value

$$P_{\text{cl}}(x) = \langle \delta(x - \bar{x}) \rangle_{\omega, \text{cl}} = Z_{\text{cl}}^{-1} \int_{-\infty}^{\infty} \frac{d\bar{x}}{\sqrt{2\pi\hbar^2\beta/M}} \delta(x - \bar{x}) e^{-\beta M \omega^2 x^2 / 2}. \quad (4.14)$$

Which fluctuations cause the divergence of the Gaussian width (4.8) for high temperatures? In order to answer this question we exclude from the path integral (4.2) the zero-frequency contributions, which we have identified in (4.5) to be equal to the temporal mean value $\overline{x(\tau)}$ of the path. Thus, we define for each x_0 new local expectation values

$$\langle O_1(x(\tau_1))O_2(x(\tau_2))\cdots \rangle_\omega^{x_0} = \frac{\langle \delta(x_0 - \overline{x(\tau)})O_1(x(\tau_1))O_2(x(\tau_2))\cdots \rangle_\omega}{\langle \delta(x_0 - \overline{x(\tau)}) \rangle_\omega}. \quad (4.15)$$

The original quantum statistical distribution of the harmonic oscillator (4.7) collects fluctuations of $x_0 = \overline{x(\tau)}$ and those around x_0 , and can therefore be written as the convolution integral

$$P(x) = \int_{-\infty}^{\infty} dx_0 P_{x_0}(x - x_0)P_{cl}(x_0) \quad (4.16)$$

over the classical distribution (4.10) and the local one

$$P_{x_0}(x) = \langle \delta(x - x(\tau)) \rangle_\omega^{x_0} = \frac{1}{\sqrt{2\pi a_{x_0}^2}} \exp \left[-\frac{(x - x_0)^2}{2a_{x_0}^2} \right]. \quad (4.17)$$

Such a convolution of Gaussian distributions as in Eq. (4.16) leads to another Gaussian distribution with added widths, so that the width of the local distribution is given by the difference

$$a_{x_0}^2 = a^2 - a_{cl}^2 = \frac{\hbar}{2M\omega} \left(\coth \frac{\hbar\beta\omega}{2} - \frac{2}{\hbar\beta\omega} \right), \quad (4.18)$$

which starts out at the finite value (4.9) for $T = 1/k_B\beta = 0$, and goes to zero for $T \rightarrow \infty$ with the asymptotic behavior $\hbar\beta\omega/12$ (see Fig. 4.1). The latter property suppresses all fluctuations around $\overline{x(\tau)}$. Thus it turns out that the zero-frequency fluctuations x_0 lead to the divergence of the fluctuation width for $T \rightarrow \infty$. Such violent fluctuations cannot be treated by perturbation theory. They must be separated from the path integral (4.2) and integrated at the end of the calculation. Thus we shall revise the perturbative treatment for the free energy in Section 3.7.

4.1.2 Fluctuation Width for Fixed Ends

Now we dwell on the question how the fluctuation width behaves for a system with fixed ends. We consider the unnormalized density matrix $\tilde{\varrho}(x_b, x_a)$, which is expressed by the path integral

$$\tilde{\varrho}(x_b, x_a) = \int_{x(0)=x_a}^{x(\hbar\beta)=x_b} \mathcal{D}x e^{-\mathcal{A}[x]/\hbar} \quad (4.19)$$

over all paths with the fixed end points $x(0) = x_a$ and $x(\hbar\beta) = x_b$. For a harmonic oscillator (4.1), the path integral (4.19) can easily be done, with the result

$$\tilde{\varrho}_\omega(x_b, x_a) = \sqrt{\frac{M\omega}{2\pi\hbar \sinh \hbar\beta\omega}} \exp \left\{ -\frac{M\omega}{2\hbar \sinh \hbar\beta\omega} [(x_b^2 + x_a^2) \cosh \hbar\beta\omega - 2x_b x_a] \right\}. \quad (4.20)$$

At fixed end points x_b, x_a , the quantum mechanical correlation functions are

$$\langle O_1(x(\tau_1))O_2(x(\tau_2))\cdots \rangle_\omega^{x_b, x_a} = \frac{1}{\tilde{\varrho}_\omega(x_b, x_a)} \int_{x(0)=x_a}^{x(\hbar\beta)=x_b} \mathcal{D}x O_1(x(\tau_1))O_2(x(\tau_2))\cdots e^{-\mathcal{A}[x]/\hbar} \quad (4.21)$$

and the distribution function is found to be

$$p(x, \tau) \equiv \langle \delta(x - x(\tau)) \rangle_\omega^{x_b, x_a} = \frac{1}{\sqrt{2\pi b^2(\tau)}} \exp \left[-\frac{(x - x_{cl}(\tau))^2}{2b^2(\tau)} \right]. \quad (4.22)$$

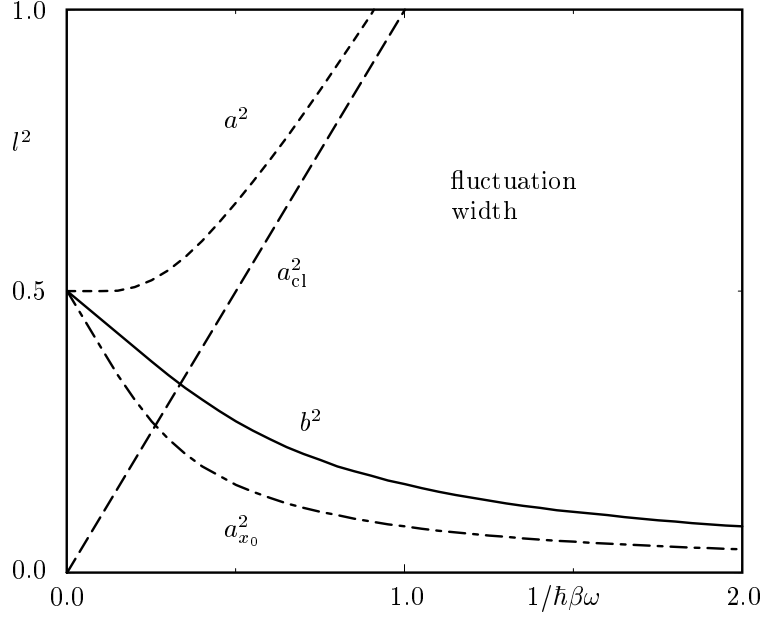


FIGURE 4.1: Temperature dependence of fluctuation widths of any point $x(\tau)$ on the path in a harmonic oscillator (l^2 is a square length in units of $\hbar/M\omega$). The quantity a^2 (dashed) is the quantum mechanical width, whereas $a_{x_0}^2$ (dash-dotted) is the width after separating out the fluctuations around the path average x_0 . The quantity a_{cl}^2 (long-dashed) is the width of the classical distribution, and b^2 (solid curve) is the fluctuation width at fixed ends.

The classical path of a particle in a harmonic potential is given by Eq. (3.47), and the time-dependent width $b^2(\tau)$ is found to be

$$b^2(\tau) = G_{xx}^D(\tau, \tau) = \frac{\hbar}{2M\omega} \left\{ \coth \hbar\beta\omega - \frac{\cosh[\omega(2\tau - \hbar\beta)]}{\sinh \hbar\beta\omega} \right\}, \quad (4.23)$$

and is thus identical with the harmonic equal-time Green function (3.54) for Dirichlet boundary conditions. Since the Euclidean time τ lies in the interval $0 \leq \tau \leq \hbar\beta$, the width (4.23) is bounded by

$$b^2(\tau) \leq \frac{\hbar}{2M\omega} \tanh \frac{\hbar\beta\omega}{2}, \quad (4.24)$$

thus remaining finite at all temperatures. The temporal average of (4.23) is

$$b^2 = \frac{1}{\hbar\beta} \int_0^{\hbar\beta} d\tau b^2(\tau) = \frac{\hbar}{2M\omega} \left(\coth \hbar\beta\omega - \frac{1}{\hbar\beta\omega} \right). \quad (4.25)$$

Just as $a_{x_0}^2$, this goes to zero for $T \rightarrow \infty$ with an asymptotic behavior $\hbar\beta\omega/6$, which is twice as big as that of $a_{x_0}^2$ (see Fig. 4.1). Because of the finiteness of the fluctuation width b^2 at all temperatures, which is similar to that of $a_{x_0}^2$, the special treatment of $\bar{x} = x_0$ becomes superfluous for paths with fixed end points x_b, x_a . While the separation of x_0 was necessary to deal with the diverging fluctuation width of the path average \bar{x} , paths with fixed ends have fluctuations of the path average, which are governed by the distribution

$$p_{x_0}(x_b, x_a) \equiv \langle \delta(x_0 - \bar{x}) \rangle_{\omega}^{x_b, x_a} = \frac{1}{\sqrt{2\pi b_{x_0}^2}} \exp \left\{ -\frac{1}{2b_{x_0}^2} \left[x_0 - \frac{1}{2}(x_b + x_a) \frac{2}{\hbar\beta\omega} \tanh \frac{\hbar\beta\omega}{2} \right]^2 \right\} \quad (4.26)$$

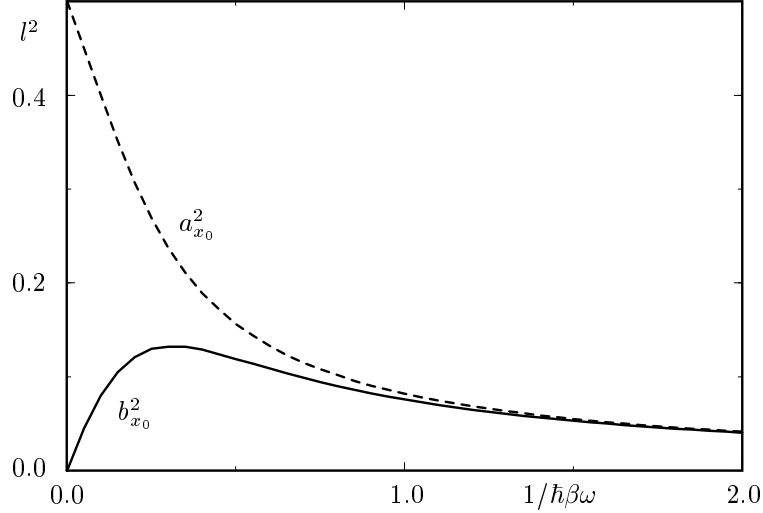


FIGURE 4.2: Temperature dependence of the width of fluctuations around the path average $x_0 = \bar{x}$ at fixed ends. For comparison we also show the width $a_{x_0}^2$ of Fig. 4.1. The vertical axis gives these square lengths l^2 in units of $\hbar/M\omega$ again.

with the width

$$b_{x_0}^2 = \frac{1}{M\beta\omega^2} \left[1 - \frac{2}{\hbar\beta\omega} \tanh \frac{\hbar\beta\omega}{2} \right], \quad (4.27)$$

which goes to zero for both limits $\beta \rightarrow \infty$ and $\beta \rightarrow 0$ (see Fig. 4.2). At each Euclidean time, $x(\tau)$ fluctuates narrowly around the classical path $x_{cl}(\tau)$ connecting x_b and x_a . This is the reason why we may treat the fluctuations of $\bar{x} = x_0$ by perturbation theory, just as the other fluctuations.

Thus there is no need for particularly treating certain fluctuations for quantities with fixed bounds.

4.2 Restricted Partition Function and Effective Classical Hamiltonian

As was shown in the previous section, a separate treatment of the zero-frequency fluctuations for periodic paths is necessary. We illustrate how this separation leads to a reformulation of quantum statistics, which is then governed by an effective classical Hamiltonian.

We rewrite the partition function

$$Z = \oint \mathcal{D}^d x \mathcal{D}^d p e^{-\mathcal{A}[\mathbf{p}, \mathbf{x}]/\hbar} \quad (4.28)$$

for an arbitrary system as

$$Z = \int \frac{d^d x_0 d^d p_0}{(2\pi\hbar)^d} e^{-\beta H_{\text{eff}}(\mathbf{p}_0, \mathbf{x}_0)} = \int \frac{d^d x_0 d^d p_0}{(2\pi\hbar)^d} Z^{\mathbf{p}_0 \mathbf{x}_0}, \quad (4.29)$$

where we have introduced the restricted partition function

$$Z^{\mathbf{p}_0 \mathbf{x}_0} = (2\pi\hbar)^d \oint \mathcal{D}^d x \mathcal{D}^d p \delta(\mathbf{p}_0 - \overline{\mathbf{p}(\tau)}) \delta(\mathbf{x}_0 - \overline{\mathbf{x}(\tau)}) e^{-\mathcal{A}[\mathbf{p}, \mathbf{x}]/\hbar}. \quad (4.30)$$

From (4.29) follows that the effective classical Hamiltonian $H_{\text{eff}}(\mathbf{p}_0, \mathbf{x}_0)$ and the restricted partition function $Z^{\mathbf{p}_0 \mathbf{x}_0}$ are related by

$$H_{\text{eff}}(\mathbf{p}_0, \mathbf{x}_0) = -\frac{1}{\beta} \ln Z^{\mathbf{p}_0 \mathbf{x}_0}. \quad (4.31)$$

This expression for the effective classical Hamiltonian has a similar form like a free energy, which is here local in phase space. Thus, we can also write

$$F^{\mathbf{p}_0 \mathbf{x}_0} \equiv H_{\text{eff}}(\mathbf{p}_0, \mathbf{x}_0). \quad (4.32)$$

Now we turn to the general Gaussian action (3.1), which we will use in the form (3.8), and calculate the restricted functional

$$\begin{aligned} Z_0^{\mathbf{w}_0}[\mathbf{C}] &= (2\pi\hbar)^d \oint \mathcal{D}^{2d}w \delta(\mathbf{w}_0 - \overline{\mathbf{w}(\tau)}) \\ &\times \exp \left[-\frac{1}{2} \int_0^{\hbar\beta} d\tau \int_0^{\hbar\beta} d\tau' \mathbf{w}^T(\tau) S(\tau, \tau') \mathbf{w}(\tau') - \frac{1}{\hbar} \int_0^{\hbar\beta} d\tau \mathbf{C}^T(\tau) \mathbf{w}(\tau) \right], \end{aligned} \quad (4.33)$$

with $\mathbf{w}^T(\tau) = (\mathbf{x}^T(\tau), \mathbf{p}^T(\tau))$ and $\mathbf{C}^T(\tau) = (\mathbf{j}^T(\tau), \mathbf{v}^T(\tau))$. The temporal mean value of $\mathbf{w}(\tau)$ is defined as before, $\overline{\mathbf{w}(\tau)} = \int_0^{\hbar\beta} d\tau \mathbf{w}(\tau) / \hbar\beta$. The symmetric matrix S is given by (3.10). There is no difficulty to calculate $Z_0^{\mathbf{w}_0}$. Along similar lines as in Section 3.5, we express the δ function by its Fourier transform

$$\delta(\mathbf{w}_0 - \overline{\mathbf{w}(\tau)}) = \int \frac{d^{2d}\mathbf{k}}{(2\pi)^{2d}} \exp \left[i\mathbf{w}_0^T \mathbf{k} - \frac{1}{\hbar} \int_0^{\hbar\beta} d\tau \mathbf{C}_0^T \mathbf{w}(\tau) \right], \quad (4.34)$$

where \mathbf{C}_0 is a constant current vector,

$$\mathbf{C}_0 = \frac{i}{\beta} \mathbf{k}. \quad (4.35)$$

The functional (4.33) becomes

$$\begin{aligned} Z_0^{\mathbf{w}_0}[\tilde{\mathbf{C}}] &= (2\pi\hbar)^d \int \frac{d^{2d}\mathbf{k}}{(2\pi)^{2d}} e^{i\mathbf{w}_0^T \mathbf{k}} \oint \mathcal{D}^{2d}w \\ &\times \exp \left[-\frac{1}{2} \int_0^{\hbar\beta} d\tau \int_0^{\hbar\beta} d\tau' \mathbf{w}^T(\tau) S(\tau, \tau') \mathbf{w}(\tau') - \frac{1}{\hbar} \int_0^{\hbar\beta} d\tau \tilde{\mathbf{C}}^T(\tau) \mathbf{w}(\tau) \right], \end{aligned} \quad (4.36)$$

where we have introduced the current

$$\tilde{\mathbf{C}}(\tau) = \mathbf{C}(\tau) + \mathbf{C}_0. \quad (4.37)$$

The path integral is calculated on equal footing as for the particle density (3.144) and yields an expression similar to the partition function (3.155). We obtain

$$Z_0^{\mathbf{w}_0}[\mathbf{C}] = \frac{(2\pi\hbar)^d}{\sqrt{\det S}} \int \frac{d^{2d}\mathbf{k}}{(2\pi)^{2d}} e^{i\mathbf{w}_0^T \mathbf{k}} \exp \left\{ \frac{1}{2\hbar^2} \int_0^{\hbar\beta} d\tau \int_0^{\hbar\beta} d\tau' \tilde{\mathbf{C}}^T(\tau) S^{-1}(\tau, \tau') \tilde{\mathbf{C}}(\tau') \right\}, \quad (4.38)$$

with the $2d$ -fold k integral still to be done. Re-expressing the current $\tilde{\mathbf{C}}$ by (4.37) and inserting (4.35), the integrations over k turn out to be simple Gaussian ones. Executing the usual procedure of completing the square, rotation in phase space to find a diagonal representation to decouple the k -components, and translation of the components of k enables us to solve the k integrals, yielding

$$Z_0^{\mathbf{w}_0}[\mathbf{C}] = \frac{1}{\sqrt{\det_{\text{ps}} B' \det S}} \exp \left\{ -\frac{\hbar^2 \beta^2}{2} \mathbf{w}_0^T B'^{-1} \mathbf{w}_0 - \beta \int_0^{\hbar\beta} d\tau \int_0^{\hbar\beta} d\tau' \mathbf{C}^T(\tau) S^{-1}(\tau, \tau') B'^{-1} \mathbf{w}_0 \right\}$$

$$\times \exp \left\{ \frac{1}{2\hbar^2} \int_0^{\hbar\beta} d\tau \int_0^{\hbar\beta} d\tau' \mathbf{C}^T(\tau) \left[S^{-1}(\tau, \tau') - \int_0^{\hbar\beta} d\tau_1 \int_0^{\hbar\beta} d\tau_2 S^{-1}(\tau, \tau_1) B'^{-1} S^{-1}(\tau_2, \tau') \right] \mathbf{C}(\tau') \right\}. \quad (4.39)$$

We have introduced the $2d \times 2d$ matrix

$$B' = \int_0^{\hbar\beta} d\tau \int_0^{\hbar\beta} d\tau' S^{-1}(\tau, \tau'), \quad (4.40)$$

which is constant in time and therefore its determinant is calculated in phase space only. This differs from the calculation of the determinant of S , which is done in phase and time space. A similar case has been considered below Eq. (3.153).

It is revealing to continue the discussion of the expressions (4.39) and (4.40) in frequency space. We write the matrix $S(\tau, \tau')$ and its inverse in Fourier space as

$$S(\tau, \tau') = \frac{1}{\hbar\beta} S_0 + \frac{1}{\hbar\beta} \sum_{m=1}^{\infty} \left[S(\omega_m) e^{-i\omega_m(\tau-\tau')} + S(-\omega_m) e^{i\omega_m(\tau-\tau')} \right], \quad (4.41)$$

$$S^{-1}(\tau, \tau') = \frac{1}{\hbar\beta} S_0^{-1} + \frac{1}{\hbar\beta} \sum_{m=1}^{\infty} \left[S^{-1}(\omega_m) e^{-i\omega_m(\tau-\tau')} + S^{-1}(-\omega_m) e^{i\omega_m(\tau-\tau')} \right], \quad (4.42)$$

where we have abbreviated the zero-frequency components by $S_0 \equiv S(\omega_m = 0)$ and $S_0^{-1} \equiv S^{-1}(\omega_m = 0)$, respectively. In particular, we are interested in time integrations of $S^{-1}(\tau, \tau')$. Inserting the Fourier decomposition the integration over one time argument yields the result

$$\int_0^{\hbar\beta} d\tau S^{-1}(\tau, \tau') = S_0^{-1}, \quad (4.43)$$

which is independent of time. This is obvious, since $S^{-1}(\tau, \tau') = S^{-1}(\tau - \tau')$ is invariant under translations of time. Thus, an additional integration of (4.43) over τ' only contributes a ‘‘volume factor’’ $\hbar\beta$:

$$\int_0^{\hbar\beta} d\tau' \int_0^{\hbar\beta} d\tau S^{-1}(\tau, \tau') = \hbar\beta S_0^{-1} \equiv B'. \quad (4.44)$$

An alternative representation is to use temporal mean values:

$$\overline{\overline{S^{-1}(\tau, \tau')}} = \frac{1}{\hbar^2 \beta^2} \int_0^{\hbar\beta} d\tau \int_0^{\hbar\beta} d\tau' S^{-1}(\tau, \tau') = \frac{1}{\hbar\beta} S_0^{-1}. \quad (4.45)$$

These results are very useful to simplify the expression (4.39). We obtain

$$\begin{aligned} Z_0^{\mathbf{w}_0}[\mathbf{C}] &= \frac{1}{\sqrt{\det_{\text{ps}} S_0^{-1} \det S}} \exp \left\{ -\frac{1}{2} \int_0^{\hbar\beta} d\tau \int_0^{\hbar\beta} d\tau' \mathbf{w}_0^T S(\tau, \tau') \mathbf{w}_0 - \frac{1}{\hbar} \int_0^{\hbar\beta} d\tau \mathbf{C}^T(\tau) \mathbf{w}_0 \right\} \\ &\times \exp \left\{ \frac{1}{2\hbar^2} \int_0^{\hbar\beta} d\tau \int_0^{\hbar\beta} d\tau' \mathbf{C}^T(\tau) G^{\mathbf{w}_0}(\tau, \tau') \mathbf{C}(\tau') \right\}, \end{aligned} \quad (4.46)$$

where the $2d \times 2d$ matrix $G^{\mathbf{w}_0}(\tau, \tau')$ of Green functions is defined as

$$G^{\mathbf{w}_0}(\tau, \tau') = S^{-1}(\tau, \tau') - \overline{\overline{S^{-1}(\tau, \tau')}} \equiv \begin{pmatrix} G_{\mathbf{xx}}^{\mathbf{p}_0 \mathbf{x}_0}(\tau, \tau') & G_{\mathbf{xp}}^{\mathbf{p}_0 \mathbf{x}_0}(\tau, \tau') \\ G_{\mathbf{px}}^{\mathbf{p}_0 \mathbf{x}_0}(\tau, \tau') & G_{\mathbf{pp}}^{\mathbf{p}_0 \mathbf{x}_0}(\tau, \tau') \end{pmatrix}. \quad (4.47)$$

The elements are $d \times d$ block matrices and identified with the Green functions (3.157)–(3.160) with *excluded* zero-frequency mode:

$$G_{\mathbf{xx}}^{\mathbf{p}_0 \mathbf{x}_0}(\tau, \tau') = G_{\mathbf{xx}}^{\mathbf{p}}(\tau, \tau') - \overline{\overline{G_{\mathbf{xx}}^{\mathbf{p}}(\tau, \tau')}} = G_{\mathbf{xx}}^{\mathbf{p}}(\tau, \tau') - G_{\mathbf{xx}, \text{cl}}^{\mathbf{p}}, \quad (4.48)$$

$$G_{\mathbf{x}\mathbf{p}}^{\mathbf{p}_0\mathbf{x}_0}(\tau, \tau') = G_{\mathbf{x}\mathbf{p}}^{\mathbf{p}}(\tau, \tau') - \overline{\overline{G_{\mathbf{x}\mathbf{p}}^{\mathbf{p}}(\tau, \tau')}} = G_{\mathbf{x}\mathbf{p}}^{\mathbf{p}}(\tau, \tau') - G_{\mathbf{x}\mathbf{p}, \text{cl}}^{\mathbf{p}}, \quad (4.49)$$

$$G_{\mathbf{p}\mathbf{x}}^{\mathbf{p}_0\mathbf{x}_0}(\tau, \tau') = G_{\mathbf{p}\mathbf{x}}^{\mathbf{p}}(\tau, \tau') - \overline{\overline{G_{\mathbf{p}\mathbf{x}}^{\mathbf{p}}(\tau, \tau')}} = G_{\mathbf{p}\mathbf{x}}^{\mathbf{p}}(\tau, \tau') - G_{\mathbf{p}\mathbf{x}, \text{cl}}^{\mathbf{p}} = G_{\mathbf{x}\mathbf{p}}^{\mathbf{p}_0\mathbf{x}_0}(\tau', \tau), \quad (4.50)$$

$$G_{\mathbf{p}\mathbf{p}}^{\mathbf{p}_0\mathbf{x}_0}(\tau, \tau') = G_{\mathbf{p}\mathbf{p}}^{\mathbf{p}}(\tau, \tau') - \overline{\overline{G_{\mathbf{p}\mathbf{p}}^{\mathbf{p}}(\tau, \tau')}} = G_{\mathbf{p}\mathbf{p}}^{\mathbf{p}}(\tau, \tau') - G_{\mathbf{p}\mathbf{p}, \text{cl}}^{\mathbf{p}}, \quad (4.51)$$

where we have used the identity of the zero-frequency component of the quantum statistical Green functions and the classical fluctuation width. As a consequence of the relations (4.31) and (4.32), and the zero-temperature limit (3.191), the restricted partition function (4.46) is the fundamental quantity, which enables us to calculate the free energy and the effective classical Hamiltonian of any system with Gaussian action. For later use, we introduce expectation values in phase space with the zero-frequency modes excluded in a similar manner as in Eq. (4.15). Defining the restricted partition function as the functional (4.46) with vanishing currents,

$$Z_0^{\mathbf{w}_0} \equiv Z_0^{\mathbf{w}_0}[0] = \frac{1}{\sqrt{\det_{\text{ps}} S_0^{-1} \det S}} \exp \left\{ -\frac{1}{2} \int_0^{\hbar\beta} d\tau \int_0^{\hbar\beta} d\tau' \mathbf{w}_0^T S(\tau, \tau') \mathbf{w}_0 \right\}, \quad (4.52)$$

the restricted expectation value for any quantity, which depends on position and/or momentum is expressed as

$$\langle \dots \rangle^{\mathbf{p}_0\mathbf{x}_0} = (2\pi\hbar)^d [Z_0^{\mathbf{w}_0}]^{-1} \oint \mathcal{D}^{2d} w \delta(\mathbf{w}_0 - \overline{\mathbf{w}(\tau)}) \dots \exp \left[-\frac{1}{2} \int_0^{\hbar\beta} d\tau \int_0^{\hbar\beta} d\tau' \mathbf{w}^T(\tau) S(\tau, \tau') \mathbf{w}(\tau') \right]. \quad (4.53)$$

Similar to the method of calculating expectation values and the results obtained in Section 3.2.3, we find that the one-point function is

$$\langle \mathbf{w}(\tau) \rangle^{\mathbf{p}_0\mathbf{x}_0} = \mathbf{w}_0, \quad (4.54)$$

and the two-point functions are evaluated as

$$\langle w_m(\tau) w_n(\tau') \rangle^{\mathbf{p}_0\mathbf{x}_0} = G_{w_m w_n}^{\mathbf{p}_0\mathbf{x}_0} + w_{0,m} w_{0,n}, \quad m, n = 1, \dots, 2d. \quad (4.55)$$

This makes it possible to rewrite the Green functions (4.48)–(4.51) as two-point correlation functions

$$\begin{aligned} G_{x_k x_l}^{\mathbf{p}_0\mathbf{x}_0}(\tau, \tau') &= \langle \tilde{x}_k(\tau) \tilde{x}_l(\tau') \rangle^{\mathbf{p}_0\mathbf{x}_0}, & G_{p_k p_l}^{\mathbf{p}_0\mathbf{x}_0}(\tau, \tau') &= \langle \tilde{p}_k(\tau) \tilde{p}_l(\tau') \rangle^{\mathbf{p}_0\mathbf{x}_0}, \\ G_{x_k p_l}^{\mathbf{p}_0\mathbf{x}_0}(\tau, \tau') &= \langle \tilde{x}_k(\tau) \tilde{p}_l(\tau') \rangle^{\mathbf{p}_0\mathbf{x}_0}, & G_{p_k x_l}^{\mathbf{p}_0\mathbf{x}_0}(\tau, \tau') &= \langle \tilde{p}_k(\tau) \tilde{x}_l(\tau') \rangle^{\mathbf{p}_0\mathbf{x}_0}, \end{aligned} \quad k, l = 1, \dots, d, \quad (4.56)$$

with abbreviations

$$\tilde{\mathbf{x}}(\tau) = \mathbf{x}(\tau) - \mathbf{x}_0, \quad \tilde{\mathbf{p}}(\tau) = \mathbf{p}(\tau) - \mathbf{p}_0. \quad (4.57)$$

For the calculation of an expectation value of a quantity, which is a nonpolynomial function F of \mathbf{x} or \mathbf{p} , we need the smearing formula. The derivation of this multiple convolution integral follows along a similar procedure as presented in Section 3.3.2 for the density matrix. We do not repeat it here and give only the result for the general case of a product of $N + M$ functions, where N of which may depend on \mathbf{x} and M on \mathbf{p} :

$$\begin{aligned} & \langle F_1(\mathbf{x}(\tau_1)) F_2(\mathbf{x}(\tau_2)) \dots F_N(\mathbf{x}(\tau_N)) F_{N+1}(\mathbf{p}(\tau_{N+1})) F_{N+2}(\mathbf{p}(\tau_{N+2})) \dots F_{N+M}(\mathbf{x}(\tau_{N+M})) \rangle^{\mathbf{p}_0\mathbf{x}_0} \\ &= \frac{1}{\sqrt{G^{\mathbf{p}_0\mathbf{x}_0}}} \prod_{n=1}^N \left[\int d^d x_n F_n(\mathbf{x}_n) \right] \prod_{m=1}^M \left[\frac{d^d p_m}{(2\pi\hbar)^d} F_{N+m}(\mathbf{p}_m) \right] \exp \left\{ -\frac{1}{2} \mathbf{y}^T [G^{\mathbf{p}_0\mathbf{x}_0}]^{-1} \mathbf{y} \right\}, \end{aligned} \quad (4.58)$$

where \mathbf{y} is the $(N + M)d$ -dimensional vector

$$\mathbf{y}^T = (\mathbf{x}_1(\tau_1) - \mathbf{x}_0, \dots, \mathbf{x}_N(\tau_N) - \mathbf{x}_0, \mathbf{p}_1(\tau_{N+1}) - \mathbf{p}_0, \dots, \mathbf{p}_M(\tau_{N+M}) - \mathbf{p}_0). \quad (4.59)$$

The $(N + M)d \times (N + M)d$ -matrix

$$G^{\mathbf{p}_0\mathbf{x}_0} = \begin{pmatrix} A & B \\ B^T & C \end{pmatrix} \quad (4.60)$$

is composed of the $Nd \times Nd$ -matrix A and the $Md \times Md$ -matrix C ,

$$A = \begin{pmatrix} G_{\mathbf{xx}}^{\mathbf{p}_0 \mathbf{x}_0}(\tau_1, \tau_1) & G_{\mathbf{xx}}^{\mathbf{p}_0 \mathbf{x}_0}(\tau_1, \tau_2) & \cdots & G_{\mathbf{xx}}^{\mathbf{p}_0 \mathbf{x}_0}(\tau_1, \tau_N) \\ G_{\mathbf{xx}}^{\mathbf{p}_0 \mathbf{x}_0}(\tau_1, \tau_2) & G_{\mathbf{xx}}^{\mathbf{p}_0 \mathbf{x}_0}(\tau_1, \tau_1) & \cdots & G_{\mathbf{xx}}^{\mathbf{p}_0 \mathbf{x}_0}(\tau_2, \tau_N) \\ \vdots & \vdots & \ddots & \vdots \\ G_{\mathbf{xx}}^{\mathbf{p}_0 \mathbf{x}_0}(\tau_1, \tau_N) & G_{\mathbf{xx}}^{\mathbf{p}_0 \mathbf{x}_0}(\tau_2, \tau_N) & \cdots & G_{\mathbf{xx}}^{\mathbf{p}_0 \mathbf{x}_0}(\tau_1, \tau_1) \end{pmatrix}, \quad (4.61)$$

$$C = \begin{pmatrix} G_{\mathbf{pp}}^{\mathbf{p}_0 \mathbf{x}_0}(\tau_1, \tau_1) & G_{\mathbf{pp}}^{\mathbf{p}_0 \mathbf{x}_0}(\tau_1, \tau_2) & \cdots & G_{\mathbf{pp}}^{\mathbf{p}_0 \mathbf{x}_0}(\tau_1, \tau_M) \\ G_{\mathbf{pp}}^{\mathbf{p}_0 \mathbf{x}_0}(\tau_1, \tau_2) & G_{\mathbf{pp}}^{\mathbf{p}_0 \mathbf{x}_0}(\tau_1, \tau_1) & \cdots & G_{\mathbf{pp}}^{\mathbf{p}_0 \mathbf{x}_0}(\tau_2, \tau_M) \\ \vdots & \vdots & \ddots & \vdots \\ G_{\mathbf{pp}}^{\mathbf{p}_0 \mathbf{x}_0}(\tau_1, \tau_M) & G_{\mathbf{pp}}^{\mathbf{p}_0 \mathbf{x}_0}(\tau_2, \tau_M) & \cdots & G_{\mathbf{pp}}^{\mathbf{p}_0 \mathbf{x}_0}(\tau_1, \tau_1) \end{pmatrix}, \quad (4.62)$$

as well as the $Nd \times Md$ -matrix

$$B = \begin{pmatrix} -G_{\mathbf{xp}}^{\mathbf{p}_0 \mathbf{x}_0}(\tau_1, \tau_1) & -G_{\mathbf{xp}}^{\mathbf{p}_0 \mathbf{x}_0}(\tau_1, \tau_2) & \cdots & -G_{\mathbf{xp}}^{\mathbf{p}_0 \mathbf{x}_0}(\tau_1, \tau_M) \\ -G_{\mathbf{xp}}^{\mathbf{p}_0 \mathbf{x}_0}(\tau_2, \tau_1) & -G_{\mathbf{xp}}^{\mathbf{p}_0 \mathbf{x}_0}(\tau_1, \tau_1) & \cdots & -G_{\mathbf{xp}}^{\mathbf{p}_0 \mathbf{x}_0}(\tau_2, \tau_M) \\ \vdots & \vdots & \ddots & \vdots \\ -G_{\mathbf{xp}}^{\mathbf{p}_0 \mathbf{x}_0}(\tau_N, \tau_1) & -G_{\mathbf{xp}}^{\mathbf{p}_0 \mathbf{x}_0}(\tau_N, \tau_2) & \cdots & -G_{\mathbf{xp}}^{\mathbf{p}_0 \mathbf{x}_0}(\tau_N, \tau_M) \end{pmatrix}. \quad (4.63)$$

The inverse and the determinant of the block matrix $G^{\mathbf{p}_0 \mathbf{x}_0}$ are calculated as described in Appendix 3A.

We calculate now the appropriate Green functions and the partition function (4.46) for the harmonic oscillator. The calculation of the Green functions with the zero-frequency components excluded is simply done, since we know the complete Green functions for the harmonic oscillator from Eqs. (3.166)–(3.169). Subtracting the twice-averaged terms, we obtain

$$G_{xx,\omega}^{p_0 x_0}(\tau, \tau') = G_{xx,\omega}^p(\tau, \tau') - \frac{1}{M\beta\omega^2}, \quad (4.64)$$

$$G_{xp,\omega}^{p_0 x_0}(\tau, \tau') = G_{xp,\omega}^p(\tau, \tau'), \quad (4.65)$$

$$G_{px,\omega}^{p_0 x_0}(\tau, \tau') = G_{px,\omega}^p(\tau, \tau'), \quad (4.66)$$

$$G_{pp,\omega}^{p_0 x_0}(\tau, \tau') = G_{pp,\omega}^p(\tau, \tau') - \frac{M}{\beta}. \quad (4.67)$$

The zero-frequency modes of the mixed two-point functions vanish. Thus, the matrix of the zero components simply reads

$$S_0 = \begin{pmatrix} M\hbar^{-1}\omega^2 & 0 \\ 0 & (\hbar M)^{-1} \end{pmatrix}. \quad (4.68)$$

The determinant is easily calculated and yields $\det_{\text{ps}} S_0 = \omega^2$ in units, where $\hbar = \beta = M = 1$. Together with the result (3.175) for the partition function of the harmonic oscillator, this gives the restricted partition function

$$Z_\omega^{p_0 x_0} = \frac{\hbar\beta\omega}{2 \sinh \hbar\beta\omega/2} \exp \left[-\beta \left(\frac{p_0^2}{2M} + \frac{1}{2} M\omega^2 x_0^2 \right) \right], \quad (4.69)$$

where the exponential contains the effective classical Hamiltonian of the harmonic oscillator, $H_{\text{eff},\omega} = p_0^2/2M + M\omega^2 x_0^2/2$. Performing the integral over the zero-frequency components x_0 and p_0 leads to the known partition function (3.175) of the harmonic oscillator.

Part II

Graphical Recursion Relations for Feynman Diagrams

Quantum Statistics

The free energy of a quantum statistical system with polynomial interaction can be considered as a functional of the free correlation function (3.182). As such it obeys a nonlinear functional differential equation which can be turned into a recursion relation [21–23]. This is solved order by order in the coupling constant of the interaction to find all connected vacuum diagrams with their proper multiplicities. The procedure is applied here to a system with quartic interaction as it occurs for the anharmonic oscillator or the double well. The results obtained with this method are, of course, the same as for a scalar field theory with a ϕ^4 self interaction.

All Feynman diagrams with external lines are obtained from functional derivatives of the connected vacuum diagrams with respect to the free correlation function. The recursive graphical construction can efficiently be automatized by computer algebra with the help of a unique matrix notation for the Feynman diagrams [23].

5.1 Introduction

Within the path integral (3.178) for the partition function Z we have expanded the Boltzmann factor of the action into a Taylor series with respect to the potential and obtained the general perturbative expansion (3.188) for the free energy F of a quantum statistical system. The perturbative coefficients are mainly determined by the time integrals over the connected correlation functions of the potential. As known from the “ordinary” Wick rule, presented for the density matrix in Section 3.4.1, these correlation functions can easily be decomposed into products of two-point functions, if the potential is of polynomial type. For the expansion of the free energy (3.188), the two-point correlation functions (3.182)–(3.185) must be used.

Since the number of contributions to the perturbative coefficients rapidly increases from order to order, it is troublesome to write them down for high orders. Moreover, many contributions are identical. The number of such repetitions is called the *multiplicity* of this contribution. It was a main simplification, when Feynman introduced his pictorial representation. The two-point correlation functions were displayed by lines with ends representing the time arguments of these two-point functions. Lines with joint end points are connected. The joint point is integrated over and is called *vertex*. In diagrams for interacting quantum fields, particles hit each other in these interaction points. Examples for the decomposition of a second-order perturbation contribution for a quartic potential into Feynman diagrams are given in Eqs. (3.140) and (3.141).

In order to circumvent the use of the lengthy analytic description of perturbative contributions for the construction of Feynman diagrams, one can approach from a topological point of view. In

any order, which is in our case characterized by the number of vertices, all topologically different diagrams having the appropriate number of vertices and obeying the condition that the number of legs connected by a vertex is identical with the polynomial degree of the potential contribute to the perturbative coefficient of this order. The multiplicity of each Feynman diagram follows combinatorially from its symmetry interchanging its lines and vertices. Although the topological point of view is a main progress in comparison with the naive analytic description of perturbative coefficients, it remains a tedious task to determine all possible topologically different diagrams and their correct multiplicities of a high-order perturbative coefficient. There exist various convenient computer programs, for instance *FeynArts* [24,25] or *QGRAF* [26], for constructing and counting Feynman graphs in different field theories. These programs are based on a combinatorial enumeration of all possible ways of connecting vertices by lines according to Feynman's rules.

We develop an alternative systematic approach to construct all topologically different Feynman diagrams with their multiplicities. It relies on considering a Feynman diagram as a functional of its graphical elements, i.e. its lines and vertices. Functional derivatives with respect to these elements are represented by graphical operations which remove lines or vertices of a Feynman diagram in all possible ways. With these operations, our approach proceeds in two steps. First the connected vacuum diagrams are constructed as solutions of a graphical recursion relation derived from a nonlinear functional differential equation. In a second step, all connected diagrams with external lines are obtained from functional derivatives of the connected vacuum diagrams with respect to the free correlation function. The recursion relation enables one to automatize the process of constructing Feynman diagrams and to count the multiplicity with the help of an efficient computer algorithm which is based on a practical matrix notation for these diagrams [23].

In the following, the graphical recursion relation for the free energy of a system with x^4 potential is derived and graphically solved.

5.2 Systematic Construction of Feynman Diagrams for the Quartic Oscillator Free Energy

In order to illustrate the power of the recursive graphical construction for Feynman diagrams for quantum statistical systems with polynomial interaction, we consider the quartic oscillator in one dimension, whose thermal fluctuations are controlled by a path integral

$$Z = \oint \mathcal{D}x e^{-\mathcal{A}[x]} \quad (5.1)$$

over the Boltzmann factor containing the action

$$\mathcal{A}[x] = \frac{1}{2} \int_{12} x_1 G_{12}^{-1} x_2 + \frac{g}{4!} \int_{1234} V_{1234} x_1 x_2 x_3 x_4 \quad (5.2)$$

with some coupling constant g . In this short-hand notation, where we have also used natural units ($\hbar = k_B = M = 1$), the argument of the coordinate x , the bilocal kernel G^{-1} , and the quartic interaction V are indicated by simple number indices, i.e.

$$x_i \equiv x(\tau_i), \quad \int_i \equiv \int_0^1 d\tau_i, \quad G_{12}^{-1} \equiv G^{-1}(\tau_1, \tau_2), \quad V_{1234} \equiv V(\tau_1, \tau_2, \tau_3, \tau_4). \quad (5.3)$$

The kernel is a functional matrix G^{-1} , while V is a functional tensor, both being symmetric in their indices.

In the following we shall leave G^{-1} and V completely general, except for the symmetry with respect to their indices, and insert the physical values

$$G^{-1}(\tau_1, \tau_2) = \left(-\frac{\partial^2}{\partial \tau_1^2} + \omega^2 \right) \delta(\tau_1 - \tau_2), \quad V(\tau_1, \tau_2, \tau_3, \tau_4) = \delta(\tau_1 - \tau_2) \delta(\tau_1 - \tau_3) \delta(\tau_1 - \tau_4) \quad (5.4)$$

at the end.

We may evaluate the partition function (5.1) perturbatively as a power series in the coupling constant g . From this we obtain the functional $W = \ln Z$, which is related to the free energy F of the system by $W = -\beta F$, as an expansion

$$W = \sum_{p=0}^{\infty} \frac{1}{p!} \left(\frac{-g}{4!} \right)^p W^{(p)}. \tag{5.5}$$

The coefficients $W^{(p)}$ may be displayed as connected vacuum diagrams constructed from lines and vertices. Each line represents a free correlation function

$$1 \text{ --- } 2 \equiv G_{12}, \tag{5.6}$$

which is the functional inverse of the kernel G^{-1} in the energy functional (5.2), defined by

$$\int_2 G_{12} G_{23}^{-1} = \delta_{13}. \tag{5.7}$$

The vertices represent an integral over the interaction

$$\text{X} \equiv \int_{1234} V_{1234}. \tag{5.8}$$

To construct all connected vacuum diagrams contributing to $W^{(p)}$ to each order p in perturbation theory, one connects p vertices with $4p$ legs in all possible ways according to Feynman's rules which follow from Wick's expansion of correlation functions into a sum of all pair contractions. This yields an increasing number of Feynman diagrams, each with a certain multiplicity which follows from combinatorics. In total there are $4!^p p!$ ways of ordering the $4p$ legs of the p vertices. This number is reduced by permutations of the legs and the vertices which leave a vacuum diagram invariant. Denoting the number of self, double, triple and fourfold connections with S, D, T, F , there are $2!^S, 2!^D, 3!^T, 4!^F$ leg permutations. An additional reduction arises from the number N of identical vertex permutations, where the vertices remain attached to the lines emerging from them in the same way as before. The resulting multiplicity of a connected vacuum diagram in the ϕ^4 theory is therefore given by the formula [5,27]

$$M^{E=0} = \frac{4!^p p!}{2!^{S+D} 3!^T 4!^F N}, \tag{5.9}$$


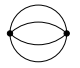
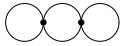

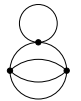
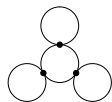

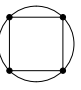
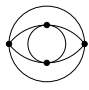
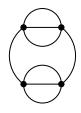
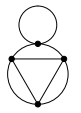
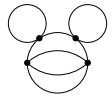
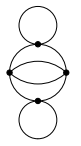
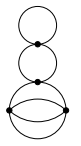
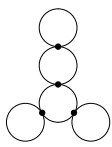
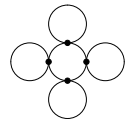
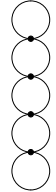
where $E = 0$ records that the number of external legs of vacuum diagrams is zero. The diagrammatic representation of the coefficients $W^{(p)}$ in the expansion (5.5) of the quantity W is displayed in Table 5.1 up to five loops [28–30]. For higher orders, the factorially increasing number of diagrams makes it more and more difficult to construct all topologically different diagrams and to count their multiplicities. In particular, it becomes quite hard to identify by inspection the number N of identical vertex permutations. This identification problem is solved by introducing a unique matrix notation for the graphs [23].

In the following, we shall generate iteratively all connected vacuum diagrams. We start by identifying graphical operations associated with functional derivatives with respect to the kernel G^{-1} , or the propagator G . Then we show that these operations can be applied to the one-loop contribution of the free partition function to generate all perturbative contributions to the partition function (5.1). After deriving a nonlinear functional differential equation for W , its graphical solution yields all connected vacuum diagrams order by order in the coupling strength.

5.2.1 Basic Graphical Operations

Each Feynman diagram is composed of integrals over products of free correlation functions G and may thus be considered as a functional of the kernel G^{-1} . The connected vacuum diagrams satisfy a

TABLE 5.1: Connected vacuum diagrams and their multiplicities of the x^4 theory up to five loops. Each diagram is characterized by the vector $(S, D, T, F; N)$ whose components specify the number of self, double, triple and fourfold connections, and of the identical vertex permutations leaving the vacuum diagram unchanged, respectively.

p	$W(p)$									
1	#1 3 (2,1,0,0;1) 									
2	#2 24 (0,0,0,1;2) 					#3 72 (2,1,0,0;2) 				
3	#4 1728 (0,3,0,0;6) 	#5 3456 (1,0,1,0;2) 	#6 1728 (3,0,0,0;6) 	#7 2592 (2,2,0,0;2) 						
4	#8 62208 (0,4,0,0;8) 	#9 248832 (0,2,0,0;8) 	#10 55296 (0,0,2,0;4) 	#11 497664 (1,2,0,0;2) 	#12 165888 (2,0,1,0;2) 	#13 248832 (2,1,0,0;4) 	#14 165888 (1,1,1,0;2) 	#15 248832 (3,1,0,0;2) 	#16 62208 (4,0,0,0;8) 	#17 124416 (2,3,0,0;2) 

certain functional differential equation, from which they will be constructed recursively. This will be done by a graphical procedure, for which we set up the necessary graphical rules now. First we observe that functional derivatives with respect to the kernel G^{-1} or to the free propagator G correspond to the graphical prescriptions of cutting or of removing a single line of a diagram in all possible ways, respectively.

Cutting Lines

Since x is a real scalar coordinate, the kernel G^{-1} is a symmetric functional matrix. This property has to be taken into account when performing functional derivatives with respect to the kernel G^{-1} , whose basic rule is

$$\frac{\delta G_{12}^{-1}}{\delta G_{34}^{-1}} = \frac{1}{2} \{ \delta_{13} \delta_{42} + \delta_{14} \delta_{32} \}. \quad (5.10)$$

From the identity (5.7) and the functional chain rule, we find the effect of this derivative on the free correlation function

$$-2 \frac{\delta G_{12}}{\delta G_{34}^{-1}} = G_{13} G_{42} + G_{14} G_{32} \quad (5.11)$$

which has the graphical representation

$$-2 \frac{\delta}{\delta G_{34}^{-1}} \text{1} \text{---} \text{2} = \text{1} \text{---} \text{3} \text{---} \text{4} \text{---} \text{2} + \text{1} \text{---} \text{4} \text{---} \text{3} \text{---} \text{2} . \quad (5.12)$$

Thus differentiating a propagator with respect to the kernel G^{-1} amounts to cutting the associated line into two pieces. The differentiation rule (5.10) ensures that the spatial indices of the kernel are symmetrically attached to the newly created line ends in the two possible ways. When differentiating a general Feynman integral with respect to G^{-1} , the product rule of functional differentiation leads to a sum of diagrams in which each line is cut once.

With this graphical operation, the product of two fields can be rewritten as a derivative of the action with respect to the kernel

$$x_1 x_2 = 2 \frac{\delta \mathcal{A}[x]}{\delta G_{12}^{-1}}, \quad (5.13)$$

as follows directly from (5.2) and (5.10). Applying the substitution rule (5.13) to the functional integral for the fully interacting two-point function

$$\mathbf{G}_{12} = \frac{1}{Z} \int \mathcal{D}x \, x_1 x_2 e^{-\mathcal{A}[x]}, \quad (5.14)$$

we obtain the fundamental identity

$$\mathbf{G}_{12} = -2 \frac{\delta W}{\delta G_{12}^{-1}}. \quad (5.15)$$

Thus, by cutting a line of the connected vacuum diagrams in all possible ways, we obtain all diagrams of the fully interacting two-point function. Analytically this has a Taylor series expansion in powers of the coupling constant g similar to (5.5)

$$\mathbf{G}_{12} = \sum_{p=0}^{\infty} \frac{1}{p!} \left(\frac{-g}{4!} \right)^p \mathbf{G}_{12}^{(p)} \quad (5.16)$$

with coefficients

$$\mathbf{G}_{12}^{(p)} = -2 \frac{\delta W^{(p)}}{\delta G_{12}^{-1}}. \quad (5.17)$$

The cutting prescription (5.17) converts the vacuum diagrams of p th order in the coefficients $W^{(p)}$ in Table 5.1 to the corresponding ones in the coefficients $\mathbf{G}_{12}^{(p)}$ of the two-point function. The results are shown in Table 5.2 up to four loops. The numbering of diagrams used in Table 5.2 reveals from which connected vacuum diagrams they are obtained by cutting a line.

For instance, the diagrams #15.1–#15.5 and their multiplicities in Table 5.2 follow from the connected vacuum diagram #15 in Table 5.1. We observe that the multiplicity of a diagram of a two-point function obeys a formula similar to (5.9):

$$M^{E=2} = \frac{4!^p p! 2!}{2!^{S+D} 3!^T N}. \quad (5.18)$$

In the numerator, the $4!^p p!$ permutations of the $4p$ legs of the p vertices are multiplied by a factor $2!$ for the permutations of the two end points of the two-point function. The number N in the denominator counts the identical permutations of both the p vertices and the two end points.


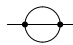
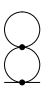

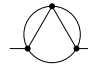
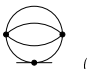
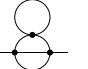

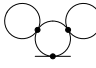

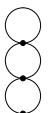
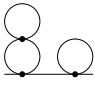
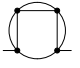
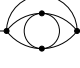
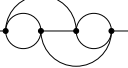
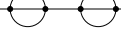
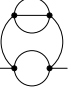

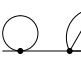
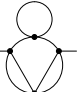
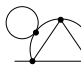
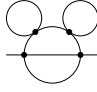
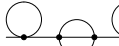
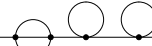
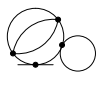
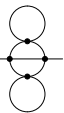
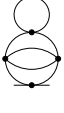
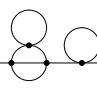
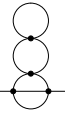
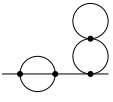
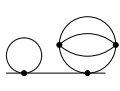
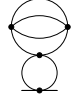
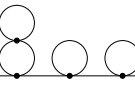
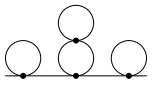
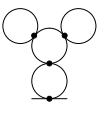
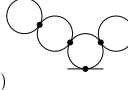
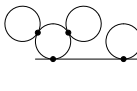
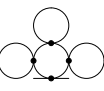
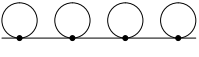

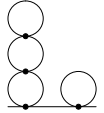
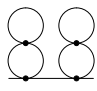
Performing a differentiation of the two-point function (5.14) with respect to the kernel G^{-1} yields

$$-2 \frac{\delta \mathbf{G}_{12}}{\delta G_{34}^{-1}} = \mathbf{G}_{1234} - \mathbf{G}_{12} \mathbf{G}_{34}, \quad (5.19)$$

where \mathbf{G}_{1234} denotes the fully interacting four-point function

$$\mathbf{G}_{1234} = \frac{1}{Z} \int \mathcal{D}x \, x_1 x_2 x_3 x_4 e^{-\mathcal{A}[x]}. \quad (5.20)$$

TABLE 5.2: Connected diagrams of the two-point function and their multiplicities of the x^4 theory up to four loops. Each diagram is characterized by the vector $(S, D, T; N)$ whose components specify the number of self, double, triple connections, and of the combined permutations of vertices and external lines leaving the diagram unchanged, respectively.

p	$G_{12}^{(p)}$									
1	#1.1 12 (1,0,0;2)									
2	#2.1 192 (0,0,1;2)		#3.1 288 (1,1,0;2)		#3.2 288 (2,0,0;2)					
3	#4.1 20736 (0,2,0;2)		#5.1 6912 (0,0,1;4)		#5.2 20736 (1,1,0;2)		#5.3 13824 (1,0,1;1)			
	#6.1 10368 (2,0,0;4)		#6.2 10368 (3,0,0;2)		#7.1 10368 (1,2,0;2)		#7.2 20736 (2,1,0;1)			
4	#8.1 995328 (0,3,0;2)		#9.1 1990656 (0,1,0;4)		#9.2 1990656 (0,2,0;2)		#10.1 221184 (0,0,2;2)		#10.2 663552 (0,1,1;2)	
	#11.1 995328 (0,2,0;4)		#11.2 1990656 (1,2,0;1)		#11.3 995328 (1,2,0;2)		#11.4 3981312 (1,1,0;1)		#12.1 995328 (2,1,0;2)	
	#12.2 331776 (2,0,1;2)		#12.3 663552 (2,0,1;1)		#12.4 663552 (1,0,1;2)		#13.1 995328 (2,0,0;4)		#13.2 995328 (1,1,0;4)	
	#13.3 1990656 (2,1,0;1)		#14.1 995328 (1,2,0;2)		#14.2 663552 (1,1,1;1)		#14.3 663552 (1,0,1;2)		#14.4 331776 (0,1,1;4)	
	#15.1 995328 (3,1,0;1)		#15.2 497664 (3,1,0;2)		#15.3 497664 (2,1,0;4)		#15.4 995328 (2,1,0;2)		#15.5 995328 (3,0,0;2)	
	#16.1 497664 (3,0,0;4)		#16.2 497664 (4,0,0;2)		#17.1 497664 (1,3,0;2)		#17.2 995328 (2,2,0;1)		#17.3 497664 (2,2,0;2)	

The term $\mathbf{G}_{12}\mathbf{G}_{34}$ in (5.19) subtracts a certain set of disconnected diagrams from \mathbf{G}_{1234} . By subtracting *all* disconnected diagrams from \mathbf{G}_{1234} , we obtain the connected four-point function

$$\mathbf{G}_{1234}^c \equiv \mathbf{G}_{1234} - \mathbf{G}_{12}\mathbf{G}_{34} - \mathbf{G}_{13}\mathbf{G}_{24} - \mathbf{G}_{14}\mathbf{G}_{23} \quad (5.21)$$

in the form

$$\mathbf{G}_{1234}^c = -2 \frac{\delta \mathbf{G}_{12}}{\delta G_{34}^{-1}} - \mathbf{G}_{13}\mathbf{G}_{24} - \mathbf{G}_{14}\mathbf{G}_{23}. \quad (5.22)$$

The first term contains all diagrams obtained by cutting a line in the diagrams of the two-point-function \mathbf{G}_{12} . The second and third terms remove from these the disconnected diagrams. In this way we obtain the perturbative expansion

$$\mathbf{G}_{1234}^c = \sum_{p=1}^{\infty} \frac{1}{p!} \left(\frac{-g}{4!} \right)^p \mathbf{G}_{1234}^{c,(p)} \quad (5.23)$$

with coefficients

$$\mathbf{G}_{1234}^{c,(p)} = -2 \frac{\delta \mathbf{G}_{12}^{(p)}}{\delta G_{34}^{-1}} - \sum_{q=0}^p \binom{p}{q} \left(\mathbf{G}_{13}^{(p-q)} \mathbf{G}_{24}^{(q)} + \mathbf{G}_{14}^{(p-q)} \mathbf{G}_{23}^{(q)} \right). \quad (5.24)$$

They are listed diagrammatically in Table 5.3 up to three loops. As before in Table 5.2, the multiple numbering in Table 5.3 indicates the origin of each diagram of the connected four-point function. For instance, the diagram #11.2.2, #11.4.3, #14.1.2, #14.3.3 in Table 5.3 stems together with its multiplicity from the diagrams #11.2, #11.4, #14.1, #14.3 in Table 5.2.

The multiplicity of each diagram of a connected four-point function obeys a formula similar to (5.18):

$$M^{E=4} = \frac{4!^p p! 4!}{2!^{S+D} 3!^T N}. \quad (5.25)$$

This multiplicity decomposes into equal parts if the spatial indices 1, 2, 3, 4 are assigned to the four end points of the connected four-point function, for instance:

$$62208 \quad \begin{array}{c} \diagup \quad \diagdown \\ \circ \quad \circ \\ \diagdown \quad \diagup \end{array} \equiv 20736 \begin{array}{c} 1 \quad 3 \\ \diagup \quad \diagdown \\ \circ \quad \circ \\ \diagdown \quad \diagup \\ 2 \quad 4 \end{array} + 20736 \begin{array}{c} 1 \quad 2 \\ \diagup \quad \diagdown \\ \circ \quad \circ \\ \diagdown \quad \diagup \\ 3 \quad 4 \end{array} + 20736 \begin{array}{c} 1 \quad 4 \\ \diagup \quad \diagdown \\ \circ \quad \circ \\ \diagdown \quad \diagup \\ 2 \quad 3 \end{array}. \quad (5.26)$$

Generalizing the multiplicities (5.9), (5.18), and (5.25) for connected vacuum diagrams, two- and four-point functions to an arbitrary connected correlation function with an even number E of end points, we see that

$$M^E = \frac{4!^p p! E!}{2!^{S+D} 3!^T 4!^F N}, \quad (5.27)$$

where N counts the number of permutations of vertices and external lines which leave the diagram unchanged.

Removing Lines

We now study the graphical effect of functional derivatives with respect to the free propagator G , where the basic differentiation rule (5.10) becomes

$$\frac{\delta G_{12}}{\delta G_{34}} = \frac{1}{2} \{ \delta_{13} \delta_{42} + \delta_{14} \delta_{32} \}. \quad (5.28)$$

We represent this graphically by extending the elements of Feynman diagrams by an open dot with two labeled line ends representing the δ function:

$$1 \text{ --- } 2 = \delta_{12}. \quad (5.29)$$

TABLE 5.3: Connected diagrams of the four-point function and their multiplicities of the x^4 theory up to four loops. Each diagram is characterized by the vector $(S, D, T; N)$ whose components specify the number of self, double, triple connections, and of the combined permutations of vertices and external lines leaving the diagram unchanged, respectively.


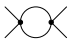
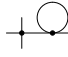

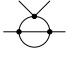

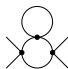
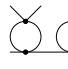
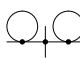
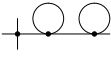
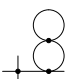

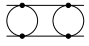

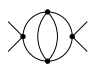
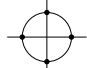
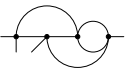
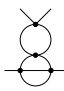
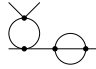
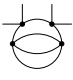
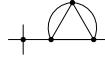
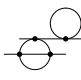
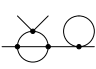
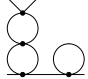
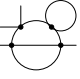
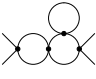
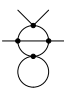
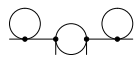
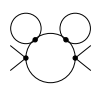
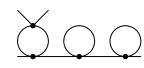
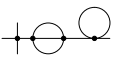

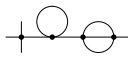
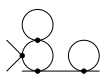
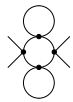
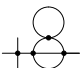
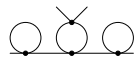
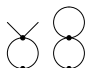
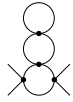
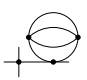
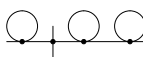
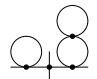
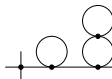
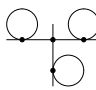
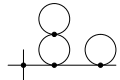
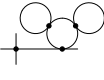
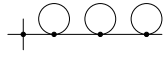
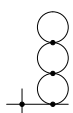
p	$G_{1234}^{c,(p)}$														
1	#1.1.1 24 (0,0,0;24) 														
2	#2.1.1, #3.1.1 1152,576 1728 (0,1,0;8) 	#3.1.2, #3.2.1 1152,1152 2304 (1,0,0;6) 													
3	#4.1.1, #7.1.1 41472,20736 62208 (0,2,0;8) 	#4.1.2, #5.1.1, #5.2.1 165888,41472,41472 248832 (0,1,0;4) 	#5.1.2, #5.3.2 27648,27648 55296 (0,0,1;6) 	#5.2.2, #6.1.1 82944,41472 124416 (1,0,0;8) 	#5.2.3, #5.3.1, #7.1.2, #7.2.1 82944,82944,41472,41472 248832 (1,1,0;2) 	#6.1.2, #6.2.2, #7.2.2 20736,20736,82944 124416 (2,0,0;4) 	#6.1.3, #6.2.1 41472,41472 82944 (2,0,0;6) 	#7.1.3, #7.2.3 41472,41472 82944 (1,1,0;6) 							
4	#8.1.1, #17.1.1 1990656,995328 2985984 (0,3,0;8) 	#8.1.2, #9.2.1, #10.2.1 3981312,3981312,3981312 11943936 (0,2,0;4) 	#8.1.3, #11.1.2, #11.3.1 7962624,1990656,1990656 11943936 (0,2,0;4) 	#9.1.1, #13.2.1 3981312,1990656 5971968 (0,1,0;16) 	#9.1.2 7962624 (0,0,0;24) 	#9.1.3, #9.2.3, #11.1.1, #11.4.1 15925248,15925248,7962624,7962624 47775744 (0,1,0;2) 	#9.2.2, #14.1.1, #14.4.3 7962624,1990656,1990656 11943936 (0,2,0;4) 	#10.1.1, #10.2.3, #14.2.1, #14.4.2 2654208,2654208,1327104,1327104 7962624 (0,1,1;2) 	#10.2.2, #12.4.1 2654208,1327104 3981312 (0,0,1;8) 	#11.1.3, #11.2.1 3981312,3981312 7962624 (0,2,0;6) 	#11.2.2, #11.4.3, #14.1.2, #14.3.3 7962624,7962624,3981312,3981312 23887872 (1,1,0;2) 	#11.2.3, #11.4.2, #13.2.2, #13.3.1 7962624,7962624,3981312,3981312 23887872 (1,1,0;2) 	#11.2.4, #11.3.2, #17.1.2, #17.2.1 3981312,3981312,1990656,1990656 11943936 (1,2,0;2) 	#11.3.3, #11.4.4, #12.1.1, #12.4.5 7962624,7962624,3981312,3981312 23887872 (1,1,0;2) 	#11.4.5, #15.3.1, #15.4.1 7962624,1990656,1990656 11943936 (1,1,0;4) 

Table 5.3 (Continued)

4	#11.4.6, #13.1.1, #13.2.3 15925248, 3981312, 3981312 23887872 (1,0,0:4)		#12.1.2, #12.2.2, #13.3.3, #17.2.2 1990656, 1990656, 3981312, 3981312 11943936 (2,1,0:2)		#12.1.3, #16.1.2 3981312, 1990656 5971968 (2,0,0:8)	
	#12.1.4, #12.3.3, #15.1.1, #15.3.2 3981312, 3981312, 1990656, 1990656 11943936 (2,1,0:2)		#12.2.1, #12.4.2 1327104, 1327104 2654208 (1,0,1:6)		#12.3.2, #12.4.3, #14.2.2, #14.3.2 1327104, 1327104, 2654208, 2654208 7962624 (1,0,1:2)	
	#12.3.1, #12.4.4 1327104, 1327104 2654208 (1,0,1:6)		#13.1.2, #13.3.4, #15.4.2, #15.5.1 7962624, 7962624, 3981312, 3981312 23887872 (2,0,0:2)		#13.1.3, #16.1.1 1990656, 995328 2985984 (2,0,0:16)	
	#13.2.4, #13.3.5 3981312, 3981312 7962624 (1,1,0:6)		#13.3.2, #15.2.1, #15.3.3 3981312, 995328, 995328 5971968 (2,1,0:4)		#14.1.3, #14.2.3, #17.1.3, #17.3.1 3981312, 3981312, 1990656, 1990656 11943936 (1,2,0:2)	
	#14.1.4, #15.4.4 3981312, 1990656 5971968 (1,1,0:8)		#14.3.1, #14.4.1 1327104, 1327104 2654208 (0,0,1:12)		#15.1.2, #15.5.3, #16.1.3, #16.2.2 3981312, 3981312, 1990656, 1990656 11943936 (3,0,0:2)	
	#15.1.3, #15.4.3, #17.2.3, #17.3.2 1990656, 1990656, 3981312, 3981312 11943936 (2,1,0:2)		#15.1.4, #15.4.5 1990656, 1990656 3981312 (2,1,0:6)		#15.2.2, #15.5.2 1990656, 1990656 3981312 (3,0,0:6)	
	#15.2.3, #15.4.6 1990656, 1990656 3981312 (2,1,0:6)		#15.3.4, #15.5.4 1990656, 1990656 3981312 (2,0,0:12)		#16.1.4, #16.2.1 1990656, 1990656 3981312 (3,0,0:6)	
			#17.1.4, #17.2.4 1990656, 1990656 3981312 (1,2,0:6)			

Thus we can write the differentiation (5.28) graphically as follows:

$$\frac{\delta}{\delta 3 \text{---} 4} 1 \text{---} 2 = \frac{1}{2} \left\{ 1 \text{---} 3 \quad 4 \text{---} 2 \quad + \quad 1 \text{---} 4 \quad 3 \text{---} 2 \right\}. \quad (5.30)$$

Differentiating a line with respect to the free correlation function removes the line, leaving in a symmetrized way the spatial indices of the free correlation function on the vertices to which the line was connected.

The effect of this derivative is illustrated by studying the diagrammatic effect of the operator

$$\hat{L} = \int_{12} G_{12} \frac{\delta}{\delta G_{12}}. \quad (5.31)$$

Applying \hat{L} to a connected vacuum diagram in $W^{(p)}$, the functional derivative $\delta/\delta G_{12}$ generates diagrams in each of which one of the $2p$ lines of the original vacuum diagram is removed. Subsequently, the removed lines are again reinserted, so that the connected vacuum diagrams $W^{(p)}$ are eigenfunctions

of \hat{L} , whose eigenvalues $2p$ count the lines of the diagrams:

$$\hat{L} W^{(p)} = 2p W^{(p)}. \quad (5.32)$$

As an example, take the explicit first-order expression for the vacuum diagrams, i.e.

$$W^{(1)} = 3 \int_{1234} V_{1234} G_{12} G_{34}, \quad (5.33)$$

and apply the basic rule (5.28), leading to the desired eigenvalue 2.

5.2.2 Perturbation Theory

We introduce an external current J into the functional (5.2) which is linearly coupled to the coordinate x . Thus the partition function (5.1) becomes the generating functional $Z[J]$ which allows us to find all free n -point functions from functional derivatives with respect to this external current J . Due to the shape of the functional (5.2) the expectation value of the coordinate x is zero and only correlation functions of an even number of coordinates are nonzero. To calculate all of these, it is possible to substitute two functional derivatives with respect to the current J by one functional derivative with respect to the kernel G^{-1} . This reduces the number of functional derivatives in each order of perturbation theory by one half and has the additional advantage that the introduction of the current J becomes superfluous.

Current Approach

Recall briefly the standard perturbative treatment, in which the energy functional (5.2) is artificially extended by a source term

$$\mathcal{A}[x, J] = \mathcal{A}[x] - \int_1 J_1 x_1. \quad (5.34)$$

The functional integral for the generating functional

$$Z[J] = \int \mathcal{D}x e^{-\mathcal{A}[x, J]} \quad (5.35)$$

is first explicitly calculated for a vanishing coupling constant g , yielding

$$Z^{(0)}[J] = \exp \left\{ -\frac{1}{2} \text{Tr} \ln G^{-1} + \frac{1}{2} \int_{12} J_1 G_{12} J_2 \right\}, \quad (5.36)$$

where the trace of the logarithm of the kernel is defined by the series [31]

$$\text{Tr} \ln G^{-1} = \sum_{n=1}^{\infty} \frac{(-1)^{n+1}}{n} \int_{1\dots n} \{G_{12}^{-1} - \delta_{12}\} \cdots \{G_{n1}^{-1} - \delta_{n1}\}. \quad (5.37)$$

If the coupling constant g does not vanish, one expands the generating functional $Z[J]$ in powers of the quartic interaction V , and re-expresses the resulting powers of the coordinate within the functional integral (5.35) as functional derivatives with respect to the current J . The original partition function (5.1) can thus be obtained from the free generating functional (5.36) by the formula

$$Z = \exp \left\{ -\frac{g}{4!} \int_{1234} V_{1234} \frac{\delta^4}{\delta J_1 \delta J_2 \delta J_3 \delta J_4} \right\} Z^{(0)}[J] \Big|_{J=0}. \quad (5.38)$$

Expanding the exponential in a power series, we arrive at the perturbation expansion

$$Z = \left\{ 1 - \frac{g}{4!} \int_{1234} V_{1234} \frac{\delta^4}{\delta J_1 \delta J_2 \delta J_3 \delta J_4} + \frac{1}{2} \frac{g^2}{(4!)^2} \int_{12345678} V_{1234} V_{5678} \frac{\delta^8}{\delta J_1 \delta J_2 \delta J_3 \delta J_4 \delta J_5 \delta J_6 \delta J_7 \delta J_8} + \dots \right\} Z^{(0)}[J] \Big|_{J=0}, \quad (5.39)$$

in which the p th order contribution for the partition function requires the evaluation of $4p$ functional derivatives with respect to the current J .

Kernel Approach

The derivation of the perturbation expansion simplifies, if we use functional derivatives with respect to the kernel G^{-1} in the action (5.2) rather than with respect to the current J . This allows us to substitute the previous expression (5.38) for the partition function by

$$Z = \exp \left\{ -\frac{g}{6} \int_{1234} V_{1234} \frac{\delta^2}{\delta G_{12}^{-1} \delta G_{34}^{-1}} \right\} e^{W^{(0)}}, \quad (5.40)$$

where the zeroth order of the negative free energy has the diagrammatic representation

$$W^{(0)} = -\frac{1}{2} \text{Tr} \ln G^{-1} \equiv \frac{1}{2} \bigcirc. \quad (5.41)$$

Expanding again the exponential into a power series, we obtain

$$Z = \left\{ 1 - \frac{g}{6} \int_{1234} V_{1234} \frac{\delta^2}{\delta G_{12}^{-1} \delta G_{34}^{-1}} + \frac{1}{2} \frac{g^2}{36} \int_{12345678} V_{1234} V_{5678} \frac{\delta^4}{\delta G_{12}^{-1} \delta G_{34}^{-1} \delta G_{56}^{-1} \delta G_{78}^{-1}} + \dots \right\} e^{W^{(0)}}. \quad (5.42)$$

Thus we need only half as many functional derivatives than in (5.39). Taking into account (5.10), (5.11), and (5.37), we obtain

$$\frac{\delta W^{(0)}}{\delta G_{12}^{-1}} = -\frac{1}{2} G_{12}, \quad \frac{\delta^2 W^{(0)}}{\delta G_{12}^{-1} \delta G_{34}^{-1}} = \frac{1}{4} \{G_{13} G_{24} + G_{14} G_{23}\}, \quad (5.43)$$

such that the partition function Z becomes

$$Z = \left\{ 1 - 3 \frac{g}{4!} \int_{1234} V_{1234} G_{12} G_{34} + \frac{1}{2} \frac{g^2}{(4!)^2} \int_{12345678} V_{1234} V_{5678} \right. \\ \left. \times \left[9 G_{12} G_{34} G_{56} G_{78} + 24 G_{15} G_{26} G_{37} G_{48} + 72 G_{12} G_{35} G_{46} G_{78} \right] + \dots \right\} e^{W^{(0)}}. \quad (5.44)$$

This has the diagrammatic representation

$$Z = \left\{ 1 - \frac{g}{4!} 3 \bigcirc\bigcirc + \frac{1}{2} \frac{g^2}{(4!)^2} \left[9 \bigcirc\bigcirc\bigcirc\bigcirc + 24 \bigcirc\bigcirc\bigcirc\bigcirc + 72 \bigcirc\bigcirc\bigcirc\bigcirc \right] + \dots \right\} e^{W^{(0)}}. \quad (5.45)$$

All diagrams in this expansion follow directly by successively cutting lines of the basic one-loop vacuum diagram (5.41) according to (5.42). By going to the logarithm of the partition function Z , we find a diagrammatic expansion for W

$$W = \frac{1}{2} \bigcirc - \frac{g}{4!} 3 \bigcirc\bigcirc + \frac{1}{2} \frac{g^2}{(4!)^2} \left\{ 24 \bigcirc\bigcirc\bigcirc\bigcirc + 72 \bigcirc\bigcirc\bigcirc\bigcirc \right\} + \dots, \quad (5.46)$$

which turns out to contain precisely all connected diagrams in (5.45) with the same multiplicities. In the next section we show that this diagrammatic expansion for W can be derived more efficiently by solving a differential equation.

5.2.3 Functional Differential Equation for $W = \ln Z$

Regarding the partition function Z as a functional of the kernel G^{-1} , we derive a functional differential equation for Z . We start with the trivial identity

$$\int \mathcal{D}x \frac{\delta}{\delta x_1} \{x_2 e^{-\mathcal{A}[x]}\} = 0. \quad (5.47)$$

Taking into account the explicit form of the action (5.2), we perform the functional derivative with respect to the coordinate and obtain

$$\int \mathcal{D}x \left\{ \delta_{12} - \int_3 G_{13}^{-1} x_2 x_3 - \frac{g}{6} \int_{345} V_{1345} x_2 x_3 x_4 x_5 \right\} e^{-\mathcal{A}[x]} = 0. \quad (5.48)$$

Applying the substitution rule (5.13), this equation can be expressed in terms of the partition function (5.1) and its derivatives with respect to the kernel G^{-1} :

$$\delta_{12} Z + 2 \int_3 G_{13}^{-1} \frac{\delta Z}{\delta G_{23}^{-1}} = \frac{2}{3} g \int_{345} V_{1345} \frac{\delta^2 Z}{\delta G_{23}^{-1} \delta G_{45}^{-1}}. \quad (5.49)$$

Note that this linear functional differential equation for the partition function Z is, indeed, solved by (5.40) due to the commutation relation

$$\begin{aligned} & \exp \left\{ -\frac{g}{6} \int_{1234} V_{1234} \frac{\delta^2}{\delta G_{12}^{-1} \delta G_{34}^{-1}} \right\} G_{56}^{-1} - G_{56}^{-1} \exp \left\{ -\frac{g}{6} \int_{1234} V_{1234} \frac{\delta^2}{\delta G_{12}^{-1} \delta G_{34}^{-1}} \right\} \\ &= -\frac{g}{3} \int_{78} V_{5678} \frac{\delta}{\delta G_{78}^{-1}} \exp \left\{ -\frac{g}{6} \int_{1234} V_{1234} \frac{\delta^2}{\delta G_{12}^{-1} \delta G_{34}^{-1}} \right\} \end{aligned} \quad (5.50)$$

which follows from the canonical one

$$\frac{\delta}{\delta G_{12}^{-1}} G_{34}^{-1} - G_{34}^{-1} \frac{\delta}{\delta G_{12}^{-1}} = \frac{1}{2} \{ \delta_{13} \delta_{24} + \delta_{14} \delta_{23} \}. \quad (5.51)$$

Going over from Z to $W = \ln Z$, the linear functional differential equation (5.49) turns into a nonlinear one:

$$\delta_{12} + 2 \int_3 G_{13}^{-1} \frac{\delta W}{\delta G_{23}^{-1}} = \frac{2}{3} g \int_{345} V_{1345} \left\{ \frac{\delta^2 W}{\delta G_{23}^{-1} \delta G_{45}^{-1}} + \frac{\delta W}{\delta G_{23}^{-1}} \frac{\delta W}{\delta G_{45}^{-1}} \right\}. \quad (5.52)$$

If the coupling constant g vanishes, this is immediately solved by (5.41). For a nonvanishing coupling constant g , the right-hand side in (5.52) produces corrections to (5.41) which we shall denote with $W^{(\text{int})}$. Thus the quantity W decomposes according to

$$W = W^{(0)} + W^{(\text{int})}. \quad (5.53)$$

Inserting this into (5.52) and taking into account (5.43), we obtain the following functional differential equation for $W^{(\text{int})}$:

$$\begin{aligned} \int_{12} G_{12}^{-1} \frac{\delta W^{(\text{int})}}{\delta G_{12}^{-1}} &= \frac{g}{4} \int_{1234} V_{1234} G_{12} G_{34} - \frac{g}{3} \int_{1234} V_{1234} G_{12} \frac{\delta W^{(\text{int})}}{\delta G_{34}^{-1}} \\ &+ \frac{g}{3} \int_{1234} V_{1234} \left\{ \frac{\delta^2 W^{(\text{int})}}{\delta G_{12}^{-1} \delta G_{34}^{-1}} + \frac{\delta W^{(\text{int})}}{\delta G_{12}^{-1}} \frac{\delta W^{(\text{int})}}{\delta G_{34}^{-1}} \right\}. \end{aligned} \quad (5.54)$$

With the help of the functional chain rule, the first and second derivatives with respect to the kernel G^{-1} are rewritten as

$$\frac{\delta}{\delta G_{12}^{-1}} = - \int_{34} G_{13} G_{24} \frac{\delta}{\delta G_{34}^{-1}} \quad (5.55)$$

and

$$\begin{aligned} \frac{\delta^2}{\delta G_{12}^{-1} \delta G_{34}^{-1}} &= \int_{5678} G_{15} G_{26} G_{37} G_{48} \frac{\delta^2}{\delta G_{56}^{-1} \delta G_{78}^{-1}} \\ &+ \frac{1}{2} \int_{56} \{ G_{13} G_{25} G_{46} + G_{14} G_{25} G_{36} + G_{23} G_{15} G_{46} + G_{24} G_{15} G_{36} \} \frac{\delta}{\delta G_{56}^{-1}}, \end{aligned} \quad (5.56)$$

respectively, so that the functional differential equation (5.54) for $W^{(\text{int})}$ takes the form

$$\begin{aligned} \int_{12} G_{12} \frac{\delta W^{(\text{int})}}{\delta G_{12}^{-1}} &= -\frac{g}{4} \int_{1234} V_{1234} G_{12} G_{34} - g \int_{123456} V_{1234} G_{12} G_{35} G_{46} \frac{\delta W^{(\text{int})}}{\delta G_{56}^{-1}} \\ &- \frac{g}{3} \int_{12345678} V_{1234} G_{15} G_{26} G_{37} G_{48} \left\{ \frac{\delta^2 W^{(\text{int})}}{\delta G_{56}^{-1} \delta G_{78}^{-1}} + \frac{\delta W^{(\text{int})}}{\delta G_{56}^{-1}} \frac{\delta W^{(\text{int})}}{\delta G_{78}^{-1}} \right\}. \end{aligned} \quad (5.57)$$

5.2.4 Recursion Relation and Graphical Solution

We now convert the functional differential equation (5.57) into a recursion relation by expanding $W^{(\text{int})}$ into a power series in g :

$$W^{(\text{int})} = \sum_{p=1}^{\infty} \frac{1}{p!} \left(\frac{-g}{4!} \right)^p W^{(p)}. \quad (5.58)$$

Using the property (5.32) that the coefficient $W^{(p)}$ satisfies the eigenvalue problem of the line numbering operator (5.31), we obtain the recursion relation

$$\begin{aligned} W^{(p+1)} = & 12 \int_{123456} V_{1234} G_{12} G_{35} G_{46} \frac{\delta W^{(p)}}{\delta G_{56}} + 4 \int_{12345678} V_{1234} G_{15} G_{26} G_{37} G_{48} \frac{\delta^2 W^{(p)}}{\delta G_{56} \delta G_{78}} \\ & + 4 \sum_{q=1}^{p-1} \binom{p}{q} \int_{12345678} V_{1234} G_{15} G_{26} G_{37} G_{48} \frac{\delta W^{(p-q)}}{\delta G_{56}} \frac{\delta W^{(q)}}{\delta G_{78}} \end{aligned} \quad (5.59)$$

and the initial condition (5.33). With the help of the graphical rules of Section 5.2.1, the recursion relation (5.59) can be written diagrammatically as follows

$$\begin{aligned} W^{(p+1)} = & 4 \frac{\delta^2 W^{(p)}}{\delta_{1-2} \delta_{3-4}} \begin{array}{c} 1 \\ 2 \\ 3 \\ 4 \end{array} \begin{array}{c} \diagup \\ \diagdown \\ \diagup \\ \diagdown \end{array} + 12 \frac{\delta W^{(p)}}{\delta_{1-2}} \begin{array}{c} 1 \\ 2 \end{array} \begin{array}{c} \diagup \\ \diagdown \end{array} \\ & + 4 \sum_{q=1}^{p-1} \binom{p}{q} \frac{\delta W^{(p-q)}}{\delta_{1-2}} \begin{array}{c} 1 \\ 2 \end{array} \begin{array}{c} 3 \\ 4 \end{array} \frac{\delta W^{(q)}}{\delta_{3-4}}, \quad p \geq 1. \end{aligned} \quad (5.60)$$

This is iterated starting from

$$W^{(1)} = 3 \begin{array}{c} \circ \\ \circ \end{array}. \quad (5.61)$$

The right-hand side of (5.60) contains three different graphical operations. The first two are linear and involve one or two line amputations of the previous perturbative order. The third operation is nonlinear and mixes two different one-line amputations of lower orders.

To demonstrate the working of (5.60), we calculate the connected vacuum diagrams up to five loops. Applying the linear operations to (5.59), we obtain immediately

$$\frac{\delta W^{(1)}}{\delta_{1-2}} = 6 \begin{array}{c} 1 \\ 2 \end{array} \begin{array}{c} \diagup \\ \diagdown \end{array} \begin{array}{c} \circ \\ \circ \end{array}, \quad \frac{\delta^2 W^{(1)}}{\delta_{1-2} \delta_{3-4}} = 6 \begin{array}{c} 1 \\ 2 \end{array} \begin{array}{c} 3 \\ 4 \end{array} \begin{array}{c} \diagup \\ \diagdown \end{array} \begin{array}{c} \circ \\ \circ \end{array}. \quad (5.62)$$

Inserted into (5.60), these lead to the three-loop vacuum diagrams

$$W^{(2)} = 24 \begin{array}{c} \circ \\ \circ \\ \circ \end{array} + 72 \begin{array}{c} \circ \\ \circ \\ \circ \end{array}. \quad (5.63)$$

Proceeding to the next order, we have to perform one- and two-line amputations on the vacuum graphs in (5.63), leading to

$$\frac{\delta W^{(2)}}{\delta_{1-2}} = 96 \begin{array}{c} 1 \\ 2 \end{array} \begin{array}{c} \circ \\ \circ \end{array} + 144 \begin{array}{c} \circ \\ \circ \\ \circ \end{array} + 144 \begin{array}{c} \circ \\ \circ \\ \circ \end{array}, \quad (5.64)$$

and subsequently to

$$\begin{aligned} \frac{\delta^2 W^{(2)}}{\delta 1 \text{---} 2 \delta 3 \text{---} 4} = & 288 \begin{array}{c} 1 \\ \diagdown \quad \diagup \\ \text{---} \text{---} \text{---} \\ \diagup \quad \diagdown \\ 3 \quad 4 \end{array} + 144 \begin{array}{c} 1 \\ \diagdown \quad \diagup \\ \text{---} \text{---} \text{---} \\ \diagup \quad \diagdown \\ 2 \quad 4 \end{array} + 288 \begin{array}{c} 1 \\ \text{---} \text{---} \text{---} \\ \text{---} \text{---} \text{---} \\ \text{---} \text{---} \text{---} \\ 3 \end{array} \\ & + 144 \begin{array}{c} 1 \\ \text{---} \text{---} \text{---} \\ \text{---} \text{---} \text{---} \\ \text{---} \text{---} \text{---} \\ 4 \end{array} + 144 \begin{array}{c} 2 \\ \text{---} \text{---} \text{---} \\ \text{---} \text{---} \text{---} \\ \text{---} \text{---} \text{---} \\ 1 \quad 3 \end{array} + 144 \begin{array}{c} 1 \\ \text{---} \text{---} \text{---} \\ \text{---} \text{---} \text{---} \\ \text{---} \text{---} \text{---} \\ 2 \quad 3 \end{array} + 144 \begin{array}{c} 1 \\ \text{---} \text{---} \text{---} \\ \text{---} \text{---} \text{---} \\ \text{---} \text{---} \text{---} \\ 3 \quad 4 \end{array} . \quad (5.65) \end{aligned}$$

Inserting (5.64) and (5.65) into (5.60) and taking into account (5.62), we find the connected vacuum diagrams of order $p = 3$ with their multiplicities as shown in Table 5.1. We observe that the nonlinear operation in (5.60) does not lead to topologically new diagrams. It only corrects the multiplicities of the diagrams generated from the first two operations. This is true also in higher orders. The connected vacuum diagrams of the subsequent order $p = 4$ and their multiplicities are listed in Table 5.1.

As a cross-check we can also determine the total multiplicities $M^{(p)}$ of all connected vacuum diagrams contributing to $W^{(p)}$. To this end we recall that each of the $M^{(p)}$ diagrams in $W^{(p)}$ consists of $2p$ lines. The amputation of one or two lines therefore leads to $2pM^{(p)}$ and $2p(2p-1)M^{(p)}$ diagrams with $2p-1$ and $2p-2$ lines, respectively. Considering only the total multiplicities, the graphical recursion relations (5.60) reduce to the form derived before in Ref. [22]

$$M^{(p+1)} = 16p(p+1)M^{(p)} + 16 \sum_{q=1}^{p-1} \frac{p!}{(p-q-1)!(q-1)!} M^{(q)} M^{(p-q)}, \quad p \geq 1. \quad (5.66)$$

These are solved starting with the initial value

$$M^{(1)} = 3, \quad (5.67)$$

leading to the total multiplicities

$$M^{(2)} = 96, \quad M^{(3)} = 9504, \quad M^{(4)} = 1880064, \quad (5.68)$$

which agree with the results listed in Table 5.1. In addition we note that the next orders would contain

$$M^{(5)} = 616108032, \quad M^{(6)} = 301093355520, \quad M^{(7)} = 205062331760640 \quad (5.69)$$

connected vacuum diagrams.

Quantum Field Theory

We present a method for a recursive graphical construction of Feynman diagrams with their correct multiplicities in quantum electrodynamics (QED) [32]. The method is first applied to find all diagrams contributing to the vacuum energy from which all n -point functions are derived by functional differentiation with respect to electron and photon propagators, and to the interaction. Basis for our construction is a functional differential equation obeyed by the vacuum energy when considered as a functional of the free propagators and the interaction. Our method does not employ external sources in contrast to traditional approaches.

6.1 Introduction

In quantum field theory, it is well known [33,34] that the complete knowledge of all vacuum diagrams implies the knowledge of the entire theory (“the vacuum is the world”). Indeed, it is possible to derive all correlation functions and scattering amplitudes from the vacuum diagrams. This has been elaborated explicitly for ϕ^4 theory in the disordered phase in Refs. [5,23] and for the ordered phase in Ref. [35,36], following a general theoretical framework laid out some time ago [21,22]. This knowledge is now applied for constructing an efficient algebraic method along these lines for field theories of fundamental particles [32].

The purpose of the present chapter is to do this for quantum electrodynamics (QED). We show how to derive systematically all Feynman diagrams of the theory together with their correct multiplicities in a two step process: First we find the vacuum energy from a sum over all vacuum diagrams by a recursive graphical procedure. This is developed by solving a functional differential equation which involves functional derivatives with respect to the free electron and photon propagators. In a second step, we find all correlation functions by a diagrammatic application of functional derivatives upon the vacuum energy. In contrast to conventional procedures [6,37–41], no external currents coupled to single fields are used, such that there is no need for Grassmann sources for the electron fields. An additional advantage of our procedure is that the number of derivatives to be performed for a certain correlation function is half as big as with external sources.

In Section 6.2 we establish the partition function of Euclidean QED as a functional with respect to the inverse electron and photon propagators as well as a generalized interaction. By setting up graphical representations for functional derivatives with respect to these bilocal and trilocal functions, we show in Section 6.3 that the partition function constitutes a generating functional for all correlation functions. This forms the basis for a perturbative expansion of the vacuum energy in terms of connected vacuum diagrams. In Section 6.4 we then derive a recursion relation which allows to graphically construct

the connected vacuum diagrams order by order. From these we obtain in Section 6.5 all diagrams for self interactions and scattering processes by cutting electron as well as photon lines or by removing vertices. Along similar lines we apply in Section 6.6 our method for scattering processes in the presence of an external electromagnetic field.

6.2 Generating Functional without Particle Sources

We begin by setting up a generating functional for all Feynman diagrams of quantum electrodynamics which does not employ external particle sources coupled linearly to the fields.

6.2.1 Partition Function of QED

Our notation for the action of QED in Euclidean spacetime with a gauge fixing of Feynman type is

$$\mathcal{A}_{\text{QED}}[\bar{\psi}, \psi, A] = \int d^4x \left[\bar{\psi}_\alpha (i\gamma_{\alpha\beta}^\mu \partial_\mu + m) \psi_\beta + \frac{1}{2} A_\mu (-\partial^2) A^\mu - e \bar{\psi}_\alpha \gamma_{\alpha\beta}^\mu A_\mu \psi_\beta \right] \quad (6.1)$$

with Dirac spinor fields $\psi_\alpha, \bar{\psi}_\beta = \psi_\alpha^\dagger \gamma_{\alpha\beta}^0$ ($\alpha, \beta = 1, \dots, 4$) and Maxwell's vector field A_μ ($\mu = 0, \dots, 3$). The properties of the vacuum are completely described by the partition function

$$Z_{\text{QED}} = \oint \mathcal{D}\bar{\psi} \mathcal{D}\psi \mathcal{D}A e^{-\mathcal{A}_{\text{QED}}[\bar{\psi}, \psi, A]}, \quad (6.2)$$

where the electron fields $\bar{\psi}$ and ψ are Grassmannian. Let us split the action into the three terms

$$\mathcal{A}_{\text{QED}}[\bar{\psi}, \psi, A] = \mathcal{A}_\psi[\bar{\psi}, \psi] + \mathcal{A}_A[A] + \mathcal{A}_{\text{int}}[\bar{\psi}, \psi, A], \quad (6.3)$$

corresponding to the Dirac, Maxwell, and interaction terms in (6.1). For the upcoming development it will be useful to consider the free parts of the action as bilocal functionals. The free action for the Dirac fields is

$$\mathcal{A}_\psi[\bar{\psi}, \psi] = \iint d^4x d^4x' \bar{\psi}_\alpha(x) S_{\text{F}\alpha\beta}^{-1}(x, x') \psi_\beta(x'), \quad (6.4)$$

with a kernel

$$S_{\text{F}\alpha\beta}^{-1}(x, x') = (i\gamma_{\alpha\beta}^\mu \partial_\mu + m\delta_{\alpha\beta}) \delta(x - x'), \quad (6.5)$$

while the free action for the Maxwell field reads

$$\mathcal{A}_A[A] = \frac{1}{2} \iint d^4x d^4x' A^\mu(x) D_{\text{F}\mu\nu}^{-1}(x, x') A^\nu(x') \quad (6.6)$$

with a kernel

$$D_{\text{F}\mu\nu}^{-1}(x, x') = -\partial^2 \delta(x - x') \delta_{\mu\nu}. \quad (6.7)$$

In the following, we shall omit all vector and spinor indices, for brevity.

6.2.2 Generalized Action

Our generating functional will arise from a generalization of the free action

$$\mathcal{A}^{(0)}[\bar{\psi}, \psi, A] = \mathcal{A}_\psi[\bar{\psi}, \psi] + \mathcal{A}_A[A] \quad (6.8)$$

to bilocal functionals of arbitrary kernels $S^{-1}(x_1, x_2)$ and $D^{-1}(x_1, x_2) = D^{-1}(x_2, x_1)$ according to

$$\mathcal{A}_\psi[\bar{\psi}, \psi] \rightarrow \mathcal{A}_\psi[\bar{\psi}, \psi; S^{-1}] = \iint d^4x_1 d^4x_2 \bar{\psi}(x_1) S^{-1}(x_1, x_2) \psi(x_2), \quad (6.9)$$

$$\mathcal{A}_A[A] \rightarrow \mathcal{A}_A[A; D^{-1}] = \frac{1}{2} \iint d^4x_1 d^4x_2 A(x_1) D^{-1}(x_1, x_2) A(x_2). \quad (6.10)$$

The kernels $S^{-1}(x_1, x_2)$ and $D^{-1}(x_1, x_2)$ are only required to possess a functional inverse $S(x_1, x_2)$ and $D(x_1, x_2)$. Similarly, we shall generalize the interaction to

$$\mathcal{A}_{\text{int}}[\bar{\psi}, \psi, A] \rightarrow \mathcal{A}_{\text{int}}[\bar{\psi}, \psi, A; V] = -e \iiint d^4x_1 d^4x_2 d^4x_3 V(x_1, x_2; x_3) \bar{\psi}(x_1) \psi(x_2) A(x_3), \quad (6.11)$$

where $V(x_1, x_2; x_3)$ is an arbitrary trilocal function. At the end we shall return to QED by substituting $S \rightarrow S_F, D \rightarrow D_F$ and $eV(x_1, x_2; x_3) \rightarrow e\gamma_\mu \delta(x_1 - x_2) \delta(x_1 - x_3)$.

The generalized partition function

$$Z = \oint \mathcal{D}\bar{\psi} \mathcal{D}\psi \mathcal{D}A e^{-\mathcal{A}[\bar{\psi}, \psi, A; S^{-1}, D^{-1}, V]} \quad (6.12)$$

with the action

$$\mathcal{A}[\bar{\psi}, \psi, A; S^{-1}, D^{-1}, V] = \mathcal{A}_\psi[\bar{\psi}, \psi; S^{-1}] + \mathcal{A}_A[\bar{\psi}, \psi; D^{-1}] + \mathcal{A}_{\text{int}}[\bar{\psi}, \psi, A; V] \quad (6.13)$$

then represents a functional of the bilocal quantities $S^{-1}(x_1, x_2), D^{-1}(x_1, x_2)$, and of the trilocal function $V(x_1, x_2; x_3)$. All n -point correlation functions of the theory are obtained from expectation values defined by

$$\langle \hat{O}_1(x_1) \hat{O}_2(x_2) \dots \rangle = Z^{-1} \oint \mathcal{D}\bar{\psi} \mathcal{D}\psi \mathcal{D}A O_1(x_1) O_2(x_2) \dots e^{-\mathcal{A}[\bar{\psi}, \psi, A; S^{-1}, D^{-1}, V]}, \quad (6.14)$$

where the local operators $\hat{O}_i(x)$ are products of field operators $\hat{\psi}(x), \hat{\bar{\psi}}(x)$, and $\hat{A}(x)$ at the same spacetime point. Important examples for expectation values of this kind are the photon and the electron propagators of the interacting theory

$$\gamma G^2(x_1, x_2) \equiv \langle \hat{A}(x_1) \hat{A}(x_2) \rangle = Z^{-1} \oint \mathcal{D}\bar{\psi} \mathcal{D}\psi \mathcal{D}A A(x_1) A(x_2) e^{-\mathcal{A}[\bar{\psi}, \psi, A; S^{-1}, D^{-1}, V]}, \quad (6.15)$$

$$e G^2(x_1, x_2) \equiv \langle \hat{\psi}(x_1) \hat{\bar{\psi}}(x_2) \rangle = Z^{-1} \oint \mathcal{D}\bar{\psi} \mathcal{D}\psi \mathcal{D}A \psi(x_1) \bar{\psi}(x_2) e^{-\mathcal{A}[\bar{\psi}, \psi, A; S^{-1}, D^{-1}, V]}. \quad (6.16)$$

For a perturbative calculation of the partition function Z we define the free vacuum functional

$$Z^{(0)} \equiv \oint \mathcal{D}\bar{\psi} \mathcal{D}\psi \mathcal{D}A e^{-\mathcal{A}^{(0)}[\bar{\psi}, \psi, A; S^{-1}, D^{-1}]}, \quad (6.17)$$

whose action is quadratic in the fields. The path integral is Gaussian and yields

$$Z^{(0)} = \exp[\text{Tr} \ln S^{-1}] \exp\left[-\frac{1}{2} \text{Tr} \ln D^{-1}\right]. \quad (6.18)$$

The free correlation functions of arbitrary local electron and photon operators $\hat{O}(x)$ are defined by the free part of the expectation values (6.14)

$$\langle \hat{O}_1(x_1) \hat{O}_2(x_2) \dots \rangle^{(0)} = [Z^{(0)}]^{-1} \oint \mathcal{D}\bar{\psi} \mathcal{D}\psi \mathcal{D}A O_1(x_1) O_2(x_2) \dots e^{-\mathcal{A}^{(0)}[\bar{\psi}, \psi, A; S^{-1}, D^{-1}]}, \quad (6.19)$$

and the free-field propagators are the expectation values

$$\gamma G^{2(0)}(x_1, x_2) = D(x_1, x_2) \equiv \langle \hat{A}(x_1) \hat{A}(x_2) \rangle^{(0)} \equiv D(x_2, x_1), \quad (6.20)$$

$$e G^{2(0)}(x_1, x_2) = S(x_1, x_2) \equiv \langle \hat{\psi}(x_1) \hat{\bar{\psi}}(x_2) \rangle^{(0)}. \quad (6.21)$$

To avoid a pile up of infinite volume factors in a perturbation expansion, it is favorable to go over from $Z^{(0)}$ to the vacuum energy $W^{(0)}$ defined by

$$W^{(0)} \equiv \ln Z^{(0)} = W_\psi^{(0)} + W_A^{(0)}, \quad (6.22)$$

where the free electron and photon parts are

$$W_{\psi}^{(0)} = \text{Tr} \ln S^{-1} \quad (6.23)$$

and

$$W_A^{(0)} = -\frac{1}{2} \text{Tr} \ln D^{-1}. \quad (6.24)$$

The total vacuum energy

$$W = \ln Z \quad (6.25)$$

is obtained perturbatively by expanding the functional integral (6.12) in powers of the coupling constant e :

$$W = \sum_{p=0}^{\infty} e^{2p} W^{(p)}, \quad (6.26)$$

where the quantities $W^{(p)}$ with $p \geq 1$ are free-field expectation values of the type (6.19):

$$W^{(p)} = \int_{1 \dots 6p} V_{123} \cdots V_{6p-2 \ 6p-1 \ 6p} \langle \hat{\psi}_{6p-1} \cdots \hat{\psi}_5 \hat{\psi}_2 \hat{\psi}_1 \hat{\psi}_4 \cdots \hat{\psi}_{6p-2} \hat{A}_3 \hat{A}_6 \cdots \hat{A}_{6p} \rangle^{(0)}, \quad p \geq 1. \quad (6.27)$$

In the sequel we shall use from now on the short-hand notation $1 = x_1, 2 = x_2, \dots$ and $\int_{1 \dots} = \int d^4 x_1 \cdots$. The expectation values in (6.27) are evaluated with the help of Wick's rule as a sum of Feynman integrals, which are pictured as connected vacuum diagrams constructed from lines and vertices. A straight line with an arrow represents an electron propagator

$$1 \longleftarrow 2 \equiv S_{12}, \quad (6.28)$$

whereas a wiggly line stands for a photon propagator

$$1 \rightsquigarrow 2 \equiv D_{12}. \quad (6.29)$$

The vertex represents an integral over the interaction potential:

$$\text{---} \equiv e \int_{123} V_{123}. \quad (6.30)$$

The vacuum energies (6.23) and (6.24) will be represented by single-loop diagrams

$$W_{\psi}^{(0)} = - \text{---} \quad (6.31)$$

and

$$W_A^{(0)} = \frac{1}{2} \text{---} \quad (6.32)$$

This leaves us with the important problem of finding all connected vacuum diagrams. For this we shall exploit that the partition function (6.12) is a functional of the bilocal functions $S^{-1}(x_1, x_2)$, $D^{-1}(x_1, x_2)$, and of the trilocal function $V(x_1, x_2; x_3)$.

6.3 Perturbation Theory

As a preparation for our generation procedure for vacuum diagrams, we set up a graphical representation of functional derivatives with respect to the kernels S^{-1} , D^{-1} , the propagators S , D , and the interaction function V . After this we express the vacuum functional W in terms of a series of functional derivatives of the free partition function $Z^{(0)}$ with respect to the kernels.

6.3.1 Functional Derivatives with Respect to $S^{-1}(x_1, x_2)$, $D^{-1}(x_1, x_2)$, and $V(x_1, x_2; x_3)$

Each Feynman diagram is composed of integrals over products of the propagators S , D and may thus be considered as a functional of the kernels S^{-1} , D^{-1} . In the following we set up the graphical rules for performing functional derivatives with respect to these functional matrices. With these rules we can generate all $2n$ -point correlation functions with $n = 1, 2, \dots$ from vacuum diagrams. To produce also $(2n + 1)$ -point correlation functions with $n = 1, 2, \dots$ such as the fundamental three-point vertex function from vacuum diagrams, it is useful to introduce additionally a functional derivative with respect to the interaction function V_{123} .

Functional Derivative with Respect to the Photon Kernel

The kernel D_{12}^{-1} of the photon is symmetric $D_{12}^{-1} = D_{21}^{-1}$, so that the basic functional derivatives are also symmetric [23],

$$\frac{\delta D_{12}^{-1}}{\delta D_{34}^{-1}} \equiv \frac{1}{2} \{ \delta_{13} \delta_{42} + \delta_{14} \delta_{32} \}, \quad (6.33)$$

as is discussed in detail in Ref. [35]. By the chain rule of differentiation, this defines the functional derivative with respect to D^{-1} for all functionals of D^{-1} . As an example, we calculate the free photon propagator (6.20) by applying the operator $\delta/\delta D_{12}^{-1}$ to Eq. (6.17). Taking into account Eq. (6.22) and Eq. (6.33), we find

$$D_{12} = -2 \frac{\delta W_A^{(0)}}{\delta D_{12}^{-1}}. \quad (6.34)$$

Inserting the explicit form (6.24), we obtain

$$D_{12} = \frac{\delta}{\delta D_{12}^{-1}} \text{Tr} \ln D^{-1}. \quad (6.35)$$

With the notation (6.29) and (6.32), we can write relation (6.34) graphically as

$$1 \text{ --- } 2 = -\frac{\delta}{\delta D_{12}^{-1}} \text{ (loop) }. \quad (6.36)$$

This diagrammatic equation may be viewed as a special case of a general graphical rule derived as follows: Let us apply the functional derivative (6.33) to a photon propagator D_{12} . Because of the identity

$$\int_{\bar{1}} D_{1\bar{1}} D_{\bar{1}2}^{-1} = \delta_{12} \quad (6.37)$$

we find

$$-\frac{\delta D_{12}}{\delta D_{34}^{-1}} = \frac{1}{2} \{ D_{13} D_{42} + D_{14} D_{32} \}. \quad (6.38)$$

Diagrammatically, this equation implies that the operation $-\delta/\delta D_{34}^{-1}$ applied to a photon line (6.29) amounts to cutting the line:

$$-\frac{\delta}{\delta D_{34}^{-1}} 1 \text{ --- } 2 = \frac{1}{2} \left\{ 1 \text{ --- } 3 \quad 4 \text{ --- } 2 + 1 \text{ --- } 4 \quad 3 \text{ --- } 2 \right\}. \quad (6.39)$$

Note that the indices of the kernel D_{34}^{-1} are symmetrically attached to the newly created line ends in the two possible ways due to the differentiation rule (6.33). This rule implies directly the diagrammatic equation (6.36).

Consider now higher-order correlation functions which follow from higher functional derivatives of $W_A^{(0)}$. From the definition (6.19) and Eq. (6.10), we obtain the free four-point function as the second functional derivative

$$\gamma G_{1234}^{4(0)} \equiv \langle \hat{A}_1 \hat{A}_2 \hat{A}_3 \hat{A}_4 \rangle^{(0)} = 4 e^{-W_A^{(0)}} \frac{\delta^2}{\delta D_{12}^{-1} \delta D_{34}^{-1}} e^{W_A^{(0)}}. \quad (6.40)$$

Because of the symmetry of D_{12} , the order in which the spacetime arguments appear in the inverse propagators is of no importance. Inserting for $W_A^{(0)}$ the explicit form (6.24), the first derivative yields via Eq. (6.35) just $-D_{34} \exp\{W_A^{(0)}\}$, the second derivative applied to this gives with the rule (6.38) and, once more (6.35),

$$\gamma G_{1234}^{4(0)} = D_{13}D_{24} + D_{32}D_{14} + D_{12}D_{34}. \quad (6.41)$$

The right-hand side has the graphical representation

$$\gamma G_{1234}^{4(0)} = \begin{array}{c} 2 \quad 3 \\ \diagdown \quad \diagup \\ 1 \quad 4 \end{array} + \begin{array}{c} 2 \quad 3 \\ \text{---} \quad \text{---} \\ 1 \quad 4 \end{array} + \begin{array}{c} 2 \quad 3 \\ \text{---} \quad \text{---} \\ 1 \quad 4 \end{array}. \quad (6.42)$$

The same diagrams are obtained by applying the cutting rule (6.39) twice to the single-loop diagram (6.32).

While derivatives with respect to the kernel D^{-1} amount to cutting photon lines, we show now that derivatives with respect to the photon propagator D lead to line amputations. The transformation rule between the two operations follows from relation (6.38):

$$\frac{\delta}{\delta D_{12}^{-1}} = - \int_{34} D_{13}D_{24} \frac{\delta}{\delta D_{34}}, \quad (6.43)$$

which is equivalent to

$$\frac{\delta}{\delta D_{12}} = - \int_{34} D_{13}^{-1}D_{24}^{-1} \frac{\delta}{\delta D_{34}^{-1}}. \quad (6.44)$$

The functional derivative with respect to D_{12} satisfies of course the fundamental relation (6.33):

$$\frac{\delta D_{12}}{\delta D_{34}} = \frac{1}{2} \{\delta_{13}\delta_{42} + \delta_{14}\delta_{32}\}. \quad (6.45)$$

We shall represent the right-hand side graphically by extending the Feynman diagrams by the symbol:

$$1 \text{ --- } 2 \equiv \delta_{12}. \quad (6.46)$$

If we write the functional derivative with respect to the propagator D_{12} graphically as

$$\frac{\delta}{\delta D_{12}} \equiv \frac{\delta}{\delta 1 \text{ --- } 2}, \quad (6.47)$$

we may express Eq. (6.45) as

$$\frac{\delta}{\delta 1 \text{ --- } 2} \begin{array}{c} 3 \quad 4 \\ \text{---} \quad \text{---} \end{array} = \frac{1}{2} \left\{ \begin{array}{c} 1 \text{ --- } 2 \quad 4 \text{ --- } 2 \\ + \quad 1 \text{ --- } 4 \quad 3 \text{ --- } 2 \end{array} \right\}. \quad (6.48)$$

Thus, differentiating a photon line with respect to the corresponding propagator amputates this line, leaving only the symmetrized indices at the end points.

Functional Derivative with Respect to the Electron Kernel

Setting up graphical representations for functional derivatives for electrons is different from that in the photon case since the kernel S^{-1} is no longer symmetric. The functional derivative is therefore the usual one

$$\frac{\delta S_{12}^{-1}}{\delta S_{34}^{-1}} = \delta_{13}\delta_{42}, \quad (6.49)$$

from which all others are derived via the chain rule of differentiation. The free electron propagator S_{12} is found in analogy to (6.34) by differentiating the free electron vacuum functional (6.23) with respect to the inverse electron propagator S^{-1} :

$$S_{12} = \frac{\delta W_{\psi}^{(0)}}{\delta S_{21}^{-1}}. \quad (6.50)$$

This implies

$$S_{12} = \frac{\delta}{\delta S_{21}^{-1}} \text{Tr} \ln S^{-1}, \quad (6.51)$$

which follows also from Eq. (6.49) and the chain rule of differentiation. The graphical interpretation of the functional derivative $\delta/\delta S_{21}^{-1}$ is quite analogous to the photon case. In analogy to Eq. (6.36), we write expression (6.51) diagrammatically as

$$1 \longleftarrow 2 = -\frac{\delta}{\delta S_{21}^{-1}} \bigcirc. \quad (6.52)$$

This, in turn, can be understood as being a consequence of the general cutting rule for electron lines:

$$\frac{\delta}{\delta S_{43}^{-1}} 1 \longleftarrow 2 = - \begin{array}{c} 1 \quad 2 \\ \diagdown \quad \diagup \\ 3 \quad 4 \end{array}, \quad (6.53)$$

which graphically expresses the derivative relation

$$\frac{\delta S_{12}}{\delta S_{43}^{-1}} = -S_{14}S_{32}. \quad (6.54)$$

The free electron 4-point function is obtained from two functional derivatives according to

$${}^e G_{1234}^{4(0)} \equiv \langle \hat{\psi}_1 \hat{\psi}_2 \hat{\psi}_3 \hat{\psi}_4 \rangle^{(0)} = e^{-W_{\psi}^{(0)}} \frac{\delta^2}{\delta S_{32}^{-1} \delta S_{41}^{-1}} e^{W_{\psi}^{(0)}}. \quad (6.55)$$

Here, the electron fields must be properly rearranged to $\hat{\psi}_2 \hat{\psi}_3 \hat{\psi}_1 \hat{\psi}_4$ for applying the functional derivatives with respect to S^{-1} . Using Eqs. (6.50) and (6.54) we obtain from Eq. (6.55)

$${}^e G_{1234}^{4(0)} = S_{23}S_{14} - S_{24}S_{13}, \quad (6.56)$$

or graphically

$${}^e G_{1234}^{4(0)} = \begin{array}{c} 2 \longleftarrow 3 \\ 1 \longleftarrow 4 \end{array} - \begin{array}{c} 2 \quad 3 \\ \diagdown \quad \diagup \\ 1 \quad 4 \end{array}. \quad (6.57)$$

Derivatives with respect to the propagators S satisfy the relation

$$\frac{\delta S_{12}}{\delta S_{34}} = \delta_{13}\delta_{42}, \quad (6.58)$$

which in analogy to (6.45) is represented graphically as an amputation of an electron line

$$\frac{\delta}{\delta 3 \longleftarrow 4} 1 \longleftarrow 2 = 1 \longleftarrow 3 \quad 4 \longleftarrow 2. \quad (6.59)$$

Here we have introduced the additional diagrammatic symbols

$$1 \begin{array}{c} \leftarrow \\ \leftrightarrow \\ \rightarrow \end{array} 2 \equiv \delta_{12}, \quad (6.60)$$

$$\frac{\delta}{\delta S_{12}} \equiv \frac{\delta}{\delta 1 \begin{array}{c} \leftarrow \\ \leftrightarrow \\ \rightarrow \end{array} 2}. \quad (6.61)$$

Differentiating an electron line with respect to the corresponding propagator removes this line, leaving only the indices at the end points of the remaining lines.

The analytic relations between cutting and amputating lines are now, just as in Eqs. (6.43) and (6.44):

$$\frac{\delta}{\delta S_{12}^{-1}} = - \int_{34} S_{31} S_{24} \frac{\delta}{\delta S_{34}}, \quad (6.62)$$

$$\frac{\delta}{\delta S_{12}} = - \int_{34} S_{31}^{-1} S_{24}^{-1} \frac{\delta}{\delta S_{34}^{-1}}. \quad (6.63)$$

With the above graphical representations of the functional derivatives, it will be possible to derive systematically all vacuum diagrams of the interacting theory order by order in the coupling strength e , and from these all diagrams with an even number of legs.

Functional Derivative with Respect to the Interaction

If we want to find amplitudes involving an odd number of photons such as the three-point function from vacuum diagrams, the derivatives with respect to the kernels S^{-1} , D^{-1} are not enough. Here the general trilocal interaction function V_{123} of Eq. (6.11) is needed. Thus, we define an associated functional derivative with respect to this interaction to satisfy

$$\frac{\delta V_{123}}{\delta V_{456}} = \delta_{14} \delta_{52} \delta_{36}. \quad (6.64)$$

By introducing the graphical rule

$$\frac{\delta}{\delta \begin{array}{c} 3 \\ \text{---} \\ 1 \text{---} 2 \end{array}} \equiv \frac{\delta}{\delta V_{123}}, \quad (6.65)$$

the definition of the functional derivative (6.64) can be expressed as

$$\frac{\delta}{\delta \begin{array}{c} 6 \\ \text{---} \\ 4 \text{---} 5 \end{array}} \begin{array}{c} 3 \\ \text{---} \\ 1 \text{---} 2 \end{array} = \begin{array}{c} 3 \\ \text{---} \\ 6 \\ \text{---} \\ 4 \text{---} 5 \end{array} \begin{array}{c} 1 \\ \text{---} \\ 1 \text{---} 2 \end{array}, \quad (6.66)$$

where the right-hand side represents a product of δ functions as defined in Eqs. (6.46) and (6.60).

6.3.2 Vacuum Energy as Generating Functional

With the above-introduced diagrammatic operations, the vacuum energy $W[S^{-1}, D^{-1}, V]$ constitutes a generating functional for all correlation functions. Its evaluation proceeds by expanding the exponential in the partition function (6.12) in powers of the coupling constant e , leading to the Taylor series

$$Z = \sum_{p=0}^{\infty} \frac{e^{2p}}{(2p)!} \oint \mathcal{D}\bar{\psi} \mathcal{D}\psi \mathcal{D}A \left(\int_{1\dots 6} V_{123} V_{456} \bar{\psi}_1 \psi_2 A_3 \bar{\psi}_4 \psi_5 A_6 \right)^p e^{-\mathcal{A}^{(0)}[\bar{\psi}, \psi, A; S^{-1}, D^{-1}]}. \quad (6.67)$$

The products of pairs of fields $\bar{\psi}_1 \psi_2$ and $A_3 A_6$ can be substituted by a functional derivative with respect to S^{-1} and D^{-1} , leading to the perturbation expansion

$$Z \equiv \sum_{p=0}^{\infty} e^{2p} Z^{(p)} = \sum_{p=0}^{\infty} \frac{(-2e^2)^p}{(2p)!} \left(\int_{1\dots 6} V_{123} V_{456} \frac{\delta^3}{\delta S_{12}^{-1} \delta S_{45}^{-1} \delta D_{36}^{-1}} \right)^p Z^{(0)}. \quad (6.68)$$

Note the two advantages of this expansion over the conventional one in terms of currents coupled linearly to the fields. First, it contains only half as many functional derivatives. Second, it does not contain derivatives with respect to Grassmann variables.

Inserting for $Z^{(0)}$ the free vacuum functional (6.22), we obtain for the first-order term $Z^{(1)}$

$$Z^{(1)} = \frac{1}{2!} \int_{1\dots 6} V_{123} V_{456} (-2) \frac{\delta^3}{\delta D_{36}^{-1} \delta S_{12}^{-1} \delta S_{45}^{-1}} Z^{(0)}. \quad (6.69)$$

Since

$$Z = Z^{(0)} + e^2 Z^{(1)} + \dots = \exp \left\{ W^{(0)} + e^2 W^{(1)} + \dots \right\}, \quad (6.70)$$

this corresponds to a first-order correction $W^{(1)}$ to the vacuum energy $W^{(0)}$:

$$W^{(1)} = \frac{1}{2!} \int_{1\dots 6} V_{123} V_{456} (-2) \frac{\delta W_A^{(0)}}{\delta D_{36}^{-1}} \left(\frac{\delta^2 W_\psi^{(0)}}{\delta S_{12}^{-1} \delta S_{45}^{-1}} + \frac{\delta W_\psi^{(0)}}{\delta S_{12}^{-1}} \frac{\delta W_\psi^{(0)}}{\delta S_{45}^{-1}} \right). \quad (6.71)$$

Expressing the derivatives with respect to the kernels by the corresponding propagators via Eqs. (6.34), (6.50), and taking into account (6.54), $W^{(1)}$ becomes

$$W^{(1)} = \frac{1}{2} \int_{1\dots 6} V_{123} V_{456} D_{36} (S_{21} S_{54} - S_{24} S_{51}). \quad (6.72)$$

According to the Feynman rules (6.28)–(6.30), this is represented by the diagrams

$$W^{(1)} = \frac{1}{2} \left(\text{Diagram 1} \right) - \frac{1}{2} \left(\text{Diagram 2} \right). \quad (6.73)$$

Note that each closed electron loop causes a factor -1 .

6.4 Graphical Recursion Relation for Connected Vacuum Diagrams

In this section, we derive a functional differential equation for the vacuum functional $W[S^{-1}, D^{-1}, V]$ whose solution leads to a graphical recursion relation for all connected vacuum diagrams.

6.4.1 Functional Differential Equation for $W = \ln Z$

The functional differential equation for the vacuum functional $W[S^{-1}, D^{-1}, V]$ is derived from the following functional integral identity

$$\oint \mathcal{D}\bar{\psi} \mathcal{D}\psi \mathcal{D}A \frac{\delta}{\delta \psi_1} \left\{ \bar{\psi}_2 e^{-\mathcal{A}[\bar{\psi}, \psi, A; S^{-1}, D^{-1}, V]} \right\} = 0 \quad (6.74)$$

with the action (6.13). This identity is the functional generalization of the trivial integral identity $\int_{-\infty}^{+\infty} dx f'(x) = 0$ for functions $f(x)$ which vanish at infinity. Nontrivial consequences of Eq. (6.74) are obtained by performing the functional derivative in the integrand which yields

$$\oint \mathcal{D}\bar{\psi} \mathcal{D}\psi \mathcal{D}A \left\{ \delta_{12} + \int_3 \bar{\psi}_2 S_{13}^{-1} \psi_3 - e \int_{34} V_{134} \bar{\psi}_2 \psi_3 A_4 \right\} e^{-\mathcal{A}[\bar{\psi}, \psi, A; S^{-1}, D^{-1}, V]} = 0. \quad (6.75)$$

Substituting the field product $\bar{\psi}_2 \psi_3$ by functional derivatives with respect to the electron kernel S_{23}^{-1} , this equation can be expressed in terms of the partition function (6.12):

$$Z \delta_{12} - \int_3 S_{13}^{-1} \frac{\delta Z}{\delta S_{23}^{-1}} + e \int_{34} V_{134} \frac{\delta}{\delta S_{23}^{-1}} [\langle \hat{A}_4 \rangle Z] = 0. \quad (6.76)$$

To bring this functional differential equation into a more convenient form, we calculate explicitly the term containing the expectation of the field A . This is done starting from the integral identity

$$\oint \mathcal{D}\bar{\psi}\mathcal{D}\psi\mathcal{D}A \frac{\delta}{\delta A_1} e^{-\mathcal{A}[\bar{\psi},\psi,A,S^{-1},D^{-1},V]} = 0. \quad (6.77)$$

Note this identity is not endangered by the gauge freedom in the electromagnetic vector potential A_μ due to the presence of a gauge fixing term in the action (6.1). This ensures that the exponential vanishes at the boundary of all A field directions.

After differentiating the action in the exponential of Eq. (6.77), we find the expectation of the photon field

$$\int_1 \langle \hat{A}_1 \rangle D_{12}^{-1} = -e \int_{34} V_{342} \langle \psi_4 \bar{\psi}_3 \rangle. \quad (6.78)$$

Multiplying this with $\int_2 D_{25}$, we yield

$$\langle \hat{A}_5 \rangle = -e \int_{234} V_{342} D_{25} \frac{\delta W}{\delta S_{34}^{-1}}, \quad (6.79)$$

where we have used $Z = e^W$. Inserting this into Eq. (6.76), we obtain

$$\delta_{12} - \int_3 S_{13}^{-1} \frac{\delta W}{\delta S_{23}^{-1}} = e^2 \int_{3\dots 7} V_{134} V_{567} D_{47} \left\{ \frac{\delta^2 W}{\delta S_{23}^{-1} \delta S_{56}^{-1}} + \frac{\delta W}{\delta S_{23}^{-1}} \frac{\delta W}{\delta S_{56}^{-1}} \right\}. \quad (6.80)$$

Setting $x_1 = x_2$ and performing the integration over x_1 , this leads to the nonlinear functional differential equation for the vacuum functional W

$$\int_1 \delta_{11} - \int_{12} S_{12}^{-1} \frac{\delta W}{\delta S_{12}^{-1}} = e^2 \int_{1\dots 6} V_{123} V_{456} D_{36} \left\{ \frac{\delta^2 W}{\delta S_{12}^{-1} \delta S_{45}^{-1}} + \frac{\delta W}{\delta S_{12}^{-1}} \frac{\delta W}{\delta S_{45}^{-1}} \right\}, \quad (6.81)$$

which will form the basis for deriving the desired recursion relation for the vacuum diagrams. The first term on the left-hand side of Eq. (6.81) is infinite, but in the next section we will show that this cancels against an infinity in the second term.

6.4.2 Recursion Relation

Equation (6.81) contains functional derivatives with respect to the electron kernel S^{-1} which are equivalent to cutting lines in the vacuum diagrams. For practical purposes it will be more convenient to work with derivatives with respect to the propagators S which remove electron lines. The second term on the left-hand side of Eq. (6.81) contains the operation $-\int_{12} S_{12}^{-1} \delta/\delta S_{12}^{-1}$, which we convert into the differential operator

$$\hat{N}_F = \int_{12} S_{12} \frac{\delta}{\delta S_{12}} \quad (6.82)$$

with the help of (6.62). This operator has a simple graphical interpretation. The derivative $\delta/\delta S_{12}$ removes an electron line from a Feynman diagram, and the factor S_{12} restores it. This operation is familiar from the number operator in second quantization. The operator \hat{N}_F counts the number of electron lines in a Feynman diagram G :

$$\hat{N}_F G = N_F G. \quad (6.83)$$

When applied to the vacuum diagrams $W^{(p)}$ of order $p \geq 1$, this operator gives

$$\hat{N}_F W^{(p)} = 2p W^{(p)}, \quad p \geq 1, \quad (6.84)$$

since the number of electron lines in a vacuum diagram without external sources in quantum electrodynamics is equal to the number of vertices. The restriction in Eq. (6.84) to $p \geq 1$ is necessary due

to a special role of the vacuum diagram. Take, for example, the electron vacuum diagram of the free theory (6.23). By applying the operator \hat{N}_F , we obtain with (6.50)

$$\hat{N}_F W_\psi^{(0)} = - \int_{12} S_{12}^{-1} S_{21} = - \int_1 \delta_{11}, \quad (6.85)$$

which is a divergent trace integral precisely canceling the infinite first term in Eq. (6.81).

Separating out $W^{(0)}$ in the expansion (6.26) of the vacuum functional, the left-hand side of the functional differential equation (6.81) has the expansion

$$\int_1 \delta_{11} + \hat{N}_F W = \sum_{p=1}^{\infty} 2p e^{2p} W^{(p)} = \sum_{p=0}^{\infty} 2(p+1) e^{2(p+1)} W^{(p+1)}. \quad (6.86)$$

On the right hand side of Eq. (6.81), we express the first and second functional derivatives with respect to the kernel S^{-1} in terms of functional derivatives with respect to the propagator S by using Eq. (6.62) and

$$\frac{\delta^2}{\delta S_{12}^{-1} \delta S_{34}^{-1}} = \int_{5678} S_{51} S_{26} S_{73} S_{48} \frac{\delta^2}{\delta S_{56} \delta S_{78}} + \int_{56} [S_{53} S_{41} S_{26} + S_{23} S_{46} S_{51}] \frac{\delta}{\delta S_{56}}. \quad (6.87)$$

Inserting here the expansion (6.26) and comparing equal powers in e with those in Eq. (6.86), we obtain the following recursion formula for the expansion coefficients of the vacuum functional

$$W^{(p+1)} = \frac{1}{2(p+1)} \left\{ \int_{1\dots 10} V_{123} V_{456} D_{36} S_{71} S_{28} S_{94} S_{510} \frac{\delta^2 W^{(p)}}{\delta S_{78} \delta S_{910}} \right. \\ \left. + 2 \int_{1\dots 8} V_{123} V_{456} D_{36} (S_{51} S_{28} S_{74} - S_{71} S_{28} S_{54}) \frac{\delta W^{(p)}}{\delta S_{78}} \right. \\ \left. + \sum_{q=1}^{p-1} \int_{1\dots 10} V_{123} V_{456} D_{36} S_{71} S_{28} S_{94} S_{510} \frac{\delta W^{(q)}}{\delta S_{78}} \frac{\delta W^{(p-q)}}{\delta S_{910}} \right\}, \quad p \geq 1 \quad (6.88)$$

and the initial value (6.72). This equation enables us to derive the connected vacuum diagrams systematically to any desired order from the diagrams of the previous orders, as will now be shown.

6.4.3 Graphical Solution

With the help of the Feynman rules (6.28)–(6.30), the functional recursion relation (6.88) can be written diagrammatically as follows

$$W^{(p+1)} \equiv \frac{1}{2(p+1)} \left\{ \begin{array}{l} \text{Diagram 1: } \frac{\delta^2 W^{(p)}}{\delta 1 \leftarrow 2 \delta 3 \leftarrow 4} \\ \text{Diagram 2: } \left[\text{Diagram 2a} - \text{Diagram 2b} \right] \frac{\delta W^{(p)}}{\delta 1 \leftarrow 2} \\ \text{Diagram 3: } \sum_{q=1}^{p-1} \frac{\delta W^{(p-q)}}{\delta 1 \leftarrow 2} \text{Diagram 3a} \frac{\delta W^{(q)}}{\delta 3 \leftarrow 4} \end{array} \right\}, \quad p \geq 1 \quad (6.89)$$

and the first-order result is given by Eq. (6.73). The right-hand side contains four graphical operations. The first three are linear and involve one or two electron line amputations of the previous perturbative order. The fourth operation is nonlinear and mixes two different electron line amputations of lower orders. To demonstrate the working of this formula, we calculate the connected vacuum diagrams in second and third order. We start with the amputation of one or two electron lines in first order (6.73):

$$\frac{\delta W^{(1)}}{\delta 1 \leftarrow 2} \equiv \text{Diagram 4a} - \text{Diagram 4b}, \quad \frac{\delta^2 W^{(1)}}{\delta 1 \leftarrow 2 \delta 3 \leftarrow 4} \equiv \text{Diagram 5a} - \text{Diagram 5b}. \quad (6.90)$$

Inserting (6.90) into (6.89), where we have to take care of connecting only legs with the same label, we find the second-order correction of the vacuum functional W :

$$W^{(2)} \equiv \frac{1}{4} \text{diagram}_1 + \text{diagram}_2 - \frac{1}{2} \text{diagram}_3 - \frac{1}{4} \text{diagram}_4 - \frac{1}{2} \text{diagram}_5. \quad (6.91)$$

The calculation of the third-order correction $W^{(3)}$ leads to the following 20 diagrams:

$$\begin{aligned} W^{(3)} \equiv & \frac{1}{2} \text{diagram}_1 + \frac{1}{6} \text{diagram}_2 + \frac{1}{6} \text{diagram}_3 + \text{diagram}_4 - \frac{1}{6} \text{diagram}_5 \\ & + \frac{1}{2} \text{diagram}_6 + \text{diagram}_7 + \text{diagram}_8 + \text{diagram}_9 - \text{diagram}_{10} \\ & - \frac{1}{2} \text{diagram}_{11} - \text{diagram}_{12} - \text{diagram}_{13} + \frac{1}{3} \text{diagram}_{14} \\ & + \frac{1}{2} \text{diagram}_{15} - \frac{1}{2} \text{diagram}_{16} - \frac{1}{6} \text{diagram}_{17} - \text{diagram}_{18} - \frac{1}{2} \text{diagram}_{19} - \frac{1}{3} \text{diagram}_{20}. \end{aligned} \quad (6.92)$$

From the vacuum diagrams (6.73), (6.91), and (6.92), we observe a simple mnemonic rule for the weights of the connected vacuum diagrams in QED. At least up to four loops, each weight is equal to the reciprocal number of electron lines, which, by cutting, generate the same two-point diagrams. The sign is given by $(-1)^L$, where L denotes the number of electron loops. Note that the total weight, which is the sum over all weights of the vacuum diagrams in the order to be considered, vanishes in QED. The simplicity of the weights is a consequence of the Fermi statistics and the three-point form of interaction (6.11). The weights of the vacuum diagrams in other theories, like ϕ^4 theory [5,21,23], follow more complicated rules.

6.5 Scattering Between Electrons and Photons

From the above vacuum diagrams, we obtain all even-point correlation functions by cutting electron or photon lines. For the generation of the odd-point functions we use the functional derivative (6.66) with respect to the interaction function V which removes a vertex from a diagram.

As an illustration, we generate the diagrams for the self interactions described by the propagators (6.15) and (6.16)

$${}^\gamma G_{12}^2 = \langle \hat{A}_1 \hat{A}_2 \rangle, \quad {}^e G_{12}^2 = \langle \hat{\psi}_1 \hat{\psi}_2 \rangle \quad (6.93)$$

and the four-point functions

$${}^{\gamma\gamma} G_{1234}^4 = \langle \hat{A}_1 \hat{A}_2 \hat{A}_3 \hat{A}_4 \rangle, \quad {}^{ee} G_{1234}^4 = \langle \hat{\psi}_1 \hat{\psi}_2 \hat{\psi}_3 \hat{\psi}_4 \rangle, \quad {}^{e\gamma} G_{1234}^4 = \langle \hat{\psi}_1 \hat{A}_2 \hat{A}_3 \hat{\psi}_4 \rangle, \quad (6.94)$$

which represent the simplest scattering processes of the theory. In addition, we give the perturbative expansion of the three-point vertex function

$$G_{123}^3 = \langle \hat{\psi}_1 \hat{\psi}_2 \hat{A}_3 \rangle. \quad (6.95)$$

The following examples illustrate the simple weights $(-1)^L$ of diagrams contributing to an n -point function with $n \geq 2$, with L being the number of electron loops.

6.5.1 Self Interactions

Substituting the product of the photon fields $A_1 A_2$ in the functional integral (6.15) by the photonic functional derivative $-2\delta/\delta D_{12}^{-1}$, the photonic two-point function of the interacting theory is given by

$$\gamma G_{12}^2 = -2 \frac{\delta}{\delta D_{12}^{-1}} W[S^{-1}, D^{-1}, V]. \quad (6.96)$$

Applying the associated cutting rule (6.39) to the vacuum diagrams (6.73) and (6.91) leads to the connected diagrams

$$\begin{aligned} \gamma G_{12}^{2,c} \equiv & \text{1} \text{---} \text{2} - e^2 \text{---} \text{---} \text{---} + e^4 \left[\text{---} \text{---} \text{---} - \text{---} \text{---} \text{---} - \text{---} \text{---} \text{---} \right. \\ & \left. + \text{---} \text{---} \text{---} + \text{---} \text{---} \text{---} + \text{---} \text{---} \text{---} \right] + \mathcal{O}(e^6). \end{aligned} \quad (6.97)$$

For brevity, we have omitted the labels 1 and 2 at the ends of the higher-order diagrams. The full and the connected propagators γG_{12}^2 and $\gamma G_{12}^{2,c}$ satisfy the cumulant relation

$$\gamma G_{12}^{2,c} = \gamma G_{12}^2 - \langle \hat{A}_1 \rangle \langle \hat{A}_2 \rangle. \quad (6.98)$$

Note that although the expectation value of the electromagnetic field $\langle \hat{A}_\mu(x) \rangle$ is zero in quantum electrodynamics, it does not vanish in our generalized theory with arbitrary propagators S and D [see Eq. (6.79)].

The derivative of vacuum diagrams with respect to the electron kernel S^{-1} ,

$${}^e G_{12}^2 = \frac{\delta}{\delta S_{21}^{-1}} W[S^{-1}, D^{-1}, V], \quad (6.99)$$

leads to the electronic two-point function, whose diagrams are

$$\begin{aligned} {}^e G_{12}^2 \equiv & \text{1} \text{---} \text{2} + e^2 \left[\text{---} \text{---} \text{---} - \text{---} \text{---} \text{---} \right] + e^4 \left[\text{---} \text{---} \text{---} + \text{---} \text{---} \text{---} \right. \\ & + \text{---} \text{---} \text{---} - \text{---} \text{---} \text{---} - \text{---} \text{---} \text{---} - \text{---} \text{---} \text{---} \\ & \left. - \text{---} \text{---} \text{---} - \text{---} \text{---} \text{---} + \text{---} \text{---} \text{---} - \text{---} \text{---} \text{---} \right] + \mathcal{O}(e^6). \end{aligned} \quad (6.100)$$

6.5.2 Scattering Processes

The generation of diagrams for scattering processes between electrons and photons (6.94) and higher even-point functions is now straightforward.

Photon-Photon-Scattering

The four-point function of photons is obtained by cutting two photon lines in the vacuum diagrams or one photon line in the photonic two-point function:

$$\gamma\gamma G_{1234}^4 = 4 \left\{ \frac{\delta^2 W}{\delta D_{12}^{-1} \delta D_{34}^{-1}} + \frac{\delta W}{\delta D_{12}^{-1}} \frac{\delta W}{\delta D_{34}^{-1}} \right\} = -2 \frac{\delta \gamma G_{12}^2}{\delta D_{34}^{-1}} + \gamma G_{12}^2 \gamma G_{34}^2. \quad (6.101)$$

After applying one of the two possible operations in (6.101), the resulting connected diagrams to order e^4 are

$$\gamma\gamma G_{1234}^{4,c} \equiv -e^4 \left[\begin{array}{c} 2 \\ \text{---} \\ \text{---} \text{---} \text{---} \\ \text{---} \\ 1 \end{array} \text{---} \begin{array}{c} 3 \\ \text{---} \\ \text{---} \text{---} \text{---} \\ \text{---} \\ 4 \end{array} + 5 \text{ perm.} \right] + \mathcal{O}(e^6), \quad (6.102)$$

each permutation of two external spacetime coordinates leading to a different diagram.

Møller and Bhabba Scattering

The scattering of two electrons (Møller scattering) is described by the electronic four-point function

$$ee G_{1234}^4 = \frac{\delta^2 W}{\delta S_{41}^{-1} \delta S_{32}^{-1}} + \frac{\delta W}{\delta S_{41}^{-1}} \frac{\delta W}{\delta S_{32}^{-1}} = \frac{\delta e G_{23}^2}{\delta S_{41}^{-1}} + e G_{14}^2 e G_{23}^2. \quad (6.103)$$

To order e^4 , the connected diagrams contributing to the fermionic four-point function are

$$ee G_{1234}^{4,c} \equiv e^2 \left[\begin{array}{c} 2 \\ \text{---} \\ \text{---} \text{---} \text{---} \\ \text{---} \\ 1 \end{array} \text{---} \begin{array}{c} 3 \\ \text{---} \\ \text{---} \text{---} \text{---} \\ \text{---} \\ 4 \end{array} - (3 \leftrightarrow 4) \right] + e^4 \left[\begin{array}{c} \text{---} \\ \text{---} \\ \text{---} \text{---} \text{---} \\ \text{---} \\ \text{---} \end{array} + \begin{array}{c} \text{---} \\ \text{---} \\ \text{---} \text{---} \text{---} \\ \text{---} \\ \text{---} \end{array} + \begin{array}{c} \text{---} \\ \text{---} \\ \text{---} \text{---} \text{---} \\ \text{---} \\ \text{---} \end{array} \\ + \begin{array}{c} \text{---} \\ \text{---} \\ \text{---} \text{---} \text{---} \\ \text{---} \\ \text{---} \end{array} + \begin{array}{c} \text{---} \\ \text{---} \\ \text{---} \text{---} \text{---} \\ \text{---} \\ \text{---} \end{array} + \begin{array}{c} \text{---} \\ \text{---} \\ \text{---} \text{---} \text{---} \\ \text{---} \\ \text{---} \end{array} + \begin{array}{c} \text{---} \\ \text{---} \\ \text{---} \text{---} \text{---} \\ \text{---} \\ \text{---} \end{array} - \begin{array}{c} \text{---} \\ \text{---} \\ \text{---} \text{---} \text{---} \\ \text{---} \\ \text{---} \end{array} \\ - \begin{array}{c} \text{---} \\ \text{---} \\ \text{---} \text{---} \text{---} \\ \text{---} \\ \text{---} \end{array} - \begin{array}{c} \text{---} \\ \text{---} \\ \text{---} \text{---} \text{---} \\ \text{---} \\ \text{---} \end{array} - \begin{array}{c} \text{---} \\ \text{---} \\ \text{---} \text{---} \text{---} \\ \text{---} \\ \text{---} \end{array} - \begin{array}{c} \text{---} \\ \text{---} \\ \text{---} \text{---} \text{---} \\ \text{---} \\ \text{---} \end{array} - (3 \leftrightarrow 4) \right] + \mathcal{O}(e^6), \quad (6.104)$$

where the spacetime indices in all diagrams are arranged as in the first. Each diagram on the right-hand side has a partner with opposite sign, where the spacetime indices either of the incoming or of the outgoing electrons are interchanged. The tadpole diagrams vanish for physical propagators $S = S_F$, $D = D_F$, and the corresponding corrections attached to external legs do not contribute when calculating the S -matrix elements. In our general vacuum functional, however, we must not discard them, since they contribute to higher functional derivatives, which would be needed for the calculation of, e.g. the six-point function.

By interchanging spacetime arguments in the kernels of Eq. (6.104) apparently, the Feynman diagrams (6.104) describe also scattering of electron and positron (Bhabba scattering) and scattering of two positrons.

Compton Scattering

The amplitude of Compton scattering is given by the mixed four-point function $e\gamma G_{1234}^4$. To obtain the relevant Feynman diagrams, we have to perform one of the possible operations

$$e\gamma G_{1234}^4 = -2 \left\{ \frac{\delta^2 W}{\delta D_{23}^{-1} \delta S_{41}^{-1}} + \frac{\delta W}{\delta D_{23}^{-1}} \frac{\delta W}{\delta S_{41}^{-1}} \right\} = \frac{\delta \gamma G_{23}^2}{\delta S_{41}^{-1}} + e G_{14}^2 \gamma G_{23}^2 = -2 \frac{\delta e G_{14}^2}{\delta D_{23}^{-1}} + e G_{14}^2 \gamma G_{23}^2. \quad (6.105)$$

The resulting connected Feynman diagrams to order e^4 are

$$\begin{aligned}
 e\gamma G_{1234}^{4,c} \equiv & e^2 \left[\begin{array}{c} 2 \\ \diagup \quad \diagdown \\ 1 \quad \quad 4 \end{array} \begin{array}{c} \diagdown \quad \diagup \\ 3 \\ 4 \end{array} + (2 \leftrightarrow 3) \right] + e^4 \left[\begin{array}{c} \diagdown \quad \diagup \\ \diagdown \quad \diagup \\ \diagdown \quad \diagup \end{array} + \begin{array}{c} \diagdown \quad \diagup \\ \diagdown \quad \diagup \\ \diagdown \quad \diagup \end{array} + \begin{array}{c} \diagdown \quad \diagup \\ \diagdown \quad \diagup \\ \diagdown \quad \diagup \end{array} \right. \\
 & + \begin{array}{c} \diagdown \quad \diagup \\ \diagdown \quad \diagup \\ \diagdown \quad \diagup \end{array} + \begin{array}{c} \diagdown \quad \diagup \\ \diagdown \quad \diagup \\ \diagdown \quad \diagup \end{array} + \begin{array}{c} \diagdown \quad \diagup \\ \diagdown \quad \diagup \\ \diagdown \quad \diagup \end{array} - \begin{array}{c} \diagdown \quad \diagup \\ \diagdown \quad \diagup \\ \diagdown \quad \diagup \end{array} - \begin{array}{c} \diagdown \quad \diagup \\ \diagdown \quad \diagup \\ \diagdown \quad \diagup \end{array} - \begin{array}{c} \diagdown \quad \diagup \\ \diagdown \quad \diagup \\ \diagdown \quad \diagup \end{array} \\
 & \left. - \begin{array}{c} \diagdown \quad \diagup \\ \diagdown \quad \diagup \\ \diagdown \quad \diagup \end{array} - \begin{array}{c} \diagdown \quad \diagup \\ \diagdown \quad \diagup \\ \diagdown \quad \diagup \end{array} - \begin{array}{c} \diagdown \quad \diagup \\ \diagdown \quad \diagup \\ \diagdown \quad \diagup \end{array} + (2 \leftrightarrow 3) \right] + \mathcal{O}(e^6), \quad (6.106)
 \end{aligned}$$

where the diagrams with interchanged photon coordinates $2 \leftrightarrow 3$ possess the same sign as the original one.

6.5.3 Three-Point Vertex Function

The three-point vertex function is obtained from the vacuum energy W by performing the derivative with respect to the interaction function V_{123} , which we have defined in Eq. (6.64):

$$G_{123}^3 = -\frac{1}{e} \frac{\delta W}{\delta V_{213}}. \quad (6.107)$$

The easiest way to find the associated Feynman diagrams is to apply the graphical operation (6.65), which removes a vertex from the vacuum diagrams in all possible ways and lets the remaining legs open. Dropping disconnected diagrams by considering the cumulant

$$G_{123}^{3,c} = G_{123}^3 - \langle \hat{\psi}_1 \hat{\psi}_2 \rangle \langle \hat{A}_3 \rangle \quad (6.108)$$

we obtain

$$\begin{aligned}
 G_{123}^{3,c} = & e \begin{array}{c} 3 \\ \diagup \quad \diagdown \\ 1 \quad \quad 2 \end{array} + e^3 \left[\begin{array}{c} \diagdown \quad \diagup \\ \diagdown \quad \diagup \\ \diagdown \quad \diagup \end{array} + \begin{array}{c} \diagdown \quad \diagup \\ \diagdown \quad \diagup \\ \diagdown \quad \diagup \end{array} + \begin{array}{c} \diagdown \quad \diagup \\ \diagdown \quad \diagup \\ \diagdown \quad \diagup \end{array} - \begin{array}{c} \diagdown \quad \diagup \\ \diagdown \quad \diagup \\ \diagdown \quad \diagup \end{array} - \begin{array}{c} \diagdown \quad \diagup \\ \diagdown \quad \diagup \\ \diagdown \quad \diagup \end{array} \right. \\
 & \left. - \begin{array}{c} \diagdown \quad \diagup \\ \diagdown \quad \diagup \\ \diagdown \quad \diagup \end{array} \right] + \mathcal{O}(e^5). \quad (6.109)
 \end{aligned}$$

6.6 Scattering of Electrons and Photons in the Presence of an External Electromagnetic Field

To describe the scattering of electrons and photons on external electromagnetic fields, the action $\mathcal{A}[\bar{\psi}, \psi, A]$ in Eq. (6.13) must be extended by an additional external current J , which is coupled linearly to the electromagnetic field A :

$$\mathcal{A}^J[\bar{\psi}, \psi, A, J] = \mathcal{A}[\bar{\psi}, \psi, A] - e \int_1 J_1 A_1. \quad (6.110)$$

Then the partition function (6.12) becomes a functional in the physical current J and is given by

$$Z[J] = \oint \mathcal{D}\bar{\psi} \mathcal{D}\psi \mathcal{D}A e^{-\mathcal{A}^J[\bar{\psi}, \psi, A, J]} \quad (6.111)$$

with $Z = Z[0]$. The external current is usually supplied by some atomic nucleus of charge Ne with integer number N . For this reason, the factor e is removed from the current in Eq. (6.110) to be able to collect systematically all Feynman diagrams of the same order in e . This organization may not always be the most useful one. If we consider, for instance, an external heavy nucleus with a high charge Ne , we may have to include many more orders in the external charge Ne than in the internal charge e . Such subtleties will be ignored here, for simplicity.

6.6.1 Recursion Relation for the Vacuum Energy with External Source

Along similar lines as before, we derive the recursion relation for the vacuum energy in the presence of an external current, $W[J] = \ln Z[J]$ which is now also a functional of J (suppressing the other arguments D^{-1}, S^{-1}, V). After that, we derive a recursion relation *only* producing those vacuum diagrams which contain a coupling to the source. It turns out that the resulting recursion relation for current diagrams is extremely simple. Hence, this recursion relation is the ideal extension of the former Eq. (6.89) which generates only the source-free diagrams.

Complete Recursion Relation for All Vacuum Diagrams

The recursion relation for *all* vacuum diagrams with and without external source is derived in a similar manner as that for all source-free vacuum diagrams (6.89). There will be, however, a few significant differences in comparison with the procedure in Section 6.4. Since the current J couples to the electromagnetic field A , vacuum diagrams with external current always contain photon lines. For this reason, we start with the identity

$$\oint \mathcal{D}\bar{\psi}\mathcal{D}\psi\mathcal{D}A \frac{\delta}{\delta A_1} \left\{ A_2 e^{-\mathcal{A}^J[\bar{\psi}, \psi, A, J]} \right\} = 0 \quad (6.112)$$

instead of Eq. (6.74). Performing the functional derivative leads to

$$Z[J]\delta_{12} + 2 \int_3 D_{13}^{-1} \frac{\delta Z[J]}{\delta D_{23}^{-1}} - e \int_{34} V_{341} \frac{\delta}{\delta S_{34}^{-1}} [\langle \hat{A}_2 \rangle^J Z[J]] + e J_1 \langle \hat{A}_2 \rangle^J Z[J] = 0 \quad (6.113)$$

in analogy to Eq. (6.76). The expectation value of the electromagnetic field A in the presence of an external source J is found by exploiting the identity

$$\oint \mathcal{D}\bar{\psi}\mathcal{D}\psi\mathcal{D}A \frac{\delta}{\delta A_1} e^{-\mathcal{A}^J[\bar{\psi}, \psi, A, J]} = 0 \quad (6.114)$$

to derive, as in Eqs. (6.77)–(6.79),

$$\langle \hat{A}_1 \rangle^J = -e \int_{234} V_{234} D_{14} \frac{\delta W[J]}{\delta S_{23}^{-1}} + e \int_2 D_{12} J_2, \quad (6.115)$$

where we have set $W[J] = \ln Z[J]$. Inserting the expectation value (6.115) into Eq. (6.113), the resulting functional differential equation reads

$$\begin{aligned} \delta_{12} + 2 \int_3 D_{13}^{-1} \frac{\delta W[J]}{\delta D_{23}^{-1}} &= -e^2 \int_{3\dots 7} V_{341} V_{567} D_{27} \left\{ \frac{\delta^2 W[J]}{\delta S_{34}^{-1} \delta S_{56}^{-1}} + \frac{\delta W[J]}{\delta S_{34}^{-1}} \frac{\delta W[J]}{\delta S_{56}^{-1}} \right\} \\ &+ 2e^2 \int_{345} V_{345} D_{25} J_1 \frac{\delta W[J]}{\delta S_{34}^{-1}} - e^2 \int_3 J_1 D_{23} J_3. \end{aligned} \quad (6.116)$$

Using relations (6.43) and (6.62), and taking the trace, this becomes

$$\begin{aligned} & - \int_1 \delta_{11} + 2 \int_{12} D_{12} \frac{\delta W[J]}{\delta D_{12}} \\ &= 2e^2 \int_{1\dots 8} V_{123} V_{456} D_{36} S_{71} S_{24} S_{58} \frac{\delta W[J]}{\delta S_{78}} + e^2 \int_{1\dots 10} V_{123} V_{456} D_{36} S_{71} S_{28} S_{94} S_{510} \end{aligned}$$

$$\times \left\{ \frac{\delta^2 W[J]}{\delta S_{78} \delta S_{910}} + \frac{\delta W[J]}{\delta S_{78}} \frac{\delta W[J]}{\delta S_{910}} \right\} + 2e^2 \int_{1\dots 6} V_{123} D_{34} J_4 S_{51} S_{26} \frac{\delta W[J]}{\delta S_{56}} + e^2 \int_{12} J_1 D_{12} J_2, \quad (6.117)$$

which generalizes Eq. (6.81). Expanding $W[J]$ as in Eq. (6.26),

$$W[J] = W^{(0)} + \sum_{p=1}^{\infty} e^{2p} W^{(p)}[J], \quad (6.118)$$

and using the fact that the free vacuum energy $W^{(0)}[J] = W^{(0)}[0] = W^{(0)}$ is independent of the external current, the first term on the left-hand side in Eq. (6.117) is canceled by an identity following from Eq. (6.34)

$$2 \int_{12} D_{12} \frac{\delta W^{(0)}}{\delta D_{12}} = \int_1 \delta_{11}. \quad (6.119)$$

Introducing a Feynman diagram for the coupling to the current J

$$\begin{array}{c} \nearrow \\ \searrow \end{array} \text{---} 1 \equiv J_1, \quad (6.120)$$

we obtain the graphical recursion relation

$$\begin{aligned} 2 \begin{array}{c} \nearrow \\ \searrow \end{array} \text{---} 1 \frac{\delta W^{(p+1)}[J]}{\delta \text{---} 2} &\equiv \begin{array}{c} \nearrow \\ \searrow \end{array} \begin{array}{c} 1 \\ 2 \\ 3 \\ 4 \end{array} \frac{\delta^2 W^{(p)}[J]}{\delta \text{---} 2 \delta \text{---} 4} + 2 \left[\begin{array}{c} \nearrow \\ \searrow \end{array} \begin{array}{c} 1 \\ 2 \end{array} - \begin{array}{c} \circ \\ \nearrow \\ \searrow \end{array} \begin{array}{c} 1 \\ 2 \end{array} \right] \frac{\delta W^{(p)}[J]}{\delta \text{---} 2} \\ + \sum_{q=1}^{p-1} \frac{\delta W^{(p-q)}[J]}{\delta \text{---} 2} & \begin{array}{c} \nearrow \\ \searrow \end{array} \begin{array}{c} 1 \\ 2 \\ 3 \\ 4 \end{array} \frac{\delta W^{(q)}[J]}{\delta \text{---} 4} + 2 \begin{array}{c} \nearrow \\ \searrow \end{array} \begin{array}{c} 1 \\ 2 \end{array} \frac{\delta W^{(p)}[J]}{\delta \text{---} 2}, \quad p \geq 1, \quad (6.121) \end{aligned}$$

and the first-order diagrams

$$W^{(1)}[J] = W^{(1)}[0] + \frac{1}{2} \begin{array}{c} \nearrow \\ \searrow \end{array} \begin{array}{c} \nearrow \\ \searrow \end{array} - \begin{array}{c} \nearrow \\ \searrow \end{array} \begin{array}{c} \circ \end{array}, \quad (6.122)$$

where $W^{(1)}[0] = W^{(1)}$ contains the source-free first-order vacuum diagrams (6.73). An important difference between the recursion relation (6.121) and the previous (6.89) is that the vacuum diagrams in a series of the coupling constant e contain different numbers of photon (or electron) lines, thus not satisfying a simple eigenvalue equation like (6.84). In fact, each vacuum diagram, generated by using the right-hand side of the recursion relation (6.121), must be divided by twice the number of photon lines in the diagram to obtain the correct weight factor. This procedure is a consequence of the left-hand side of Eq. (6.121), which counts the number of photon lines in each diagram separately. By taking this into consideration, the second-order vacuum diagrams are given by

$$W^{(2)}[J] = W^{(2)}[0] - \begin{array}{c} \nearrow \\ \searrow \end{array} \begin{array}{c} \circ \end{array} \begin{array}{c} \circ \end{array} - \begin{array}{c} \nearrow \\ \searrow \end{array} \begin{array}{c} \circ \end{array} - \frac{1}{2} \begin{array}{c} \nearrow \\ \searrow \end{array} \begin{array}{c} \circ \end{array} \begin{array}{c} \nearrow \\ \searrow \end{array} \quad (6.123)$$

with the source-free diagrams given in (6.91). In third order, there are 15 diagrams which couple to the physical source:

$$\begin{aligned} W^{(3)}[J] = W^{(3)}[0] &- \begin{array}{c} \nearrow \\ \searrow \end{array} \begin{array}{c} \circ \end{array} \begin{array}{c} \circ \end{array} \begin{array}{c} \circ \end{array} - \begin{array}{c} \nearrow \\ \searrow \end{array} \begin{array}{c} \circ \end{array} \begin{array}{c} \circ \end{array} - \begin{array}{c} \nearrow \\ \searrow \end{array} \begin{array}{c} \circ \end{array} \begin{array}{c} \circ \end{array} + \begin{array}{c} \nearrow \\ \searrow \end{array} \begin{array}{c} \circ \end{array} \begin{array}{c} \circ \end{array} \begin{array}{c} \circ \end{array} + \begin{array}{c} \nearrow \\ \searrow \end{array} \begin{array}{c} \circ \end{array} \begin{array}{c} \circ \end{array} \\ + \begin{array}{c} \nearrow \\ \searrow \end{array} \begin{array}{c} \circ \end{array} \begin{array}{c} \circ \end{array} \begin{array}{c} \circ \end{array} &+ \begin{array}{c} \nearrow \\ \searrow \end{array} \begin{array}{c} \circ \end{array} \begin{array}{c} \circ \end{array} \begin{array}{c} \circ \end{array} + \begin{array}{c} \nearrow \\ \searrow \end{array} \begin{array}{c} \circ \end{array} \begin{array}{c} \circ \end{array} \begin{array}{c} \circ \end{array} - \begin{array}{c} \nearrow \\ \searrow \end{array} \begin{array}{c} \circ \end{array} \begin{array}{c} \circ \end{array} \begin{array}{c} \circ \end{array} \begin{array}{c} \circ \end{array} - \begin{array}{c} \nearrow \\ \searrow \end{array} \begin{array}{c} \circ \end{array} \begin{array}{c} \circ \end{array} \begin{array}{c} \circ \end{array} \begin{array}{c} \circ \end{array} \end{aligned}$$

$$-\frac{1}{2} \begin{array}{c} \diagup \\ \diagdown \end{array} \text{---} \text{---} \text{---} \text{---} \begin{array}{c} \diagdown \\ \diagup \end{array} - \begin{array}{c} \diagup \\ \diagdown \end{array} \text{---} \text{---} \text{---} \text{---} \begin{array}{c} \diagdown \\ \diagup \end{array} - \begin{array}{c} \diagup \\ \diagdown \end{array} \text{---} \text{---} \text{---} \text{---} \begin{array}{c} \diagdown \\ \diagup \end{array} + \frac{1}{2} \begin{array}{c} \diagup \\ \diagdown \end{array} \text{---} \text{---} \text{---} \text{---} \begin{array}{c} \diagdown \\ \diagup \end{array} - \frac{1}{3} \begin{array}{c} \diagup \\ \diagdown \end{array} \text{---} \text{---} \text{---} \text{---} \begin{array}{c} \diagdown \\ \diagup \end{array} . \quad (6.124)$$

In the following we derive a recursion relation which allows us to generate *only* those vacuum diagrams which contain a coupling to the source.

Recursion Relation for Vacuum Diagrams Coupled to the External Source

Since we have the possibility to generate all source-free vacuum diagrams with the help of the recursion relation (6.89), we are able to set up a recursion relation to generate only the diagrams with source coupling. Inserting on the left-hand side of Eq. (6.115) the equation

$$\langle \hat{A}_1 \rangle^J = \frac{1}{e} \frac{\delta W[J]}{\delta J_1}, \quad (6.125)$$

multiplying both sides with J_1 , and performing the integral \int_1 yields

$$\int_1 J_1 \frac{\delta W[J]}{\delta J_1} = e^2 \int_{1\dots 6} V_{234} D_{14} J_1 S_{52} S_{36} \frac{\delta W[J]}{\delta S_{56}} + e^2 \int_{12} J_1 D_{12} J_2. \quad (6.126)$$

On the right-hand side we have changed the functional derivatives with respect to the kernel S^{-1} into functional derivatives with respect to the propagator S using Eq. (6.62). Inserting the decomposition (6.118) and utilizing the fact that $W^{(0)}$ from Eq. (6.22) is source-free, $\delta W^{(0)}/\delta J_1 = 0$, we find

$$\int_1 J_1 \frac{\delta W^{(1)}[J]}{\delta J_1} + \sum_{n=1}^{\infty} e^{2n} \int_1 J_1 \frac{\delta W^{(n+1)}[J]}{\delta J_1} = - \int_{1\dots 4} V_{234} D_{14} J_1 S_{32} + \int_{12} J_1 D_{12} J_2 + \sum_{n=1}^{\infty} e^{2n} \int_{1\dots 6} V_{234} D_{14} J_1 S_{52} S_{36} \frac{\delta W^{(n)}[J]}{\delta S_{56}}. \quad (6.127)$$

To lowest order, the right-hand side yields the source diagrams

$$\tilde{W}^{(1)}[J] = \frac{1}{2} \begin{array}{c} \diagup \\ \diagdown \end{array} \text{---} \text{---} \text{---} \begin{array}{c} \diagdown \\ \diagup \end{array} - \begin{array}{c} \diagup \\ \diagdown \end{array} \text{---} \text{---} \text{---} \text{---} \begin{array}{c} \diagdown \\ \diagup \end{array}, \quad (6.128)$$

where we have used the wobble to indicate the restriction to the source diagrams of $W^{(1)}[J]$ in Eq. (6.122). The full functional solving Eq. (6.127) consists of the terms

$$W^{(n)}[J] = W^{(n)}[0] + \tilde{W}^{(n)}[J], \quad (6.129)$$

where the source-free contributions $W^{(n)}[0] = W^{(n)}$ of Section 6.4 represent integration constants undetermined by Eq. (6.127). Introducing a diagram for the functional derivative with respect to the current J ,

$$\frac{\delta}{\delta \text{---}_1} \equiv \frac{\delta}{\delta J_1}, \quad (6.130)$$

the recursion relation for the vacuum diagrams with source-coupling Eq. (6.127) is graphically written for $n \geq 1$ as

$$\begin{array}{c} \diagup \\ \diagdown \end{array} \text{---}_1 \frac{\delta W^{(n+1)}[J]}{\delta \text{---}_1} \equiv \begin{array}{c} \diagup \\ \diagdown \end{array} \text{---}_1 \frac{\delta W^{(n)}[J]}{\delta \text{---}_1 \text{---}_2}. \quad (6.131)$$

The graphical operation on the right-hand side means that an external current is attached through a photon line to a fermion line in all possible ways. The iteration of this recursion relation is very simple since the right-hand side is linear. Each diagram calculated with the right-hand side of this equation must be divided by the number of source-coupling within the diagram since the operation on the left-hand side counts the number of source-couplings in the diagram. By considering Eq. (6.129), one easily reproduces the higher-order vacuum diagrams given in the Eqs. (6.123) and (6.124).

6.6.2 Scattering of Electrons and Photons in the Presence of an External Source

Typically, an external electromagnetic field is produced by a heavy particle such as a nucleus or an ion. Quantum electrodynamical effects like pair creation, Bremsstrahlung, and Lamb shift are caused by such electromagnetic fields. The Feynman diagrams for the n -point functions associated with these processes are again obtained by cutting electron or photon lines from the just-derived vacuum diagrams.

Vacuum Polarization Induced by External Field

The photon propagator in the presence of an external source

$$\gamma G_{12}^2[J] = -2 \frac{\delta W[J]}{\delta D_{12}^{-1}} \tag{6.132}$$

is found by cutting a photon line in the vacuum diagrams (6.122)–(6.124):

$$\gamma G_{12}^{2,c}[J] = \gamma G_{12}^{2,c}[0] + e^4 \left[- \text{diagram} - (1 \leftrightarrow 2) \right] + \mathcal{O}(e^6), \tag{6.133}$$

showing polarization caused by the external field.

Lamb Shift and Anomalous Magnetic Moment

The important phenomena of Lamb shift and anomalous magnetic moments are obtained from the perturbative corrections in the electron propagator:

$${}^e G_{12}^2[J] = \frac{\delta W[J]}{\delta S_{21}^{-1}}, \tag{6.134}$$

whose diagrams come from cutting an electron line in the vacuum diagrams (6.122)–(6.124). To order e^4 , we have

$${}^e G_{12}^2[J] = {}^e G_{12}^2[0] + e^2 \text{diagram} + e^4 \left[\text{diagram} + \text{diagram} + \text{diagram} - \text{diagram} - \text{diagram} - \text{diagram} - \text{diagram} + \text{diagram} \right] + \mathcal{O}(e^6). \tag{6.135}$$

As already mentioned before, diagrams with corrections on external legs and tadpole graphs do not contribute to S -matrix elements. In some problems, diagrams with more than one source-coupling are irrelevant.

Pair Creation, Pair Annihilation, and Bremsstrahlung

By differentiating the vacuum energy diagrams (6.122)–(6.124) with respect to the interaction function V_{123} , we obtain the vertex function in the presence of an external field:

$$G_{123}^3[J] = -\frac{1}{e} \frac{\delta W[J]}{\delta V_{213}}. \quad (6.136)$$

The connected Feynman diagrams are to order e^3 :

$$G_{123}^{3,c}[J] = G_{123}^{3,c}[0] + e^3 \left[\begin{array}{c} \text{Diagram 1} \\ \text{Diagram 2} \end{array} \right] + \mathcal{O}(e^5) \quad (6.137)$$

with $G_{123}^{3,c}[0] = G_{123}^{3,c}$ of Eq. (6.109). These diagrams appear in pair creation, pair annihilation, or Bremsstrahlung processes.

Part III

Variational Perturbation Theory in Quantum Statistics

Introduction

The exact calculation of path integrals is only possible, if they are or can be transformed in a Gaussian shape. In Part II of this thesis, we have considered a very general Gaussian action (3.1) and calculated the quantum-statistical properties of systems governed by such an action. All Euclidean systems, where the action only contains terms of the form $x^m(\tau)p^n(\tau)$ with $(m, n) \in \{(2, 0), (1, 1), (0, 2)\}$, belong to this class of exactly solvable problems. An example is a particle in a harmonic potential and influenced by external sources which linearly couple to particle position or momentum. In order to motivate the general theory in Part II, we have investigated the quantum statistics of the one-dimensional problem in detail. Another system in this class is a charged particle in static electric and/or magnetic field, since the scalar potential of the electric field couples linearly to the position, and the vector potential of the magnetic field is minimally coupled to the momentum. We will consider an application in this part, where we investigate the quantum-statistical properties of hydrogen in uniform magnetic field. As a warm-up exercise, we will treat there the exactly solvable problem of a single electron in magnetic field at arbitrary temperature. It is worth noting that the calculation of the path amplitude for the three-dimensional hydrogen atom is also exactly done after mapping it to a four-dimensional oscillator [4].

Nevertheless, most of the interesting systems have nontrivial interactions, which prevent an exact evaluation of quantum-statistical quantities. A characteristic property of such systems is that they are usually governed by potentials, which “disturb” the Gaussian shape of the action, for example the x^4 term of the anharmonic oscillator, its pendant in the field theory of critical phenomena, ϕ^4 , or the interaction $\bar{\psi}\gamma_\mu\psi A^\mu$ between matter fields $\bar{\psi}$, ψ and electromagnetic field A_μ in quantum electrodynamics (QED). The coupling strength between these fields in QED is rather small, it is the fine structure constant $\alpha = e^2/4\pi\epsilon_0\hbar c \approx 1/137$. In cases, where the coupling constant is small, it is useful to expand the time evolution operator (or the corresponding action exponential in the functional integral) into a Taylor series and to calculate perturbative corrections to the result of the exactly solvable unperturbed system. Since it is usually impossible to evaluate the corrections in all orders, the perturbation series must be broken up after any order n . For weak coupling, the first contributing perturbative order yields already satisfactory results for many systems. There is no guarantee, however, that, despite a small coupling constant, the perturbative series converges. The reason is that the number of terms contributing to a certain order of perturbation is extremely increasing from order to order. A practical quantity for checking the convergence of a series is its radius of convergence, which is defined as the infinite-order limit of the absolute ratio of contributions

a_n of successive orders:

$$R = \lim_{n \rightarrow \infty} \left| \frac{a_n}{a_{n+1}} \right|. \quad (7.1)$$

The series *converges*, if $R > 1$, and *diverges* for $R < 1$. Since in n th order $a_n = c_n g^n$, where c_n is the expansion coefficient and g the coupling constant, we find

$$R = \frac{r}{g}, \quad r = \lim_{n \rightarrow \infty} \left| \frac{c_n}{c_{n+1}} \right|. \quad (7.2)$$

In this relation, the competitive character of expansion coefficients and coupling strength turns out clearly. Thus, a perturbative series converges, if $r > g$, since the overall contribution decreases for successive orders of perturbation. A diverging series is characterized by $r < g$. Unfortunately, the radius of convergence can only be evaluated exactly, if a recursion equation for the perturbative coefficients exists, which relates c_n and c_{n+1} . For most problems, it is not possible to exactly determine R , and one can only make an extrapolation estimated from successive low orders, for which the coefficients c_n are known. Following Dyson [42], even perturbative series in QED will diverge for orders of perturbation higher than the inverse fine structure constant, i.e. $n > 1/\alpha$.

In order to obtain finite results from truncated perturbative expansions, it is necessary to apply methods, which perform an approximate summation of the series. It is even possible to use such summation methods for strong-coupling series, where the perturbations are not small in comparison with the unperturbed contribution. Well-known summation methods were developed by Euler, Borel, and Padé. The applicability of such methods is usually restricted to series obeying some requirements regarding the growth of the expansion coefficients for large orders [43]. Alternative promising procedures are based on nonlinear transformations, e.g. sequence transformations [44], for accelerating the convergence of originally diverging series.

We use a different powerful method for the summation of perturbative series, which is called *variational perturbation theory* [4, Chap. 5]. A first approach was used by Feynman in 1954 for discussing the polaron problem [45]. This procedure was improved by Feynman and Kleinert [8] and, independently, by Giachetti and Tognetti [9] in 1985/86. In this approach, the action of a harmonic oscillator with trial frequency $\Omega(x_0)$ serves as trial system and the remainder as perturbation. The correctly treated zero-frequency mode x_0 of the path by a separate x_0 -integration makes it possible to reexpress the quantum-statistical partition function by an integral over a classically looking Boltzmann factor, which contains the *effective classical potential*. Based on the Jensen-Peierls inequality, variation with respect to the trial frequency $\Omega(x_0)$ yields an upper bound for the effective classical potential. Meanwhile, this method is denoted as *variational approach*, since a systematic extension to higher-order variational perturbation theory was developed by Kleinert [4,46,47]. We will review the fundamentals of the approach and the systematic theory in the following sections.

In the following chapters, we present generalizations of this theory, which enable us to enlarge the range of applicability of variational perturbation theory. We develop variational perturbation theory for density matrices [20] and calculate the density of a particle in the double-well potential. Furthermore, we investigate the pair-distribution function for hydrogen, which is a characteristic quantity of hydrogen plasma. By extending variational perturbation theory for applications in phase space, where we practically introduce the *effective classical Hamiltonian*, we calculate the quantum-statistical properties of hydrogen in magnetic fields [18,19]. The zero-temperature limit of the effective classical Hamiltonian yields the binding energy. This quantity possesses quite different asymptotic behaviors for weak and strong magnetic fields. We investigate these limits in detail, and the results confirm the power of the variational summation method. Finally, in Part IV of this thesis, we turn to membrane physics, where we calculate the fluctuation pressure which fluid membranes exert upon hard walls [48,49]. By an analytic strong-coupling calculation, we evaluate the constants occurring in Helfrich's ideal-gas-like pressure law [50] to such a high accuracy that their values lie well within the error bounds of Monte-Carlo simulations. Aside from the very successful calculation of critical exponents in ϕ^4 theory [5], the results for the fluctuating membranes show that variational perturbation theory is also applicable for the summation of perturbation series arising from field theories.

7.1 Variational Approach via Jensen-Peierls Inequality

We review the variational approach [4,8,45] for the calculation of the quantum-statistical partition function Z in the more general phase space representation. As shown in Eq. (4.29), we express the partition function (4.28) as an integral of the restricted partition function $Z^{\mathbf{p}_0 \mathbf{x}_0}$ over the zero-frequency phase space coordinates \mathbf{p}_0 and \mathbf{x}_0 . The relation between $Z^{\mathbf{p}_0 \mathbf{x}_0}$ and the effective classical Hamiltonian $H_{\text{eff}}(p_0, x_0)$ is given by Eq. (4.31). We write the restricted partition function for any system with an dimensionless action $\mathcal{A}[\mathbf{p}, \mathbf{x}]$ as a path integral over the phase space coordinates $\mathbf{w}^T = (\mathbf{x}^T, \mathbf{p}^T)$ as

$$Z^{\mathbf{w}_0} = (2\pi\hbar)^d \oint \mathcal{D}^{2d} w \delta(\mathbf{w}_0 - \overline{\mathbf{w}(\tau)}) e^{-\mathcal{A}[\mathbf{w}]/\hbar}. \quad (7.3)$$

In general, this quantity cannot be calculated exactly, and therefore we decompose the action $\mathcal{A}[\mathbf{w}]$ into a part $\mathcal{A}_{\Omega}^{\mathbf{w}_0}[\mathbf{w}]$, for which the restricted partition function is known, and a remainder, which we call the interaction term $\mathcal{A}_{\text{int}}[\mathbf{w}]$:

$$\mathcal{A}[\mathbf{w}] = \mathcal{A}_{\Omega}^{\mathbf{w}_0}[\mathbf{w}] + \mathcal{A}_{\text{int}}[\mathbf{w}]. \quad (7.4)$$

The action of the exactly solvable system shall be expressed as

$$\mathcal{A}_{\Omega}^{\mathbf{w}_0}[\mathbf{w}] = \frac{\hbar}{2} \int_0^{\hbar\beta} d\tau \int_0^{\hbar\beta} d\tau' (\mathbf{w}^T(\tau) - \mathbf{w}_0^T) S_{\Omega}(\tau, \tau') (\mathbf{w}(\tau') - \mathbf{w}_0), \quad (7.5)$$

where we have subtracted the zero-frequency mode from the phase space coordinates. The elements of the symmetric matrix S_{Ω} are of the form $S_{\Omega,ij} = \Omega_{ij} S_{ij}$, where the $2d^2 + d$ parameters $\Omega_{ij} = \Omega_{ji}$ are still undetermined. The matrix S shall be of the form (3.10), which makes it possible to exactly calculate the corresponding restricted partition function:

$$\begin{aligned} Z_{\Omega}^{\mathbf{w}_0} &= (2\pi\hbar)^d \oint \mathcal{D}^{2d} w \delta(\mathbf{w}_0 - \overline{\mathbf{w}(\tau)}) \exp \left\{ -\frac{1}{2} \int_0^{\hbar\beta} d\tau \int_0^{\hbar\beta} d\tau' (\mathbf{w}^T(\tau) - \mathbf{w}_0^T) S_{\Omega}(\tau, \tau') (\mathbf{w}(\tau') - \mathbf{w}_0) \right\} \\ &= \frac{1}{\sqrt{\det_{\text{ps}} S_{\Omega,0}^{-1} \det S_{\Omega}}}. \end{aligned} \quad (7.6)$$

Here, we have made use of the calculation for the restricted partition function in Section 4.2, with the result (4.52). The exponential function occurring in (4.52) is absent in Eq. (7.6) due to the subtraction of the zero-frequency modes of the phase space path in the action of Eq. (7.5). In analogy to Eq. (4.53), we use the path integral (7.6) to define expectation values

$$\begin{aligned} \langle O_1(\mathbf{w}(\tau_1)) O_2(\mathbf{w}(\tau_2)) \cdots \rangle_{\Omega}^{\mathbf{w}_0} &= (2\pi\hbar)^d [Z_{\Omega}^{\mathbf{w}_0}]^{-1} \oint \mathcal{D}^{2d} w \delta(\mathbf{w}_0 - \overline{\mathbf{w}(\tau)}) \\ &\quad \times O_1(\mathbf{w}(\tau_1)) O_2(\mathbf{w}(\tau_2)) \cdots e^{-\mathcal{A}_{\Omega}^{\mathbf{w}_0}[\mathbf{w}]/\hbar}. \end{aligned} \quad (7.7)$$

By adding and subtracting the trial action (7.5) to the full action in the Boltzmann factor of expression (7.3), we obtain

$$Z^{\mathbf{w}_0} = (2\pi\hbar)^d \oint \mathcal{D}^{2d} w \delta(\mathbf{w}_0 - \overline{\mathbf{w}(\tau)}) e^{-\mathcal{A}_{\Omega}^{\mathbf{w}_0}[\mathbf{w}]/\hbar} \exp \{ -(\mathcal{A}[\mathbf{w}] - \mathcal{A}_{\Omega}^{\mathbf{w}_0}[\mathbf{w}]) / \hbar \}. \quad (7.8)$$

With the definition (7.7), the right-hand side of this equation can be written as expectation value of the exponential function containing the perturbation $\mathcal{A}[\mathbf{w}] - \mathcal{A}_{\Omega}^{\mathbf{w}_0}[\mathbf{w}] \equiv \mathcal{A}_{\text{int}}[\mathbf{w}]$:

$$Z^{\mathbf{w}_0} = Z_{\Omega}^{\mathbf{w}_0} \left\langle e^{-\mathcal{A}_{\text{int}}[\mathbf{w}]/\hbar} \right\rangle_{\Omega}^{\mathbf{w}_0}. \quad (7.9)$$

With the help of the Jensen-Peierls inequality,

$$\langle e^{-O} \rangle \geq e^{-\langle O \rangle}, \quad (7.10)$$

we can estimate Eq. (7.9) by

$$Z^{\mathbf{w}_0} \geq Z_{\Omega}^{\mathbf{w}_0} e^{-\langle \mathcal{A}_{\text{int}}[\mathbf{w}] / \hbar \rangle_{\Omega}^{\mathbf{w}_0}}. \quad (7.11)$$

Since the restricted partition functions are related to the effective classical Hamiltonians via

$$Z^{\mathbf{w}_0} = e^{-\beta H_{\text{eff}}(\mathbf{w}_0)}, \quad Z_{\Omega}^{\mathbf{w}_0} = e^{-\beta H_{\text{eff},\Omega}(\mathbf{w}_0)}, \quad (7.12)$$

the inequality (7.11) can be written as

$$H_{\text{eff}}(\mathbf{w}_0) \leq H_{\text{eff},\Omega}(\mathbf{w}_0) + \frac{1}{\hbar\beta} \langle \mathcal{A}_{\text{int}}[\mathbf{w}] \rangle_{\Omega}^{\mathbf{w}_0} \equiv \mathcal{H}_{\Omega}^{(1)}(\mathbf{w}_0). \quad (7.13)$$

We express the action $\mathcal{A}_{\text{int}}[\mathbf{w}]$ as a time integral over an interaction potential $V_{\text{int}}(\mathbf{w}(\tau))$,

$$\mathcal{A}_{\text{int}}[\mathbf{w}] = \int_0^{\hbar\beta} d\tau V_{\text{int}}(\mathbf{w}(\tau)). \quad (7.14)$$

The invariance of the expectation value under time translations makes the time integral trivial and the expectation value of the action becomes

$$\langle \mathcal{A}_{\text{int}}[\mathbf{w}] \rangle_{\Omega}^{\mathbf{w}_0} = \int_0^{\hbar\beta} d\tau \langle V_{\text{int}}(\mathbf{w}(\tau)) \rangle_{\Omega}^{\mathbf{w}_0} = \hbar\beta \langle V_{\text{int}}(\mathbf{w}) \rangle_{\Omega}^{\mathbf{w}_0}. \quad (7.15)$$

Thus the estimate $\mathcal{H}_{\Omega}^{(1)}(\mathbf{w}_0)$ can be written as

$$\mathcal{H}_{\Omega}^{(1)}(\mathbf{w}_0) = H_{\text{eff},\Omega}(\mathbf{w}_0) + \langle V_{\text{int}}(\mathbf{w}) \rangle_{\Omega}^{\mathbf{w}_0}. \quad (7.16)$$

This quantity is now optimized with respect to the set of parameters Ω_{ij} to yield the optimal upper bound for the effective classical Hamiltonian:

$$\frac{\partial \mathcal{H}_{\Omega}^{(1)}(\mathbf{w}_0)}{\partial \Omega_{ij}} \stackrel{!}{=} 0. \quad (7.17)$$

Let us denote the set of optimal parameters satisfying these $2d^2 + d$ equations as $\Omega_{ij}^{(1)}(\mathbf{w}_0)$. Inserting these results into (7.16), the optimal upper bound for the effective classical Hamiltonian is given by

$$\mathcal{H}^{(1)}(\mathbf{w}_0) = \mathcal{H}_{\Omega^{(1)}}^{(1)}(\mathbf{w}_0). \quad (7.18)$$

If more than one solution to the equations (7.17) exist, the smallest must be chosen, since the effective Hamiltonian (which can also be considered as a local free energy $F^{\mathbf{w}_0}$) must be minimal in the equilibrium state of the system. Should no solutions exist, the parameters are chosen from the flattest region, i.e. where $\mathcal{H}_{\Omega^{(1)}}^{(1)}(\mathbf{w}_0)$ depends *minimally* on the parameters Ω_{ij} . This is the principle of minimal sensitivity, which states that the best estimate possesses the least dependence of the variational parameters [51]. This is a conclusion of the independence of the exact effective classical Hamiltonian from these parameters.

The simplest case for the trial action (7.5) is the usual harmonic oscillator in one dimension

$$\mathcal{A}_{\Omega}^{p_0 x_0}[p, x] = \int_0^{\hbar\beta} d\tau \left\{ \frac{1}{2M} [p(\tau) - p_0]^2 + \frac{1}{2} M \Omega^2 [x(\tau) - x_0]^2 \right\}, \quad (7.19)$$

where only the potential contains a trial parameter Ω .

7.2 Variational Perturbation Theory to Any Order

A Taylor expansion of the exponential function in the expectation value of Eq. (7.9) in powers of the interaction $\mathcal{A}_{\text{int}}[\mathbf{w}]$ makes it possible to systematically improve the variational approach. Since

the summations of perturbative expansions truncated in different orders of perturbation can yield approximations for the effective classical Hamiltonian, which alternate around the exact result, the inequality (7.10) does not hold in general.

Performing the Taylor expansion, Eq. (7.9) becomes

$$Z^{\mathbf{w}_0} = Z_{\Omega}^{\mathbf{w}_0} \sum_{n=0}^{\infty} \frac{(-1)^n}{\hbar^n n!} \left\langle \left(\int_0^{\hbar\beta} d\tau V_{\text{int}}(\mathbf{w}(\tau)) \right)^n \right\rangle_{\Omega}^{\mathbf{w}_0}. \quad (7.20)$$

This can be written in the exponential form

$$Z^{\mathbf{w}_0} = Z_{\Omega}^{\mathbf{w}_0} \exp \left\{ \sum_{n=1}^{\infty} \frac{(-1)^n}{\hbar^n n!} \left\langle \left(\int_0^{\hbar\beta} d\tau V_{\text{int}}(\mathbf{w}(\tau)) \right)^n \right\rangle_{\Omega, c}^{\mathbf{w}_0} \right\}, \quad (7.21)$$

where the subscript c indicates as usual cumulants. The lowest cumulants are related to the full expectation values as follows:

$$\begin{aligned} \langle O_1(\mathbf{w}(\tau_1)) \rangle_{\Omega, c}^{\mathbf{w}_0} &= \langle O_1(\mathbf{w}(\tau_1)) \rangle_{\Omega}^{\mathbf{w}_0}, \\ \langle O_1(\mathbf{w}(\tau_1)) O_2(\mathbf{w}(\tau_2)) \rangle_{\Omega, c}^{\mathbf{w}_0} &= \langle O_1(\mathbf{w}(\tau_1)) O_2(\mathbf{w}(\tau_2)) \rangle_{\Omega}^{\mathbf{w}_0} - \langle O_1(\mathbf{w}(\tau_1)) \rangle_{\Omega}^{\mathbf{w}_0} \langle O_2(\mathbf{w}(\tau_2)) \rangle_{\Omega}^{\mathbf{w}_0}, \\ &\vdots, \end{aligned} \quad (7.22)$$

where $O_i(\mathbf{w}(\tau_j))$ denotes any observable depending on position and momentum. Recalling the relations (7.12) between partition functions and effective classical Hamiltonians we obtain from (7.21) the effective classical Hamiltonian as a cumulant expansion:

$$H_{\text{eff}}(\mathbf{w}_0) = -\frac{1}{\beta} \ln Z_{\Omega}^{\mathbf{w}_0} + \frac{1}{\beta} \sum_{n=1}^{\infty} \frac{(-1)^{n+1}}{\hbar^n n!} \left\langle \left(\int_0^{\hbar\beta} d\tau V_{\text{int}}(\mathbf{w}(\tau)) \right)^n \right\rangle_{\Omega, c}^{\mathbf{w}_0}. \quad (7.23)$$

Up to now, we did not make any approximation. The expansion on the right-hand side is an exact expression for the effective classical Hamiltonian for all components of Ω .

For systems with a nontrivial interaction, we are capable of calculating only some initial truncated part of the series (7.23), say up to the N th order, leading to the approximate effective classical Hamiltonian

$$\mathcal{H}_{\Omega}^{(N)}(\mathbf{w}_0) = -\frac{1}{\beta} \ln Z_{\Omega}^{\mathbf{w}_0} + \frac{1}{\beta} \sum_{n=1}^N \frac{(-1)^{n+1}}{\hbar^n n!} \left\langle \left(\int_0^{\hbar\beta} d\tau V_{\text{int}}(\mathbf{w}(\tau)) \right)^n \right\rangle_{\Omega, c}^{\mathbf{w}_0}. \quad (7.24)$$

This depends explicitly on the parameters Ω . Since the exact expression (7.23) is independent of Ω , the best approximation for $\mathcal{H}_{\Omega}^{(N)}(\mathbf{w}_0)$ should depend on Ω *minimally*. Thus the optimal solution will be found by determining the parameters from the $2d^2 + d$ conditions

$$\frac{\partial}{\partial \Omega_{ij}} \mathcal{H}_{\Omega}^{(N)}(\mathbf{w}_0) \stackrel{!}{=} 0. \quad (7.25)$$

Let us denote the optimal variational parameters to N th order by $\Omega_{ij}^{(N)}(\mathbf{w}_0)$. Inserting these into Eq. (7.24) yields the optimal effective classical Hamiltonian $\mathcal{H}^{(N)}(\mathbf{w}_0)$.

Variational Perturbation Theory for Density Matrices

We develop a convergent variational perturbation theory for quantum statistical density matrices, which is applicable to polynomial as well as nonpolynomial interactions [20]. We illustrate the power of the theory by calculating the temperature-dependent density of a particle in the double-well potential to second order, and of the electron in the hydrogen atom to first order.

8.1 Introduction

Variational perturbation theory [4,46] transforms divergent perturbation expansions into convergent ones, where the resulting convergence even extends to infinitely strong couplings [52]. The theory has first been developed in quantum mechanics for the path integral representation of the free energy of the anharmonic oscillator [47] and the hydrogen atom [4,53]. Local quantities such as quantum statistical density matrices have been treated so far only to lowest order for the anharmonic oscillator and the hydrogen atom [54,55].

In this chapter, we develop a systematic convergent variational perturbation theory for the path integral representation of density matrices of a point particle moving in a polynomial as well as a nonpolynomial potential. By systematically taking into account higher orders, we thus go beyond related first-order treatments in classical phase space [56] and early Rayleigh-Ritz type variational approximations [57]. With the help of a generalized smearing formula, which accounts for the effects of quantum fluctuations, we can furthermore treat nonpolynomial interactions, thus extending the range of applicability of the work in Ref. [58]. As a first application, we calculate here the particle density in the double-well potential to second order and then the electron density in the hydrogen atom to first order.

8.2 General Features

Variational perturbation theory approximates a quantum statistical system by perturbation expansions around harmonic oscillators with trial frequencies, which are optimized differently for each order of the expansions. We have shown in Section 4.1.1 that, when dealing with the free energy, it is essential to give a special treatment to the fluctuations of the path average $\bar{x} \equiv (k_B T / \hbar) \int_0^{\hbar/k_B T} d\tau x(\tau)$, since this

performs violent fluctuations at high temperatures T . These cannot be treated by any expansion, unless the potential is close to harmonic. The effect of these fluctuations may, however, easily be calculated at the end by a single numerical fluctuation integral. For this reason, variational perturbation expansions are performed for each position x_0 of the path average separately, yielding an N th order approximation $W_N(x_0)$ to the local free energy $V_{\text{eff,cl}}(x_0)$, called the *effective classical potential* [59]. The name indicates that one may obtain the full quantum partition function Z from this object by a simple integral over x_0 just as in classical statistics,

$$Z = \int_{-\infty}^{+\infty} \frac{dx_0}{\sqrt{2\pi\hbar^2/Mk_B T}} e^{-V_{\text{eff,cl}}(x_0)/k_B T}. \quad (8.1)$$

Having calculated $W_N(x_0)$, we obtain the N th-order approximation to the partition function

$$Z_N = \int_{-\infty}^{+\infty} \frac{dx_0}{\sqrt{2\pi\hbar^2/Mk_B T}} e^{-W_N(x_0)/k_B T}. \quad (8.2)$$

The separate treatment of the path average is important to ensure a fast convergence at larger temperatures. In the high-temperature limit, $W_N(x_0)$ converges against the initial potential $V(x_0)$ for any order N .

Consider the Euclidean path integral over all periodic paths $x(\tau)$, with $x(0) = x(\hbar/k_B T)$, for a harmonic oscillator with minimum at x_m , where the action is

$$\mathcal{A}^{\Omega, x_m}[x] = \int_0^{\hbar\beta} d\tau \left\{ \frac{1}{2} M \dot{x}^2(\tau) + \frac{1}{2} M \Omega^2 [x(\tau) - x_m]^2 \right\}. \quad (8.3)$$

Its partition function is

$$Z^{\Omega, x_m} = \oint \mathcal{D}x \exp \{ -\mathcal{A}^{\Omega, x_m}[x]/\hbar \} = \frac{1}{2 \sinh \hbar\beta\Omega/2}, \quad (8.4)$$

and the unnormalized density matrix is given by

$$\tilde{\varrho}_0^{\Omega, x_m}(x_b, x_a) = \sqrt{\frac{M\Omega}{2\pi\hbar \sinh \hbar\beta\Omega}} \exp \left\{ -\frac{M\Omega}{2\hbar \sinh \hbar\beta\Omega} [(\tilde{x}_b^2 + \tilde{x}_a^2) \cosh \hbar\beta\Omega - 2\tilde{x}_b\tilde{x}_a] \right\}, \quad (8.5)$$

where we have introduced the abbreviation

$$\tilde{x}(\tau) = x(\tau) - x_m. \quad (8.6)$$

At fixed end points x_b, x_a , the quantum mechanical correlation functions are

$$\begin{aligned} \langle O_1(x(\tau_1)) O_2(x(\tau_2)) \dots \rangle_{x_b, x_a}^{\Omega, x_m} &= \frac{1}{\tilde{\varrho}_0^{\Omega, x_m}(x_b, x_a)} \int_{x(0)=x_a}^{x(\hbar\beta)=x_b} \mathcal{D}x O_1(x(\tau_1)) O_2(x(\tau_2)) \dots \\ &\times \exp \{ -\mathcal{A}^{\Omega, x_m}[x]/\hbar \}. \end{aligned} \quad (8.7)$$

The classical path of a particle in a translated harmonic potential is

$$x_{\text{cl}}(\tau) = \frac{\tilde{x}_b \sinh \Omega\tau + \tilde{x}_a \sinh \Omega(\hbar\beta - \tau)}{\sinh \hbar\beta\Omega}. \quad (8.8)$$

8.3 Variational Perturbation Theory

To obtain a variational approximation for the density matrix, it is useful to separate the general action

$$\mathcal{A}[x] = \int_0^{\hbar\beta} d\tau \left[\frac{M}{2} \dot{x}^2(\tau) + V(x(\tau)) \right] \quad (8.9)$$

into a trial one, for which the density matrix is known, and a remainder containing the original potential.

We have pointed out in Section 4.1.2 that a separate treatment of the fluctuations $x_0 = \bar{x} = \int_0^{\hbar\beta} d\tau x(\tau)/\hbar\beta$ is not necessary for paths with fixed ends. As a remnant of the extra treatment of x_0 we must, however, perform the initial perturbation expansion around the minimum of the effective classical potential, which will lie at some point x_m determined by the end points x_b, x_a , and by the minimum of the potential $V(x)$. Thus we shall use the Euclidean path integral for the density matrix of the harmonic oscillator centered at x_m as the trial system around which to perform the variational perturbation theory, treating the fluctuations of x_0 around x_m on the same footing as the remaining fluctuations. The position x_m of the minimum is a function $x_m = x_m(x_b, x_a)$, and has to be optimized with respect to the trial frequency, which itself is a function $\Omega = \Omega(x_b, x_a)$ to be optimized.

Hence we start by decomposing the action (8.9) as

$$\mathcal{A}[x] = \mathcal{A}^{\Omega, x_m}[x] + \mathcal{A}_{\text{int}}[x] \quad (8.10)$$

with an interaction

$$\mathcal{A}_{\text{int}}[x] = \int_0^{\hbar\beta} d\tau V_{\text{int}}(x(\tau)), \quad (8.11)$$

where the interaction potential is the difference between the original one $V(x)$ and the inserted displaced harmonic oscillator:

$$V_{\text{int}}(x(\tau)) = V(x(\tau)) - \frac{1}{2}M\Omega^2[x(\tau) - x_m]^2. \quad (8.12)$$

Now we evaluate the path integral for the unnormalized density matrix

$$\tilde{\varrho}(x_b, x_a) = \int_{x(0)=x_a}^{x(\hbar\beta)=x_b} \mathcal{D}x e^{-\mathcal{A}[x]/\hbar} \quad (8.13)$$

by treating the interaction (8.11) as a perturbation, leading to a moment expansion

$$\tilde{\varrho}(x_b, x_a) = \tilde{\varrho}_0^{\Omega, x_m}(x_b, x_a) \left[1 - \frac{1}{\hbar} \langle \mathcal{A}_{\text{int}}[x] \rangle_{x_b, x_a}^{\Omega, x_m} + \frac{1}{2\hbar^2} \langle \mathcal{A}_{\text{int}}^2[x] \rangle_{x_b, x_a}^{\Omega, x_m} - \dots \right], \quad (8.14)$$

with expectation values defined in (8.7). The zeroth order consists of the harmonic contribution (8.5) and higher orders contain harmonic averages of the interaction (8.11). The correlation functions in (8.14) can be decomposed into connected ones by going over to cumulants, yielding

$$\tilde{\varrho}(x_b, x_a) = \tilde{\varrho}_0^{\Omega, x_m}(x_b, x_a) \exp \left[-\frac{1}{\hbar} \langle \mathcal{A}_{\text{int}}[x] \rangle_{x_b, x_a, c}^{\Omega, x_m} + \frac{1}{2\hbar^2} \langle \mathcal{A}_{\text{int}}^2[x] \rangle_{x_b, x_a, c}^{\Omega, x_m} - \dots \right], \quad (8.15)$$

where the first cumulants are defined as usual:

$$\begin{aligned} \langle O_1(x(\tau_1)) \rangle_{x_b, x_a, c}^{\Omega, x_m} &= \langle O_1(x(\tau_1)) \rangle_{x_b, x_a}^{\Omega, x_m}, \\ \langle O_1(x(\tau_1)) O_2(x(\tau_2)) \rangle_{x_b, x_a, c}^{\Omega, x_m} &= \langle O_1(x(\tau_1)) O_2(x(\tau_2)) \rangle_{x_b, x_a}^{\Omega, x_m} - \langle O_1(x(\tau_1)) \rangle_{x_b, x_a}^{\Omega, x_m} \langle O_2(x(\tau_2)) \rangle_{x_b, x_a}^{\Omega, x_m}, \\ &\vdots \end{aligned} \quad (8.16)$$

The series (8.15) is truncated after the N th term, resulting in the N th-order approximant for the quantum statistical density matrix

$$\tilde{\varrho}_N^{\Omega, x_m}(x_b, x_a) = \tilde{\varrho}_0^{\Omega, x_m}(x_b, x_a) \exp \left[\sum_{n=1}^N \frac{(-1)^n}{n! \hbar^n} \langle \mathcal{A}_{\text{int}}^n[x] \rangle_{x_b, x_a, c}^{\Omega, x_m} \right], \quad (8.17)$$

which explicitly depends on both variational parameters Ω and x_m .

In analogy to classical statistics, where the Boltzmann distribution in configuration space is controlled by the classical potential $V(x)$ according to

$$\tilde{\varrho}_{\text{cl}}(x) = \sqrt{\frac{M}{2\pi\hbar^2\beta}} \exp[-\beta V(x)], \quad (8.18)$$

we now introduce a new type of *effective classical potential* $V_{\text{eff,cl}}(x_b, x_a)$, which governs the unnormalized density matrix

$$\tilde{\varrho}(x_b, x_a) = \sqrt{\frac{M}{2\pi\hbar^2\beta}} \exp[-\beta V_{\text{eff,cl}}(x_b, x_a)]. \quad (8.19)$$

Its N th-order approximation is obtained from (8.5), (8.17), and (8.19) via the cumulant expansion

$$\begin{aligned} W_N^{\Omega, x_m}(x_b, x_a) &= \frac{1}{2\beta} \ln \frac{\sinh \hbar\beta\Omega}{\hbar\beta\Omega} + \frac{M\Omega}{2\hbar\beta \sinh \hbar\beta\Omega} \{(\tilde{x}_b^2 + \tilde{x}_a^2) \cosh \hbar\beta\Omega - 2\tilde{x}_b\tilde{x}_a\} \\ &\quad - \frac{1}{\beta} \sum_{n=1}^N \frac{(-1)^n}{n! \hbar^n} \langle \mathcal{A}_{\text{int}}^n[x] \rangle_{x_b, x_a, c}^{\Omega, x_m}, \end{aligned} \quad (8.20)$$

which is optimized for each set of end points x_b, x_a in the variational parameters Ω^2 and x_m , the result being denoted by $W_N(x_b, x_a)$. The optimal values $\Omega^2(x_b, x_a)$ and $x_m(x_b, x_a)$ are determined from the extremality conditions

$$\frac{\partial W_N^{\Omega, x_m}(x_b, x_a)}{\partial \Omega^2} \stackrel{!}{=} 0, \quad \frac{\partial W_N^{\Omega, x_m}(x_b, x_a)}{\partial x_m} \stackrel{!}{=} 0. \quad (8.21)$$

The solutions are denoted by Ω^{2N}, x_m^N , both being functions of x_b, x_a . If no extrema are found, one has to look for the flattest region of the function (8.20), where the lowest higher-order derivative disappears. Eventually the N th-order approximation for the normalized density matrix is obtained from

$$\varrho_N(x_b, x_a) = Z_N^{-1} \tilde{\varrho}_N^{\Omega^{2N}, x_m^N}(x_b, x_a), \quad (8.22)$$

where the corresponding partition function reads

$$Z_N = \int_{-\infty}^{+\infty} dx \tilde{\varrho}_N^{\Omega^{2N}, x_m^N}(x_b, x_a). \quad (8.23)$$

In principle, one could also optimize the entire ratio (8.22), but this would be harder to do in practice. Moreover, the optimization of the unnormalized density matrix is the only option, if the normalization diverges due to singularities of the potential. This will be seen in Section 8.7.2 by the example of the hydrogen atom.

8.4 Smearing Formula for Density Matrices

In order to calculate the connected correlation functions in the variational perturbation expansion (8.17), we must find efficient formulas for evaluating expectation values (8.7) of any power of the interaction (8.11)

$$\langle \mathcal{A}_{\text{int}}^n[x] \rangle_{x_b, x_a}^{\Omega, x_m} = \frac{1}{\tilde{\varrho}_0^{\Omega, x_m}(x_b, x_a)} \int_{\tilde{x}_a, 0}^{\tilde{x}_b, \hbar\beta} \mathcal{D}\tilde{x} \prod_{l=1}^n \left[\int_0^{\hbar\beta} d\tau_l V_{\text{int}}(\tilde{x}(\tau_l) + x_m) \right] \exp \left\{ -\frac{1}{\hbar} \mathcal{A}^{\Omega, x_m}[\tilde{x} + x_m] \right\}. \quad (8.24)$$

This can be done by an extension of the smearing formalism, which is developed in Ref. [53]. To this end we rewrite the interaction potential as

$$V_{\text{int}}(\tilde{x}(\tau_l) + x_m) = \int_{-\infty}^{+\infty} dz_l V_{\text{int}}(z_l + x_m) \int_{-\infty}^{+\infty} \frac{d\lambda_l}{2\pi} \exp\{i\lambda_l z_l\} \exp\left[-\int_0^{\hbar\beta} d\tau i\lambda_l \delta(\tau - \tau_l) \tilde{x}(\tau)\right] \quad (8.25)$$

and introduce a current

$$J(\tau) = \sum_{l=1}^n i\hbar\lambda_l \delta(\tau - \tau_l), \quad (8.26)$$

so that (8.24) becomes

$$\begin{aligned} \langle \mathcal{A}_{\text{int}}^n[x] \rangle_{x_b, x_a}^{\Omega, x_m} &= \frac{1}{\tilde{\varrho}_0^{\Omega, x_m}(x_b, x_a)} \\ &\times \prod_{l=1}^n \left[\int_0^{\hbar\beta} d\tau_l \int_{-\infty}^{+\infty} dz_l V_{\text{int}}(z_l + x_{\text{min}}) \int_{-\infty}^{+\infty} \frac{d\lambda_l}{2\pi} \exp\{i\lambda_l z_l\} \right] K^{\Omega, x_m}[J]. \end{aligned} \quad (8.27)$$

The kernel $K^{\Omega, x_m}[J]$ represents the generating functional for all correlation functions of the displaced harmonic oscillator

$$K^{\Omega, x_m}[J] = \int_{\tilde{x}_a, 0}^{\tilde{x}_b, \hbar\beta} \mathcal{D}\tilde{x} \exp\left\{-\frac{1}{\hbar} \int_0^{\hbar\beta} d\tau \left[\frac{m}{2} \dot{\tilde{x}}^2(\tau) + \frac{1}{2} M \Omega^2 \tilde{x}^2(\tau) + J(\tau) \tilde{x}(\tau) \right]\right\}. \quad (8.28)$$

For zero current J , this generating functional reduces to the Euclidean harmonic propagator (8.5):

$$K^{\Omega, x_m}[J=0] = \tilde{\varrho}_0^{\Omega, x_m}(x_b, x_a). \quad (8.29)$$

For nonzero J , the solution of the functional integral (8.28) is given by

$$K^{\Omega, x_m}[J] = \tilde{\varrho}_0^{\Omega, x_m}(x_b, x_a) \exp\left[-\frac{1}{\hbar} \int_0^{\hbar\beta} d\tau J(\tau) x_{\text{cl}}(\tau) + \frac{1}{2\hbar^2} \int_0^{\hbar\beta} d\tau \int_0^{\hbar\beta} d\tau' J(\tau) G^{\Omega}(\tau, \tau') J(\tau')\right], \quad (8.30)$$

where $x_{\text{cl}}(\tau)$ denotes the classical path (8.8) and $G^{\Omega}(\tau, \tau')$ the harmonic Green function

$$G^{\Omega}(\tau, \tau') = \frac{\hbar}{2M\Omega} \frac{\cosh\Omega(|\tau - \tau'| - \hbar\beta) - \cosh\Omega(\tau + \tau' - \hbar\beta)}{\sinh\hbar\beta\Omega}. \quad (8.31)$$

The expression (8.30) can be simplified by using the explicit expression (8.26) for the current J . This leads to a generating functional

$$K^{\Omega, x_m}[J] = \tilde{\varrho}_0^{\Omega, x_m}(x_b, x_a) \exp\left(-i\boldsymbol{\lambda}^T \mathbf{x}_{\text{cl}} - \frac{1}{2} \boldsymbol{\lambda}^T G \boldsymbol{\lambda}\right), \quad (8.32)$$

where we have introduced the n -dimensional vectors $\boldsymbol{\lambda} = (\lambda_1, \dots, \lambda_n)^T$, $\mathbf{x}_{\text{cl}} = (x_{\text{cl}}(\tau_1), \dots, x_{\text{cl}}(\tau_n))^T$ with the superscript T denoting transposition, and the symmetric $n \times n$ -matrix G whose elements are $G_{kl} = G^{\Omega}(\tau_k, \tau_l)$. Inserting (8.32) into (8.27), and performing the integrals with respect to $\lambda_1, \dots, \lambda_n$, we obtain the n th-order smearing formula for the density matrix

$$\begin{aligned} \langle \mathcal{A}_{\text{int}}^n[x] \rangle_{x_b, x_a}^{\Omega, x_m} &= \prod_{l=1}^n \left[\int_0^{\hbar\beta} d\tau_l \int_{-\infty}^{+\infty} dz_l V_{\text{int}}(z_l + x_m) \right] \\ &\times \frac{1}{\sqrt{(2\pi)^n \det G}} \exp\left\{-\frac{1}{2} \sum_{k,l=1}^n [z_k - x_{\text{cl}}(\tau_k)] G_{kl}^{-1} [z_l - x_{\text{cl}}(\tau_l)]\right\}. \end{aligned} \quad (8.33)$$

The integrand contains an n -dimensional Gaussian distribution describing both thermal and quantum fluctuations around the harmonic classical path $x_{cl}(\tau)$ of Eq. (8.8) in a trial oscillator centered at x_m , whose width is governed by the Green function (8.31).

For closed paths with coinciding end points ($x_b = x_a$), formula (8.33) leads to the n th-order smearing formula for particle densities

$$\rho(x_a) = \frac{1}{Z} \tilde{\rho}(x_a, x_a) = \frac{1}{Z} \oint \mathcal{D}x \delta(x(\tau=0) - x_a) \exp\{-\mathcal{A}[x]/\hbar\}, \quad (8.34)$$

which can be written as

$$\begin{aligned} \langle \mathcal{A}_{\text{int}}^n[x] \rangle_{x_a, x_a}^{\Omega, x_m} &= \frac{1}{\varrho_0^{\Omega, x_m}(x_a)} \prod_{l=1}^n \left[\int_0^{\hbar\beta} d\tau_l \int_{-\infty}^{+\infty} dz_l V_{\text{int}}(z_l + x_m) \right] \\ &\times \frac{1}{\sqrt{(2\pi)^{n+1} \det a^2}} \exp\left(-\frac{1}{2} \sum_{k,l=0}^n z_k a_{kl}^{-2} z_l\right) \end{aligned} \quad (8.35)$$

with $z_0 = \tilde{x}_a$. Here a^2 denotes a symmetric $(n+1) \times (n+1)$ -matrix whose elements $a_{kl}^2 = a^2(\tau_k, \tau_l)$ are obtained from the harmonic Green function for periodic paths $G^{\Omega, \text{p}}(\tau, \tau')$ as (see Chapters 3 and 5 in Ref. [4])

$$a^2(\tau, \tau') \equiv \frac{\hbar}{M} G^{\Omega, \text{p}}(\tau, \tau') = \frac{\hbar}{2M\Omega} \frac{\cosh \Omega(|\tau - \tau'| - \hbar\beta/2)}{\sinh \hbar\beta\Omega/2}. \quad (8.36)$$

The diagonal elements $a^2 = a^2(\tau, \tau)$ represent the fluctuation width (4.8), which behaves in the classical limit like (4.11) and at zero temperature like (4.9).

Both smearing formulas (8.33) and (8.35) allow in principle to determine all harmonic expectation values for the variational perturbation theory of density matrices and particle densities in terms of ordinary Gaussian integrals. Unfortunately, in many applications containing nonpolynomial potentials, it is impossible to solve neither the spatial nor the temporal integrals analytically. This circumstance drastically increases the numerical effort in higher-order calculations.

8.5 First-Order Variational Results

The first-order variational approximation gives usually a reasonable estimate for any desired quantity. Let us investigate the classical and the quantum mechanical limit of this approximation. To facilitate the discussion, we first derive a new representation for the first-order smearing formula (8.35), which allows a direct evaluation of the imaginary time integral. The resulting expression will depend only on temperature, whose low- and high-temperature limits can easily be extracted.

8.5.1 Alternative Formula for First-Order Smearing

For simplicity, we restrict ourselves to the case of particle densities and allow only symmetric potentials $V(x)$ centered at the origin. If $V(x)$ has only one minimum at the origin, then also x_m will be zero. If $V(x)$ has several symmetric minima, then x_m goes to zero only at sufficiently high temperatures. To first order, the smearing formula (8.35) reads

$$\langle \mathcal{A}_{\text{int}}[x] \rangle_{x_a, x_a}^{\Omega} = \frac{1}{\varrho_0^{\Omega}(x_a)} \int_0^{\hbar\beta} d\tau \int_{-\infty}^{+\infty} \frac{dz}{2\pi} V_{\text{int}}(z) \frac{1}{\sqrt{a_{00}^4 - a_{01}^4}} \exp\left\{-\frac{1}{2} \frac{(z^2 + x_a^2)a_{00}^2 - 2zx_a a_{01}^2}{a_{00}^4 - a_{01}^4}\right\}, \quad (8.37)$$

so that Mehler's summation formula

$$\frac{1}{\sqrt{1-b^2}} \exp\left\{-\frac{(x^2 + x'^2)(1+b^2) - 4xx'b}{2(1-b^2)}\right\} = \exp\left\{-\frac{1}{2}(x^2 + x'^2)\right\} \sum_{n=0}^{\infty} \frac{b^n}{2^n n!} H_n(x) H_n(x') \quad (8.38)$$

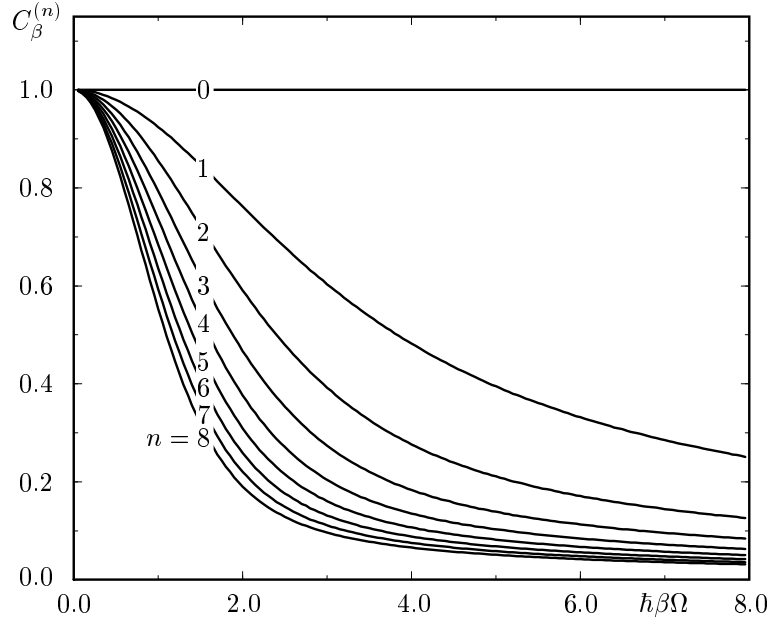


FIGURE 8.1: Temperature-dependence of the first 9 functions $C_\beta^{(n)}$, where $\beta = 1/k_B T$.

leads to an expansion in terms of Hermite polynomials $H_n(x)$, whose temperature dependence stems from the diagonal elements of the harmonic Green function (8.36):

$$\langle \mathcal{A}_{\text{int}}[x] \rangle_{x_a, x_a}^\Omega = \sum_{n=0}^{\infty} \frac{\hbar\beta}{2^n n!} C_\beta^{(n)} H_n \left(x_a / \sqrt{2a_{00}^2} \right) \int_{-\infty}^{+\infty} \frac{dz}{\sqrt{2\pi a_{00}^2}} V_{\text{int}}(z) e^{-z^2/2a_{00}^2} H_n \left(z / \sqrt{2a_{00}^2} \right). \quad (8.39)$$

Here the dimensionless functions $C_\beta^{(n)}$ are defined by

$$C_\beta^{(n)} = \frac{1}{\hbar\beta} \int_0^{\hbar\beta} d\tau \left(\frac{a_{01}^2}{a_{00}^2} \right)^n. \quad (8.40)$$

We have plotted the functions $C_\beta^{(n)}$ for $n = 0, \dots, 8$ in Fig. 8.1. Inserting (8.36) and performing the integral over τ , we obtain

$$C_\beta^{(n)} = \frac{1}{2^n \cosh^n \hbar\beta\Omega/2} \sum_{k=0}^n \binom{n}{k} \frac{\sinh \hbar\beta\Omega(n/2 - k)}{\hbar\beta\Omega(n/2 - k)}. \quad (8.41)$$

At high temperatures, these functions of β go all to unity,

$$\lim_{\beta \rightarrow 0} C_\beta^{(n)} = 1, \quad (8.42)$$

whereas for zero temperature we yield

$$\lim_{\beta \rightarrow \infty} C_\beta^{(n)} = \begin{cases} 1, & n = 0, \\ \frac{1}{\hbar\beta\Omega n}, & n > 0. \end{cases} \quad (8.43)$$

According to (8.20), the first-order approximation to the effective classical potential is given by

$$W_1^\Omega(x_a) = \frac{1}{2\beta} \ln \frac{\sinh \hbar\beta\Omega}{\hbar\beta\Omega} + \frac{M\Omega}{\hbar\beta} x_a^2 \tanh \frac{\hbar\beta\Omega}{2} + V_{a^2}^\Omega(x_a) \quad (8.44)$$

with the smeared interaction potential

$$V_{a^2}^\Omega(x_a) = \frac{1}{\hbar\beta} \langle \mathcal{A}_{\text{int}}[x] \rangle_{x_a, x_a}^\Omega. \quad (8.45)$$

It is instructive to discuss separately the limits $\beta \rightarrow 0$ and $\beta \rightarrow \infty$ of dominating thermal and quantum fluctuations, respectively.

8.5.2 Classical Limit of Effective Classical Potential

In the classical limit $\beta \rightarrow 0$, the first-order effective classical potential (8.44) reduces to

$$W_1^{\Omega, \text{cl}}(x_a) = \frac{1}{2} M \Omega^2 x_a^2 + \lim_{\beta \rightarrow 0} V_{a^2}^\Omega(x_a). \quad (8.46)$$

The second term is determined by inserting the high-temperature limit of the fluctuation width (4.11) and of the polynomials (8.42) into the expansion (8.39), leading to

$$\begin{aligned} \lim_{\beta \rightarrow 0} V_{a^2}^\Omega(x_a) &= \lim_{\beta \rightarrow 0} \sum_{n=0}^{\infty} \frac{1}{2^n n!} H_n \left(\sqrt{M\Omega^2\beta/2} x_a \right) \\ &\times \int_{-\infty}^{+\infty} \frac{dz}{\sqrt{2\pi/M\Omega^2\beta}} V_{\text{int}}(z) e^{-M\Omega^2\beta z^2/2} H_n \left(\sqrt{M\Omega^2\beta/2} z \right). \end{aligned} \quad (8.47)$$

Then we make use of the completeness relation for Hermite polynomials

$$\frac{1}{\sqrt{\pi}} e^{-x^2} \sum_{n=0}^{\infty} \frac{1}{2^n n!} H_n(x) H_n(x') = \delta(x - x'), \quad (8.48)$$

which may be derived from Mehler's summation formula (8.38) in the limit $b \rightarrow 1^-$, to reduce the smeared interaction potential $V_{a^2}^\Omega(x_a)$ to the pure interaction potential (8.12):

$$\lim_{\beta \rightarrow 0} V_{a^2}^\Omega(x_a) = V_{\text{int}}(x_a). \quad (8.49)$$

Recalling (8.12) we see that the first-order effective classical potential (8.46) approaches the classical one:

$$\lim_{\beta \rightarrow 0} W_1^{\Omega, \text{cl}}(x_a) = V(x_a). \quad (8.50)$$

This is a consequence of the vanishing fluctuation width b^2 [see Eq. (4.25)] of the paths around the classical orbits. This property is universal to all higher-order approximations to the effective classical potential (8.20). Thus all correction terms with $n > 1$ must disappear in the limit $\beta \rightarrow 0$,

$$\lim_{\beta \rightarrow 0} \frac{-1}{\beta} \sum_{n=2}^{\infty} \frac{(-1)^n}{n! \hbar^n} \langle \mathcal{A}_{\text{int}}^n[x] \rangle_{x_a, x_a, c}^\Omega = 0. \quad (8.51)$$

8.5.3 Zero-Temperature Limit

At low temperatures, the first-order effective classical potential (8.44) becomes

$$W_1^{\Omega, \text{qm}}(x_a) = \frac{\hbar\Omega}{2} + \lim_{\beta \rightarrow \infty} V_{a^2}^\Omega(x_a). \quad (8.52)$$

The zero-temperature limit of the smeared potential in the second term defined in (8.45) follows from Eq. (8.39) by taking into account the limiting procedure for the polynomials $C_\beta^{(n)}$ in (8.43) and for the fluctuation width a_{qm}^2 (4.9). Thus we obtain with $H_0(x) = 1$ and the inverse length $\kappa = \sqrt{M\Omega/\hbar}$:

$$\lim_{\beta \rightarrow \infty} V_a^\Omega(x_a) = \int_{-\infty}^{+\infty} dz \sqrt{\frac{\kappa^2}{\pi}} H_0(\kappa z)^2 \exp\{-\kappa^2 z^2\} V_{\text{int}}(z). \quad (8.53)$$

Introducing the harmonic eigenvalues

$$E_n^\Omega = \hbar\Omega \left(n + \frac{1}{2} \right), \quad (8.54)$$

and the harmonic eigenfunctions

$$\psi_n^\Omega(x) = \frac{1}{\sqrt{n!2^n}} \left(\frac{\kappa^2}{\pi} \right)^{1/4} e^{-\kappa^2 x^2/2} H_n(\kappa x), \quad (8.55)$$

we can re-express the zero-temperature limit of the first-order effective classical potential (8.52) with (8.53) by

$$W_1^{\Omega, \text{qm}}(x_a) = E_0^\Omega + \langle \psi_0^\Omega | V_{\text{int}} | \psi_0^\Omega \rangle. \quad (8.56)$$

This is recognized as the first-order harmonic Rayleigh-Schrödinger perturbative result for the ground-state energy.

For the discussion of the quantum mechanical limit of the first-order normalized density,

$$\varrho_1^\Omega(x_a) = \frac{\tilde{\varrho}_1^\Omega(x_a)}{Z} = \varrho_0^\Omega(x_a) \frac{\exp\left\{-\frac{1}{\hbar} \langle \mathcal{A}_{\text{int}}[x] \rangle_{x_a, x_a}^\Omega\right\}}{\int_{-\infty}^{+\infty} dx_a \varrho_0^\Omega(x_a) \exp\left\{-\frac{1}{\hbar} \langle \mathcal{A}_{\text{int}}[x] \rangle_{x_a, x_a}^\Omega\right\}}, \quad (8.57)$$

we proceed as follows. First we expand (8.57) up to first order in the interaction, leading to

$$\varrho_1^\Omega(x_a) = \varrho_0^\Omega(x_a) \left[1 - \frac{1}{\hbar} \left(\langle \mathcal{A}_{\text{int}}[x] \rangle_{x_a, x_a}^\Omega - \int_{-\infty}^{+\infty} dx_a \varrho_0^\Omega(x_a) \langle \mathcal{A}_{\text{int}}[x] \rangle_{x_a, x_a}^\Omega \right) \right]. \quad (8.58)$$

Inserting (8.5) and (8.39) into the third term in (8.58), and assuming Ω not to depend explicitly on x_a , the x_a -integral reduces to the orthonormality relation for Hermite polynomials

$$\frac{1}{2^n n! \sqrt{\pi}} \int_{-\infty}^{+\infty} dx_a H_n(x_a) H_0(x_a) e^{-x_a^2} = \delta_{n0}, \quad (8.59)$$

so that the third term in (8.58) eventually becomes

$$- \int_{-\infty}^{+\infty} dx_a \varrho_0^\Omega(x_a) \langle \mathcal{A}_{\text{int}}[x] \rangle_{x_a, x_a}^\Omega = -\beta \int_{-\infty}^{+\infty} dz \sqrt{\frac{\kappa^2}{\pi}} V_{\text{int}}(z) \exp\{-\kappa^2 z^2\} H_0(\kappa z). \quad (8.60)$$

But this is just the $n = 0$ -term of (8.39) with an opposite sign, thus canceling the zeroth component of the second term in (8.58), which would have been divergent for $\beta \rightarrow \infty$.

The resulting expression for the first-order normalized density is

$$\varrho_1^\Omega(x_a) = \varrho_0^\Omega(x_a) \left[1 - \sum_{n=1}^{\infty} \frac{\beta}{2^n n!} C_\beta^{(n)} H_n(\kappa x_a) \int_{-\infty}^{+\infty} dz \sqrt{\frac{\kappa^2}{\pi}} V_{\text{int}}(z) \exp(-\kappa^2 z^2) H_n(\kappa z) \right]. \quad (8.61)$$

The zero-temperature limit of $C_\beta^{(n)}$ is from (8.43) and (8.54)

$$\lim_{\beta \rightarrow \infty} \beta C_\beta^{(n)} = \frac{2}{E_n^\Omega - E_0^\Omega}, \quad (8.62)$$

so that we obtain from (8.61) the limit

$$\varrho_1^\Omega(x_a) = \varrho_0^\Omega(x_a) \left[1 - 2 \sum_{n=1}^{\infty} \frac{1}{2^n n!} \frac{1}{E_n^\Omega - E_0^\Omega} H_n(\kappa x_a) \int_{-\infty}^{\infty} dz \sqrt{\frac{\kappa^2}{\pi}} V_{\text{int}}(z) \exp\{-\kappa^2 z^2\} H_n(\kappa z) H_0(\kappa z) \right]. \quad (8.63)$$

Taking into account the harmonic eigenfunctions (8.55), we can rewrite (8.63) as

$$\varrho_1^\Omega(x_a) = |\psi_0(x_a)|^2 = [\psi_0^\Omega(x_a)]^2 - 2\psi_0^\Omega(x_a) \sum_{n>0} \psi_n^\Omega(x_a) \frac{\langle \psi_n^\Omega | V_{\text{int}} | \psi_0^\Omega \rangle}{E_n^\Omega - E_0^\Omega}, \quad (8.64)$$

which is just equivalent to the harmonic first-order Rayleigh-Schrödinger result for particle densities.

Summarizing the results of this section, we have shown that our method has properly reproduced the high- and low-temperature limits. Because of relation (8.64), the variational approach for particle densities can be used to determine approximately the ground-state wave function $\psi_0(x_a)$ for the system of interest. Thus our method supplies earlier perturbative [60] and variational [61] attempts to directly compute the ground-state wave function.

8.6 Smearing Formula in Higher Spatial Dimensions

Most physical systems possess many degrees of freedom. This requires an extension of our method to higher spatial dimensions. In general, we must consider anisotropic harmonic trial systems, where the previous variational parameter Ω^2 becomes a $d \times d$ -matrix $\Omega_{\mu\nu}^2$, with $\mu, \nu = 1, 2, \dots, d$.

8.6.1 Isotropic Approximation

An isotropic trial ansatz

$$\Omega_{\mu\nu}^2 = \Omega^2 \delta_{\mu\nu} \quad (8.65)$$

can give rough initial estimates for the properties of the system. In this case, the n th-order smearing formula (8.35) generalizes directly to

$$\langle \mathcal{A}_{\text{int}}^n[\mathbf{r}] \rangle_{\mathbf{r}_a, \mathbf{r}_a}^\Omega = \frac{1}{\varrho_0^\Omega(\mathbf{r}_a)} \prod_{l=1}^n \left[\int_0^{\hbar\beta} d\tau_l \int d^d z_l V_{\text{int}}(\mathbf{z}_l) \right] \frac{1}{\sqrt{(2\pi)^{n+1} \det a^2}} \exp \left[-\frac{1}{2} \sum_{k,l=0}^n \mathbf{z}_k a_{kl}^{-2} \mathbf{z}_l \right] \quad (8.66)$$

with the d -dimensional vectors $\mathbf{z}_l = (z_{1l}, z_{2l}, \dots, z_{dl})^T$. Note, that Greek labels $\mu, \nu, \dots = 1, 2, \dots, d$ specify spatial indices and Latin labels $k, l, \dots = 0, 1, 2, \dots, n$ refer to the different imaginary times. The vector \mathbf{z}_0 denotes \mathbf{r}_a , the matrix a^2 is the same as in Section 8.4. The harmonic density reads

$$\varrho_0^\Omega(\mathbf{r}) = \sqrt{\frac{1}{(2\pi a_{00}^2)^d}} \exp \left[-\frac{1}{2 a_{00}^2} \sum_{\mu=1}^d x_\mu^2 \right]. \quad (8.67)$$

8.6.2 Anisotropic Approximation

In the discussion of the anisotropic approximation, we shall only consider radially-symmetric potentials $V(\mathbf{r}) = V(|\mathbf{r}|)$ because of their simplicity and their major occurrence in physics. The trial frequencies decompose naturally into a radial frequency Ω_L and a transversal one Ω_T (see Ref. [4]):

$$\Omega_{\mu\nu}^2 = \Omega_L^2 \frac{x_a \mu x_{a\nu}}{r_a^2} + \Omega_T^2 \left(\delta_{\mu\nu} - \frac{x_a \mu x_{a\nu}}{r_a^2} \right) \quad (8.68)$$

with $r_a = |\mathbf{r}_a|$. For practical reasons we rotate the coordinate system by $\bar{\mathbf{x}}_n = U \mathbf{x}_n$ so that $\bar{\mathbf{r}}_a$ points along the first coordinate axis,

$$(\bar{\mathbf{r}}_a)_\mu \equiv \bar{z}_{\mu 0} = \begin{cases} r_a, & \mu = 1, \\ 0, & 2 \leq \mu \leq d, \end{cases} \quad (8.69)$$

and rotated Ω^2 -matrix is diagonal:

$$\bar{\Omega}^2 = \begin{pmatrix} \Omega_L^2 & 0 & 0 & \cdots & 0 \\ 0 & \Omega_T^2 & 0 & \cdots & 0 \\ 0 & 0 & \Omega_T^2 & \cdots & 0 \\ \vdots & \vdots & \vdots & \ddots & \vdots \\ 0 & 0 & 0 & \cdots & \Omega_T^2 \end{pmatrix} = U \Omega^2 U^{-1}. \quad (8.70)$$

After this rotation, the *anisotropic* n th-order smearing formula in d dimensions reads

$$\begin{aligned} \langle \mathcal{A}_{\text{int}}^n[\mathbf{r}] \rangle_{\mathbf{r}_a, \mathbf{r}_a}^{\Omega_L, \Omega_T} &= \frac{(2\pi)^{-d(n+1)/2}}{\varrho_0^{\Omega_L, \Omega_T}(\bar{\mathbf{r}}_a)} \prod_{l=1}^n \left[\int_0^{\hbar\beta} d\tau_l \int d^d \bar{z}_l V_{\text{int}}(|\bar{z}_l|) \right] (\det a_L^2)^{-1/2} (\det a_T^2)^{-(d-1)/2} \\ &\times \exp \left\{ -\frac{1}{2} \sum_{k,l=0}^n \bar{z}_{1k} a_{Lkl}^{-2} \bar{z}_{1l} \right\} \exp \left\{ -\frac{1}{2} \sum_{\mu=2}^d \sum_{k,l=1}^n \bar{z}_{\mu k} a_{Tkl}^{-2} \bar{z}_{\mu l} \right\}. \end{aligned} \quad (8.71)$$

The components of the longitudinal and transversal matrices a_L^2 and a_T^2 are

$$a_{Lkl}^2 = a_L^2(\tau_k, \tau_l), \quad a_{Tkl}^2 = a_T^2(\tau_k, \tau_l), \quad (8.72)$$

where the frequency Ω in (8.36) must be substituted by the new variational parameters Ω_L, Ω_T , respectively. For the harmonic density in the rotated system $\varrho_0^{\Omega_L, \Omega_T}(\bar{\mathbf{r}})$, which is used to normalize (8.71), we find

$$\varrho_0^{\Omega_L, \Omega_T}(\bar{\mathbf{r}}) = \sqrt{\frac{1}{2\pi a_{L00}^2}} \sqrt{\frac{1}{(2\pi a_{T00}^2)^{d-1}}} \exp \left[-\frac{1}{2 a_{L00}^2} \bar{x}_1^2 - \frac{1}{2 a_{T00}^2} \sum_{\mu=2}^d \bar{x}_\mu^2 \right]. \quad (8.73)$$

8.7 Applications

By discussing the applications, we shall employ for simplicity natural units with $\hbar = k_B = M = 1$. In order to develop some feeling how our variational method works, we approximate at first the particle density in the double-well potential in second order. After that we approximate the temperature-dependent electron density of the hydrogen atom in first order.

8.7.1 The Double Well

A detailed analysis of the first-order approximation shows that the particle density in the double-well potential is nearly exact for all temperatures if we use the two variational parameters Ω^2 and x_m , whereas one variational parameter Ω^2 leads to larger deviations at low temperatures and coupling strengths. For such conditions, leading to a maximum of the density far away from origin $x_a = 0$, the displacement of the trial oscillator x_m may not be supposed to vanish. Considering that, our first-order results improve those obtained in Ref. [58]. Since the differences between the optimization procedures using one or two variational parameters become less significant in higher orders, the subsequent second-order calculation is restricted to the optimization in Ω .

First-Order Approximation

In the case of the double-well potential

$$V(x) = -\frac{1}{2}\omega^2 x^2 + \frac{1}{4}gx^4 + \frac{1}{4g} \quad (8.74)$$

with coupling constant g , we obtain for the expectation of the interaction (8.39) to first order, also setting $\omega^2 = 1$,

$$\begin{aligned} \langle \mathcal{A}_{\text{int}}[x] \rangle_{x_a, x_m}^{\Omega, x_m} &= \frac{1}{2}\beta g_0 + \frac{1}{2}g_1 C_\beta^{(1)} H_1 \left((x_a - x_m) / \sqrt{2a_{00}^2} \right) + \frac{1}{4}g_2 C_\beta^{(2)} H_2 \left((x_a - x_m) / \sqrt{2a_{00}^2} \right) \\ &\quad + \frac{1}{8}g_3 C_\beta^{(3)} H_3 \left((x_a - x_m) / \sqrt{2a_{00}^2} \right) + \frac{1}{16}g_4 C_\beta^{(4)} H_4 \left((x_a - x_m) / \sqrt{2a_{00}^2} \right) \end{aligned} \quad (8.75)$$

with

$$\begin{aligned} g_0 &= -a_{00}^2(\Omega^2 + 1) + \frac{3}{2}ga_{00}^4 + 3ga_{00}^2x_m^2 + \frac{1}{2}gx_m^4 + \frac{1}{2g} - \frac{1}{2}x_m^2, \\ g_1 &= -\sqrt{2a_{00}^2}x_m + \frac{3}{4}g(2a_{00}^2)^{3/2}x_m + g\sqrt{2a_{00}^2}x_m^3, \\ g_2 &= -a_{00}^2(\Omega^2 + 1) + 3ga_{00}^4 + 3ga_{00}^2x_m^2, \\ g_3 &= g(2a_{00}^2)^{3/2}x_m, \\ g_4 &= ga_{00}^4. \end{aligned}$$

Inserting (8.75) in (8.45), we obtain the unnormalized double-well density

$$\tilde{\varrho}_1^{\Omega, x_m}(x_a) = \frac{1}{\sqrt{2\pi\beta}} \exp[-\beta W_1^{\Omega, x_m}(x_a)] \quad (8.76)$$

with the first-order effective classical potential

$$W_1^{\Omega, x_m}(x_a) = \frac{1}{2} \ln \frac{\sinh \beta \Omega}{\beta \Omega} + \frac{\Omega}{\beta} (x_a - x_m)^2 \tanh \frac{\beta \Omega}{2} + \frac{1}{\beta} \langle \mathcal{A}_{\text{int}}[x] \rangle_{x_a, x_m}^{\Omega, x_m}. \quad (8.77)$$

After optimizing $W_1^{\Omega, x_m}(x_a)$, the normalized first-order particle density $\varrho_1(x_a)$ is found by dividing $\tilde{\varrho}_1(x_a)$ by the first-order partition function

$$Z_1 = \frac{1}{\sqrt{2\pi\beta}} \int_{-\infty}^{+\infty} dx_a \exp[-\beta W_1(x_a)]. \quad (8.78)$$

Subjecting $W_1^{\Omega, x_m}(x_a)$ to the extremality conditions (8.21), we obtain optimal values for the variational parameters $\Omega^2(x_a)$ and $x_m(x_a)$. Usually there is a unique minimum, but sometimes this does not exist and a turning point or a vanishing higher derivative must be used for optimization. Fortunately, the first case is often realized. Figure 8.2 shows the dependence of the first-order effective classical potential $W_1^{\Omega, x_m}(x_a)$ at $\beta = 10$ and $g = 0.4$ for two fixed values of position x_a as a function of the variational parameters $\Omega^2(x_a)$ and $x_m(x_a)$ in a three-dimensional plot. Thereby, the darker the region the smaller the value of W_1^{Ω, x_m} . We can distinguish between deep valleys (darkgray), in which the global minimum resides, and hills (lightgray). After having determined roughly the area around the expected minimum, one solves numerically the extremality conditions (8.21) with some nearby starting values, to find the exact locations of the minimum.

The example in Fig. 8.2 gives an impression of the general features of this minimization process. Furthermore we note that for symmetry reasons,

$$x_m(x_a) = -x_m(-x_a), \quad (8.79)$$

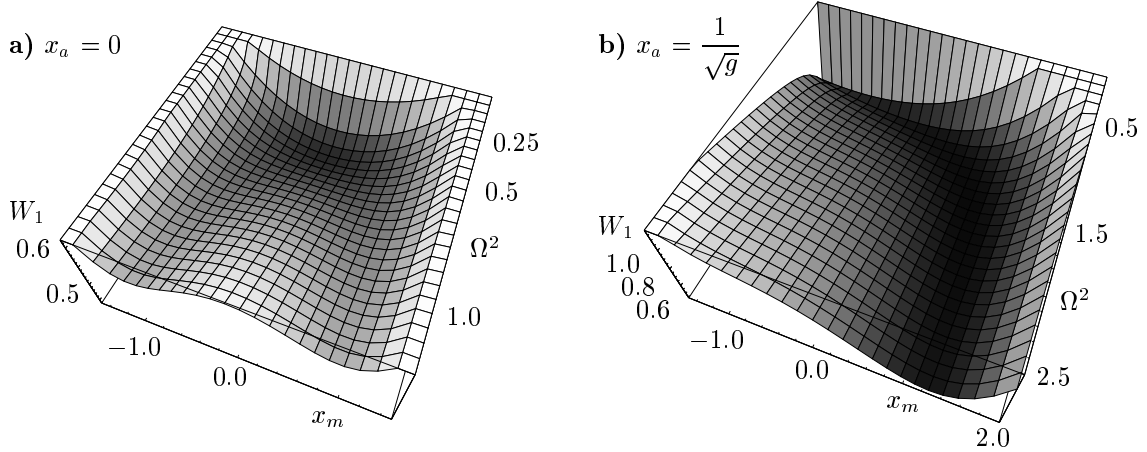


FIGURE 8.2: Plots of the first-order approximation $W_1^{\Omega, x_m}(x_a)$ to the effective classical potential as a function of the two variational parameters $\Omega^2(x_a), x_m(x_a)$ at $g = 0.4$ and $\beta = 10$ for two different values of x_a .

and

$$\Omega^2(x_a) = \Omega^2(-x_a). \quad (8.80)$$

Some first-order approximations to the effective classical potential $W_1(x_a)$ are shown in Fig. 8.3, which are obtained by optimizing with respect to $\Omega^2(x_a)$ and $x_m(x_a)$. The sharp maximum occurring for weak-coupling is a consequence of a nonvanishing $x_m(x_a = 0)$. In the strong-coupling regime, on the other hand, where $x_m(x_a = 0) \approx 0$, the sharp top is absent. This behavior is illustrated in of Figs. 8.4b) and 8.5b) at different temperatures.

The influence of the center parameter x_m diminishes for increasing values of g and decreasing height $1/4g$ of the central barrier (see Fig. 8.3). The same thing is true at high temperatures and large values of x_a , where the precise knowledge of the optimal value of x_m is irrelevant. In these limits, the particle density can be determined without optimizing in x_m , i.e. setting simply $x_m = 0$, where the expectation value (8.75) reduces to

$$\begin{aligned} \langle \mathcal{A}_{\text{int}}[x] \rangle_{x_a, x_a}^{\Omega} &= \frac{1}{4} C_{\beta}^{(2)} H_2 \left(x_a / \sqrt{2a_{00}^2} \right) (g_1 + 3g_2) + \frac{1}{16} g_2 C_{\beta}^{(4)} H_4 \left(x_a / \sqrt{2a_{00}^2} \right) \\ &+ \beta \left(\frac{1}{2} g_1 + \frac{3}{4} g_2 + g_3 \right), \end{aligned} \quad (8.81)$$

with the abbreviations

$$g_1 = -a_{00}^2(\Omega^2 + 1), \quad g_2 = ga_{00}^4, \quad g_3 = \frac{1}{4g}.$$

Inserting (8.81) in (8.45) we obtain the unnormalized double-well density

$$\tilde{\rho}_1^{\Omega}(x_a) = \frac{1}{\sqrt{2\pi\beta}} \exp[-\beta W_1^{\Omega}(x_a)] \quad (8.82)$$

with the first-order effective classical potential

$$W_1^{\Omega}(x_a) = \frac{1}{2} \ln \frac{\sinh \beta \Omega}{\beta \Omega} + \frac{\Omega}{\beta} x_a^2 \tanh \frac{\beta \Omega}{2} + \frac{1}{\beta} \langle \mathcal{A}_{\text{int}}[x] \rangle_{x_a, x_a}^{\Omega}. \quad (8.83)$$

The optimization at $x_m = 0$ gives reasonable results for moderate temperatures at couplings such as $g = 0.4$, as shown in Fig. 8.6 by a comparison with the exact density, which is obtained from numerical solutions of the Schrödinger equation. An additional optimization in x_m cannot be distinguished on

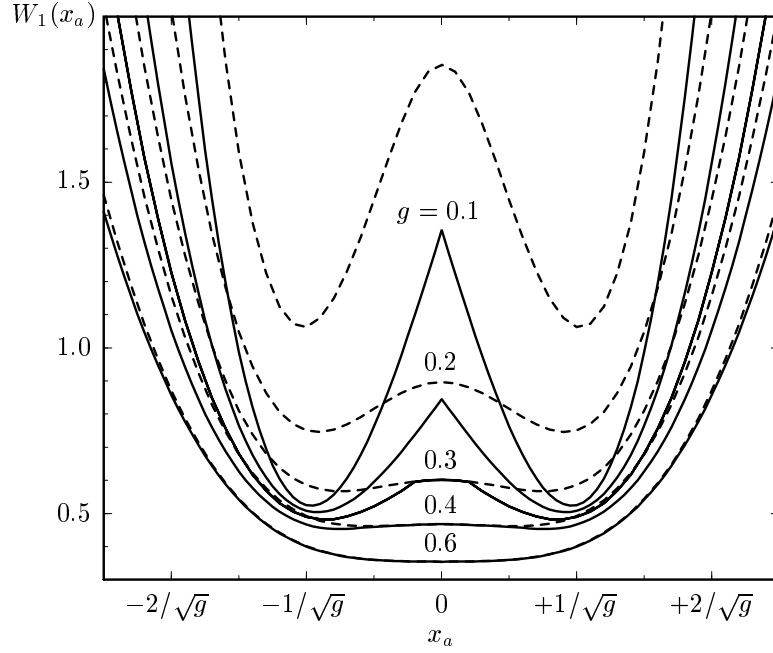


FIGURE 8.3: First-order approximation to the effective classical potential, $W_1(x_a)$, for different coupling strengths g as a function of the position x_a at $\beta = 10$ by optimizing in both variational parameters Ω^2, x_m (solid curves) in comparison with the approximations obtained by variation in Ω^2 only (dashed curves).

the plot. An example, where the second variational parameter x_m becomes important, is shown in Fig. 8.7, where we compare the first-order approximation with one (Ω) and two variational parameters (Ω, x_m) with the exact density for different temperatures at the smaller coupling strength $g = 0.1$. In Fig. 8.4 we see that for $x_a > 0$, the optimal x_m -values lie close to the right hand minimum of the double-well potential, which we only want to consider here. The minimum is located at $1/\sqrt{g} \approx 3.16$. We observe that, with two variational parameters, the first-order approximation is nearly exact for all temperatures, in contrast to the results with only one variational parameter at low temperatures (see the curve for $\beta = 20$ in Fig. 8.7).

Second-Order Approximation

In second-order variational perturbation theory, the differences between the optimization procedures using one or two variational parameters become less significant. Thus, we restrict ourselves to the optimization in $\Omega(x_a)$ and set $x_m = 0$.

The second-order density

$$\tilde{\rho}_2^\Omega(x_a) = \frac{1}{\sqrt{2\pi\beta}} \exp[-\beta W_2^\Omega(x_a)] \quad (8.84)$$

with the second-order approximation of the effective classical potential

$$W_2^\Omega(x_a) = \frac{1}{2} \ln \frac{\sinh \beta\Omega}{\beta\Omega} + \frac{\Omega}{\beta} x_a^2 \tanh \frac{\beta\Omega}{2} + \frac{1}{\beta} \langle \mathcal{A}_{\text{int}}[x] \rangle_{x_a, x_a}^\Omega - \frac{1}{2\beta} \langle \mathcal{A}_{\text{int}}^2[x] \rangle_{x_a, x_a, c}^\Omega \quad (8.85)$$

requires evaluating the smearing formula (8.33) for $n = 1$, which is given in (8.81) and $n = 2$ to be calculated. Going immediately to the cumulant we have

$$\langle \mathcal{A}_{\text{int}}^2[x] \rangle_{x_a, x_a, c}^\Omega = \int_0^\beta d\tau_1 \int_0^\beta d\tau_2 \left\{ \frac{1}{4} (\Omega^2 + 1)^2 [I_{22}(\tau_1, \tau_2) - I_2(\tau_1)I_2(\tau_2)] \right.$$

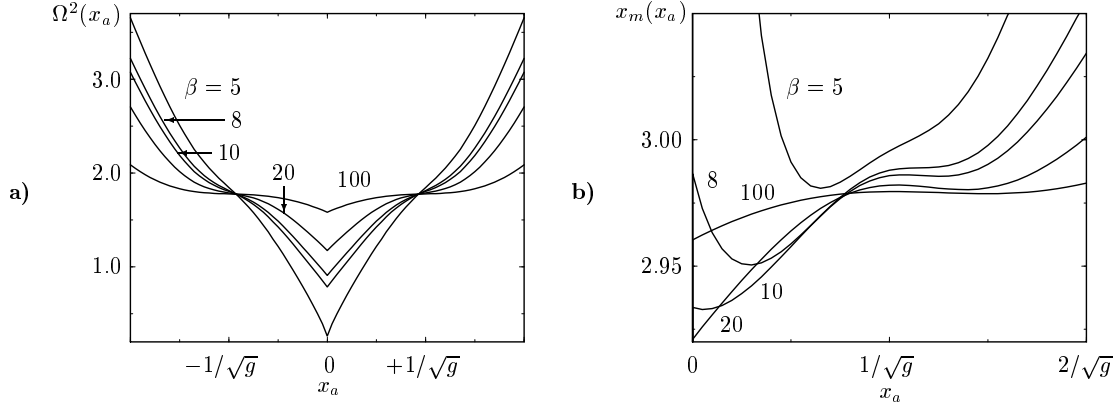


FIGURE 8.4: **a)** Trial frequency $\Omega^2(x_a)$ at different temperatures and coupling strength $g = 0.1$. **b)** Minimum of trial oscillator $x_m(x_a)$ at different temperatures and coupling $g = 0.1$.

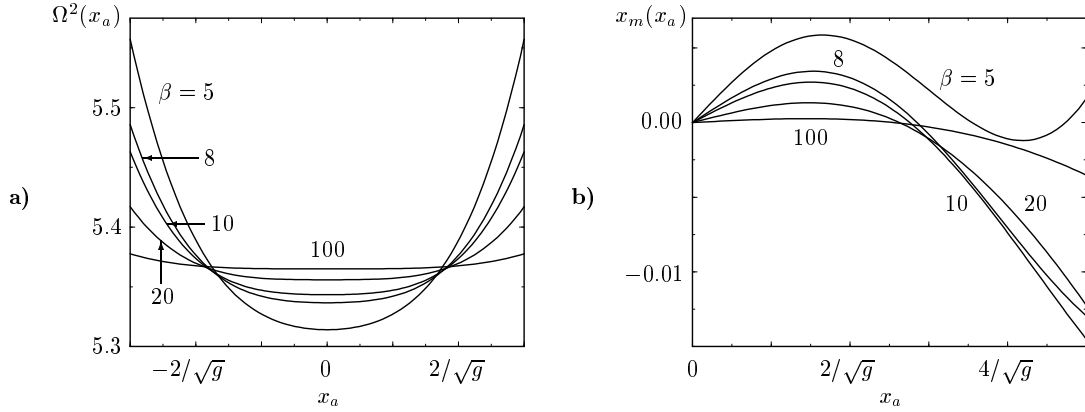


FIGURE 8.5: **a)** Trial frequency $\Omega^2(x_a)$ at different temperatures and coupling strength $g = 10$. **b)** Minimum of trial oscillator $x_m(x_a)$ at different temperatures and coupling $g = 10$.

$$\left. -\frac{1}{4}g(\Omega^2 + 1) [I_{24}(\tau_1, \tau_2) - I_2(\tau_1)I_4(\tau_2)] + \frac{1}{16}g^2 [I_{44}(\tau_1, \tau_2) - I_4(\tau_1)I_4(\tau_2)] \right\} \quad (8.86)$$

with

$$I_m(\tau_k) = (a_{00}^4 - a_{0k}^4)^m \frac{\partial^m}{\partial j^m} \exp \left[\frac{j^2 + 2x_a a_{0k}^2 j}{2a_{00}^2 (a_{00}^4 - a_{0k}^4)} \right]_{j=0}, \quad k = 1, 2 \quad (8.87)$$

and

$$I_{mn}(\tau_1, \tau_2) = (-\det A)^{m+n} \frac{\partial^m}{\partial j_1^m} \frac{\partial^n}{\partial j_2^n} \exp \left[\frac{F(j_1, j_2)}{2a_{00}^2 (\det A)^2} \right]_{j_1=j_2=0} \quad (8.88)$$

$$\det A = a_{00}^6 + 2a_{01}^2 a_{02}^2 a_{12}^2 - a_{00}^2 (a_{01}^4 + a_{02}^4 + a_{12}^4).$$

The generating function is

$$F(j_1, j_2) = a_{00}^4 (j_1^2 + j_2^2) - 2a_{00}^6 (a_{01}^2 j_1 + a_{02}^2 j_2) x_a + 2a_{00}^2 (a_{12}^2 j_1 j_2 + (a_{01}^4 + a_{02}^4 + a_{12}^4) (a_{01}^2 j_1 + a_{02}^2 j_2) x_a) - (a_{01}^2 j_1 + a_{02}^2 j_2) (a_{01}^2 j_1 + a_{02}^2 j_2 + 4a_{01}^2 a_{02}^2 a_{12}^2 x_a). \quad (8.89)$$

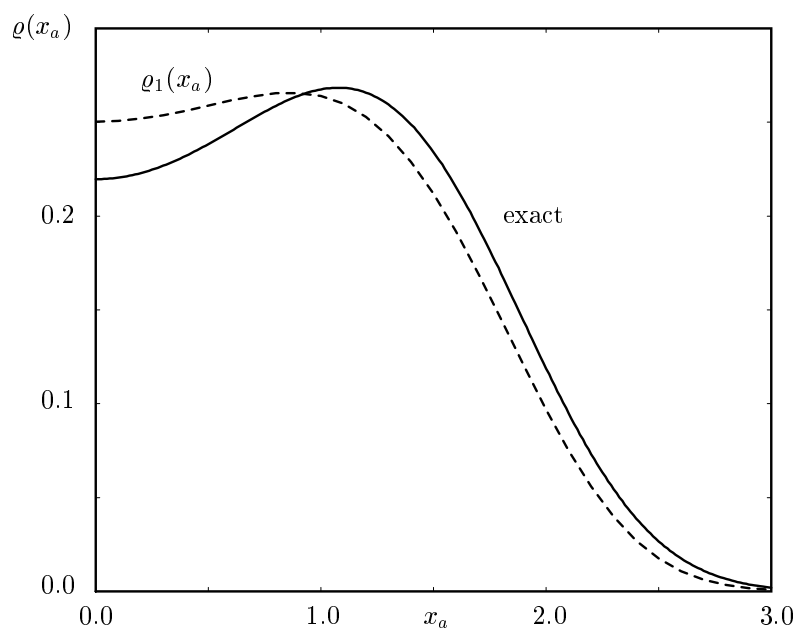


FIGURE 8.6: First-order approximation of the double-well particle density for $\beta = 10$ and $g = 0.4$ compared with the exact particle density in a double well from numerical solution of the Schrödinger equation. All values are in natural units.

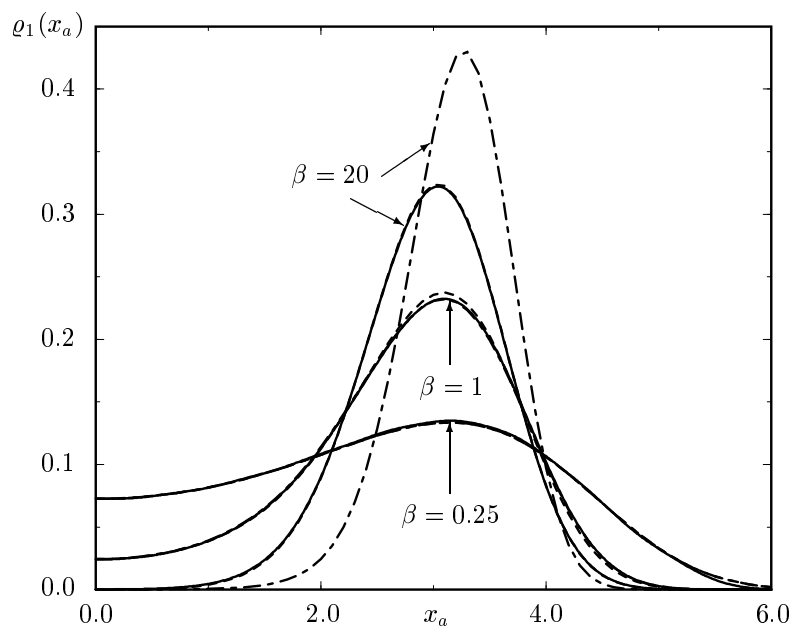


FIGURE 8.7: First-order particle densities of the double well for $g = 0.1$ obtained by optimizing with respect to two variational parameters Ω^2, x_m (dashed curves) and with only Ω^2 (dash-dotted) vs. exact distributions (solid) for different temperatures. The parameter x_m is very important for low temperatures.

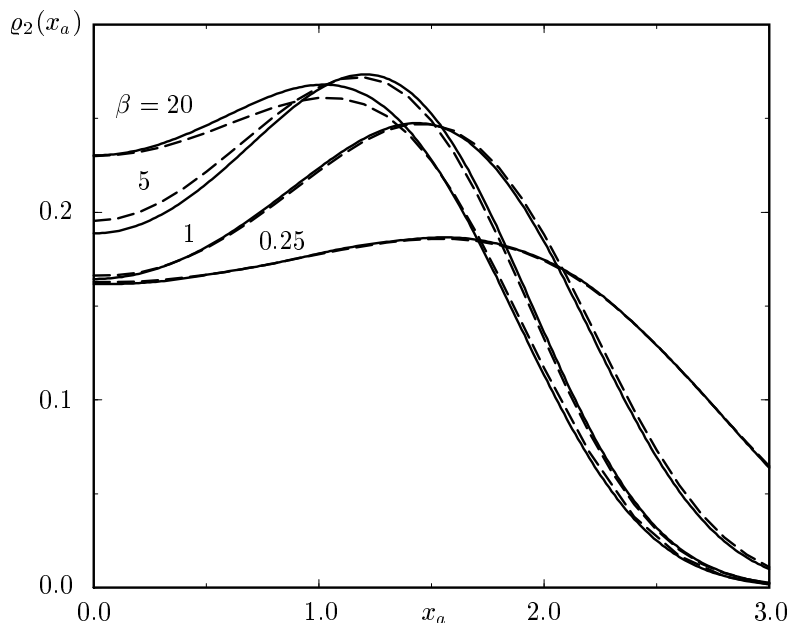


FIGURE 8.8: Second-order particle density (dashed) compared with exact results from numerical solutions of the Schrödinger equation (solid) in a double well at different inverse temperatures. The coupling strength is $g = 0.4$.

All necessary derivatives and the imaginary time integrations in (8.86) have been calculated analytically. After optimizing the unnormalized second-order density (8.84) in Ω we obtain the results depicted in Fig. 8.8. Comparing the second-order results with the exact densities obtained from numerical solutions of the Schrödinger equation, we see that the deviations are strongest in the region of intermediate β , as expected. Quantum mechanical limits are reproduced very well, classical limits exactly.

8.7.2 Distribution Function for the Electron in the Hydrogen Atom

With the insights gained in the last section by discussing the double-well potential, we are prepared to apply our method to the electron in the hydrogen atom, which is exposed to the attractive Coulomb interaction

$$V(\mathbf{r}) = -\frac{e^2}{r}. \quad (8.90)$$

Apart from its physical significance, the theoretical interest in this problem originates from the non-polynomial nature of the attractive Coulomb interaction. The usual Wick rules or Feynman diagrams do not allow to evaluate harmonic expectation values in this case. Only by the aid of the above-mentioned smearing formula we are able to compute the variational expansion. Since we learned from the double-well potential that the importance of the second variational parameter \mathbf{r}_m diminishes for a decreasing height of the central barrier, it is sufficient for the Coulomb potential with an absent central barrier to set $\mathbf{r}_m = 0$ and to take into account only one variational parameter Ω^2 . By doing so we will see in the first order that the anisotropic variational approximation becomes significant at low temperatures, where radial and transversal quantum fluctuations have quite different weights. The effect of anisotropy disappears completely in the classical limit.

Isotropic First-Order Approximation

In the first-order approximation for the unnormalized density, we must calculate the harmonic expectation value of the action

$$\mathcal{A}_{\text{int}}[\mathbf{r}] = \int_0^{\hbar\beta} d\tau_1 V_{\text{int}}(\mathbf{r}(\tau_1)) \quad (8.91)$$

with the interaction potential

$$V_{\text{int}}(\mathbf{r}) = - \left(\frac{e^2}{r} + \frac{1}{2} \mathbf{r}^T \Omega^2 \mathbf{r} \right), \quad (8.92)$$

where the matrix $\Omega_{\mu\nu}^2$ has the form (8.68). Applying the isotropic smearing formula (8.66) for $n = 1$ to the harmonic term in (8.91) we easily find

$$\langle \mathbf{r}^2(\tau_1) \rangle_{\mathbf{r}_a, \mathbf{r}_a}^\Omega = 3 \frac{a_{00}^4 - a_{01}^4}{a_{00}^2} + \frac{a_{01}^4}{a_{00}^4} r_a^2. \quad (8.93)$$

For the Coulomb potential we obtain the local average

$$\left\langle \frac{e^2}{r(\tau_1)} \right\rangle_{\mathbf{r}_a, \mathbf{r}_a}^\Omega = \frac{e^2}{r_a} \frac{a_{00}^2}{a_{01}^2} \operatorname{erf} \left(\frac{a_{01}^2}{\sqrt{2a_{00}^2(a_{00}^4 - a_{01}^4)}} r_a \right). \quad (8.94)$$

The time integration in (8.91) cannot be done in an analytical manner and must be performed numerically. Alternatively we can use the expansion method introduced in Section 8.5.1 for evaluating the smearing formula in three dimensions, which yields

$$\langle \mathcal{A}_{\text{int}}[\mathbf{r}] \rangle_{\mathbf{r}_a, \mathbf{r}_a}^\Omega = [\varrho_0^\Omega(\mathbf{r}_a)]^{-1} \frac{e^{-r_a^2/2a_{00}^2}}{\pi^2 a_{00}^2 r_a} \sum_{n=0}^{\infty} \frac{H_{2n+1}(r_a/\sqrt{2a_{00}^2})}{2^{2n+1} (2n+1)!} C_\beta^{(2n)} \int_0^\infty dy y V_{\text{int}}(\sqrt{2a_{00}^2} y) e^{-y^2} H_{2n+1}(y). \quad (8.95)$$

This can be rewritten in terms of Laguerre polynomials $L_n^\mu(r)$ as

$$\begin{aligned} \langle \mathcal{A}_{\text{int}}[\mathbf{r}] \rangle_{\mathbf{r}_a, \mathbf{r}_a}^\Omega &= \sqrt{\frac{2a_{00}^2}{\pi}} \frac{1}{r_a} \sum_{n=0}^{\infty} \frac{(-1)^n n!}{(2n+1)!} C_\beta^{(2n)} H_{2n+1} \left(r_a / \sqrt{2a_{00}^2} \right) \\ &\quad \times \int_0^\infty dy y^{1/2} V_{\text{int}} \left(\sqrt{2a_{00}^2} y^{1/2} \right) e^{-y} L_n^{1/2}(y) L_0^{1/2}(y). \end{aligned} \quad (8.96)$$

Using the integral formula [62, Eq. 2.19.14.15]

$$\int_0^\infty dx x^{\alpha-1} e^{-cx} L_m^\gamma(cx) L_n^\lambda(cx) = \frac{(1+\gamma)_m (\lambda - \alpha + 1)_n \Gamma(\alpha)}{m! n! c^\alpha} {}_3F_2(-m, \alpha, \alpha - \lambda; \gamma + 1, \alpha - \lambda - n; 1), \quad (8.97)$$

where the $(\alpha)_n$ are Pochhammer symbols, ${}_pF_q(a_1, \dots, a_p; b_1, \dots, b_q; x)$ denotes the confluent hypergeometric function, and $\Gamma(x)$ is the Gamma function, we apply the smearing formula to the interaction potential (8.92) and find

$$\begin{aligned} \langle \mathcal{A}_{\text{int}}[\mathbf{r}] \rangle_{\mathbf{r}_a, \mathbf{r}_a}^\Omega &= - \frac{e^2}{\sqrt{\pi} r_a} \sum_{n=0}^{\infty} \frac{(-1)^n (2n-1)!!}{2^n (2n+1)!} C_\beta^{(2n)} H_{2n+1}(r_a/\sqrt{2a_{00}^2}) \\ &\quad - \frac{3}{4} \sqrt{2a_{00}^6} \Omega^4 \frac{1}{r_a} \left\{ C_\beta^{(0)} H_1(r_a/\sqrt{2a_{00}^2}) + \frac{1}{6} C_\beta^{(2)} H_3(r_a/\sqrt{2a_{00}^2}) \right\}. \end{aligned} \quad (8.98)$$

The first term comes from the Coulomb potential, the second from the harmonic potential. Inserting (8.98) in (8.17), we compute the first-order isotropic form of the radial distribution function

$$g(\mathbf{r}) = \sqrt{2\pi\beta}^3 \tilde{\rho}(\mathbf{r}). \quad (8.99)$$

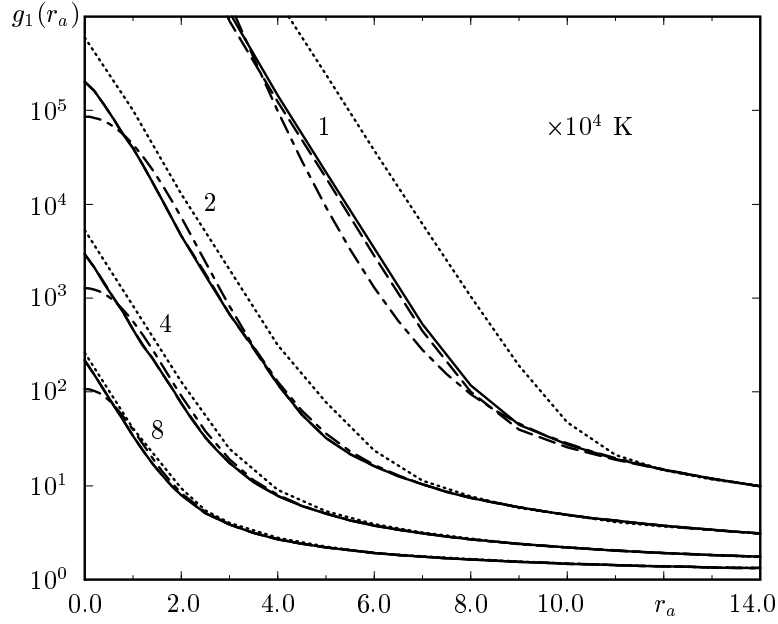


FIGURE 8.9: Radial distribution function for an electron–proton pair at different temperatures. The first-order results obtained with isotropic (dashed curves) and anisotropic (solid) variational perturbation theory are compared with Storer’s numerical results [63] (dotted) and an earlier approximation derived from the variational effective potential method to first order in Ref. [55] (dash-dotted).

This can be written as

$$g_1^\Omega(\mathbf{r}_a) = \exp[-\beta W_1^\Omega(\mathbf{r}_a)] \quad (8.100)$$

with the isotropic first-order approximation of the effective classical potential

$$W_1^\Omega(\mathbf{r}_a) = \frac{3}{2\beta} \ln \frac{\sinh \beta\Omega}{\beta\Omega} + \frac{\Omega}{\beta} r_a^2 \tanh \frac{\beta\Omega}{2} + \frac{1}{\beta} \langle \mathcal{A}_{\text{int}}[\mathbf{r}] \rangle_{\mathbf{r}_a, \mathbf{r}_a}^\Omega, \quad (8.101)$$

which is shown in Fig. 8.9 for various temperatures. The results compare well with Storer’s precise numerical results [63]. Near the origin, our results are better than those obtained with an earlier approximation derived from lowest-order effective classical potential $W_1(x_0)$ [55].

Anisotropic First-Order Approximation

The above results can be improved by taking care of the anisotropy of the problem. For the harmonic part of the action (8.91),

$$\mathcal{A}_{\text{int}}[\mathbf{r}] = \mathcal{A}^\Omega[\mathbf{r}] + \mathcal{A}_C[\mathbf{r}], \quad (8.102)$$

the smearing formula (8.71) yields the expectation value

$$\langle \mathcal{A}^\Omega[\mathbf{r}] \rangle_{\mathbf{r}_a, \mathbf{r}_a}^{\Omega_{L,T}} = -\frac{1}{2} \left\{ \Omega_L^2 a_{L00}^2 \left(C_\beta^{(0)} + \frac{1}{2} C_{\beta,L}^{(2)} H_2(r_a / \sqrt{2a_{L00}^2}) \right) + 2\Omega_T^2 a_{T00}^2 (C_\beta^{(0)} - C_{\beta,T}^{(2)}) \right\}, \quad (8.103)$$

where the $C_{\beta,L(T)}^{(n)}$ are the polynomials (8.41) with Ω replaced by the longitudinal or transverse frequency. For the Coulomb part of action, the smearing formula (8.71) leads to a double integral

$$\langle \mathcal{A}_C[\mathbf{r}] \rangle_{\mathbf{r}_a, \mathbf{r}_a}^{\Omega_{L,T}} = -e^2 \int_0^{\hbar\beta} d\tau_1 \sqrt{\frac{2}{\pi a_{L00}^2 (1 - a_L^4)}} \int_0^1 d\lambda \left\{ 1 + \lambda^2 \left[\frac{a_{T00}^2 (1 - a_T^4)}{a_{L00}^2 (1 - a_L^4)} - 1 \right] \right\}^{-1}$$

$$\times \exp \left\{ -\frac{r_a^2 a_L^4 \lambda^2}{2a_{L00}^2 (1 - a_L^4)} \right\} \quad (8.104)$$

with the abbreviations

$$a_L^2 = \frac{a_{L01}^2}{a_{L00}^2}, \quad a_T^2 = \frac{a_{T01}^2}{a_{T00}^2}. \quad (8.105)$$

The integrals must be done numerically and the first-order approximation of the radial distribution function can be expressed by

$$g_1^{\Omega_L, T}(\mathbf{r}_a) = \exp[-\beta W_1^{\Omega_L, T}(\mathbf{r}_a)] \quad (8.106)$$

with

$$W_1^{\Omega_L, T}(\mathbf{r}_a) = \frac{1}{2\beta} \ln \frac{\sinh \beta \Omega_L}{\beta \Omega_L} + \frac{1}{\beta} \ln \frac{\sinh \beta \Omega_T}{\beta \Omega_T} + \frac{\Omega_L}{\beta} r_a^2 \tanh \frac{\beta \Omega_L}{2} + \frac{1}{\beta} \langle \mathcal{A}_{\text{int}}[\mathbf{r}] \rangle_{\mathbf{r}_a, \mathbf{r}_a}^{\Omega_L, T}. \quad (8.107)$$

This is optimized in $\Omega_L(\mathbf{r}_a), \Omega_T(\mathbf{r}_a)$ with the results shown in Fig. 8.9. The anisotropic approach improves the isotropic result for temperatures below 10^4 K.

Variational Approach to Hydrogen Atom in Uniform Magnetic Field

Applying the generalized variational approach presented in Section 7.1, we calculate the temperature-dependent effective classical potential governing the quantum statistics of a hydrogen atom in a uniform magnetic at all temperatures [18,19]. The zero-temperature limit yields the binding energy of the electron which is quite accurate for all magnetic field strengths and exhibits, in particular, the correct logarithmic growth at large fields.

9.1 Introduction

The quantum statistical and quantum mechanical properties of a hydrogen atom in an external magnetic field are not exactly calculable. Perturbative approaches yield good results only for weak uniform fields as discussed in detail by Le Guillou and Zinn-Justin [64], who interpolated with analytic mapping techniques the ground-state energy between weak- and strong-field regime. Other approaches are based on recursive procedures in higher-order perturbation theory [65–67]. Zero-temperature properties were also investigated with the help of an operator optimization method in a second-quantized variational procedure [68]. The behavior at high uniform fields was inferred from treatments of the one-dimensional hydrogen atom [69–71]. Hydrogen in strong magnetic fields is still a problem under investigation, since its solution is necessary to understand the properties of white dwarfs and neutron stars, as emphasized in Refs. [72–75].

A compact and detailed presentation of the bound states and highly accurate numerical values for the energy levels are given in Ref. [76].

Equations for a first-order variational approach to the ground-state energy of hydrogen in a uniform magnetic field based on the Jensen-Peierls inequality were written down a long time ago [77], but never evaluated. Apparently, they merely served as a preparation for attacking the more complicated problem of a polaron in a magnetic field [77–79].

In plasma physics, the equation of state of a hydrogen plasma, which is influenced by a magnetic field, was recently investigated with the help of fugacity expansions for weak and strong fields [80–82].

In our approach, we calculate the quantum statistical properties of the system by an extension of variational perturbation theory [4]. The crucial quantity is the effective classical potential. In the zero-temperature limit, it yields the ground-state energy. Our calculations in a magnetic field require an extension of the formalism in Ref. [4] which derives the effective classical potential from the phase

space representation of the partition function.

Variational perturbation theory has an important advantage over other approaches: The calculation yields a good effective classical potential for *all* temperatures and coupling strengths. The quantum statistical partition function is obtained from a simple integral over a Boltzmann-factor involving the effective classical potential. The ground-state energy is then obtained from its zero-temperature limit. The asymptotic behavior in the strong-coupling limit is emerging automatically and does not have to be derived from other sources.

9.2 Effective Classical Representations for the Quantum Statistical Partition Function

A point particle in d dimensions with a potential $V(\mathbf{x})$ and a vector potential $\mathbf{A}(\mathbf{x})$ is described by a Hamiltonian

$$H(\mathbf{p}, \mathbf{x}) = \frac{1}{2M} [\mathbf{p} - e\mathbf{A}(\mathbf{x})]^2 + V(\mathbf{x}). \quad (9.1)$$

The quantum statistical partition function is given by the Euclidean phase space path integral

$$Z = \oint \mathcal{D}'^d x \mathcal{D}^d p e^{-\mathcal{A}[\mathbf{p}, \mathbf{x}]/\hbar} \quad (9.2)$$

with an action

$$\mathcal{A}[\mathbf{p}, \mathbf{x}] = \int_0^{\hbar\beta} d\tau [-i\mathbf{p}(\tau) \cdot \dot{\mathbf{x}}(\tau) + H(\mathbf{p}(\tau), \mathbf{x}(\tau))], \quad (9.3)$$

and the path measure

$$\oint \mathcal{D}'^d x \mathcal{D}^d p = \lim_{N \rightarrow \infty} \prod_{n=1}^{N+1} \left[\int \frac{d^d x_n d^d p_n}{(2\pi\hbar)^d} \right]. \quad (9.4)$$

The parameter $\beta = 1/k_B T$ denotes the usual inverse thermal energy at temperature T , where k_B is the Boltzmann constant. From Z we obtain the free energy of the system:

$$F = -\frac{1}{\beta} \ln Z. \quad (9.5)$$

In perturbation theory, one treats the external potential $V(\mathbf{x})$ as a small quantity, and expands the partition function into powers of $V(\mathbf{x})$. Such a naive expansion is applicable only for extremely weak couplings, and has a vanishing radius of convergence. Convergence is achieved by variational perturbation theory [4], which yields good approximations for all potential strengths, as we shall see in the sequel.

9.2.1 Effective Classical Potential

All quantum mechanical systems studied so far in variational perturbation theory were governed by a Hamiltonian of the standard form

$$H(\mathbf{p}, \mathbf{x}) = \frac{\mathbf{p}^2}{2M} + V(\mathbf{x}). \quad (9.6)$$

The simple quadratic dependence on the momenta makes the momentum integrals in the path integral (9.2) trivial. The remaining configuration space representation of the partition function is used to define an effective classical potential $V_{\text{eff}}(\mathbf{x}_0)$, from which the quantum mechanical partition function is found by a classically looking integral

$$Z = \int \frac{d^d x_0}{\lambda_{\text{th}}^d} \exp[-\beta V_{\text{eff}}(\mathbf{x}_0)], \quad (9.7)$$

where $\lambda_{\text{th}} = \sqrt{2\pi\hbar^2\beta/M}$ is the thermal wavelength. The Boltzmann factor plays the role of a *local partition function* $Z^{\mathbf{x}_0}$, which is calculated from the restricted path integral

$$e^{-\beta V_{\text{eff}}(\mathbf{x}_0)} \equiv Z^{\mathbf{x}_0} = \lambda_{\text{th}}^d \oint \mathcal{D}^d x \delta(\mathbf{x}_0 - \overline{\mathbf{x}(\tau)}) e^{-\mathcal{A}[\mathbf{x}]/\hbar}, \quad (9.8)$$

with the action

$$\mathcal{A}[\mathbf{x}] = \int_0^{\hbar\beta} d\tau \left[\frac{M}{2} \dot{\mathbf{x}}^2(\tau) + V(\mathbf{x}(\tau)) \right], \quad (9.9)$$

and the path measure

$$\oint \mathcal{D}^d x = \lim_{N \rightarrow \infty} \prod_{n=1}^{N+1} \left\{ \int \frac{d^d x_n}{[2\pi\hbar^2\beta/M(N+1)]^{d/2}} \right\}. \quad (9.10)$$

As pointed out in Section 4.1, the special treatment of the temporal average of the Fourier path

$$\mathbf{x}_0 = \overline{\mathbf{x}(\tau)} = \frac{1}{\hbar\beta} \int_0^{\hbar\beta} d\tau \mathbf{x}(\tau) \quad (9.11)$$

is essential for the quality of the results. It subtracts from the harmonic fluctuation width $\langle \mathbf{x}^2 \rangle^{\text{cl}}$ the classical divergence proportional to $T = 1/k_B\beta$ of the Dulong-Petit law [4,20]. Such diverging fluctuations cannot be treated perturbatively, and require the final integration in expression (9.7) to be done numerically.

For the Coulomb potential $V(\mathbf{x}) = -e^2/4\pi\epsilon_0 |\mathbf{x}|$ in three dimensions, the effective classical potential in Eq. (9.8) can be approximated well by variational perturbation theory [4,20,53,55].

9.2.2 Effective Classical Hamiltonian

In order to deal with Hamiltonians like (9.1) which contain a $\mathbf{p} \cdot \mathbf{A}(\mathbf{x})$ -term, we must apply the generalized variational procedure introduced in Section 7.2. Extending (9.8), we define an *effective classical Hamiltonian* by the phase space path integral

$$e^{-\beta H_{\text{eff}}(\mathbf{p}_0, \mathbf{x}_0)} \equiv Z^{\mathbf{p}_0, \mathbf{x}_0} = (2\pi\hbar)^d \oint \mathcal{D}^d x \mathcal{D}^d p \delta(\mathbf{x}_0 - \overline{\mathbf{x}(\tau)}) \delta(\mathbf{p}_0 - \overline{\mathbf{p}(\tau)}) e^{-\mathcal{A}[\mathbf{p}, \mathbf{x}]/\hbar}, \quad (9.12)$$

with the action (9.3) and the measure (9.4). This allows us to express the partition function as the classically looking phase space integral

$$Z = \int \frac{d^d x_0 d^d p_0}{(2\pi\hbar)^d} \exp[-\beta H_{\text{eff}}(\mathbf{p}_0, \mathbf{x}_0)], \quad (9.13)$$

where \mathbf{p}_0 is the temporal average of the momentum:

$$\mathbf{p}_0 = \overline{\mathbf{p}(\tau)} = \frac{1}{\hbar\beta} \int_0^{\hbar\beta} d\tau \mathbf{p}(\tau). \quad (9.14)$$

The fixing of \mathbf{p}_0 is done for the same reason as that for \mathbf{x}_0 , since the classical expectation value $\langle \mathbf{p}^2 \rangle^{\text{cl}}$ is diverging linearly with T , just as $\langle \mathbf{x}^2 \rangle^{\text{cl}}$.

In the special case of a standard Hamiltonian (9.6), the effective Hamiltonian in Eq. (9.13) reduces to the effective classical potential, since the momentum integral in Eq. (9.12) can then be easily performed, and the resulting restricted partition function becomes

$$Z^{\mathbf{p}_0, \mathbf{x}_0} = \exp\left(-\beta \frac{\mathbf{p}_0^2}{2M}\right) Z^{\mathbf{x}_0} \quad (9.15)$$

with the local partition function of Eq. (9.8). Thus the complete quantum statistical partition function is given by (9.13), with an effective classical Hamilton function

$$H_{\text{eff}}(\mathbf{p}_0, \mathbf{x}_0) = \frac{\mathbf{p}_0^2}{2M} + V_{\text{eff}}(\mathbf{x}_0). \quad (9.16)$$

As a consequence of the purely quadratic momentum dependence of $H(\mathbf{p}, \mathbf{x})$ in (9.6), the \mathbf{p}_0 -integral in (9.13) can be done, thus expressing the quantum statistical partition function as a pure configuration space integral over the Boltzmann factor involving the effective classical potential $V_{\text{eff}}(\mathbf{x}_0)$, as in Eq. (9.7).

9.2.3 Exact Effective Classical Hamiltonian for an Electron in a Constant Magnetic Field

The effective classical Hamiltonian for the electron moving in a constant magnetic field can be calculated exactly. We consider a magnetic field $\mathbf{B} = B\mathbf{e}_z$ pointing along the positive z -axis. The only nontrivial motion of the electron is in the x - y -plane. In symmetric gauge the vector potential is given by

$$\mathbf{A}(\mathbf{x}) = \frac{B}{2}(-y, x, 0). \quad (9.17)$$

The choice of the gauge does not affect the partition function since the periodic path integral (9.2) is gauge invariant. Ignoring the trivial free particle motion along the z -direction, we may restrict our attention to the two-dimensional Hamiltonian

$$H(\mathbf{p}, \mathbf{x}) = \frac{\mathbf{p}^2}{2M} - \omega_B l_z(\mathbf{p}, \mathbf{x}) + \frac{1}{2}M\omega_B^2 \mathbf{x}^2 \quad (9.18)$$

with $\mathbf{x} = (x, y)$ and $\mathbf{p} = (p_x, p_y)$. Here, $\omega_B = eB/2M$ is half the Landau frequency, and

$$l_z(\mathbf{p}, \mathbf{x}) = (\mathbf{x} \times \mathbf{p})_z = xp_y - yp_x \quad (9.19)$$

the third component of the orbital angular momentum.

It is useful at intermediate stages of the following development to treat the more general problem

$$H(\mathbf{p}, \mathbf{x}) = \frac{\mathbf{p}^2}{2M} - \omega_B l_z(\mathbf{p}, \mathbf{x}) + \frac{1}{2}M\Omega_\perp^2 \mathbf{x}^2. \quad (9.20)$$

At the end of the calculation only the limit $\Omega_\perp \rightarrow \omega_B$ will be relevant. The partition function of the problem is given by Eq. (9.13), with $d = 2$. Being interested in an effective classical formulation, we have to calculate the path integral (9.12). First we express the δ function for the averaged momentum as a Fourier integral

$$\delta(\mathbf{p}_0 - \overline{\mathbf{p}(\tau)}) = \int \frac{d^2\xi}{(2\pi\hbar)^2} \exp\left(-\frac{i}{\hbar}\xi \cdot \mathbf{p}_0\right) \exp\left[-\frac{1}{\hbar} \int_0^{\hbar\beta} d\tau \mathbf{v}_0(\xi) \cdot \mathbf{p}(\tau)\right] \quad (9.21)$$

involving an auxiliary source

$$\mathbf{v}_0(\xi) = -\frac{i}{\hbar\beta} \xi \quad (9.22)$$

which is constant in time. Substituting the δ function in Eq. (9.12) by this source representation, the partition function reads

$$\begin{aligned} Z^{\mathbf{p}_0, \mathbf{x}_0} &= \lim_{\Omega_\perp \rightarrow \omega_B} \int d^2\xi \exp\left(-\frac{i}{\hbar}\xi \cdot \mathbf{p}_0\right) \oint \mathcal{D}'^2 x \mathcal{D}^2 p \delta(\mathbf{x}_0 - \overline{\mathbf{x}(\tau)}) \\ &\quad \times \exp\left\{-\frac{1}{\hbar} \int_0^{\hbar\beta} d\tau [-i\mathbf{p}(\tau) \cdot \dot{\mathbf{x}}(\tau) + H(\mathbf{p}(\tau), \mathbf{x}(\tau)) + \mathbf{v}_0(\xi) \cdot \mathbf{p}(\tau)]\right\}. \end{aligned} \quad (9.23)$$

Evaluating the momentum integrals and utilizing the periodicity property $\mathbf{x}(0) = \mathbf{x}(\hbar\beta)$, we obtain the configuration space path integral

$$\begin{aligned} Z^{\mathbf{p}_0, \mathbf{x}_0} &= \lim_{\Omega_\perp \rightarrow \omega_B} \int d^2\xi \exp\left(-\frac{i}{\hbar}\xi \cdot \mathbf{p}_0 - \frac{M}{2\hbar^2\beta}\xi^2\right) \oint \mathcal{D}^2 x \delta(\mathbf{x}_0 - \overline{\mathbf{x}(\tau)}) \\ &\quad \times \exp\left\{-\frac{1}{\hbar} \int_0^{\hbar\beta} d\tau \left[\frac{M}{2}\dot{\mathbf{x}}^2(\tau) + \frac{1}{2}M(\Omega_\perp^2 - \omega_B^2)\mathbf{x}^2(\tau) - iM\omega_B(\mathbf{x}(\tau) \times \dot{\mathbf{x}}(\tau))_z + \mathbf{x}(\tau) \cdot \mathbf{j}_1(\xi)\right]\right\}, \end{aligned}$$

$$(9.24)$$

where the source \mathbf{v}_0 coupled to the momentum in (9.23) has turned to a source \mathbf{j}_1 coupled to the path in configuration space [17], with components

$$\mathbf{j}_1(\boldsymbol{\xi}) = M\omega_B (v_{0y}(\boldsymbol{\xi}), -v_{0x}(\boldsymbol{\xi})) = \frac{i\omega_B M}{\hbar\beta} (-\xi_y, \xi_x). \quad (9.25)$$

Expressing the δ function in the path integral of Eq. (9.24) by the Fourier integral

$$\delta(\mathbf{x}_0 - \overline{\mathbf{x}(\tau)}) = \int \frac{d^2\boldsymbol{\kappa}}{(2\pi)^2} \exp(i\boldsymbol{\kappa} \cdot \mathbf{x}_0) \exp\left[-\frac{1}{\hbar} \int_0^{\hbar\beta} d\tau \mathbf{j}_2(\boldsymbol{\kappa}) \cdot \mathbf{x}(\tau)\right] \quad (9.26)$$

with the new source

$$\mathbf{j}_2(\boldsymbol{\kappa}) = \frac{i\boldsymbol{\kappa}}{\beta}, \quad (9.27)$$

the partition function (9.24) can be written as

$$Z^{\mathbf{p}_0, \mathbf{x}_0} = \lim_{\Omega_{\perp} \rightarrow \omega_B} \int d^2\xi \exp\left(-\frac{i}{\hbar}\boldsymbol{\xi} \cdot \mathbf{p}_0 - \frac{M}{2\hbar^2\beta}\boldsymbol{\xi}^2\right) \int \frac{d^2\boldsymbol{\kappa}}{(2\pi)^2} \exp(i\boldsymbol{\kappa} \cdot \mathbf{x}_0) Z_{\Omega}[\mathbf{J}(\boldsymbol{\xi}, \boldsymbol{\kappa})]. \quad (9.28)$$

The functional $Z_{\Omega}[\mathbf{J}(\boldsymbol{\xi}, \boldsymbol{\kappa})]$ is defined as the configuration space path integral

$$Z_{\Omega}[\mathbf{J}(\boldsymbol{\xi}, \boldsymbol{\kappa})] = \oint \mathcal{D}^2x \exp\left[-\frac{1}{2} \int_0^{\hbar\beta} d\tau \int_0^{\hbar\beta} d\tau' \mathbf{x}(\tau) \mathbf{G}^{-1}(\tau, \tau') \mathbf{x}(\tau') - \frac{1}{\hbar} \int_0^{\hbar\beta} d\tau \mathbf{J}(\boldsymbol{\xi}, \boldsymbol{\kappa}) \cdot \mathbf{x}(\tau)\right], \quad (9.29)$$

where we have introduced the combined source $\mathbf{J}(\boldsymbol{\xi}, \boldsymbol{\kappa}) = \mathbf{j}_1(\boldsymbol{\xi}) + \mathbf{j}_2(\boldsymbol{\kappa})$. Formally, the solution reads

$$Z_{\Omega}[\mathbf{J}(\boldsymbol{\xi}, \boldsymbol{\kappa})] = Z_{\Omega}[0] \exp\left[\frac{1}{2\hbar^2} \int_0^{\hbar\beta} d\tau \int_0^{\hbar\beta} d\tau' \mathbf{J}(\boldsymbol{\xi}, \boldsymbol{\kappa}) \mathbf{G}(\tau, \tau') \mathbf{J}(\boldsymbol{\xi}, \boldsymbol{\kappa})\right], \quad (9.30)$$

where $\mathbf{G}(\tau, \tau')$ is the matrix of Green functions obtained by inverting

$$\mathbf{G}^{-1}(\tau, \tau') = \frac{M}{\hbar} \begin{pmatrix} -\frac{d^2}{d\tau^2} + \Omega_{\perp}^2 - \omega_B^2 & -2i\omega_B \frac{d}{d\tau} \\ 2i\omega_B \frac{d}{d\tau} & -\frac{d^2}{d\tau^2} + \Omega_{\perp}^2 - \omega_B^2 \end{pmatrix} \delta(\tau - \tau'). \quad (9.31)$$

The inversion is easily done in frequency space after spectrally decomposing the δ function into the Matsubara frequencies $\omega_m = 2\pi m/\hbar\beta$,

$$\delta(\tau - \tau') = \frac{1}{\hbar\beta} \sum_{m=-\infty}^{\infty} e^{i\omega_m(\tau - \tau')}. \quad (9.32)$$

The result is

$$\tilde{\mathbf{G}}(\omega_m) = \frac{\hbar}{M} \frac{1}{\det \tilde{\mathbf{G}}} \begin{pmatrix} \omega_m^2 + \Omega_{\perp}^2 - \omega_B^2 & -2\omega_B \omega_m \\ 2\omega_B \omega_m & \omega_m^2 + \Omega_{\perp}^2 - \omega_B^2 \end{pmatrix}. \quad (9.33)$$

At this point, the additional oscillator in Eq. (9.24) proves useful: It ensures that the determinant

$$\det \tilde{\mathbf{G}}(\omega_m) = (\omega_m^2 + \Omega_{\perp}^2 - \omega_B^2)^2 + 4\omega_B^2 \omega_m^2 \quad (9.34)$$

is nonzero for $m = 0$, thus playing the role of an infrared regulator. The Fourier expansion

$$\mathbf{G}(\tau, \tau') = \frac{1}{\hbar\beta} \sum_{m=-\infty}^{\infty} \tilde{\mathbf{G}}(\omega_m) e^{-i\omega_m(\tau - \tau')} \quad (9.35)$$

yields the matrix of Green functions

$$\mathbf{G}(\tau, \tau') = \begin{pmatrix} G_{xx}(\tau, \tau') & G_{xy}(\tau, \tau') \\ G_{yx}(\tau, \tau') & G_{yy}(\tau, \tau') \end{pmatrix} \quad (9.36)$$

which inherits the symmetry properties from the kernel (9.31):

$$G_{xx}(\tau, \tau') = G_{yy}(\tau, \tau'), \quad G_{xy}(\tau, \tau') = -G_{yx}(\tau, \tau'). \quad (9.37)$$

A more detailed description of these Green functions is given in Appendices 9A and 9B.

Since the current \mathbf{J} does not depend on the Euclidean time, the expression (9.30) simplifies therefore to

$$Z_\Omega[\mathbf{J}(\boldsymbol{\xi}, \boldsymbol{\kappa})] = Z_\Omega[0] \exp \left[\frac{1}{\hbar^2} \mathbf{J}^2(\boldsymbol{\xi}, \boldsymbol{\kappa}) \int_0^{\hbar\beta} d\tau \int_0^{\hbar\beta} d\tau' G_{xx}(\tau, \tau') \right]. \quad (9.38)$$

The Green function has the Fourier decomposition

$$G_{xx}(\tau, \tau') = \frac{1}{M\beta} \sum_{m=-\infty}^{\infty} \frac{\omega_m^2 + \Omega_\perp^2 - \omega_B^2}{(\omega_m^2 + \Omega_+^2)(\omega_m^2 + \Omega_-^2)} e^{-i\omega_m(\tau - \tau')}, \quad (9.39)$$

where Ω_\pm are the frequencies

$$\Omega_\pm = \Omega_\perp \pm \omega_B \quad (9.40)$$

and $\Omega_\perp > \omega_B$, for stability.

The ratios in the sum of (9.39) can be decomposed into two partial fractions, each of them representing a single harmonic oscillator with frequency Ω_+ and Ω_- , respectively. The analytic form of the periodic Green function of a single harmonic oscillator is well known (see Chap. 3 in Ref. [4]), and we obtain for the present Green function (9.39):

$$G_{xx}(\tau, \tau') = \frac{\hbar}{4M\Omega_\perp} \left(\frac{\cosh \Omega_+ (|\tau - \tau'| - \hbar\beta/2)}{\sinh \hbar\beta\Omega_+/2} + \frac{\cosh \Omega_- (|\tau - \tau'| - \hbar\beta/2)}{\sinh \hbar\beta\Omega_-/2} \right). \quad (9.41)$$

By factorizing the determinant (9.34) according to

$$\det \tilde{\mathbf{G}}(\omega_m) = (\omega_m^2 + \Omega_+^2)(\omega_m^2 + \Omega_-^2) \quad (9.42)$$

and summing over the logarithms of this, we calculate the partition function as a product of two single harmonic oscillators:

$$Z_\Omega = Z_\Omega[0] = \frac{1}{2 \sinh \hbar\beta\Omega_+/2} \frac{1}{2 \sinh \hbar\beta\Omega_-/2}. \quad (9.43)$$

The results (9.41) and (9.43) determine the generating functional (9.38). The Euclidean time integrations are then easily done, and subsequently the $\boldsymbol{\kappa}$ - and $\boldsymbol{\xi}$ -integrations in (9.28). As a result, we obtain the restricted partition function

$$Z^{\mathbf{p}_0, \mathbf{x}_0} = \lim_{\Omega_\perp \rightarrow \omega_B} \exp \left\{ -\beta \left(\frac{1}{\beta} \ln \frac{\sinh \hbar\beta\Omega_+/2}{\hbar\beta\Omega_+/2} \frac{\sinh \hbar\beta\Omega_-/2}{\hbar\beta\Omega_-/2} + \frac{\mathbf{p}_0^2}{2M} - \omega_B l_z(\mathbf{p}_0, \mathbf{x}_0) + \frac{1}{2} M \Omega_\perp^2 \mathbf{x}_0^2 \right) \right\}. \quad (9.44)$$

Taking the limit $\Omega_\perp \rightarrow \omega_B$, we find from (9.40): $\Omega_+ \rightarrow 2\omega_B$, $\Omega_- \rightarrow 0$, and therefore

$$\lim_{\Omega_\perp \rightarrow \omega_B} \frac{\sinh \hbar\beta\Omega_+/2}{\hbar\beta\Omega_+/2} = \frac{\sinh \hbar\beta\omega_B}{\hbar\beta\omega_B}, \quad \lim_{\Omega_\perp \rightarrow \omega_B} \frac{\sinh \hbar\beta\Omega_-/2}{\hbar\beta\Omega_-/2} = 1. \quad (9.45)$$

Recalling the definition (9.12), we identify the exact effective classical Hamiltonian for an electron in a magnetic field as

$$H_{\text{eff}}(\mathbf{p}_0, \mathbf{x}_0) = \frac{1}{\beta} \ln \frac{\sinh \hbar\beta\omega_B}{\hbar\beta\omega_B} + \frac{\mathbf{p}_0^2}{2M} - \omega_B l_z(\mathbf{p}_0, \mathbf{x}_0) + \frac{1}{2} M \omega_B^2 \mathbf{x}_0^2. \quad (9.46)$$

Integrating out the momenta in Eq. (9.13), the configuration space representation (9.7) for the partition function contains the effective classical potential for a charged particle in the plane perpendicular to the direction of a uniform magnetic field:

$$V_{\text{eff}}(\mathbf{x}_0) = \frac{1}{\beta} \ln \frac{\sinh \hbar\beta\omega_B}{\hbar\beta\omega_B}. \quad (9.47)$$

Note that this is a constant potential.

Denoting the area $\int d^2x_0$ by A , we find the exact quantum statistical partition function

$$Z = \frac{A}{\lambda_{\text{th}}^2} \frac{\hbar\beta\omega_B}{\sinh \hbar\beta\omega_B}. \quad (9.48)$$

After these preparations, we can turn our attention to the system we want to study in this chapter: the hydrogen atom in a uniform magnetic field, where the additional Coulomb interaction prevents us from finding an exact solution for the effective classical Hamilton function.

9.3 Hydrogen Atom in Constant Magnetic Field

The zero-temperature properties of the hydrogen atom without external fields are exactly known. For the quantum statistics at finite temperatures an accurate approximative result was found with the help of variational perturbation theory [53]. Similar calculations have been performed for the electron-proton pair distribution function which can be interpreted as the unnormalized density matrix [20].

Here we extend this method to the hydrogen atom in a constant magnetic field. This extension is quite nontrivial since the weak- and strong-field limits will turn out to exhibit completely different asymptotic behaviors. Let us first generalize variational perturbation theory to an electron in a constant magnetic field and arbitrary potential.

9.3.1 Generalized Variational Perturbation Theory

We consider once more the effective classical form (9.13) of the quantum statistical partition function which requires the path integration (9.12) in phase space. Fluctuations parallel and vertical to the magnetic field lines are now both nontrivial, and we must deal with the full three-dimensional system and the components of the electron position and momentum are now denoted by $\mathbf{x} = (x, y, z)$ and $\mathbf{p} = (p_x, p_y, p_z)$. For the uniform magnetic field pointing along the z -axis, the vector potential $\mathbf{A}(\mathbf{x})$ is used in the gauge (9.17). Thus the Hamilton function of an electron in a magnetic field and an arbitrary potential $V(\mathbf{x})$ is

$$H(\mathbf{p}, \mathbf{x}) = \frac{\mathbf{p}^2}{2M} - \omega_B l_z(\mathbf{p}, \mathbf{x}) + \frac{1}{2}M\omega_B^2 \mathbf{x}^2 + V(\mathbf{x}). \quad (9.49)$$

The orbital angular momentum $l_z(\mathbf{p}, \mathbf{x})$ was introduced in Eq. (9.19), and the frequency ω_B below Eq. (9.18). The importance of the separation of the zero frequency components \mathbf{x}_0 and \mathbf{p}_0 was discussed in Section 9.2. Their divergence with the temperature T prevents a perturbative treatment. Thus it is essential to set up the perturbation theory only for the fluctuations around \mathbf{x}_0 and \mathbf{p}_0 . For this we rewrite the action functional (9.3) associated with the Hamiltonian (9.49) as

$$\mathcal{A}[\mathbf{p}, \mathbf{x}] = \mathcal{A}_{\Omega}^{\mathbf{p}_0, \mathbf{x}_0}[\mathbf{p}, \mathbf{x}] + \mathcal{A}_{\text{int}}[\mathbf{p}, \mathbf{x}], \quad (9.50)$$

where we have introduced the fluctuation action

$$\begin{aligned} \mathcal{A}_{\Omega}^{\mathbf{p}_0, \mathbf{x}_0}[\mathbf{p}, \mathbf{x}] = & \int_0^{\hbar\beta} d\tau \left\{ -i[\mathbf{p}(\tau) - \mathbf{p}_0] \cdot \dot{\mathbf{x}}(\tau) + \frac{1}{2M}[\mathbf{p}(\tau) - \mathbf{p}_0]^2 - \Omega_B l_z(\mathbf{p}(\tau) - \mathbf{p}_0, \mathbf{x}(\tau) - \mathbf{x}_0) \right. \\ & \left. + \frac{1}{2}M\Omega_{\perp}^2 [\mathbf{x}^{\perp}(\tau) - \mathbf{x}_0^{\perp}]^2 + \frac{1}{2}M\Omega_{\parallel}^2 [z(\tau) - z_0]^2 \right\}, \end{aligned} \quad (9.51)$$

in which $\mathbf{x}^\perp = (x, y, 0)$ denotes the transverse part of \mathbf{x} and $\Omega_\perp > \Omega_B$, for stability. The interaction is now

$$\mathcal{A}_{\text{int}}[\mathbf{p}, \mathbf{x}] = \int_0^{\hbar\beta} d\tau V_{\text{int}}(\mathbf{p}(\tau), \mathbf{x}(\tau)) = \mathcal{A}[\mathbf{p}, \mathbf{x}] - \mathcal{A}_{\Omega}^{\mathbf{p}_0, \mathbf{x}_0}[\mathbf{p}, \mathbf{x}] \quad (9.52)$$

with the interaction potential

$$\begin{aligned} V_{\text{int}}(\mathbf{p}(\tau), \mathbf{x}(\tau)) &= \frac{1}{2M} \left\{ \mathbf{p}^2(\tau) - [\mathbf{p}(\tau) - \mathbf{p}_0]^2 \right\} - \omega_B \mathbf{x}^\perp(\tau) \times \mathbf{p}^\perp(\tau) \\ &\quad + \Omega_B (\mathbf{x}^\perp(\tau) - \mathbf{x}_0^\perp) \times (\mathbf{p}^\perp(\tau) - \mathbf{p}_0^\perp) + \frac{1}{2} M \omega_B^2 \mathbf{x}^{\perp 2}(\tau) \\ &\quad - \frac{1}{2} M \Omega_\perp^2 [\mathbf{x}^\perp(\tau) - \mathbf{x}_0^\perp]^2 - \frac{1}{2} M \Omega_\parallel^2 [z(\tau) - z_0]^2 + V(\mathbf{x}(\tau)), \end{aligned} \quad (9.53)$$

where $\mathbf{p}^\perp = (p_x, p_y, 0)$. The frequencies $\Omega = (\Omega_B, \Omega_\perp, \Omega_\parallel)$ are for the moment arbitrary. The decomposition (9.50) forms the basis for the variational approach, where the first term in the action (9.50) allows an exact treatment. The transverse part was given in Section 9.2.3 and the longitudinal part is trivial, since it is harmonic with frequency Ω_\parallel . The associated partition function is given by the path integral

$$Z_{\Omega}^{\mathbf{p}_0, \mathbf{x}_0} = \oint \mathcal{D}'^3 x \mathcal{D}^3 p \delta(\mathbf{x}_0 - \overline{\mathbf{x}(\tau)}) \delta(\mathbf{p}_0 - \overline{\mathbf{p}(\tau)}) e^{-\mathcal{A}_{\Omega}^{\mathbf{p}_0, \mathbf{x}_0}[\mathbf{p}, \mathbf{x}]/\hbar}, \quad (9.54)$$

which can be performed. Details are given in Appendix 9C. The result is

$$Z_{\Omega}^{\mathbf{p}_0, \mathbf{x}_0} = \frac{\hbar\beta\Omega_+/2}{\sinh \hbar\beta\Omega_+/2} \frac{\hbar\beta\Omega_-/2}{\sinh \hbar\beta\Omega_-/2} \frac{\hbar\beta\Omega_\parallel/2}{\sinh \hbar\beta\Omega_\parallel/2}, \quad (9.55)$$

where auxiliary frequencies are composed of the frequencies Ω_B, Ω_\perp in the action (9.51) as

$$\Omega_\pm(\Omega_B, \Omega_\perp) = \Omega_\perp \pm \Omega_B. \quad (9.56)$$

This partition function serves in the subsequent perturbation expansion as trial system which depends explicitly on the frequencies Ω . The correlation functions are a straightforward generalization of (9.36) to three dimensions:

$$\mathbf{G}^{\mathbf{x}_0}(\tau, \tau') = \begin{pmatrix} G_{xx}^{\mathbf{x}_0}(\tau, \tau') & G_{xy}^{\mathbf{x}_0}(\tau, \tau') & 0 \\ G_{yx}^{\mathbf{x}_0}(\tau, \tau') & G_{yy}^{\mathbf{x}_0}(\tau, \tau') & 0 \\ 0 & 0 & G_{zz}^{\mathbf{x}_0}(\tau, \tau') \end{pmatrix}, \quad (9.57)$$

whose explicit form is derived in Appendix 9C.

The Ω -dependent action in Eq. (9.50) is treated perturbatively. Writing the partition function (9.12) as

$$\begin{aligned} Z^{\mathbf{p}_0, \mathbf{x}_0} &= (2\pi\hbar)^3 \oint \mathcal{D}'^3 x \mathcal{D}^3 p \delta(\mathbf{x}_0 - \overline{\mathbf{x}(\tau)}) \delta(\mathbf{p}_0 - \overline{\mathbf{p}(\tau)}) \exp \left\{ -\frac{1}{\hbar} \mathcal{A}_{\Omega}^{\mathbf{p}_0, \mathbf{x}_0}[\mathbf{p}, \mathbf{x}] \right\} \\ &\quad \times \exp \left\{ -\frac{1}{\hbar} \int_0^{\hbar\beta} d\tau V_{\text{int}}(\mathbf{p}(\tau), \mathbf{x}(\tau)) \right\}, \end{aligned} \quad (9.58)$$

the second exponential is expanded into a Taylor series, yielding

$$\begin{aligned} Z^{\mathbf{p}_0, \mathbf{x}_0} &= (2\pi\hbar)^3 \oint \mathcal{D}'^3 x \mathcal{D}^3 p \delta(\mathbf{x}_0 - \overline{\mathbf{x}(\tau)}) \delta(\mathbf{p}_0 - \overline{\mathbf{p}(\tau)}) \exp \left\{ -\frac{1}{\hbar} \mathcal{A}_{\Omega}^{\mathbf{p}_0, \mathbf{x}_0}[\mathbf{p}, \mathbf{x}] \right\} \\ &\quad \times \left[1 - \frac{1}{\hbar} \int_0^{\hbar\beta} d\tau V_{\text{int}}(\mathbf{p}(\tau), \mathbf{x}(\tau)) + \frac{1}{2!\hbar^2} \int_0^{\hbar\beta} d\tau_1 \int_0^{\hbar\beta} d\tau_2 V_{\text{int}}(\mathbf{p}(\tau_1), \mathbf{x}(\tau_1)) V_{\text{int}}(\mathbf{p}(\tau_2), \mathbf{x}(\tau_2)) - \dots \right]. \end{aligned} \quad (9.59)$$

In three dimensions, the harmonic expectation values are defined with respect to the restricted path integral as

$$\langle \dots \rangle_{\Omega}^{\mathbf{p}_0, \mathbf{x}_0} = \frac{(2\pi\hbar)^3}{Z_{\Omega}^{\mathbf{p}_0, \mathbf{x}_0}} \oint \mathcal{D}'^3 x \mathcal{D}^3 p \dots \delta(\mathbf{x}_0 - \overline{\mathbf{x}(\tau)}) \delta(\mathbf{p}_0 - \overline{\mathbf{p}(\tau)}) \exp \left\{ -\frac{1}{\hbar} \mathcal{A}_{\Omega}^{\mathbf{p}_0, \mathbf{x}_0}[\mathbf{p}, \mathbf{x}] \right\}. \quad (9.60)$$

Similar to the procedure presented in Section 7.2, we rewrite the Taylor expansion (9.59) as a cumulant expansion of the form (7.21). The first cumulants are given by Eqs. (7.22). Expressing the restricted partition functions by the help of the relations (7.12), we obtain a perturbation series for the effective classical Hamiltonian:

$$H_{\text{eff}}(\mathbf{p}_0, \mathbf{x}_0) = -\frac{1}{\beta} \ln Z_{\Omega}^{\mathbf{p}_0, \mathbf{x}_0} + \frac{1}{\beta} \sum_{n=1}^{\infty} \frac{(-1)^{n+1}}{\hbar^n n!} \left\langle \left(\int_0^{\hbar\beta} d\tau V_{\text{int}}(\mathbf{p}(\tau), \mathbf{x}(\tau)) \right)^n \right\rangle_{\Omega, c}^{\mathbf{p}_0, \mathbf{x}_0}. \quad (9.61)$$

The N th-order approximation of the effective classical Hamiltonian is then given by

$$\mathcal{H}_{\Omega}^{(N)}(\mathbf{p}_0, \mathbf{x}_0) = -\frac{1}{\beta} \ln Z_{\Omega}^{\mathbf{p}_0, \mathbf{x}_0} + \frac{1}{\beta} \sum_{n=1}^N \frac{(-1)^{n+1}}{\hbar^n n!} \left\langle \left(\int_0^{\hbar\beta} d\tau V_{\text{int}}(\mathbf{p}(\tau), \mathbf{x}(\tau)) \right)^n \right\rangle_{\Omega, c}^{\mathbf{p}_0, \mathbf{x}_0}. \quad (9.62)$$

This expression depends explicitly on the three parameters Ω . Since the exact expression (9.61) is independent of Ω , the best approximation for $\mathcal{H}_{\Omega}^{(N)}(\mathbf{p}_0, \mathbf{x}_0)$ should minimally depend on Ω . The optimal solution is obtained by determining the parameters from the conditions

$$\nabla_{\Omega} \mathcal{H}_{\Omega}^{(N)}(\mathbf{p}_0, \mathbf{x}_0) \stackrel{!}{=} 0. \quad (9.63)$$

The solutions for the optimal variational parameters to N th order are given by

$$\Omega^{(N)} = \left(\Omega_B^{(N)}(\mathbf{p}_0, \mathbf{x}_0), \Omega_{\perp}^{(N)}(\mathbf{p}_0, \mathbf{x}_0), \Omega_{\parallel}^{(N)}(\mathbf{p}_0, \mathbf{x}_0) \right). \quad (9.64)$$

Inserting these into Eq. (9.62) yields the optimal effective classical Hamiltonian $\mathcal{H}^{(N)}(\mathbf{p}_0, \mathbf{x}_0)$.

9.3.2 First-Order Effective Classical Potential

The first-order approximation of the effective classical Hamiltonian (9.62) reads

$$\mathcal{H}_{\Omega}^{(1)}(\mathbf{p}_0, \mathbf{x}_0) = -\frac{1}{\beta} \ln Z_{\Omega}^{\mathbf{p}_0, \mathbf{x}_0} + \langle V_{\text{int}}(\mathbf{p}, \mathbf{x}) \rangle_{\Omega}^{\mathbf{p}_0, \mathbf{x}_0}. \quad (9.65)$$

The invariance of the system under time translations makes one of the time integrals in the expansion (9.61) trivial, yielding merely an overall factor $\hbar\beta$. In particular, the first-order expectation value of $V_{\text{int}}(\mathbf{x})$ in (9.65) is independent of the Euclidean time τ .

In order to calculate $\mathcal{H}_{\Omega}^{(1)}(\mathbf{p}_0, \mathbf{x}_0)$, we use the two-point correlation functions derived in Appendix 9C, and the vanishing of the linear expectations, e.g.

$$\langle p_x(\tau) - p_{0x} \rangle_{\Omega}^{\mathbf{p}_0, \mathbf{x}_0} = 0 \quad (9.66)$$

to find

$$\mathcal{H}_{\Omega}^{(1)}(\mathbf{p}_0, \mathbf{x}_0) = \frac{\mathbf{p}_0^2}{2M} - \omega_B l_z(\mathbf{p}_0, \mathbf{x}_0) + \frac{1}{2} M \omega_B^2 (x_0^2 + y_0^2) + W_{\Omega}^{(1)}(\mathbf{x}_0), \quad (9.67)$$

where we have collected all terms depending on the variational parameters Ω in the potential

$$\begin{aligned} W_{\Omega}^{(1)}(\mathbf{x}_0) = & -\frac{1}{\beta} \ln Z_{\Omega}^{\mathbf{p}_0, \mathbf{x}_0} - M \Omega_B (\omega_B - \Omega_B) b_{\perp}^2(\mathbf{x}_0) + M (\omega_B^2 - \Omega_{\perp}^2) a_{\perp}^2(\mathbf{x}_0) - \frac{1}{2} M \Omega_{\parallel}^2 a_{\parallel}^2(\mathbf{x}_0) \\ & + \langle V(\mathbf{x}) \rangle_{\Omega}^{\mathbf{p}_0, \mathbf{x}_0}. \end{aligned} \quad (9.68)$$

The quantities $a_{\perp}^2(\mathbf{x}_0)$, $a_{\parallel}^2(\mathbf{x}_0)$, and $b_{\perp}^2(\mathbf{x}_0)$ are the transverse and longitudinal fluctuation widths

$$a_{\perp}^2(\mathbf{x}_0) = G_{xx}^{\mathbf{p}_0, \mathbf{x}_0}(0), \quad a_{\parallel}^2(\mathbf{x}_0) = G_{zz}^{\mathbf{p}_0, \mathbf{x}_0}(0), \quad b_{\perp}^2(\mathbf{x}_0) = \frac{2}{M \Omega_B} G_{xp_y}^{\mathbf{p}_0, \mathbf{x}_0}(0). \quad (9.69)$$

Note that the potential (9.68) is independent of \mathbf{p}_0 . This means that the approximation (9.67) to the effective classical Hamiltonian contains no coupling of the momentum \mathbf{p}_0 to a variational parameter

Ω , such that the optimal $\Omega^{(1)}$ determined by minimizing $\mathcal{H}_\Omega^{(1)}(\mathbf{p}_0, \mathbf{x}_0)$ is independent of \mathbf{p}_0 . We may therefore integrate out \mathbf{p}_0 in the phase space representation of the first-order approximation for the partition function

$$Z^{(1)} = \int \frac{d^3 x_0 d^3 p_0}{(2\pi\hbar^3)} e^{-\beta \mathcal{H}_\Omega^{(1)}(\mathbf{p}_0, \mathbf{x}_0)} \quad (9.70)$$

to find the pure configuration space integral

$$Z^{(1)} = \int \frac{d^3 x_0}{\lambda_{\text{th}}^3} e^{-\beta W_\Omega^{(1)}(\mathbf{x}_0)}, \quad (9.71)$$

in which $W_\Omega^{(1)}(\mathbf{x}_0)$ represents the first-order approximation to the effective classical potential of an electron in a potential $V(\mathbf{x})$ and a uniform magnetic field.

9.3.3 Application to the Hydrogen Atom in a Magnetic Field

We now apply the formulas of the preceding section to the Hamiltonian (9.49) with an attracting Coulomb potential

$$V(\mathbf{x}) = -\frac{e^2}{4\pi\epsilon_0 |\mathbf{x}|}, \quad (9.72)$$

where $|\mathbf{x}|$ is the distance between the electron and the proton. The only nontrivial problem is the calculation of the expectation value $\langle V(\mathbf{x}(\tau)) \rangle_\Omega^{\mathbf{p}_0, \mathbf{x}_0}$ in Eq. (9.68). This is done using the so-called *smearing formula*, which is a Gaussian convolution of $V(\mathbf{x})$. This formula was first derived by Feynman and Kleinert [8], and exists now also in an extension to arbitrary order [20,53]. The generalization to position and momentum dependent observables was given in the phase space formulation [17]. We briefly re-derive the first-order smearing formula. The expectation value is defined by

$$\langle V(\mathbf{x}(\tau')) \rangle_\Omega^{\mathbf{p}_0, \mathbf{x}_0} = \frac{(2\pi\hbar)^3}{Z_\Omega^{\mathbf{p}_0, \mathbf{x}_0}} \oint \mathcal{D}'^3 x \mathcal{D}^3 p V(\mathbf{x}(\tau')) \delta(\mathbf{x}_0 - \overline{\mathbf{x}(\tau)}) \delta(\mathbf{p}_0 - \overline{\mathbf{p}(\tau)}) e^{-\mathcal{A}_\Omega^{\mathbf{p}_0, \mathbf{x}_0}[\mathbf{p}, \mathbf{x}]/\hbar}. \quad (9.73)$$

Now we substitute the potential by the expression

$$\begin{aligned} V(\mathbf{x}(\tau')) &= \int d^3 x V(\mathbf{x}) \delta(\mathbf{x} - \mathbf{x}(\tau')) \\ &= \int d^3 x V(\mathbf{x}) \int \frac{d^3 \kappa}{(2\pi)^3} \exp[i\boldsymbol{\kappa}^T(\mathbf{x} - \mathbf{x}_0)] \exp\left\{-\frac{1}{\hbar} \int_0^{\hbar\beta} d\tau \mathbf{j}^T(\tau) [\mathbf{x}(\tau) - \mathbf{x}_0]\right\}, \end{aligned} \quad (9.74)$$

where we have introduced the source

$$\mathbf{j}(\tau) = i\hbar\boldsymbol{\kappa}\delta(\tau - \tau'). \quad (9.75)$$

Inserting the expression (9.74) into Eq. (9.73) we obtain

$$\langle V(\mathbf{x}(\tau')) \rangle_\Omega^{\mathbf{p}_0, \mathbf{x}_0} = \frac{1}{Z_\Omega^{\mathbf{p}_0, \mathbf{x}_0}} \int d^3 x V(\mathbf{x}) \int \frac{d^3 \kappa}{(2\pi)^3} \exp[i\boldsymbol{\kappa} \cdot (\mathbf{x} - \mathbf{x}_0)] Z_\Omega^{\mathbf{p}_0, \mathbf{x}_0}[\mathbf{j}], \quad (9.76)$$

with the harmonic generating functional

$$\begin{aligned} Z_\Omega^{\mathbf{p}_0, \mathbf{x}_0}[\mathbf{j}] &= (2\pi\hbar)^3 \oint \mathcal{D}'^3 x \mathcal{D}^3 p \delta(\mathbf{x}_0 - \overline{\mathbf{x}(\tau)}) \delta(\mathbf{p}_0 - \overline{\mathbf{p}(\tau)}) \\ &\quad \times \exp\left\{-\frac{1}{\hbar} \mathcal{A}_\Omega^{\mathbf{p}_0, \mathbf{x}_0}[\mathbf{p}, \mathbf{x}] - \frac{1}{\hbar} \int_0^{\hbar\beta} d\tau \mathbf{j}(\tau) \cdot [\mathbf{x}(\tau) - \mathbf{x}_0]\right\}. \end{aligned} \quad (9.77)$$

The solution is

$$Z_\Omega^{\mathbf{p}_0, \mathbf{x}_0}[\mathbf{j}] = Z_\Omega^{\mathbf{p}_0, \mathbf{x}_0} \exp\left[\frac{1}{2\hbar^2} \int_0^{\hbar\beta} d\tau \int_0^{\hbar\beta} d\tau' \mathbf{j}(\tau) \mathbf{G}^{\mathbf{x}_0}(\tau, \tau') \mathbf{j}(\tau')\right] \quad (9.78)$$

with the 3×3 -matrix of Green functions of Eq. (9.57). The properties of the Green functions are discussed in the Appendices 9A and 9B. Expressing the source $\mathbf{j}(\tau)$ in terms of $\boldsymbol{\kappa}$ via Eq. (9.75) and performing the τ -integrations, we arrive at

$$\langle V(\mathbf{x}(\tau')) \rangle_{\Omega}^{\mathbf{p}_0, \mathbf{x}_0} = \int d^3x V(\mathbf{x}) \int \frac{d^3\boldsymbol{\kappa}}{(2\pi)^3} \exp\{i\boldsymbol{\kappa} \cdot [\mathbf{x} - \mathbf{x}_0]\} \exp\left[-\frac{1}{2}\boldsymbol{\kappa} \mathbf{G}^{\mathbf{x}_0}(0) \boldsymbol{\kappa}\right]. \quad (9.79)$$

Recognizing that $G_{yx}^{\mathbf{x}_0}(0) = G_{xy}^{\mathbf{x}_0}(0)$ vanish, the $\boldsymbol{\kappa}$ -integral is easily calculated and leads to the first-order smearing formula for an arbitrary position dependent potential

$$\langle V(\mathbf{x}(\tau')) \rangle_{\Omega}^{\mathbf{p}_0, \mathbf{x}_0} = \frac{1}{(2\pi)^{3/2} a_{\perp}^2(\mathbf{x}_0) \sqrt{a_{\parallel}^2(\mathbf{x}_0)}} \int d^3x V(\mathbf{x}) \exp\left[-\frac{(x-x_0)^2 + (y-y_0)^2}{2a_{\perp}^2(\mathbf{x}_0)} - \frac{(z-z_0)^2}{2a_{\parallel}^2(\mathbf{x}_0)}\right], \quad (9.80)$$

the right-hand side containing the Gaussian fluctuation widths (9.69).

For the Coulomb potential (9.72) that we are interested in, the integral in the smearing formula (9.80) can not be done exactly. An integral representation for a simple numerical treatment is

$$\left\langle -\frac{e^2}{4\pi\epsilon_0 |\mathbf{x}|} \right\rangle_{\Omega}^{\mathbf{p}_0, \mathbf{x}_0} = -\frac{e^2}{4\pi\epsilon_0} \sqrt{\frac{2}{\pi}} a_{\parallel}^2(\mathbf{x}_0) \int_0^1 \frac{d\xi}{a_{\parallel}^2(\mathbf{x}_0) + \xi^2[a_{\perp}^2(\mathbf{x}_0) - a_{\parallel}^2(\mathbf{x}_0)]} \times \exp\left\{-\frac{\xi^2}{2} \left(\frac{x_0^2 + y_0^2}{a_{\parallel}^2(\mathbf{x}_0) + \xi^2[a_{\perp}^2(\mathbf{x}_0) - a_{\parallel}^2(\mathbf{x}_0)]} + \frac{z_0^2}{a_{\parallel}^2(\mathbf{x}_0)} \right)\right\}. \quad (9.81)$$

With this expression we know the entire first-order effective classical potential (9.68) for an electron in a Coulomb potential and a uniform magnetic field which has to be optimized in the variational parameters Ω .

9.4 Results

We are now going to optimize the effective classical potential by extremizing it in Ω at different temperatures and magnetic field strengths. In the zero-temperature limit this will produce the ground-state energy.

9.4.1 Effective Classical Potential for Different Temperatures and Magnetic Field Strengths

The optimization of $W_{\Omega}^{(1)}(\mathbf{x}_0)$ proceeds by minimization in Ω and must be done for each value of \mathbf{x}_0 . Reinserting the optimal parameters $\Omega^{(1)}(\mathbf{x}_0)$ into the expressions (9.68) and (9.81), we obtain the optimal first-order effective classical potential $W^{(1)}(\mathbf{x}_0)$. The calculations are done numerically, where we used natural units $\hbar = e^2/4\pi\epsilon_0 = k_B = c = M = 1$. This means that energies are measured in units of $\epsilon_0 = Me^4/(4\pi\epsilon_0)^2\hbar^2 \equiv 2 \text{ Ry} \approx 27.21 \text{ eV}$, temperatures in $\epsilon_0/k_B \approx 3.16 \times 10^5 \text{ K}$, distances in Bohr radii $a_B = (4\pi\epsilon_0)^2\hbar^2/Me^2 \approx 0.53 \times 10^{-10} \text{ m}$, and magnetic field strengths in $B_0 = e^3M^2/\hbar^3(4\pi\epsilon_0)^2 \approx 2.35 \times 10^5 \text{ T} = 2.35 \times 10^9 \text{ G}$. Figure 9.1 shows the resulting curves for various magnetic field strengths B and an inverse temperature $\beta = 1/T = 1$. Examples of the lower temperature behavior are shown in Fig. 9.2 for $\beta = 100$. To see the expected anisotropy of the curves in the magnetic field direction and in the plane perpendicular to it, we plot simultaneously the curves for $W^{(1)}(\mathbf{x}_0)$ transversal to the magnetic field as a function of $\rho_0 = \sqrt{x_0^2 + y_0^2}$ at $z = 0$ (solid curves) and parallel as a function of z_0 at $\rho_0 = 0$ (dashed curves). The curves become strongly anisotropic for low temperatures and increasing field strengths (see Fig. 9.2). At a given field strength B , the two curves converge for large distances from the origin, where the proton resides, to the same constant depending on B . This is due to the decreasing influence of the Coulomb interaction which shows the classical $1/r$ -behavior in each direction. When approaching the classical high-temperature limit, the effect of anisotropy becomes less important since the violent thermal fluctuations do not have a preferred direction (see Fig. 9.1).

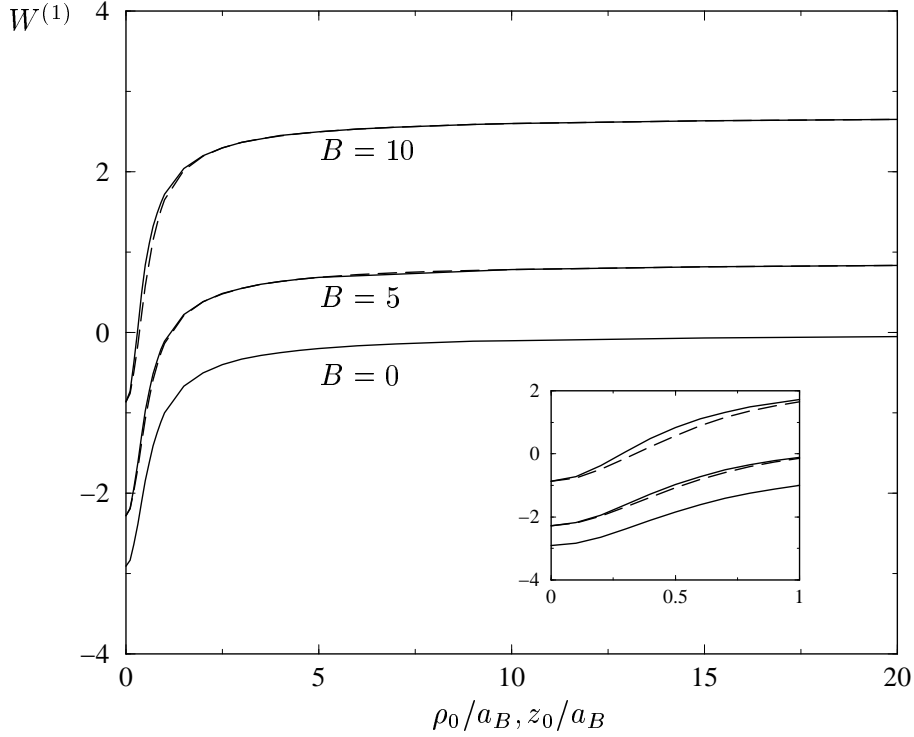


FIGURE 9.1: Effective classical potential (in units of $2Ry$) as a function of the coordinate $\rho_0 = \sqrt{x_0^2 + y_0^2}$ perpendicular to the field lines at $z_0 = 0$ (solid curves), and parallel to the magnetic field as a function of z_0 at $\rho_0 = 0$ (dashed curves). The inverse temperature is fixed at $\beta = 1$, and the strengths of the magnetic field B are varied (all in natural units). The small figure enlarges the range $0 \leq \rho_0, z_0 \leq 1$ with noticeable anisotropy.

For $\rho_0 \rightarrow \infty$ or $z_0 \rightarrow \infty$, the expectation value of the Coulomb potential (9.81) tends to zero. The remaining effective classical potential

$$W_{\Omega}^{(1)}(\mathbf{x}_0) \longrightarrow -\frac{1}{\beta} \ln Z_{\Omega}^{\mathbf{p}_0, \mathbf{x}_0} - \Omega_B (\omega_B - \Omega_B) b_{\perp}^2 + (\omega_B^2 - \Omega_{\perp}^2) a_{\perp}^2 - \frac{1}{2} \Omega_{\parallel}^2 a_{\parallel}^2 \quad (9.82)$$

is a constant with regard to the position \mathbf{x}_0 , and the optimization yields $\Omega_B^{(1)} = \Omega_{\perp}^{(1)} = \omega_B$ and $\Omega_{\parallel}^{(1)} = 0$, leading to the asymptotic constant value

$$W^{(1)}(\mathbf{x}_0) \longrightarrow -\frac{1}{\beta} \ln \frac{\beta \omega_B}{\sinh \beta \omega_B}. \quad (9.83)$$

The $B = 0$ -curves are of course identical with those obtained from variational perturbation theory for the hydrogen atom [53,55].

9.4.2 Ground-State Energy of the Hydrogen Atom in Uniform Magnetic Field

In what follows we investigate the zero-temperature behavior of the theory. Figures 9.1 and 9.2 show that the minimum of each potential curve lies at the origin. This means that the first-order approximation to the ground-state energy for a fixed magnitude of the magnetic field B is found by considering the zero-temperature limit of the first-order effective classical potential in the origin

$$E^{(1)} = \lim_{\beta \rightarrow \infty} W^{(1)}(\mathbf{0}). \quad (9.84)$$

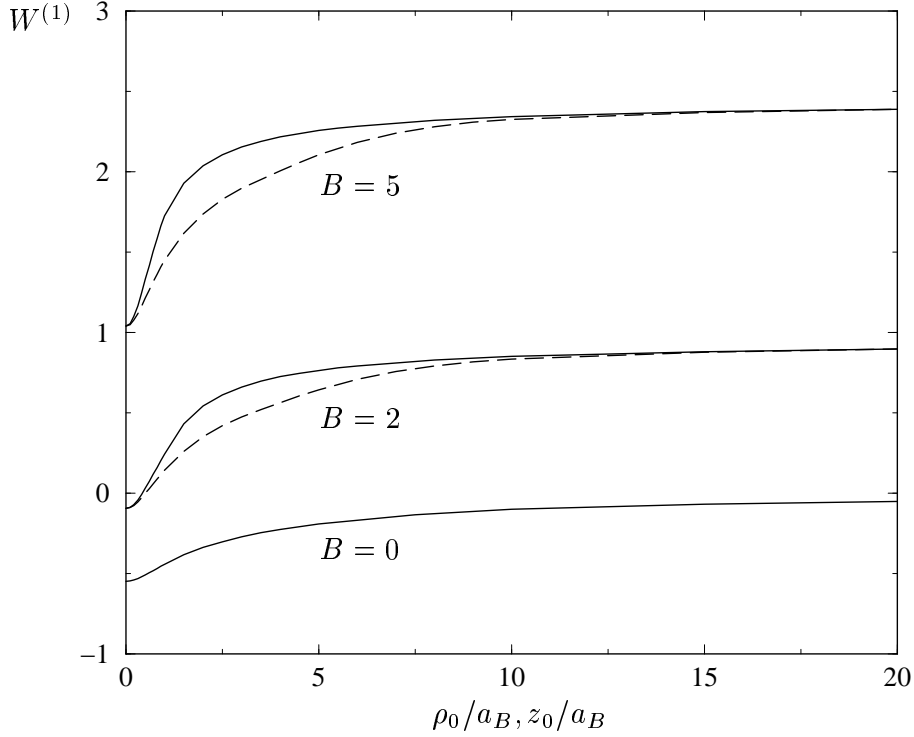


FIGURE 9.2: Analogous plot to Fig. 9.1, but at the larger inverse temperature $\beta = 100$.

Thus we obtain from Eq. (9.68) the variational expression for the ground-state energy:

$$E_{\mathbf{\Omega}}^{(1)}(B) = \frac{1}{2\Omega_{\perp}} (\Omega_{\perp}^2 + \omega_B^2) + \frac{\Omega_{\parallel}}{4} - \left\langle \frac{1}{|\mathbf{x}|} \right\rangle_{\mathbf{\Omega}}^0, \quad (9.85)$$

where the expectation value for the Coulomb potential (9.81) can now be calculated exactly since the exponential in the integral simplifies to unity:

$$\left\langle \frac{1}{|\mathbf{x}|} \right\rangle_{\mathbf{\Omega}}^0 = \sqrt{\frac{\Omega_{\parallel}}{\pi}} \frac{1}{\sqrt{1 - \Omega_{\parallel}/\Omega_{\perp}}} \ln \frac{1 - \sqrt{1 - \Omega_{\parallel}/\Omega_{\perp}}}{1 + \sqrt{1 - \Omega_{\parallel}/\Omega_{\perp}}}. \quad (9.86)$$

The equations (9.85) and (9.86) are independent of the frequency parameter Ω_B such that the optimization of the first-order expression for the ground-state energy (9.85) requires the satisfying of the equations

$$\frac{\partial E_{\mathbf{\Omega}}^{(1)}(B)}{\partial \Omega_{\perp}} \stackrel{!}{=} 0, \quad \frac{\partial E_{\mathbf{\Omega}}^{(1)}(B)}{\partial \Omega_{\parallel}} \stackrel{!}{=} 0. \quad (9.87)$$

Reinserting the resulting values $\Omega_{\perp}^{(1)}$ and $\Omega_{\parallel}^{(1)}$ into Eq. (9.85) yields the first-order approximation for the ground-state energy $E^{(1)}(B)$. In the absence of the Coulomb interaction the optimization with respect to Ω_{\perp} yields $\Omega_{\perp}^{(1)} = \omega_B$, rendering the ground-state energy $E^{(1)}(B) = \omega_B$, which is the zeroth Landau level. An optimal value for Ω_{\parallel} does not exist since the dependence of the ground-state energy of this parameter is linear in Eq. (9.85) in this special case. To obtain the lowest energy, this parameter can be set to zero (all optimal frequency parameters used in the optimization procedure turn out to be nonnegative). For a vanishing magnetic field, $B = 0$, Eq. (9.85) exactly reproduces the first-order variational result for the ground-state energy of the hydrogen atom, $E^{(1)}(B = 0) \approx -0.42$ [2 Ry], obtained in Ref. [8].

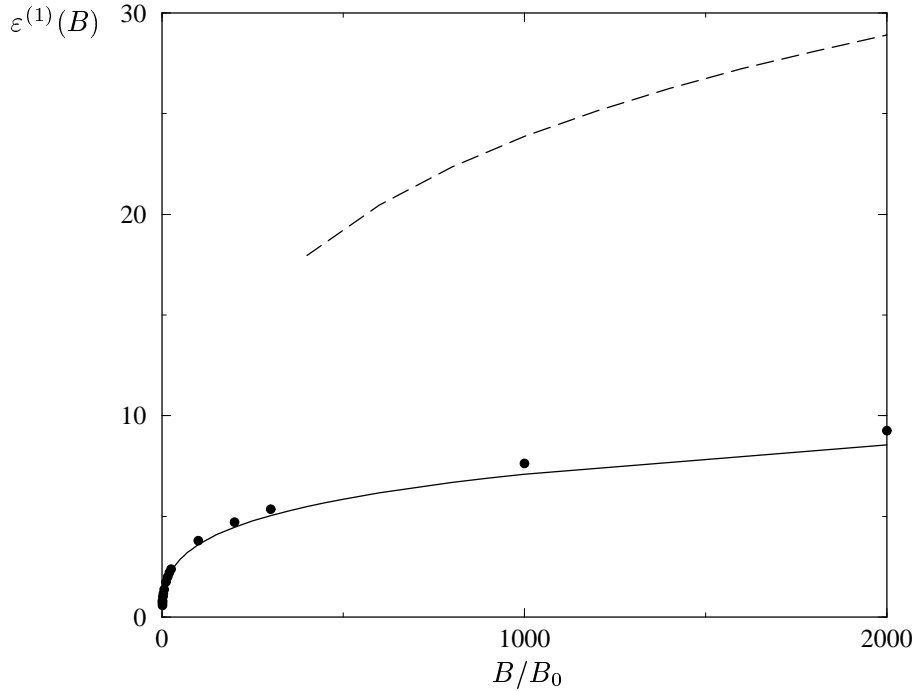


FIGURE 9.3: First-order variational result for the binding energy (in units of 2 Ry) as a function of the strength of the magnetic field. The dots indicate the values of Ref. [64]. The dashed curve shows the simple estimate of Landau-Lifschitz [69] $0.5 \ln^2 B$, which is closely related to the ground-state energy of the one-dimensional hydrogen atom [70,71].

To investigate the asymptotics in the strong-field limit $B \rightarrow \infty$, it is useful to extract the leading term ω_B . Thus we define the binding energy

$$\varepsilon(B) \equiv \omega_B - E(B) \quad (9.88)$$

which possesses a characteristic strong-field behavior to be discussed in detail subsequently. The result is shown in Fig. 9.3 as a function of the magnitude of the magnetic field B , where it is compared with the high-accuracy results of Ref. [64]. As a first-order approximation, this result is satisfactory. It is of the same quality like other first-order results, for example those from the operator optimization method in first order of Ref. [68]. The advantage of variational perturbation theory is that it yields good results over the complete range of the coupling strength, here the magnetic field. Moreover, as a consequence of the exponential convergence [4, Chap. 5], higher orders of variational perturbation theory push the approximative result of any quantity very rapidly towards the exact value.

The Weak-Field Case

We investigate now the weak-field behavior of our theory starting from the expression (9.88) and the expectation value of the Coulomb potential (9.86) in natural units:

$$\varepsilon_{\eta,\Omega}^{(1)}(B) = \frac{B}{2} - \frac{\Omega}{2} \left(1 + \frac{\eta}{2}\right) - \frac{B^2}{8\Omega} - \sqrt{\frac{\eta\Omega}{\pi}} h(\eta) \quad (9.89)$$

with

$$h(\eta) = \frac{1}{\sqrt{1-\eta}} \ln \frac{1 - \sqrt{1-\eta}}{1 + \sqrt{1-\eta}}. \quad (9.90)$$

TABLE 9.1: Perturbation coefficients up to order B^6 for the weak-field expansions of the variational parameters and the binding energy in comparison to the exact ones of Ref. [65].

n	0	1	2	3
η_n	1.0	$-\frac{405\pi^2}{7168} \approx -0.5576$	$\frac{16828965\pi^4}{1258815488} \approx 1.3023$	$-\frac{3886999332075\pi^6}{884272562962432} \approx -4.2260$
Ω_n	$\frac{16}{9\pi} \approx 0.5659$	$\frac{99\pi}{448} \approx 0.6942$	$-\frac{1293975\pi^3}{39337984} \approx -1.0199$	$\frac{524431667187\pi^5}{55267035185152} \approx 2.9038$
ε_n	$-\frac{4}{3\pi} \approx -0.4244$	$\frac{9\pi}{128} \approx 0.2209$	$-\frac{8019\pi^3}{1835008} \approx -0.1355$	$\frac{256449807\pi^5}{322256764928} \approx 0.2435$
ε_n [65]	-0.5	0.25	$-\frac{53}{192} \approx -0.2760$	$\frac{5581}{4608} \approx 1.2112$

In comparison with Eq. (9.85) we introduced new variational parameters

$$\eta \equiv \frac{\Omega_{\parallel}}{\Omega_{\perp}}, \quad \Omega \equiv \Omega_{\perp} \quad (9.91)$$

and utilized, as the calculations for the binding energy showed, that always $\eta \leq 1$. Performing the derivatives with respect to these variational parameters and setting them zero yields conditional equations which can be written after some manipulations as

$$\frac{\Omega}{4} + \sqrt{\frac{\Omega}{\pi\eta}} \frac{1}{1-\eta} \left(1 + \frac{1}{2} \frac{1}{\sqrt{1-\eta}} \ln \frac{1-\sqrt{1-\eta}}{1+\sqrt{1-\eta}} \right) \stackrel{!}{=} 0, \quad (9.92)$$

$$\frac{1}{2} + \frac{\eta}{4} - \frac{B^2}{8\Omega^2} + \frac{1}{2} \sqrt{\frac{\eta}{\pi\Omega}} \frac{1}{\sqrt{1-\eta}} \ln \frac{1-\sqrt{1-\eta}}{1+\sqrt{1-\eta}} \stackrel{!}{=} 0. \quad (9.93)$$

Expanding the variational parameters into perturbation series of the square magnetic field B^2 ,

$$\eta(B) = \sum_{n=0}^{\infty} \eta_n B^{2n}, \quad \Omega(B) = \sum_{n=0}^{\infty} \Omega_n B^{2n} \quad (9.94)$$

and inserting these expansions into the self-consistency conditions (9.92) and (9.93) we obtain order by order the coefficients given in Table 9.1. Inserting these values into the expression for the binding energy (9.89) and expand with respect to B^2 , we obtain the perturbation series

$$\varepsilon^{(1)}(B) = \frac{B}{2} - \sum_{n=0}^{\infty} \varepsilon_n B^{2n}. \quad (9.95)$$

The first coefficients are also given in Table 9.1. We find thus the important result that the first-order variational perturbation solution possesses a perturbative behavior with respect to the square magnetic field strength B^2 in the weak-field limit thus yielding the correct asymptotics. The coefficients differ in higher order from the exact ones but are improved in higher orders of the variational perturbation theory [4, Chap. 5].

Asymptotical Behavior in the Strong-Field Regime

In the discussion of the pure magnetic field below Eq. (9.87) we have mentioned that the variational calculation for the ground-state energy which is thus associated with the zeroth Landau level yields a frequency $\Omega_{\perp} \propto B$ while $\Omega_{\parallel} = 0$. Therefore we use the assumption

$$\Omega_{\perp} \gg \Omega_{\parallel}, \quad \Omega_{\parallel} \ll B \quad (9.96)$$

for the consideration of the ground-state energy (9.85) of the hydrogen atom in a strong magnetic field. In a first step we expand the last expression of the expectation value (9.86) which corresponds to the condition (9.96) in terms of $\Omega_{\parallel}/\Omega_{\perp}$ and reinsert this expansion in the equation of the ground-state energy (9.85). Then we omit all terms proportional to C/Ω_{\perp} where C stands for any expression with a value much smaller than the field strength B . In natural units, we thus obtain the strong-field approximation for the first-order binding energy (9.88)

$$\varepsilon_{\Omega_{\perp}, \Omega_{\parallel}}^{(1)} = \frac{B}{2} - \left(\frac{\Omega_{\perp}}{2} + \frac{B^2}{8\Omega_{\perp}} + \frac{\Omega_{\parallel}}{4} + \sqrt{\frac{\Omega_{\parallel}}{\pi}} \ln \frac{\Omega_{\parallel}}{4\Omega_{\perp}} \right). \quad (9.97)$$

As usual, we consider the zeros of the derivatives with respect to the variational parameters

$$\frac{\partial \varepsilon_{\Omega_{\perp}, \Omega_{\parallel}}^{(1)}}{\partial \Omega_{\parallel}} \stackrel{!}{=} 0, \quad \frac{\partial \varepsilon_{\Omega_{\perp}, \Omega_{\parallel}}^{(1)}}{\partial \Omega_{\perp}} \stackrel{!}{=} 0, \quad (9.98)$$

which lead to the self-consistence equations

$$\sqrt{\Omega_{\parallel}} = -\frac{2}{\sqrt{\pi}} (\ln \Omega_{\parallel} - \ln \Omega_{\perp} + 2 - \ln 4), \quad (9.99)$$

$$\Omega_{\perp} = \sqrt{\frac{\Omega_{\parallel}}{\pi}} + \frac{B}{2} \sqrt{1 + 4\frac{\Omega_{\parallel}}{\pi B^2}}. \quad (9.100)$$

Let us first consider the last equation. Utilizing the second of the conditions (9.96) we expand the second root around unity yielding the expression

$$\Omega_{\perp} = \frac{B}{2} + \sqrt{\frac{\Omega_{\parallel}}{\pi}} + \frac{\Omega_{\parallel}}{\pi B} - 2\frac{\Omega_{\parallel}^2}{\pi^2 B^3} + \dots, \quad (9.101)$$

where the terms are sorted with regard to their contribution starting with the biggest. Since we are interested in the strong B limit, we can obviously neglect terms suppressed by powers of $1/B$. Thus we only consider the following terms for the moment:

$$\Omega_{\perp} \approx \frac{B}{2} + \sqrt{\frac{\Omega_{\parallel}}{\pi}}. \quad (9.102)$$

Inserting this into the other condition (9.99), expanding the corresponding logarithm, and, once more, neglecting terms of order $1/B$, we find

$$\sqrt{\Omega_{\parallel}} \approx \frac{2}{\sqrt{\pi}} (\ln B - \ln \Omega_{\parallel} + \ln 2 - 2). \quad (9.103)$$

To obtain a tractable approximation for Ω_{\parallel} , we perform some iterations starting from

$$\sqrt{\Omega_{\parallel}^{(1)}} = \frac{2}{\sqrt{\pi}} \ln 2Be^{-2}. \quad (9.104)$$

Reinserting this on the right-hand side of Eq. (9.103), one obtains the second iteration $\sqrt{\Omega_{\parallel}^{(2)}}$. We stop this procedure after an additional reinsertion which yields

$$\sqrt{\Omega_{\parallel}^{(3)}} = \frac{2}{\sqrt{\pi}} \left(\ln 2Be^{-2} - 2 \ln \left[\frac{2}{\sqrt{\pi}} \left\{ \ln 2Be^{-2} - 2 \ln \left(\frac{2}{\sqrt{\pi}} \ln 2Be^{-2} \right) \right\} \right] \right). \quad (9.105)$$

The reader may convince himself that this iteration procedure indeed converges. For a subsequent systematical extraction of terms essentially contributing to the binding energy, the expression (9.105) is not satisfactory. Therefore it is better to separate the leading term in the curly brackets and expand the logarithm of the remainder. Then this proceeding is applied to the expression in the angular brackets and so on. Neglecting terms of order $\ln^{-3}B$, we obtain

$$\sqrt{\Omega_{\parallel}^{(3)}} \approx \frac{2}{\sqrt{\pi}} \left(\ln 2Be^{-2} + \ln \frac{\pi}{4} - 2 \ln \ln 2Be^{-2} \right). \quad (9.106)$$

The double-logarithmic term can be expanded in a similar way as described above:

$$\ln \ln 2Be^{-2} = \ln \left[\ln B \left(1 + \frac{\ln 2 - 2}{\ln B} \right) \right] = \ln \ln B + \frac{\ln 2 - 2}{\ln B} - \frac{1}{2} \frac{(\ln 2 - 2)^2}{\ln^2 B} + \mathcal{O}(\ln^{-3}B). \quad (9.107)$$

Thus the expression (9.106) may be rewritten as

$$\sqrt{\Omega_{\parallel}^{(3)}} = \frac{2}{\sqrt{\pi}} \left(\ln B - 2 \ln \ln B + \frac{2a}{\ln B} + \frac{a^2}{\ln^2 B} + b \right) + \mathcal{O}(\ln^{-3}B) \quad (9.108)$$

with abbreviations

$$a = 2 - \ln 2 \approx 1.307, \quad b = \ln \frac{\pi}{2} - 2 \approx -1.548. \quad (9.109)$$

The first observation is that the variational parameter Ω_{\parallel} is always much smaller than Ω_{\perp} in the high B -field limit. Thus we can further simplify the approximation (9.102) by replacing

$$\Omega_{\perp} \approx \frac{B}{2} \left(1 + \frac{2}{B} \sqrt{\frac{\Omega_{\parallel}}{\pi}} \right) \rightarrow \frac{B}{2} \quad (9.110)$$

without affecting the following expression for the binding energy. Inserting the solutions (9.108) and (9.110) into the equation for the binding energy (9.97) and expanding the logarithmic term once more as described, we find up to the order $\ln^{-2}B$:

$$\begin{aligned} \varepsilon^{(1)}(B) = & \frac{1}{\pi} \left(\ln^2 B - 4 \ln B \ln \ln B + 4 \ln^2 \ln B - 4b \ln \ln B + 2(b+2) \ln B + b^2 \right. \\ & \left. - \frac{1}{\ln B} [8 \ln^2 \ln B - 8b \ln \ln B + 2b^2] \right) + \mathcal{O}(\ln^{-2}B). \end{aligned} \quad (9.111)$$

Note that the prefactor $1/\pi$ of the leading $\ln^2 B$ -term differs from a value $1/2$ obtained by Landau and Lifschitz [69]. Our different value is a consequence of using a harmonic trial system. The calculation of higher orders in variational perturbation theory would improve the value of the prefactor.

At a magnetic field strength $B = 10^5 B_0$, which corresponds to 2.35×10^{10} T, the contribution from the first six terms is 22.87 [2 Ry]. The next three terms suppressed by a factor $\ln^{-1}B$ contribute -2.29 [2 Ry], while an estimate for the $\ln^{-2}B$ -terms yields nearly -0.3 [2 Ry]. Thus we find

$$\varepsilon^{(1)}(10^5) = 20.58 \pm 0.3 [2 \text{ Ry}]. \quad (9.112)$$

This is in very good agreement with the value 20.60 [2 Ry] obtained from the full treatment described in Section 9.4.2.

Table 9.2 lists the values of the first six terms of Eq. (9.111). This shows in particular the significance of the second-leading term $-(4/\pi) \ln B \ln \ln B$, which is of the same order of the leading term $(1/\pi) \ln^2 B$ but with an opposite sign. In Fig. 9.3, we have plotted the expression

$$\varepsilon_L(B) = \frac{1}{2} \ln^2 B \quad (9.113)$$

from Landau and Lifschitz [69] to illustrate that it gives far too large binding energies even at very large magnetic fields, e.g. at $2000B_0 \propto 10^8$ T.

TABLE 9.2: Example for the competing leading six terms in Eq. (9.111) at $B = 10^5 B_0 \approx 2.35 \times 10^{10}$ T.

$(1/\pi)\ln^2 B$	$-(4/\pi)\ln B \ln \ln B$	$(4/\pi)\ln^2 \ln B$	$-(4b/\pi)\ln \ln B$	$[2(b+2)/\pi]\ln B$	b^2/π
42.1912	-35.8181	7.6019	4.8173	3.3098	0.7632

This strength of magnetic field appears on surfaces of neutron stars ($10^6 - 10^8$ T). A recently discovered new type of neutron star is the so-called magnetar [83]. In these, charged particles such as protons and electrons, produced by decaying neutrons, give rise to the giant magnetic field of 10^{11} T. Magnetic fields of white dwarfs reach only up to $10^2 - 10^4$ T. All these magnetic field strengths are far from a direct realization in experiments. The strongest magnetic fields ever produced in a laboratory were only of the order 10 T, an order of magnitude larger than the fields in sun spots which reach about 0.4 T. Recall, for comparison, that the earth's magnetic field has the small value of 0.6×10^{-4} T.

It should, however, be noted that there are systems in solid state physics, where a rescaling of variables corresponds to extremely strong magnetic fields. In a donor impured semiconductor like GaAs, the properties of the system of an electron bound to the positively charged donor nucleus in an external magnetic field of strength 6.57 T are comparable to a hydrogen atom in a field of strength 2.35×10^5 T [84]. The reason for this is the strongly reduced effective mass of the electron bound to the donor nucleus, the large dielectric constant of the semiconductor, and thus a much larger radius of the orbit of the electron. Hence the Coulomb interaction between the donor nucleus and the electron is much weaker than in the hydrogen atom. This approximate analogy between both systems can thus be used to investigate the effects of extremely strong magnetic fields in earthbound experiments.

As we see in Fig. 9.3, the non-leading terms in Eq. (9.111) give important contributions to the asymptotic behavior even at such large magnetic fields. It is an unusual property of the asymptotic behavior that the absolute value of the difference between the Landau-expression (9.113) and our approximation (9.111) diverges with increasing magnetic field strengths B , only the relative difference decreases.

9A Generating Functional for Particle in Magnetic Field and Harmonic Oscillator Potential

For the determination of the correlation functions of a system, we need to know the solution of the two-dimensional generating functional in the presence of an external source $\mathbf{j} = (j_x, j_y)$:

$$Z^{\mathbf{x}_0}[\mathbf{j}] = \lambda_{\text{th}}^2 \oint \mathcal{D}^2 x \delta(\mathbf{x}_0 - \overline{\mathbf{x}(\tau)}) e^{-A^{\mathbf{x}_0}[\mathbf{x};\mathbf{j}]/\hbar}. \quad (9A.1)$$

The action of a particle in a magnetic field in z -direction and a harmonic oscillator reads

$$\begin{aligned} A^{\mathbf{x}_0}[\mathbf{x};\mathbf{j}] = \int_0^{\hbar\beta} d\tau \left[\frac{M}{2} \dot{\mathbf{x}}^2(\tau) - iM\Omega_B([\mathbf{x}(\tau) - \mathbf{x}_0] \times \dot{\mathbf{x}}(\tau))_z + \frac{1}{2}M(\Omega_{\perp}^2 - \Omega_B^2)[\mathbf{x}(\tau) - \mathbf{x}_0]^2 \right. \\ \left. + \mathbf{j}(\tau) \cdot (\mathbf{x}(\tau) - \mathbf{x}_0) \right], \end{aligned} \quad (9A.2)$$

where $\Omega_{\perp} > \Omega_B$, for stability. The position dependent terms are centered around $\mathbf{x}_0 = (x_0, y_0)$, which is the temporal average of the path $\mathbf{x}(\tau)$, and thus equal to the zero frequency component of the Fourier path

$$\mathbf{x}(\tau) = \mathbf{x}_0 + \sum_{m=1}^{\infty} (\mathbf{x}_m e^{i\omega_m \tau} + \mathbf{x}_m^* e^{-i\omega_m \tau}) \quad (9A.3)$$

with the Matsubara frequencies $\omega_m = 2\pi m/\hbar\beta$ and complex Fourier coefficients $\mathbf{x}_m = \mathbf{x}_m^{\text{re}} + i\mathbf{x}_m^{\text{im}}$. Introducing a similar Fourier decomposition for the current $\mathbf{j}(\tau)$ with Fourier components \mathbf{j}_m and

using the orthonormality relation

$$\frac{1}{\hbar\beta} \int_0^{\hbar\beta} d\tau e^{i(\omega_m - \omega_n)\tau} = \delta_{m n}, \quad (9A.4)$$

the generating functional can be written as

$$Z^{\mathbf{x}_0}[\mathbf{j}] = \prod_{m=1}^{\infty} \left[\int \frac{dx_m^{\text{re}} dx_m^{\text{im}} dy_m^{\text{re}} dy_m^{\text{im}}}{(\pi/M\beta\omega_m^2)^2} e^{-\mathcal{A}_m(\mathbf{x}_m, \mathbf{x}_m^*; \mathbf{j}_m, \mathbf{j}_m^*)/\hbar} \right] \quad (9A.5)$$

with

$$\begin{aligned} \mathcal{A}_m(\mathbf{x}_m, \mathbf{x}_m^*; \mathbf{j}_m, \mathbf{j}_m^*) &= \hbar\beta M (\omega_m^2 + \Omega_{\perp}^2 - \Omega_B^2) ([x_m^{\text{re}}]^2 + [x_m^{\text{im}}]^2 + [y_m^{\text{re}}]^2 + [y_m^{\text{im}}]^2) \\ &+ 4i\hbar\beta M \Omega_B \omega_m (x_m^{\text{re}} y_m^{\text{im}} - x_m^{\text{im}} y_m^{\text{re}}) + 2\hbar\beta (x_m^{\text{re}} j_{x_m}^{\text{re}} + x_m^{\text{im}} j_{x_m}^{\text{im}} + y_m^{\text{re}} j_{y_m}^{\text{re}} + y_m^{\text{im}} j_{y_m}^{\text{im}}). \end{aligned} \quad (9A.6)$$

Expression (9A.5) is equivalent to the path integral (9A.1) and after performing the integrations and re-transforming the currents

$$\mathbf{j}_m = \frac{1}{\hbar\beta} \int_0^{\hbar\beta} d\tau \mathbf{j}(\tau) e^{-i\omega_m \tau} \quad (9A.7)$$

we obtain the resulting generating functional

$$Z^{\mathbf{x}_0}[\mathbf{j}] = Z^{\mathbf{x}_0} \exp \left\{ \frac{1}{2\hbar^2} \int_0^{\hbar\beta} d\tau \int_0^{\hbar\beta} d\tau' \mathbf{j}(\tau) \mathbf{G}^{\mathbf{x}_0}(\tau, \tau') \mathbf{j}(\tau') \right\} \quad (9A.8)$$

with the partition function

$$Z^{\mathbf{x}_0} \equiv Z^{\mathbf{x}_0}[0] = \prod_{m=1}^{\infty} \frac{\omega_m^4}{4\Omega_B^2 \omega_m^2 + (\omega_m^2 + \Omega_{\perp}^2)^2} \quad (9A.9)$$

and the 2×2 -matrix of Green functions

$$\mathbf{G}^{\mathbf{x}_0}(\tau, \tau') = \begin{pmatrix} G_{xx}^{\mathbf{x}_0}(\tau, \tau') & G_{xy}^{\mathbf{x}_0}(\tau, \tau') \\ G_{yx}^{\mathbf{x}_0}(\tau, \tau') & G_{yy}^{\mathbf{x}_0}(\tau, \tau') \end{pmatrix}. \quad (9A.10)$$

The elements of this matrix are position-position correlation functions. This can easily be proved by applying two functional derivatives with respect to the desired component of the current to the functional (9A.1), for example

$$G_{xx}^{\mathbf{x}_0}(\tau, \tau') = \langle (x(\tau) - x_0)(x(\tau') - x_0) \rangle^{\mathbf{x}_0} = \left[\hbar^2 \frac{1}{Z^{\mathbf{x}_0}[\mathbf{j}]} \frac{\delta^2}{\delta j_x(\tau) \delta j_x(\tau')} Z^{\mathbf{x}_0}[\mathbf{j}] \right]_{\mathbf{j}=0}, \quad (9A.11)$$

where we have defined expectation values by

$$\langle \dots \rangle^{\mathbf{x}_0} = \frac{\lambda_{\text{th}}^2}{Z^{\mathbf{x}_0}} \oint \mathcal{D}^2 x \dots \delta(\mathbf{x}_0 - \overline{\mathbf{x}(\tau)}) e^{-\mathcal{A}^{\mathbf{x}_0}[\mathbf{x}; 0]/\hbar}. \quad (9A.12)$$

From the above calculation we find the following expressions for the Green functions in Fourier space ($0 \leq \tau, \tau' \leq \hbar\beta$):

$$\begin{aligned} G_{xx}^{\mathbf{x}_0}(\tau, \tau') &= \langle \tilde{x}(\tau) \tilde{x}(\tau') \rangle^{\mathbf{x}_0} = G_{yy}^{\mathbf{x}_0}(\tau, \tau') = \langle \tilde{y}(\tau) \tilde{y}(\tau') \rangle^{\mathbf{x}_0} \\ &= \frac{2}{M\beta} \sum_{m=1}^{\infty} \frac{\omega_m^2 + \Omega_{\perp}^2 - \Omega_B^2}{4\Omega_B^2 \omega_m^2 + (\omega_m^2 + \Omega_{\perp}^2 - \Omega_B^2)^2} e^{-i\omega_m(\tau - \tau')}, \end{aligned} \quad (9A.13)$$

$$\begin{aligned} G_{xy}^{\mathbf{x}_0}(\tau, \tau') &= \langle \tilde{x}(\tau) \tilde{y}(\tau') \rangle^{\mathbf{x}_0} = -G_{yx}^{\mathbf{x}_0}(\tau, \tau') = -\langle \tilde{y}(\tau) \tilde{x}(\tau') \rangle^{\mathbf{x}_0} \\ &= \frac{4\Omega_B}{M\beta} \sum_{m=1}^{\infty} \frac{\omega_m}{4\Omega_B^2 \omega_m^2 + (\omega_m^2 + \Omega_{\perp}^2 - \Omega_B^2)^2} e^{-i\omega_m(\tau - \tau')}, \end{aligned} \quad (9A.14)$$

where, for simplicity, $\tilde{\mathbf{x}}(\tau) = \mathbf{x}(\tau) - \mathbf{x}_0$. It is desirable to find analytical expressions for the Green functions and the partition function (9A.9). All these quantities possess the same denominator which can be decomposed as

$$4\Omega_B^2\omega_m^2 + (\omega_m^2 + \Omega_\perp^2 - \Omega_B^2)^2 = (\omega_m^2 + \Omega_+^2)(\omega_m^2 + \Omega_-^2) \quad (9A.15)$$

with frequencies

$$\Omega_\pm(\Omega_B, \Omega_\perp) = \Omega_\perp \pm \Omega_B. \quad (9A.16)$$

Therefore the partition function (9A.9) can be split into two products, each of which known from the harmonic oscillator [4, Chap. 5]:

$$Z^{\mathbf{x}_0} = \prod_{m=1}^{\infty} \left[\frac{\omega_m^2}{\omega_m^2 + \Omega_+^2} \right] \prod_{m=1}^{\infty} \left[\frac{\omega_m^2}{\omega_m^2 + \Omega_-^2} \right] = \frac{\hbar\beta\Omega_+/2}{\sinh \hbar\beta\Omega_+/2} \frac{\hbar\beta\Omega_-/2}{\sinh \hbar\beta\Omega_-/2}. \quad (9A.17)$$

Now we apply the property (9A.15) to decompose the Green functions (9A.13) into partial fractions, yielding

$$\begin{aligned} G_{xx}^{\mathbf{x}_0}(\tau, \tau') &= G_{yy}^{\mathbf{x}_0}(\tau, \tau') \\ &= \frac{1}{M\beta} \left(\alpha_1 \sum_{m=-\infty}^{\infty} \frac{1}{\omega_m^2 + \Omega_+^2} e^{-i\omega_m(\tau-\tau')} + \alpha_2 \sum_{m=-\infty}^{\infty} \frac{1}{\omega_m^2 + \Omega_-^2} e^{-i\omega_m(\tau-\tau')} - \frac{1}{\Omega_+\Omega_-} \right) \end{aligned} \quad (9A.18)$$

with coefficients

$$\alpha_1 = \frac{\Omega_+^2 - \Omega_\perp^2 + \Omega_B^2}{\Omega_+^2 - \Omega_-^2} = \frac{\Omega_\perp + \Omega_B}{2\Omega_\perp}, \quad \alpha_2 = -\frac{\Omega_-^2 - \Omega_\perp^2 + \Omega_B^2}{\Omega_+^2 - \Omega_-^2} = \frac{\Omega_\perp - \Omega_B}{2\Omega_\perp}. \quad (9A.19)$$

Following Ref. [4, Chap. 3], sums of the kind occurring in expression (9A.18) are spectral decompositions of the correlation function for the harmonic oscillator and can be summed up:

$$\sum_{m=-\infty}^{\infty} \frac{1}{\omega_m^2 + \Omega_\pm^2} e^{-i\omega_m(\tau-\tau')} = \frac{\hbar\beta}{2\Omega_\pm} g_\pm(\tau, \tau'). \quad (9A.20)$$

Here we introduced the expression

$$g_\varepsilon(\tau, \tau') = \frac{\cosh \Omega_\varepsilon(|\tau - \tau'| - \hbar\beta/2)}{\sinh \hbar\beta\Omega_\varepsilon/2}, \quad \tau, \tau' \in (0, \hbar\beta), \quad (9A.21)$$

with $\varepsilon \in \{+, -, \perp, \parallel\}$. Thus, the xx - and yy -correlation functions can be expressed by

$$G_{xx}^{\mathbf{x}_0}(\tau, \tau') = G_{yy}^{\mathbf{x}_0}(\tau, \tau') = \frac{1}{M\beta} \left(\frac{\hbar\beta}{4\Omega_\perp} g_+(\tau, \tau') + \frac{\hbar\beta}{4\Omega_\perp} g_-(\tau, \tau') - \frac{1}{\Omega_+\Omega_-} \right), \quad (9A.22)$$

where, from Eq. (9A.16), $\Omega_\pm = \Omega_\pm(\Omega_B, \Omega_\perp)$ are functions of the original frequencies Ω_B from the magnetic field and Ω_\perp from the additional harmonic oscillator (9A.2). It is obvious that expression (9A.22) reduces to the Green function of the harmonic oscillator for $\Omega_B \rightarrow 0$:

$$\lim_{\Omega_B \rightarrow 0} G_{ii}^{\mathbf{x}_0}(\tau, \tau') = \frac{1}{M\beta\Omega_\perp^2} \left(\frac{\hbar\beta\Omega_\perp}{2} g_\perp(\tau, \tau') - 1 \right) \quad (9A.23)$$

with $i \in \{x, y\}$. In this limit, the partition function (9A.17) turns out to be the usual one [4, Chap. 5] for such a harmonic oscillator

$$\lim_{\Omega_B \rightarrow 0} Z^{\mathbf{x}_0} = \frac{\hbar\beta\Omega_\perp/2}{\sinh \hbar\beta\Omega_\perp/2}. \quad (9A.24)$$

It is worth mentioning that with the last term in Green function (9A.22) the classical harmonic fluctuation width

$$G_{xx}^{\text{cl}} = \langle x^2 \rangle^{\text{cl}} = \frac{1}{M\beta(\Omega_\perp^2 - \Omega_B^2)} \quad (9A.25)$$

is subtracted. This is the consequence of the exclusion of the zero frequency mode of the Fourier path (9A.3) in the generating functional (9A.1). The necessity to do this has already been discussed in Section 9.2. The other terms in Eq. (9A.22) are those which we would have obtained *without* separating the x_0 -component. Thus these terms represent the quantum mechanical Green function containing all quantum as well as thermal fluctuations. It is a nice property of all Green functions discussed in this chapter that

$$G_{xx}^{\mathbf{x}_0}(\tau, \tau') = G_{xx}^{\text{qm}}(\tau, \tau') - G_{xx}^{\text{cl}}. \quad (9A.26)$$

Such a relation exists for all other Green functions appropriately, including momentum-position correlations which we consider subsequently.

The knowledge of relation (9A.20) makes it quite easy to determine the algebraic expression for the mixed xy -correlation functions. Rewriting Eq. (9A.14) as

$$\begin{aligned} G_{xy}^{\mathbf{x}_0}(\tau, \tau') &= -G_{yx}^{\mathbf{x}_0}(\tau, \tau') \\ &= \frac{i}{2M\beta\Omega_{\perp}} \frac{\partial}{\partial \tau} \left(\sum_{m=-\infty}^{\infty} \frac{1}{\omega_m^2 + \Omega_+^2} e^{-i\omega_m(\tau-\tau')} + \sum_{m=-\infty}^{\infty} \frac{1}{\omega_m^2 + \Omega_-^2} e^{-i\omega_m(\tau-\tau')} \right) \end{aligned} \quad (9A.27)$$

and applying the derivative with respect to τ to relation (9A.20), we obtain the following expression for the mixed Green function:

$$\begin{aligned} G_{xy}^{\mathbf{x}_0}(\tau, \tau') &= -G_{yx}^{\mathbf{x}_0}(\tau, \tau') \\ &= \frac{\hbar}{4iM\Omega_{\perp}} \{ \Theta(\tau - \tau') [h_+(\tau, \tau') - h_-(\tau, \tau')] - \Theta(\tau' - \tau) [h_+(\tau', \tau) - h_-(\tau', \tau)] \}, \end{aligned} \quad (9A.28)$$

where we have used the abbreviation

$$h_{\varepsilon}(\tau, \tau') = \frac{\sinh \Omega_{\varepsilon}(\tau - \tau' - \hbar\beta/2)}{\sinh \hbar\beta\Omega_{\varepsilon}/2}, \quad \tau, \tau' \in (0, \hbar\beta), \quad (9A.29)$$

with $\varepsilon \in \{+, -, \perp, \parallel\}$. Note that classically $\langle xy \rangle^{\text{cl}} = 0$ such that Eq. (9A.26) reduces to

$$G_{xy}^{\mathbf{x}_0}(\tau, \tau') = G_{xy}^{\text{qm}}(\tau, \tau'). \quad (9A.30)$$

The Heaviside function in Eq. (9A.28) is defined symmetrically:

$$\Theta(\tau - \tau') = \begin{cases} 1 & \tau > \tau', \\ 1/2 & \tau = \tau', \\ 0 & \tau < \tau'. \end{cases} \quad (9A.31)$$

In the quantum mechanical limit of zero-temperature ($\beta \rightarrow \infty$), the Green function (9A.22) simplifies to

$$\lim_{\beta \rightarrow \infty} G_{xx}^{\mathbf{x}_0}(\tau, \tau') = \lim_{\beta \rightarrow \infty} G_{yy}^{\mathbf{x}_0}(\tau, \tau') = \frac{\hbar}{4M\Omega_{\perp}} \left(e^{-\Omega_+|\tau-\tau'|} + e^{-\Omega_-|\tau-\tau'|} \right), \quad (9A.32)$$

while in Eq. (9A.28) only $h_{\pm}(\tau, \tau')$ changes:

$$\lim_{\beta \rightarrow \infty} h_{\pm}(\tau, \tau') = -e^{-\Omega_{\pm}(\tau-\tau')}. \quad (9A.33)$$

9B Properties of Green Functions

In this section we list properties of the Green functions (9A.22) and (9A.28) which are important for the forthcoming consideration of the generating functional with sources coupling linearly to position or momentum in Appendix 9C. For all relations we suppose that $0 \leq \tau, \tau' \leq \hbar\beta$.

9B.1 General Properties

A first observation is the temporal translational invariance of the Green functions:

$$G_{ij}^{\mathbf{x}_0}(\tau, \tau') = G_{ij}^{\mathbf{x}_0}(\tau - \tau'), \quad (9B.1)$$

where each of the indices i, j stands for x or y , respectively. For equal times we find

$$G_{ij}^{\mathbf{x}_0}(\tau, \tau) = \frac{1}{M\beta} \left(\frac{\hbar\beta}{4\Omega_{\perp}} g_+(\tau, \tau) + \frac{\hbar\beta}{4\Omega_{\perp}} g_-(\tau, \tau) - \frac{1}{\Omega_+ \Omega_-} \right) \times \begin{cases} 1 & i = j, \\ 0 & i \neq j. \end{cases} \quad (9B.2)$$

Moreover we read off the following symmetries from the expressions (9A.22) and (9A.28):

$$G_{ij}^{\mathbf{x}_0}(\tau, \tau') = G_{ij}^{\mathbf{x}_0}(\tau', \tau) \times \begin{cases} 1 & i = j, \\ -1 & i \neq j. \end{cases} \quad (9B.3)$$

Otherwise,

$$G_{ij}^{\mathbf{x}_0}(\tau, \tau') = G_{ji}^{\mathbf{x}_0}(\tau', \tau). \quad (9B.4)$$

Throughout the chapter we always use periodic paths. Hence it is obvious that all Green functions are periodic, too:

$$G_{ij}^{\mathbf{x}_0}(0, \tau') = G_{ij}^{\mathbf{x}_0}(\hbar\beta, \tau'), \quad G_{ij}^{\mathbf{x}_0}(\tau, 0) = G_{ij}^{\mathbf{x}_0}(\tau, \hbar\beta). \quad (9B.5)$$

9B.2 Derivatives of Green Functions

We now proceed with derivatives of the Green functions (9A.22) and (9A.28), since these are essential for deriving the generating functional of position and momentum dependent correlations in the forthcoming Appendix 9C.

Before considering the concrete expressions we introduce a new symbol indicating uniquely to which argument the derivative is applied. A dot on the left-hand side means to perform the derivative with respect to the first argument and the dot on the right-hand side indicates that to differentiate with respect to the other argument. Having a dot on both sides the Green function is derived with respect to both arguments:

$$\bullet G_{ij}^{\mathbf{x}_0}(\tau, \tau') = \frac{\partial G_{ij}^{\mathbf{x}_0}(\tau, \tau')}{\partial \tau}, \quad G^{\bullet \mathbf{x}_0}_{ij}(\tau, \tau') = \frac{\partial G_{ij}^{\mathbf{x}_0}(\tau, \tau')}{\partial \tau'}, \quad \bullet G^{\bullet \mathbf{x}_0}_{ij}(\tau, \tau') = \frac{\partial^2 G_{ij}^{\mathbf{x}_0}(\tau, \tau')}{\partial \tau \partial \tau'}. \quad (9B.6)$$

Applying such derivatives to the Green functions (9A.22), we obtain ($i \in \{x, y\}$):

$$\bullet G_{ii}^{\mathbf{x}_0}(\tau, \tau') = \frac{\hbar}{4M\Omega_{\perp}} [\Theta(\tau - \tau') f_1(\tau, \tau') - \Theta(\tau' - \tau) f_1(\tau', \tau)] = -G^{\bullet \mathbf{x}_0}_{ii}(\tau, \tau') \quad (9B.7)$$

with

$$f_1(\tau, \tau') = (\Omega_{\perp} + \Omega_B) h_+(\tau, \tau') + (\Omega_{\perp} - \Omega_B) h_-(\tau, \tau'), \quad (9B.8)$$

where $h_{\pm}(\tau, \tau')$ was defined in Eq. (9A.29). Performing the derivatives to both arguments leads to the expression

$$\bullet G^{\bullet \mathbf{x}_0}_{ii}(\tau, \tau') = \tilde{G}^{\bullet \mathbf{x}_0}_{ii}(\tau, \tau') + \frac{\hbar}{M} \delta(\tau - \tau'), \quad (9B.9)$$

where we have introduced the partial function

$$\bullet \tilde{G}^{\bullet \mathbf{x}_0}_{ii}(\tau, \tau') = -\frac{\hbar}{4M\Omega_{\perp}} [\Omega_+^2 g_+(\tau, \tau') + \Omega_-^2 g_-(\tau, \tau')] \quad (9B.10)$$

which is finite for equal times.

Applying derivatives with respect to the first respective second argument to the mixed correlation function (9A.28), we find

$$\bullet G^{\mathbf{x}_0}_{xy}(\tau, \tau') = \frac{\hbar}{4iM\Omega_{\perp}} [\Omega_+ g_+(\tau, \tau') - \Omega_- g_-(\tau, \tau')] = -G^{\bullet \mathbf{x}_0}_{xy}(\tau, \tau') \quad (9B.11)$$

and

$$\bullet G_{yx}^{\mathbf{x}_0}(\tau, \tau') = -\bullet G_{xy}^{\mathbf{x}_0}(\tau, \tau'). \quad (9B.12)$$

Differentiating each argument of the mixed Green function results in

$$\bullet G_{xy}^{\bullet \mathbf{x}_0}(\tau, \tau') = \frac{i\hbar}{4M\Omega_{\perp}} [\Theta(\tau - \tau')f_2(\tau, \tau') - \Theta(\tau' - \tau)f_2(\tau', \tau)] = -\bullet G_{yx}^{\bullet \mathbf{x}_0}(\tau, \tau') \quad (9B.13)$$

with

$$f_2(\tau, \tau') = (\Omega_{\perp} + \Omega_B)^2 h_+(\tau, \tau') - (\Omega_{\perp} - \Omega_B)^2 h_-(\tau, \tau'). \quad (9B.14)$$

An additional property we read off from Eqs. (9B.7) and (9B.11) is $(i, j \in \{x, y\})$:

$$\bullet G_{ij}^{\mathbf{x}_0}(\tau, \tau') = \bullet G_{ij}^{\mathbf{x}_0}(\tau', \tau) \times \begin{cases} -1 & i = j, \\ 1 & i \neq j, \end{cases} \quad (9B.15)$$

$$G_{ij}^{\bullet \mathbf{x}_0}(\tau, \tau') = G_{ij}^{\bullet \mathbf{x}_0}(\tau', \tau) \times \begin{cases} -1 & i = j, \\ 1 & i \neq j. \end{cases} \quad (9B.16)$$

The double-sided derivatives (9B.9), (9B.10), and (9B.13) imply

$$\bullet G_{ij}^{\bullet \mathbf{x}_0}(\tau, \tau') = \bullet G_{ij}^{\bullet \mathbf{x}_0}(\tau', \tau) \times \begin{cases} 1 & i = j, \\ -1 & i \neq j. \end{cases} \quad (9B.17)$$

The derivatives (9B.7), (9B.10), (9B.11), and (9B.13) are periodic:

$$\bullet G_{ij}^{\mathbf{x}_0}(\tau, 0) = \bullet G_{ij}^{\mathbf{x}_0}(\tau, \hbar\beta), \quad \bullet G_{ij}^{\mathbf{x}_0}(0, \tau') = \bullet G_{ij}^{\mathbf{x}_0}(\hbar\beta, \tau'), \quad (9B.18)$$

$$G_{ij}^{\bullet \mathbf{x}_0}(\tau, 0) = G_{ij}^{\bullet \mathbf{x}_0}(\tau, \hbar\beta), \quad G_{ij}^{\bullet \mathbf{x}_0}(0, \tau') = G_{ij}^{\bullet \mathbf{x}_0}(\hbar\beta, \tau'), \quad (9B.19)$$

$$\bullet \tilde{G}_{ii}^{\mathbf{x}_0}(\tau, 0) = \bullet \tilde{G}_{ii}^{\mathbf{x}_0}(\tau, \hbar\beta), \quad \bullet \tilde{G}_{ii}^{\mathbf{x}_0}(0, \tau') = \bullet \tilde{G}_{ii}^{\mathbf{x}_0}(\hbar\beta, \tau'), \quad (9B.20)$$

$$\bullet G_{ij}^{\bullet \mathbf{x}_0}(\tau, 0) = \bullet G_{ij}^{\bullet \mathbf{x}_0}(\tau, \hbar\beta), \quad \bullet G_{ij}^{\bullet \mathbf{x}_0}(0, \tau') = \bullet G_{ij}^{\bullet \mathbf{x}_0}(\hbar\beta, \tau'), \quad (i \neq j). \quad (9B.21)$$

9C Generating Functional for Position- and Momentum-Dependent Correlation Functions

With the discussion of the generating functional for position-dependent correlation functions and, in particular, the Green functions in Appendix 9A and their properties in Appendix 9B, we have laid the foundation to derive the generating functional for correlation functions depending on both, position and momentum. Following the framework presented in Ref. [17], such a functional involving sources coupled to the momentum can always be reduced to one containing position-coupled sources only.

We start from the three-dimensional effective classical representation for the generating functional

$$Z_{\Omega}[\mathbf{j}, \mathbf{v}] = \int \frac{d^3 x_0 d^3 p_0}{(2\pi\hbar)^3} Z_{\Omega}^{\mathbf{p}_0, \mathbf{x}_0}[\mathbf{j}, \mathbf{v}] \quad (9C.1)$$

with zero-frequency components $\mathbf{x}_0 = (x_0, y_0, z_0) = \text{const.}$ and $\mathbf{p}_0 = (p_{x_0}, p_{y_0}, p_{z_0}) = \text{const.}$ of the Fourier path separated. The reduced functional is

$$Z_{\Omega}^{\mathbf{p}_0, \mathbf{x}_0}[\mathbf{j}, \mathbf{v}] = (2\pi\hbar)^3 \oint \mathcal{D}^3 x \mathcal{D}^3 p \delta(\mathbf{x}_0 - \overline{\mathbf{x}(\tau)}) \delta(\mathbf{p}_0 - \overline{\mathbf{p}(\tau)}) \exp \left\{ -\frac{1}{\hbar} \mathcal{A}_{\Omega}^{\mathbf{p}_0, \mathbf{x}_0}[\mathbf{p}, \mathbf{x}; \mathbf{j}, \mathbf{v}] \right\}, \quad (9C.2)$$

where the path integral measure is that defined in Eq. (9.4). Extending the action (9.3) by source terms, considering a more general Hamilton function than (9.17), and introducing an additional harmonic oscillator in z -direction, the action functional in Eq. (9C.2) shall read

$$\begin{aligned} \mathcal{A}_{\Omega}^{\mathbf{p}_0, \mathbf{x}_0}[\mathbf{p}, \mathbf{x}; \mathbf{j}, \mathbf{v}] = & \int_0^{\hbar\beta} d\tau \left\{ -i\tilde{\mathbf{p}}(\tau) \cdot \dot{\tilde{\mathbf{x}}}(\tau) + \frac{1}{2M} \tilde{\mathbf{p}}^2(\tau) - \Omega_B l_z(\tilde{\mathbf{p}}, \tilde{\mathbf{x}}) + \frac{1}{2} M \Omega_{\perp}^2 [\tilde{x}^2(\tau) + \tilde{y}^2(\tau)] \right. \\ & \left. + \frac{1}{2} M \Omega_{\parallel}^2 \tilde{z}^2(\tau) + \mathbf{j}(\tau) \cdot \tilde{\mathbf{x}}(\tau) + \mathbf{v}(\tau) \cdot \tilde{\mathbf{p}}(\tau) \right\} \end{aligned} \quad (9C.3)$$

with shifted positions and momenta

$$\tilde{\mathbf{x}} = \mathbf{x}(\tau) - \mathbf{x}_0, \quad \tilde{\mathbf{p}} = \mathbf{p}(\tau) - \mathbf{p}_0. \quad (9C.4)$$

The orbital angular momentum $l_z(\mathbf{p}, \mathbf{x})$ is defined in Eq. (9.19) and is used in Eq. (9C.3) with the shifted phase space coordinates (9C.4). We have introduced three different frequencies in (9C.3), $\Omega = (\Omega_B, \Omega_{\perp}, \Omega_{\parallel})$, where the first both components are used in regard to the oscillations in the plane perpendicular to the direction of the magnetic field which shall be considered here to point into z -direction. The last component, Ω_{\parallel} , is the frequency of a trial oscillator parallel to the field lines.

Due to the periodicity of the paths, we suppose that the sources are also periodic:

$$\mathbf{j}(0) = \mathbf{j}(\hbar\beta), \quad \mathbf{v}(0) = \mathbf{v}(\hbar\beta). \quad (9C.5)$$

Since we want to simplify expression (9C.2) such that we can use the results obtained in Appendix 9A, the momentum path integral is solved in the following. In a first step we re-express the momentum δ -function in (9C.2) by

$$\delta(\mathbf{p}_0 - \overline{\mathbf{p}(\tau)}) = \int \frac{d^3 \xi}{(2\pi\hbar)^3} \exp \left\{ -\frac{1}{\hbar} \int_0^{\hbar\beta} d\tau \mathbf{v}_0 \cdot [\mathbf{p}(\tau) - \mathbf{p}_0] \right\}, \quad (9C.6)$$

where

$$\mathbf{v}_0(\xi) = \frac{i}{\hbar\beta} \xi \quad (9C.7)$$

is an additional current which is coupled to the momentum and is constant in time. Defining the sum of all sources coupled to the momentum by

$$\mathbf{V}(\xi, \tau) = \mathbf{v}(\tau) + \mathbf{v}_0(\xi), \quad (9C.8)$$

the functional (9C.2) can be written as

$$Z_{\Omega}^{\mathbf{p}_0, \mathbf{x}_0}[\mathbf{j}, \mathbf{v}] = \int d^3\xi \oint \mathcal{D}^3x \mathcal{D}^3p \delta(\mathbf{x}_0 - \overline{\mathbf{x}(\tau)}) \exp \left\{ -\frac{1}{\hbar} \int_0^{\hbar\beta} d\tau \left[-i\mathbf{p}(\tau) \cdot \dot{\mathbf{x}}(\tau) + \frac{\mathbf{p}^2(\tau)}{2M} \right. \right. \\ \left. \left. - \Omega_B l_z(\mathbf{p}(\tau), \dot{\mathbf{x}}(\tau)) + \frac{1}{2} M \Omega_{\perp}^2 \{ \tilde{x}^2(\tau) + \tilde{y}^2(\tau) \} + \frac{1}{2} M \Omega_{\parallel}^2 \tilde{z}^2(\tau) + \mathbf{j}(\tau) \cdot \dot{\mathbf{x}}(\tau) + \mathbf{V}(\boldsymbol{\xi}, \tau) \cdot \mathbf{p}(\tau) \right] \right\}, \quad (9C.9)$$

where we have used the translation invariance $\tilde{\mathbf{p}} \rightarrow \mathbf{p}$ of the path integral. To solve the momentum path integral, it is useful to express it in its discretized form. Performing quadratic completions such that the momentum path integral separates into an infinite product of simple Gaussian integrals which are easily calculated, the remaining functional is reduced to the configuration space path integral

$$Z_{\Omega}^{\mathbf{p}_0, \mathbf{x}_0}[\mathbf{j}, \mathbf{v}] = \int d^3\xi \exp \left[\frac{M}{2\hbar} \int_0^{\hbar\beta} d\tau \mathbf{V}^2(\boldsymbol{\xi}, \tau) \right] \oint \mathcal{D}^3x \delta(\mathbf{x}_0 - \overline{\mathbf{x}(\tau)}) \exp \left\{ -\frac{1}{\hbar} \mathcal{A}_{\Omega}^{\mathbf{p}_0, \mathbf{x}_0}[\mathbf{x}; \mathbf{j}, \mathbf{V}] \right\} \quad (9C.10)$$

with the measure (9.10) for $d = 3$. The action functional is

$$\mathcal{A}_{\Omega}^{\mathbf{p}_0, \mathbf{x}_0}[\mathbf{x}; \mathbf{j}, \mathbf{V}] = \int_0^{\hbar\beta} d\tau \left[\frac{M}{2} \dot{\mathbf{x}}^2(\tau) + iM\Omega_B \{ \dot{x}(\tau)\tilde{y}(\tau) - \dot{y}(\tau)\tilde{x}(\tau) \} \right. \\ \left. + \frac{1}{2} M (\Omega_{\perp}^2 - \Omega_B^2) \{ \tilde{x}^2(\tau) + \tilde{y}^2(\tau) \} + \frac{1}{2} M \Omega_{\parallel}^2 \tilde{z}^2(\tau) + \tilde{x}(\tau) [j_x(\tau) + M\Omega_B V_y(\boldsymbol{\xi}, \tau)] \right. \\ \left. + \tilde{y}(\tau) [j_y(\tau) - M\Omega_B V_x(\boldsymbol{\xi}, \tau)] + \tilde{z}(\tau) j_z(\tau) \right] - \frac{iM}{\hbar} \int_0^{\hbar\beta} d\tau \dot{\mathbf{x}}(\tau) \cdot \mathbf{V}(\boldsymbol{\xi}, \tau), \quad (9C.11)$$

where the last term simplifies by the following consideration. A partial integration of this term yields

$$\int_0^{\hbar\beta} d\tau \dot{\mathbf{x}}(\tau) \cdot \mathbf{V}(\boldsymbol{\xi}, \tau) = - \int_0^{\hbar\beta} d\tau (\mathbf{x}(\tau) - \mathbf{x}_0) \cdot \dot{\mathbf{V}}(\boldsymbol{\xi}, \tau). \quad (9C.12)$$

The surface term vanishes as a consequence of the periodicity of the path and the source. This periodicity is also the reason why we could shift $\mathbf{x}(\tau)$ by the constant \mathbf{x}_0 on the right-hand side of Eq. (9C.12). Obviously, the importance of this expression lies in the coupling of the time derivative of $\mathbf{V}(\boldsymbol{\xi}, \tau)$ to the path $\mathbf{x}(\tau)$. Thus, $\dot{\mathbf{V}}(\boldsymbol{\xi}, \tau)$ can be handled like a $\mathbf{j}(\tau)$ -current [17] and the action (9C.11) can be written as

$$\mathcal{A}_{\Omega}^{\mathbf{p}_0, \mathbf{x}_0}[\mathbf{x}; \mathbf{j}, \mathbf{V}] = \mathcal{A}_{\Omega}^{\mathbf{p}_0, \mathbf{x}_0}[\mathbf{x}; \mathbf{J}, 0] = \mathcal{A}_{\Omega}^{\mathbf{p}_0, \mathbf{x}_0}[\mathbf{x}; 0, 0] - \frac{1}{\hbar} \int_0^{\hbar\beta} d\tau \dot{\mathbf{x}}(\tau) \cdot \mathbf{J}(\boldsymbol{\xi}, \tau) \quad (9C.13)$$

with the new current vector $\mathbf{J}(\boldsymbol{\xi}, \tau)$ which has the components

$$J_x(\boldsymbol{\xi}, \tau) = j_x(\tau) + M\Omega_B V_y(\boldsymbol{\xi}, \tau) - iM\dot{V}_x(\boldsymbol{\xi}, \tau), \\ J_y(\boldsymbol{\xi}, \tau) = j_y(\tau) - M\Omega_B V_x(\boldsymbol{\xi}, \tau) - iM\dot{V}_y(\boldsymbol{\xi}, \tau), \\ J_z(\boldsymbol{\xi}, \tau) = j_z(\tau) - \frac{1}{2} M \Omega_{\parallel} V_z(\boldsymbol{\xi}, \tau) \quad (9C.14)$$

and couples to the path $\mathbf{x}(\tau)$ only. With the expression (9C.10) for the generating functional and the action (9C.13), we have derived a representation similar to Eq. (9A.1) with the action (9A.2), extended by an additional oscillator in z -direction. We identify

$$j_x \equiv J_x, \quad j_y \equiv J_y. \quad (9C.15)$$

Inserting the substitutions (9C.15) into the solution (9A.8) for the generating functional in two dimensions and performing the usual calculation for a harmonic oscillator with external source [4, Chaps. 3,5] in z -direction, we obtain an intermediate result for the generating functional in three dimensions (9C.2):

$$Z_{\Omega}^{\mathbf{p}_0, \mathbf{x}_0}[\mathbf{j}, \mathbf{v}] = \lambda_{\text{th}}^{-3} Z_{\Omega}^{\mathbf{p}_0, \mathbf{x}_0} \int d^3 \xi \exp \left\{ \frac{M}{2\hbar} \int_0^{\hbar\beta} d\tau \mathbf{V}^2(\boldsymbol{\xi}, \tau) \right\} \\ \times \exp \left\{ \frac{1}{2\hbar^2} \int_0^{\hbar\beta} d\tau \int_0^{\hbar\beta} d\tau' \mathbf{J}(\boldsymbol{\xi}, \tau) \mathbf{G}^{\mathbf{x}_0}(\tau, \tau') \mathbf{J}(\boldsymbol{\xi}, \tau') \right\}. \quad (9C.16)$$

The partition function follows from Eqs. (9A.17) and (9A.24)

$$Z_{\Omega}^{\mathbf{p}_0, \mathbf{x}_0} = Z_{\Omega}^{\mathbf{p}_0, \mathbf{x}_0}[0, 0] = \frac{\hbar\beta\Omega_+/2}{\sinh \hbar\beta\Omega_+/2} \frac{\hbar\beta\Omega_-/2}{\sinh \hbar\beta\Omega_-/2} \frac{\hbar\beta\Omega_{\parallel}/2}{\sinh \hbar\beta\Omega_{\parallel}/2} \quad (9C.17)$$

and $\mathbf{G}^{\mathbf{x}_0}(\tau, \tau')$ is the 3×3 -matrix of Green functions

$$\mathbf{G}^{\mathbf{x}_0}(\tau, \tau') = \begin{pmatrix} G_{xx}^{\mathbf{x}_0}(\tau, \tau') & G_{xy}^{\mathbf{x}_0}(\tau, \tau') & 0 \\ G_{yx}^{\mathbf{x}_0}(\tau, \tau') & G_{yy}^{\mathbf{x}_0}(\tau, \tau') & 0 \\ 0 & 0 & G_{zz}^{\mathbf{x}_0}(\tau, \tau') \end{pmatrix}. \quad (9C.18)$$

Except $G_{zz}^{\mathbf{x}_0}(\tau, \tau')$, the Green functions are given by the expressions in Eqs. (9A.22) and (9A.28). The Green function of the pure harmonic oscillator in z -direction

$$G_{zz}^{\mathbf{x}_0}(\tau, \tau') = \frac{1}{M\beta\Omega_{\parallel}^2} \left(\frac{\hbar\beta\Omega_{\parallel}}{2} g_{\parallel}(\tau, \tau') - 1 \right) \quad (9C.19)$$

follows directly from the limit (9A.23). Since the current \mathbf{J} (9C.14) still depends on time derivatives of \mathbf{V} , we have to perform some partial integrations in the functional (9C.16). This is a very extensive but straightforward work and thus we only present an instructive example. For that we apply the properties and the time derivatives of the Green functions which we presented in Appendix 9B. Consider the integral

$$I = -\frac{M^2}{2\hbar^2} \int_0^{\hbar\beta} d\tau \int_0^{\hbar\beta} d\tau' \dot{V}_i(\boldsymbol{\xi}, \tau) G_{ii}^{\mathbf{x}_0}(\tau, \tau') \dot{V}_i(\boldsymbol{\xi}, \tau') \quad (9C.20)$$

occurring in the second exponential of Eq. (9C.16) with $i \in \{x, y, z\}$. A partial integration in the τ' -integral leads to

$$I = -\frac{M^2}{2\hbar^2} \int_0^{\hbar\beta} d\tau \dot{V}_i(\boldsymbol{\xi}, \tau) \left(G_{ii}^{\mathbf{x}_0}(\tau, \tau') V_i(\boldsymbol{\xi}, \tau') \Big|_{\tau'=0}^{\tau'=\hbar\beta} - \int_0^{\hbar\beta} d\tau' \frac{\partial G_{ii}^{\mathbf{x}_0}(\tau, \tau')}{\partial \tau'} V_i(\boldsymbol{\xi}, \tau') \right) \\ = \frac{M^2}{2\hbar^2} \int_0^{\hbar\beta} d\tau \int_0^{\hbar\beta} d\tau' \dot{V}_i(\boldsymbol{\xi}, \tau) G_{ii}^{\bullet \mathbf{x}_0}(\tau, \tau') V_i(\boldsymbol{\xi}, \tau'). \quad (9C.21)$$

The surface term in the first line vanishes as a consequence of the periodicity of the current (9C.5) and the Green function (9B.5). A second partial integration, now in the τ -integral, results in

$$I = -\frac{M^2}{2\hbar^2} \int_0^{\hbar\beta} d\tau \int_0^{\hbar\beta} d\tau' V_i(\boldsymbol{\xi}, \tau) \bullet G_{ii}^{\bullet \mathbf{x}_0}(\tau, \tau') V_i(\boldsymbol{\xi}, \tau') \\ = -\frac{M^2}{2\hbar^2} \int_0^{\hbar\beta} d\tau \int_0^{\hbar\beta} d\tau' V_i(\boldsymbol{\xi}, \tau) \bullet \tilde{G}_{ii}^{\bullet \mathbf{x}_0}(\tau, \tau') V_i(\boldsymbol{\xi}, \tau') - \frac{M}{2\hbar} \int_0^{\hbar\beta} d\tau V_i^2(\boldsymbol{\xi}, \tau). \quad (9C.22)$$

Here we have applied the periodicity property of the right-hand derivative of the Green function (9B.19), leading to a vanishing surface term in this case, too. In the second line, we have used the decomposition (9B.9) of the double-sided differentiated Green function. Note that the last term just

cancels the appropriate term in the first exponential of the right-hand side of Eq. (9C.16). Eventually, after performing all such partial integrations, we re-express Eq. (9C.16) by

$$Z_{\Omega}^{\mathbf{p}_0, \mathbf{x}_0}[\mathbf{j}, \mathbf{v}] = \lambda_{\text{th}}^{-3} Z_{\Omega}^{\mathbf{p}_0, \mathbf{x}_0} \int d^3 \xi \exp \left\{ \frac{1}{2\hbar^2} \int_0^{\hbar\beta} d\tau \int_0^{\hbar\beta} d\tau' \tilde{\mathbf{s}}(\xi, \tau) \mathbf{H}^{\mathbf{x}_0}(\tau, \tau') \tilde{\mathbf{s}}(\xi, \tau') \right\} \quad (9C.23)$$

with six-dimensional sources

$$\tilde{\mathbf{s}}(\xi, \tau) = (\mathbf{j}(\tau), \mathbf{V}(\xi, \tau)). \quad (9C.24)$$

and the 6×6 -matrix $\mathbf{H}^{\mathbf{x}_0}(\tau, \tau')$ which has no significance as long as we have not done the ξ -integration. We explicitly insert the decomposition (9C.8) into expression (9C.24) of the source vector $\tilde{\mathbf{s}}$. Since $\mathbf{v}_0(\xi)$ from Eq. (9C.7) is constant in time, some temporal integrals in the exponential of Eq. (9C.23) can be calculated and we obtain

$$\begin{aligned} Z_{\Omega}^{\mathbf{p}_0, \mathbf{x}_0}[\mathbf{j}, \mathbf{v}] &= \lambda_{\text{th}}^{-3} Z_{\Omega}^{\mathbf{p}_0, \mathbf{x}_0} \exp \left\{ \frac{1}{2\hbar^2} \int_0^{\hbar\beta} d\tau \int_0^{\hbar\beta} d\tau' \mathbf{s}(\tau) \mathbf{H}^{\mathbf{x}_0}(\tau, \tau') \mathbf{s}(\tau') \right\} \\ &\times \int d^3 \xi \exp \left\{ -\frac{M}{2\hbar^2 \beta} \xi^2 + i \frac{M}{\hbar^2 \beta} \xi \cdot \int_0^{\hbar\beta} d\tau \mathbf{v}(\tau) \right\} \end{aligned} \quad (9C.25)$$

with the new 6-vector

$$\mathbf{s}(\tau) = (\mathbf{j}(\tau), \mathbf{v}(\tau)) \quad (9C.26)$$

consisting of the original sources \mathbf{j} and \mathbf{v} only. The Gaussian ξ -integral in Eq. (9C.25) can easily be solved and the terms appearing from quadratic completion modify the above matrix $\mathbf{H}^{\mathbf{x}_0}(\tau, \tau')$. The final result for the generating functional of all position and momentum dependent correlations is given by

$$Z_{\Omega}^{\mathbf{p}_0, \mathbf{x}_0}[\mathbf{j}, \mathbf{v}] = Z_{\Omega}^{\mathbf{p}_0, \mathbf{x}_0} \exp \left\{ \frac{1}{2\hbar^2} \int_0^{\hbar\beta} d\tau \int_0^{\hbar\beta} d\tau' \mathbf{s}(\tau) \mathbf{G}^{\mathbf{p}_0, \mathbf{x}_0}(\tau, \tau') \mathbf{s}(\tau') \right\}. \quad (9C.27)$$

The complete 6×6 -matrix $\mathbf{G}^{\mathbf{p}_0, \mathbf{x}_0}(\tau, \tau')$ contains all possible Green functions describing position-position, position-momentum, and momentum-momentum correlations. As a consequence of separating the fluctuations into those perpendicular and parallel to the direction of the magnetic field, all correlations between x, y on the one and z on the other hand vanish as well as those for the appropriate momenta. The symmetries for the Green functions and their derivatives were investigated in detail in Appendix 9B and lead to a further reduction of the number of significant matrix elements. It turns out that only 9 elements are independent of each other. Therefore we can write the matrix

$$\begin{aligned} &\mathbf{G}^{\mathbf{x}_0, \mathbf{p}_0}(\tau, \tau') \\ &= \begin{pmatrix} G_{xx}^{\mathbf{p}_0, \mathbf{x}_0}(\tau, \tau') & G_{xy}^{\mathbf{p}_0, \mathbf{x}_0}(\tau, \tau') & 0 & G_{xp_x}^{\mathbf{p}_0, \mathbf{x}_0}(\tau, \tau') & G_{xp_y}^{\mathbf{p}_0, \mathbf{x}_0}(\tau, \tau') & 0 \\ G_{xy}^{\mathbf{p}_0, \mathbf{x}_0}(\tau', \tau) & G_{xx}^{\mathbf{p}_0, \mathbf{x}_0}(\tau', \tau') & 0 & -G_{xpy}^{\mathbf{p}_0, \mathbf{x}_0}(\tau, \tau') & G_{xpx}^{\mathbf{p}_0, \mathbf{x}_0}(\tau, \tau') & 0 \\ 0 & 0 & G_{zz}^{\mathbf{p}_0, \mathbf{x}_0}(\tau, \tau') & 0 & 0 & G_{zpz}^{\mathbf{p}_0, \mathbf{x}_0}(\tau, \tau') \\ G_{xp_x}^{\mathbf{p}_0, \mathbf{x}_0}(\tau', \tau) & -G_{xpy}^{\mathbf{p}_0, \mathbf{x}_0}(\tau', \tau) & 0 & G_{p_x p_x}^{\mathbf{p}_0, \mathbf{x}_0}(\tau, \tau') & G_{p_x p_y}^{\mathbf{p}_0, \mathbf{x}_0}(\tau, \tau') & 0 \\ G_{xpy}^{\mathbf{p}_0, \mathbf{x}_0}(\tau', \tau) & G_{xpx}^{\mathbf{p}_0, \mathbf{x}_0}(\tau', \tau) & 0 & G_{p_x p_y}^{\mathbf{p}_0, \mathbf{x}_0}(\tau', \tau) & G_{p_x p_x}^{\mathbf{p}_0, \mathbf{x}_0}(\tau, \tau') & 0 \\ 0 & 0 & G_{zpz}^{\mathbf{p}_0, \mathbf{x}_0}(\tau', \tau) & 0 & 0 & G_{p_z p_z}^{\mathbf{p}_0, \mathbf{x}_0}(\tau, \tau') \end{pmatrix}. \end{aligned} \quad (9C.28)$$

The matrix decomposes into four 3×3 -blocks, each of the which describing another type of correlation: the upper left position-position, the upper right position-momentum (as well as the lower left one), and the lower right momentum-momentum correlations. The different elements of the matrix are

$$G_{xx}^{\mathbf{p}_0, \mathbf{x}_0}(\tau, \tau') = \langle \tilde{x}(\tau) \tilde{x}(\tau') \rangle_{\Omega}^{\mathbf{p}_0, \mathbf{x}_0} = G_{xx}^{\mathbf{x}_0}(\tau, \tau'), \quad (9C.29)$$

$$G_{xy}^{\mathbf{p}_0, \mathbf{x}_0}(\tau, \tau') = \langle \tilde{x}(\tau) \tilde{y}(\tau') \rangle_{\Omega}^{\mathbf{p}_0, \mathbf{x}_0} = G_{xy}^{\mathbf{x}_0}(\tau, \tau'), \quad (9C.30)$$

$$G_{zz}^{\mathbf{p}_0, \mathbf{x}_0}(\tau, \tau') = \langle \tilde{z}(\tau) \tilde{z}(\tau') \rangle_{\Omega}^{\mathbf{p}_0, \mathbf{x}_0} = G_{zz}^{\mathbf{x}_0}(\tau, \tau'), \quad (9C.31)$$

$$\begin{aligned}
G_{xp_x}^{\mathbf{p}^0, \mathbf{x}^0}(\tau, \tau') &= \langle \tilde{x}(\tau) \tilde{p}_x(\tau') \rangle_{\Omega}^{\mathbf{p}^0, \mathbf{x}^0} = iMG_{xx}^{\bullet \mathbf{x}^0}(\tau, \tau') - M\Omega_B G_{xy}^{\mathbf{x}^0}(\tau, \tau') \\
&= \frac{\hbar}{4i} \{ \Theta(\tau - \tau') [h_+(\tau, \tau') + h_-(\tau, \tau')] - \Theta(\tau' - \tau) [h_+(\tau', \tau) + h_-(\tau', \tau)] \}, \quad (9C.32)
\end{aligned}$$

$$\begin{aligned}
G_{xp_y}^{\mathbf{p}^0, \mathbf{x}^0}(\tau, \tau') &= \langle \tilde{x}(\tau) \tilde{p}_y(\tau') \rangle_{\Omega}^{\mathbf{p}^0, \mathbf{x}^0} = iMG_{xy}^{\bullet \mathbf{x}^0}(\tau, \tau') + M\Omega_B G_{xx}^{\mathbf{x}^0}(\tau, \tau') \\
&= -\frac{\hbar}{4} [g_+(\tau, \tau') - g_-(\tau, \tau')] - \frac{1}{\beta} \frac{\Omega_B}{\Omega_+ \Omega_-}, \quad (9C.33)
\end{aligned}$$

$$\begin{aligned}
G_{zp_z}^{\mathbf{p}^0, \mathbf{x}^0}(\tau, \tau') &= \langle \tilde{z}(\tau) \tilde{p}_z(\tau') \rangle_{\Omega}^{\mathbf{p}^0, \mathbf{x}^0} = iMG_{zz}^{\bullet \mathbf{x}^0}(\tau, \tau') \\
&= \frac{\hbar}{2i} [\Theta(\tau - \tau') h_{\parallel}(\tau, \tau') - \Theta(\tau' - \tau) h_{\parallel}(\tau', \tau)], \quad (9C.34)
\end{aligned}$$

$$\begin{aligned}
G_{p_x p_x}^{\mathbf{p}^0, \mathbf{x}^0}(\tau, \tau') &= \langle \tilde{p}_x(\tau) \tilde{p}_x(\tau') \rangle_{\Omega}^{\mathbf{p}^0, \mathbf{x}^0} = -M^2 \tilde{G}_{xx}^{\bullet \mathbf{x}^0}(\tau, \tau') - 2iM^2 \Omega_B \bullet G_{xy}^{\mathbf{x}^0}(\tau, \tau') + M^2 \Omega_B^2 G_{xx}^{\mathbf{x}^0}(\tau, \tau') - \frac{M}{\beta} \\
&= \frac{\hbar M \Omega_{\perp}}{4} [g_+(\tau, \tau') + g_-(\tau, \tau')] - \frac{M}{\beta} \left(1 - \frac{\Omega_B^2}{\Omega_+ \Omega_-} \right), \quad (9C.35)
\end{aligned}$$

$$\begin{aligned}
G_{p_x p_y}^{\mathbf{p}^0, \mathbf{x}^0}(\tau, \tau') &= \langle \tilde{p}_x(\tau) \tilde{p}_y(\tau') \rangle_{\Omega}^{\mathbf{p}^0, \mathbf{x}^0} = 2iM^2 \Omega_B \bullet G_{xx}^{\mathbf{x}^0}(\tau, \tau') - M^2 \bullet G_{xy}^{\mathbf{x}^0}(\tau, \tau') + M^2 \Omega_B^2 G_{xy}^{\mathbf{x}^0}(\tau, \tau') \\
&= \frac{\hbar M \Omega_{\perp}}{4i} \{ \Theta(\tau - \tau') [h_+(\tau, \tau') - h_-(\tau, \tau')] - \Theta(\tau' - \tau) [h_+(\tau', \tau) - h_-(\tau', \tau)] \}, \quad (9C.36)
\end{aligned}$$

$$G_{p_z p_z}^{\mathbf{p}^0, \mathbf{x}^0}(\tau, \tau') = \langle \tilde{p}_z(\tau) \tilde{p}_z(\tau') \rangle_{\Omega}^{\mathbf{p}^0, \mathbf{x}^0} = -M^2 \bullet \tilde{G}_{zz}^{\mathbf{x}^0}(\tau, \tau') - \frac{M}{\beta} = \frac{\hbar M \Omega_{\parallel}}{2} g_{\parallel}(\tau, \tau') - \frac{M}{\beta}, \quad (9C.37)$$

where the expectation values are defined by Eq. (9.60). Note that all these Green functions are invariant under time translations such that

$$G_{\mu\nu}^{\mathbf{p}^0, \mathbf{x}^0}(\tau, \tau') = G_{\mu\nu}^{\mathbf{p}^0, \mathbf{x}^0}(\tau - \tau') \quad (9C.38)$$

with $\mu, \nu \in \{x, y, z, p_x, p_y, p_z\}$.

It is quite instructive to prove that all these Green functions can be decomposed into a quantum statistical and a classical part as we did it in Eq. (9A.22). Since we know that the classical correlation functions do not depend on the Euclidean time, all derivative terms in Eqs. (9C.29)–(9C.37) do not contain a classical term. We can write each Green function

$$G_{\mu\nu}^{\mathbf{p}^0, \mathbf{x}^0}(\tau, \tau') = G_{\mu\nu}^{\text{qm}}(\tau, \tau') - G_{\mu\nu}^{\text{cl}}. \quad (9C.39)$$

This relation has been already checked for Eqs. (9C.29)–(9C.31) in Appendix 9A. The classical contribution is zero in Eqs. (9C.32), (9C.34), and (9C.36) following from the absence of classical terms in derivatives of the Green functions and mixed correlations like (9A.30). It seems surprising that the correlation (9C.33) contains a classical term while (9C.32) possesses none. This is, however, a consequence of the cross product of the orbital angular momentum appearing in the action (9C.3) and the explicit classical calculation entails

$$G_{xp_x}^{\text{cl}} = \langle xp_x \rangle^{\text{cl}} = 0, \quad G_{xp_y}^{\text{cl}} = \langle xp_y \rangle^{\text{cl}} = \frac{1}{\beta} \frac{\Omega_B}{\Omega_{\perp}^2 - \Omega_B^2}, \quad (9C.40)$$

where the latter is the subtracted classical term in Eq. (9A.22) when considering the first two substitutions in (9C.15). In Eq. (9C.37), the second term is obviously the classical one since

$$G_{p_z p_z}^{\text{cl}} = \langle p_z p_z \rangle^{\text{cl}} = \frac{M}{\beta}. \quad (9C.41)$$

The extraction of the classical terms

$$G_{p_x p_x}^{\text{cl}} = \langle p_x p_x \rangle^{\text{cl}} = \frac{M}{\beta} \left(1 + \frac{\Omega_B^2}{\Omega_{\perp}^2 - \Omega_B^2} \right) \quad (9C.42)$$

in the case of the Green function $G_{p_x p_x}^{\mathbf{p}^0, \mathbf{x}^0}(\tau, \tau')$ requires the consideration of the last two terms in Eq. (9C.35). Thus we have shown that the decomposition (9C.39) holds for each of the Green functions (9C.29)–(9C.37). Note the necessity of subtracting the classical terms since they all diverge in the classical limit of high temperatures ($\beta \rightarrow 0$).

Part IV

Strong-Coupling Theory for Membranes

Fluctuating Membranes

We investigate the violent thermal out-of-plane fluctuations of a stack of membranes between two parallel walls and calculate the pressure p that they exert upon these walls. In equilibrium with a reservoir of molecules, tension vanishes and the shape is governed by extrinsic curvature energy. The differential geometric background of this model is discussed in this chapter. The pressure law was found by Helfrich [50] and reads for N membranes

$$p_N = \frac{2N}{N+1} \alpha_N \frac{(k_B T)^2}{\kappa a^3}, \quad (10.1)$$

where $L = (N+1)a$ is the distance between the walls, and κ the bending stiffness. The universal pressure constants α_N are not calculable exactly. For a single membrane, α_1 was roughly estimated by theoretical [50] and Monte Carlo methods [85–88]. By a strong-coupling calculation [48,89], presented in Chapter 11, we find a value, which lies well within the error bounds of the latest Monte Carlo estimate [88]. In a different strong-coupling approach [49], we also calculate the pressure constants for a stack of membranes in Chapter 12. Our results are in excellent agreement with all available Monte Carlo estimates [86–88] for $N = 1, 3, 5$. By an extrapolation to $N \rightarrow \infty$ we determine the pressure constant α_∞ for infinitely many membranes.

10.1 Introduction

Membranes formed by lipid bilayers are important biophysical systems occurring as boundaries of organells and vesicles. Their tension vanishes due to the lateral motion of molecules within the membrane. The flexibility of fluid membranes leads to an amazing variety of shapes of vesicles, which are large encapsulating bags with a size of up to $100 \mu\text{m}$. Changes in temperature or osmotic conditions, e.g. the concentration of ions or molecules in the membrane, induce shape transformations of vesicles. Figure 10.1 shows schematically the process of a budding transition, where the increase of temperature entails more violent membrane fluctuations, which lead to an uncoupling of a daughter vesicle, which can move independently of the mother vesicle (see Ref. [90] for microscopic photographs of a budding transition). Eventually, it can dock to another vesicle by an inverse process. Thus, shape transformations of membranes are necessary to make possible matter and energy transport between cells and organells in a complex biological system.

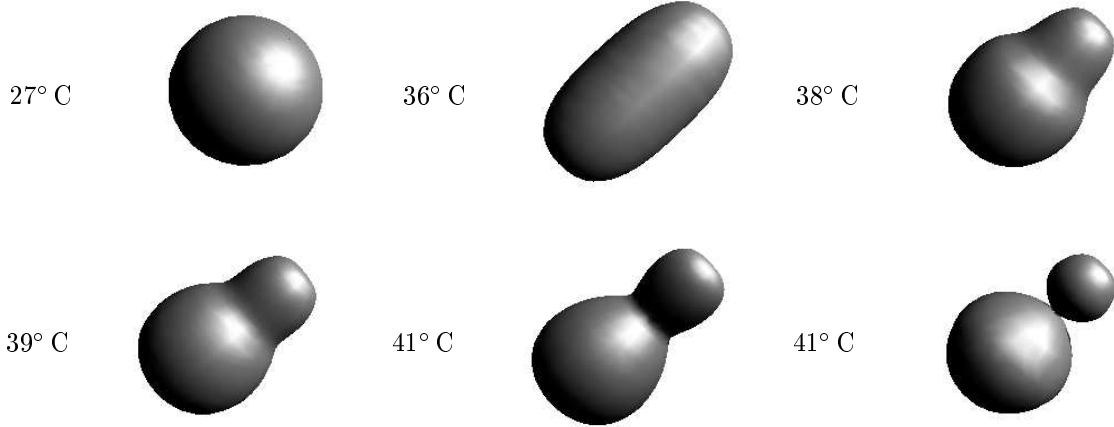


FIGURE 10.1: 3D pictures of a budding transition of a vesicle by increasing the temperature. The surfaces were modeled from microscopic photographs given in Ref. [90].

10.2 Differential Geometry for Curves and Surfaces

The geometry of the vesicle shapes can only be described locally, which means that it is necessary to apply differential geometry for modeling membranes. In what follows, we briefly review the main aspects of differential geometry.

10.2.1 Local Curvature of Curves

Topologically one-dimensional geometric objects appear in physics in different forms, for example as particle paths, polymers, strings, or vortex lines. They have in common that it is sufficient to identify each point of such a curved object by a vector in the surrounding embedding space, which depends on only one parameter. The parameter choice depends usually on the appropriate problem.

We want to describe a curve C in three-dimensional embedding space and we parameterize it with the help of the parameter s , which we choose to lie in the interval $0 \leq s \leq 1$. As Fig. 10.2 shows, a certain point of the curve C is given by the contravariant vector $\mathbf{r}(s) = (x^i(s)) = (x^1(s), x^2(s), x^3(s))^T$. The components of the tangent vector $\mathbf{t}(s) = (t^i(s))$ at the point $x^i(s)$ are given by the differential quotient

$$t^i(s) = \lim_{\Delta s \rightarrow 0} \frac{x^i(s + \Delta s) - x^i(s)}{\Delta s} = \frac{dx^i(s)}{ds}. \quad (10.2)$$

The length of an infinitesimal piece of the curve is given by

$$ds^2 = [dx^1(s)]^2 + [dx^2(s)]^2 + [dx^3(s)]^2 = \eta_{ij} dx^i(s) dx^j(s), \quad (10.3)$$

where equal indices are summed over. The identity matrix $(\eta_{ij}) = \text{diag}(1, 1, 1)$ is used to transform covariant vectors to contravariant ones: $dx_i = \eta_{ij} dx^j$. The tangent vector $t^i(s)$ is already normalized. To show this, we perform the scalar product

$$|\mathbf{t}(s)| = \sqrt{\mathbf{t}(s) \cdot \mathbf{t}(s)} = \sqrt{t_i(s) t^i(s)} = \sqrt{\eta_{ij} t^i t^j} = \sqrt{\eta_{ij} \frac{dx^i(s)}{ds} \frac{dx^j(s)}{ds}} = 1, \quad (10.4)$$

where we have used relation (10.3) in the last step. Now we determine the vectors transversal to $\mathbf{t}(s)$. We know that the number of transversal vectors is $D - 1$, where D is the dimension of the embedding space. Thus, we expect in three dimensions two independent vectors, which are orthogonal to $\mathbf{t}(s)$. One is easily determined by differentiating the scalar product $t^i(s) t_i(s) = 1$ with respect to s :

$$\frac{d}{ds} t^i(s) t_i(s) = 0 \quad \implies \quad \frac{dt^i(s)}{ds} \perp t^i(s). \quad (10.5)$$

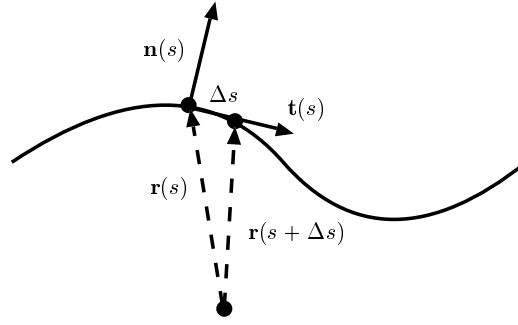


FIGURE 10.2: Curve C , parameterized by s , which we conventionally suppose to lie in the interval $0 \leq s \leq 1$.

The vector $dt^i(s)/ds$ is obviously orthogonal to $t^i(s)$, and we define the normal vector $\mathbf{n}(s)$ as

$$n^i(s) = k^{-1}(s) \frac{dt^i(s)}{ds} = k^{-1}(s) \frac{d^2x^i(s)}{ds^2}, \quad k(s) = \left| \frac{\sqrt{\eta_{ij} dt^i dt^j}}{ds} \right|. \quad (10.6)$$

The proportionality constant $k(s)$ is called the *curvature* of the curve at the point s and the components of the curvature vector $\mathbf{k}(s)$ are given by

$$k^i(s) = k(s)n^i(s), \quad (10.7)$$

thus pointing into the same direction as the normal vector. The larger its length $k(s)$, the more curved is the curve at s . The other transversal vector is called binormal vector $\mathbf{b}(s)$ and is orthogonal to $\mathbf{n}(s)$ and $\mathbf{t}(s)$:

$$b^i(s) = b^{-1}(s) \frac{dn^i(s)}{ds}, \quad (10.8)$$

where the length $b(s) = |dn^i(s)/ds|$ describes the strength of *torsion* of the curve. The more normals at neighboring points of the curve differ, the stronger is the torsion of the curve in this region.

An important quantity of a stringy object is its tension σ . This material constant is identical with the strength of the force, which acts in the opposite direction of an elongation to bring back a deformed string into its equilibrium state. In order to describe quantitatively the consequences of elongating a string with tension, we consider Fig. 10.3. The lower line represents a piece of an undeformed string. Dragging it at the position s by an amount $|\Delta \mathbf{u}(s)|$ from $\mathbf{r}(s)$ to $\mathbf{r}(s) + \Delta \mathbf{u}(s)$, where we keep the ends fixed, the overall length of this piece of string obviously increases. As we are only interested in elongations, which cause *normal* forces (which means that the force vector is parallel to the normal vector $\mathbf{n}(s)$), the displacement vector $\Delta \mathbf{u}(s)$ is parallel to the normal vector $\mathbf{n}(s)$. This ensures that the mechanical stress is the same for both legs of the triangle. It also allows us to choose one of the two rectangular triangles for the following considerations, since the ratio of the hypotenuse to the appropriate horizontal sides is identical for both. With these suppositions, we read off from Fig. 10.3:

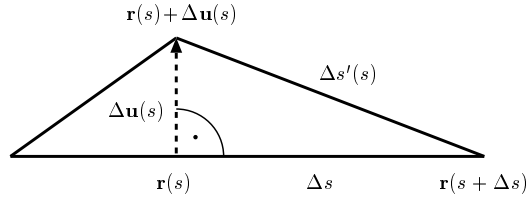
$$\Delta s'^2(s) = \Delta \mathbf{u}^2(s)/l_0^2 + \Delta s^2, \quad (10.9)$$

where we have rescaled the elongation with respect to the length of the undeformed string:

$$l_0 = l_0 \int_0^1 ds. \quad (10.10)$$

Going over to infinitesimal quantities, this relation gives us the *measure* of the deformed string

$$ds'(s) = ds \sqrt{1 + \left[\frac{d\mathbf{u}(s)}{l_0 ds} \right]^2}. \quad (10.11)$$

FIGURE 10.3: Change of scale ($\Delta s \rightarrow \Delta s'$) by elongating a string with tension.

The length of the deformed string can thus be written as

$$l = l_0 \int_0^1 ds \sqrt{1 + \left[\frac{d\mathbf{u}(s)}{l_0 ds} \right]^2} \quad (10.12)$$

in comparison to the undeformed one (10.10). Then, the energy E_σ of a deformed string due to its tension is equal to the mechanical work A_σ , which is necessary to change the length of the string from l_0 to l :

$$\begin{aligned} E_\sigma &\equiv A_\sigma = \sigma(l - l_0) = \sigma l_0 \left\{ \int_0^1 ds \sqrt{1 + \left[\frac{d\mathbf{u}(s)}{l_0 ds} \right]^2} - 1 \right\} \\ &\approx l_0 \frac{\sigma}{2} \int_0^1 ds \left[\frac{d\mathbf{u}(s)}{l_0 ds} \right]^2 = l_0 \frac{\sigma}{2} \int_0^1 ds \eta_{ij} \frac{du^i(s)}{l_0 ds} \frac{du^j(s)}{l_0 ds} = \frac{\sigma}{2} \int_0^{l_0} ds \eta_{ij} \frac{du^i(s)}{ds} \frac{du^j(s)}{ds}, \end{aligned} \quad (10.13)$$

where we have performed the scaling $s \rightarrow l_0 s$ in the last step. The approximate expression (10.13) is valid in the adiabatic limit of small elongations $|\mathbf{u}(s)|$.

If the line-like object can be deformed without changing its overall length, such as in the case of stiff polymers, another material property becomes important: the *elasticity* or *bending rigidity* κ . The degree of elastic deformation strongly depends on the curvature $k(s)$ at any position s . Thus, the bending or curvature energy is given by the curve integral

$$E_C = \frac{\kappa}{2} \int_0^1 ds k^2(s) = \frac{\kappa}{2} \int_0^1 ds \eta_{ij} \frac{dt^i(s)}{ds} \frac{dt^j(s)}{ds} = \frac{\kappa}{2} \int_0^1 ds \eta_{ij} \frac{d^2 x^i(s)}{ds^2} \frac{d^2 x^j(s)}{ds^2}, \quad (10.14)$$

where we have used the relation (10.6) between the curvature $k(s)$ and the difference of neighboring tangential vectors $\mathbf{t}(s)$ and $\mathbf{t}(s + ds)$ per length element ds and, in the last expression, the definition (10.2) of the tangential vector.

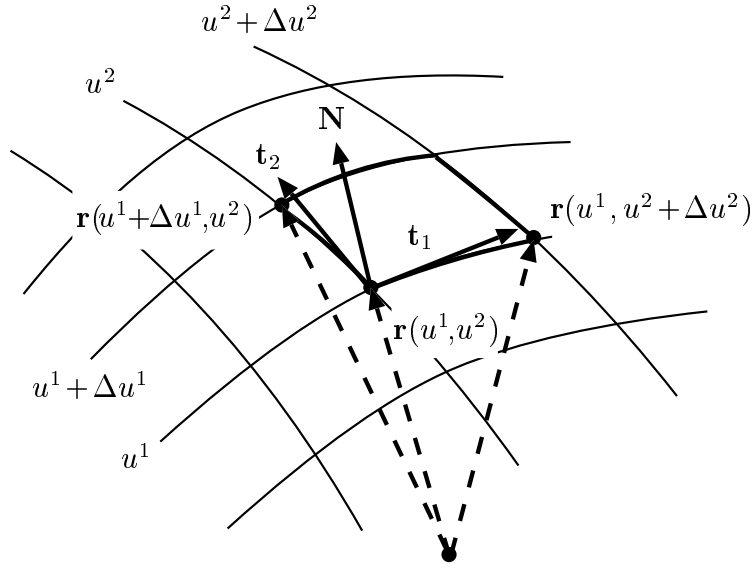
10.2.2 Local Curvature of Surfaces

In complete analogy to line-like objects in the preceding section, we investigate now topologically two-dimensional surfaces like membranes in three-dimensional embedding space. A point of a surface S may be identified by the position vector $\mathbf{r}(u^1, u^2) = x^i(u^\mu)$ with $\mu = 1, 2$, where u^1 and u^2 are suitable coordinate lines and serve as a parameterization of the surface (see Fig. 10.4). We use Latin indices for components of vectors in the embedding space, while Greek indices denote components of the intrinsic coordinates of the surface. The coordinate lines u^1, u^2 span a mesh and cover the surface completely. At the moment, the choice of these coordinates is arbitrary. Tangent vectors $\mathbf{t}_\mu(u^\mu)$ point along these coordinate lines and are introduced by

$$t_\mu^i(u^\mu) = \frac{\partial \mathbf{r}(u^\mu)}{\partial u^\mu} = \frac{\partial x^i(u^\mu)}{\partial u^\mu}, \quad \mu = 1, 2. \quad (10.15)$$

The surface normal vector $\mathbf{N}(u^\mu)$ is then given by the cross product of the tangent vectors:

$$\mathbf{N}(u^\mu) = \frac{\mathbf{t}_1(u^\mu) \times \mathbf{t}_2(u^\mu)}{|\mathbf{t}_1(u^\mu) \times \mathbf{t}_2(u^\mu)|}, \quad (10.16)$$


 FIGURE 10.4: Surface S , which is parameterized by intrinsic coordinates u^1 and u^2 .

or, written in components,

$$N^i(u^\mu) = \frac{\varepsilon_{ijk} t_1^j t_2^k}{\sqrt{\varepsilon_{ijk} t_1^j t_2^k \varepsilon^{ilm} t_{1,i} t_{2,m}}}, \quad (10.17)$$

where ε_{ijk} is the totally antisymmetric tensor

$$\varepsilon_{ijk} = \begin{cases} +1 & \{ijk\} = \{123\} \text{ or cyclic,} \\ -1 & \{ijk\} = \{213\} \text{ or cyclic,} \\ 0 & \text{else.} \end{cases} \quad (10.18)$$

An infinitesimal square length element on the surface is obviously introduced by

$$ds^2 = [dx^1(u^1, u^2)]^2 + [dx^2(u^1, u^2)]^2 + [dx^3(u^1, u^2)]^2 = dx_i(u^\mu) dx^i(u^\mu). \quad (10.19)$$

Substituting the total differentials by

$$dx^i(u^\mu) = \frac{\partial x^i(u^\mu)}{\partial u^\mu} du^\mu = t_\mu^i du^\mu, \quad (10.20)$$

Eq. (10.19) can be rewritten as the *first fundamental form*

$$ds^2 = g_{\mu\nu} du^\mu du^\nu, \quad (10.21)$$

with the metric

$$g_{\mu\nu} = t_\mu^i t_{i,\nu} = \frac{\partial x^i}{\partial u^\mu} \frac{\partial x_i}{\partial u^\nu} = \begin{pmatrix} \left(\frac{\partial \mathbf{r}}{\partial u^1}\right)^2 & \frac{\partial \mathbf{r}}{\partial u^1} \cdot \frac{\partial \mathbf{r}}{\partial u^2} \\ \frac{\partial \mathbf{r}}{\partial u^1} \cdot \frac{\partial \mathbf{r}}{\partial u^2} & \left(\frac{\partial \mathbf{r}}{\partial u^2}\right)^2 \end{pmatrix}_{\mu\nu}. \quad (10.22)$$

The metric is a symmetric tensor, which uniquely characterizes the shape of the surface. It is diagonal, if the tangent vectors are perpendicular to each other, which happens to be for orthogonal coordinates.

As the explicit calculation shows, the determinant of the metric is obtained by the square absolute value of the cross product of the tangent vectors

$$g \equiv \det g_{\mu\nu} = |\mathbf{t}_1 \times \mathbf{t}_2|^2 = \varepsilon_{ijk} t_1^i t_2^j \varepsilon^{ilm} t_{1,i} t_{2,m}. \quad (10.23)$$

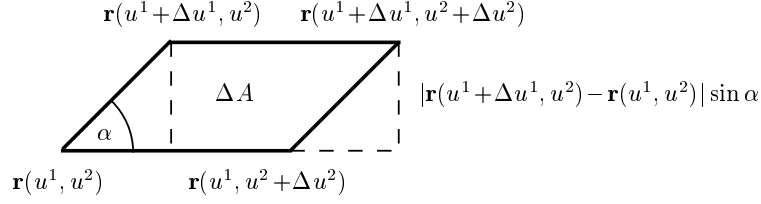


FIGURE 10.5: Planar projection of a surface element.

In Fig. 10.4, we have highlighted a surface element and we calculate its area as follows. For an infinitesimal small surface element, which is enclosed by the coordinates (u^1, u^2) , $(u^1 + du^1, u^2)$, $(u^1, u^2 + du^2)$, and $(u^1 + du^1, u^2 + du^2)$, the surface element and its planar projection are identical and we have to calculate the area of a parallelogram as shown in Fig. 10.5. Since the area of a parallelogram is identical to that of a rectangle with one shortened side, we obtain

$$\begin{aligned} dA &= |\mathbf{r}(u^1, u^2 + du^2) - \mathbf{r}(u^1, u^2)| |\mathbf{r}(u^1 + du^1, u^2) - \mathbf{r}(u^1, u^2)| \sin \alpha = \left| \frac{\partial \mathbf{r}}{\partial u^1} \right| du^1 \left| \frac{\partial \mathbf{r}}{\partial u^2} \right| du^2 \sin \alpha \\ &= \left| \frac{\partial \mathbf{r}}{\partial u^1} \times \frac{\partial \mathbf{r}}{\partial u^2} \right| du^1 du^2 = |\mathbf{t}_1 \times \mathbf{t}_2| du^1 du^2 = \sqrt{g} du^1 du^2, \end{aligned} \quad (10.24)$$

where we have used relation (10.23) in the last step. The overall area of the surface S is thus given by the parameter integral

$$A_S = \int_S dA = \int du^1 du^2 \sqrt{g}. \quad (10.25)$$

In the following we investigate the local curvature of a surface. For the one-dimensional curve, we have defined the curvature k as the proportionality constant between the normal vector $\mathbf{n}(s)$ at a position s and the derivative with respect to s of the tangent vector $\mathbf{t}(s)$ in Eq. (10.6). A surface possesses an infinite number of tangent vectors, since the two independent ones (10.15), which point along the coordinate lines u^1 and u^2 span a tangential plane, in which all possible tangential vectors at the point $\mathbf{r}(u^1, u^2)$ reside. Thus there are infinitely many curves on the surface, which touch the point $\mathbf{r}(u^1, u^2)$ and have different curvatures in this point. Thus we need a new definition for what we want to call the curvature of a surface. Let $\mathbf{r}(s)$ be a point of a curve C with curvature $k(s)$ on the surface S , where the same point is parameterized by $\mathbf{r}(u^1, u^2)$. Then, $\mathbf{n}(s) = d^2\mathbf{r}(s)/k ds^2$ denotes the normal vector of the curve and $\mathbf{N}(u^1, u^2)$ the surface normal at this point. We define the *normal curvature* k_n at this point by

$$k_n \equiv N_i \frac{d^2 x^i}{ds^2} = k_n^i N_i = k N_i n^i = k \cos \Theta, \quad (10.26)$$

where we have used the definition (10.7) for the curvature vector. The angle between \mathbf{n} and \mathbf{N} at a certain point is denoted by Θ .

If we consider the surface coordinates as functions of the curve parameter, $u^\mu = u^\mu(s)$, we rewrite the tangent and the normal vector of the curve at s as

$$\begin{aligned} \dot{x}^i(u^\mu(s)) &= \frac{dx^i(u^\mu(s))}{ds} = \frac{\partial x^i}{\partial u^\mu} \frac{du^\mu}{ds}, \\ n^i(u^\mu(s)) &= k^{-1} \frac{d^2 x^i(u^\mu(s))}{ds^2} = k^{-1} \left(\frac{\partial^2 x^i}{\partial u^\mu \partial u^\nu} \frac{du^\mu}{ds} \frac{du^\nu}{ds} + \frac{\partial x^i}{\partial u^\mu} \frac{d^2 u^\mu}{ds^2} \right). \end{aligned} \quad (10.27)$$

Multiplying the second relation by N_i and acknowledging that the second term vanishes due to $\mathbf{N}(u^\mu) \perp \partial x^i(u^\mu)/\partial u^\mu = \mathbf{t}_\mu(u^\mu)$, we obtain

$$N_i \frac{d^2 x^i}{ds^2} \equiv k_n = h_{\mu\nu} \frac{du^\mu}{ds} \frac{du^\nu}{ds}, \quad (10.28)$$

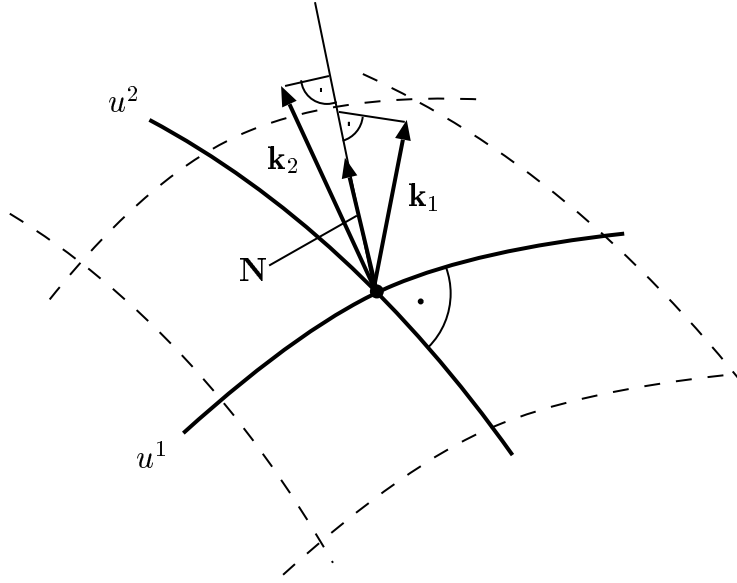


FIGURE 10.6: Definition of main curvature lines.

where we have introduced the *curvature tensor*

$$h_{\mu\nu} = N_i \frac{\partial^2 x^i}{\partial u^\mu \partial u^\nu} = N_i \frac{\partial}{\partial u^\mu} t_\nu^i. \quad (10.29)$$

Now we differentiate the relation $N_i t_\mu^i = 0$ with respect to u^ν , yielding

$$N_i \frac{\partial^2 x^i}{\partial u^\mu \partial u^\nu} \equiv h_{\mu\nu} = -\frac{\partial x^i}{\partial u^\mu} \frac{\partial N_i}{\partial u^\nu} = -\frac{dx^i}{du^\mu} \frac{dN_i}{du^\nu}, \quad (10.30)$$

where we could use total differentials since $du^\mu/du^\nu = \delta^\mu_\nu$. Expression (10.30) exhibits the *second fundamental form* [91,92]

$$-dx^i dN_i = h_{\mu\nu} du^\mu du^\nu. \quad (10.31)$$

Writing the right equation of (10.28) as $k_n ds^2 = h_{\mu\nu} du^\mu du^\nu$ and substituting ds^2 by the first fundamental form (10.21), we obtain the important expression

$$k_n = \frac{h_{\mu\nu} du^\mu du^\nu}{g_{\kappa\rho} du^\kappa du^\rho}, \quad (10.32)$$

which relates the normal curvature with the metric and the curvature tensor of the surface. As stated above, there is an infinite number of curves touching a certain point (u^1, u^2) of the surface and having a curvature vector \mathbf{k} at this point. In order to find a measure for the curvature of the surface in this point, we determine the curves with maximum and minimum curvature. This is done by extremizing the relation (10.32). Introducing abbreviations $l^\mu = du^\mu$ and $\alpha_{\mu\nu} = h_{\mu\nu} - k_n g_{\mu\nu} (= 0)$, Eq. (10.32) can be written as

$$\alpha_{\mu\nu} l^\mu l^\nu = 0. \quad (10.33)$$

Differentiating this equation with respect to l^κ yields

$$\alpha_{\mu\kappa} l^\mu = 0, \quad (10.34)$$

where we have utilized the symmetry of $\alpha_{\mu\nu}$. Re-expanding the abbreviations, multiplying by $g^{\nu\kappa}$, and substituting $g_\mu^\nu du^\mu = du^\nu$ leads to

$$h_\mu^\nu du^\mu - k_n du^\nu = 0. \quad (10.35)$$

This is a set of two equations ($\nu = 1, 2$), which constitutes an eigenvalue equation:

$$\begin{pmatrix} h_1^1 & h_2^1 \\ h_1^2 & h_2^2 \end{pmatrix} \begin{pmatrix} du^1 \\ du^2 \end{pmatrix} = k_n \begin{pmatrix} du^1 \\ du^2 \end{pmatrix}. \quad (10.36)$$

As usual, the eigenvalues k_n are obtained from the vanishing determinant

$$\begin{vmatrix} h_1^1 - k_n & h_2^1 \\ h_1^2 & h_2^2 - k_n \end{vmatrix} = 0. \quad (10.37)$$

Solving the quadratic equation $(h_1^1 - k_n)(h_2^2 - k_n) - h_1^2 h_2^1 = 0$ yields the two eigenvalues

$$k_{1,2} = \frac{1}{2} h_\mu^\mu \pm \sqrt{\frac{1}{4} (h_\mu^\mu)^2 - \det h_\mu^\nu}. \quad (10.38)$$

Defining the *Gaussian curvature*

$$K = k_1 k_2 = \det h_\mu^\nu \quad (10.39)$$

and the *mean curvature*

$$H = \frac{1}{2} (k_1 + k_2) = \frac{1}{2} h_\mu^\mu = \frac{1}{2} \text{Tr} h_\mu^\nu, \quad (10.40)$$

Eq. (10.38) can be expressed by

$$k_{1,2} = H \pm \sqrt{H^2 - K}. \quad (10.41)$$

These solutions are called *main curvatures* of the surface. The corresponding curves with curvature vectors $\mathbf{k}_{1,2}$ satisfying $k_{1,2} = \mathbf{k}_{1,2} \cdot \mathbf{N}_{1,2}$ at the point (u^1, u^2) are denoted as *main curvature lines* on the surface. Their tangent vectors $\mathbf{t}_{1,2}$ are orthogonal to another. Thus the eigenvectors of h_μ^ν form a local orthonormal coordinate system at this point of the surface as shown in Fig. 10.6.

Following Helfrich [93], the definitions of mean and Gaussian curvature are used to write the bending energy as an expansion in the curvature. The lowest-order contribution is then given by

$$E_C = \int_S dA (2\kappa H^2 + \kappa_G K), \quad (10.42)$$

which is quadratic in the main curvatures k_1 and k_2 . The elastic constants κ and κ_G are denoted as bending rigidity and Gaussian bending rigidity, respectively, and have the dimension energy. The second term in the parentheses in Eq. (10.42) is the topological invariant $4\pi\kappa_G(1 - G)$ as follows from the global Gauss-Bonnet theorem [91]. The number G counts the handles of the surface and is called the *genus* of the surface. Since we assume the surface topology to be fixed, this constant energy contribution can be omitted, leaving us with an curvature energy, which only depends on the mean curvature. Thus, Eq. (10.42) is written as

$$E_C = \frac{\kappa}{2} \int d^2u \sqrt{g} (h_\mu^\mu)^2. \quad (10.43)$$

This is the classical curvature model for bilayer membranes and is valid for curvature radii much larger than the membrane thickness (4 nm) [94]. The membrane equilibrium shape is then determined by minimizing the curvature energy.

A frequently used special parameterization of an almost planar surface is the *Monge representation*. As shown in Fig. 10.7, it is characterized by the following choice of parameters:

$$x(u^1, u^2) = u^1, \quad y(u^1, u^2) = u^2, \quad z(u^1, u^2) = z(x, y). \quad (10.44)$$

In this simple case, only deformations orthogonal to the xy -plane can be described. Although this is a strong restriction for the investigation of the influence of thermal fluctuations, which have no preferred direction upon a membrane, we will use an even more simplified form of this representation throughout the subsequent calculations. In Monge representation, the tangent vectors pointing into the direction

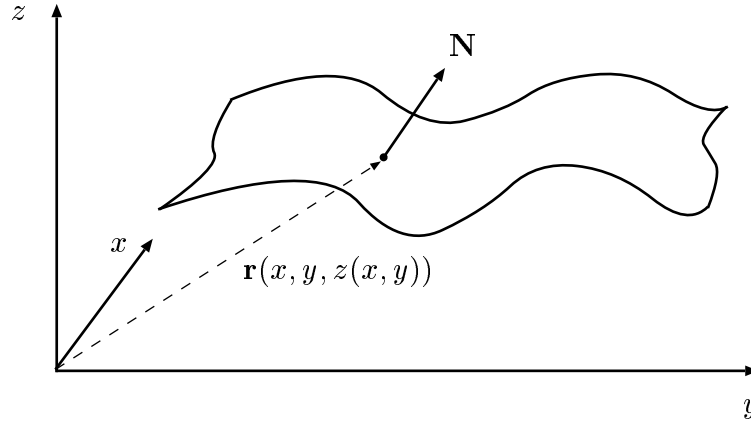


FIGURE 10.7: Out-of-plane deformations of an almost planar surface are described with the Monge representation, where Cartesian coordinates are used. The coordinates x and y span the parameter space, and only $z = z(x, y)$ depends on the parameterization.

of the x and y unit vectors read

$$\mathbf{t}_1 = (1, 0, \partial_x z)^T, \quad \mathbf{t}_2 = (0, 1, \partial_y z)^T. \quad (10.45)$$

The cross product of these tangent vectors yields the surface normal vector

$$\mathbf{N} = \frac{1}{\sqrt{1 + (\partial_x z)^2 + (\partial_y z)^2}} (-\partial_x z, -\partial_y z, 1)^T, \quad (10.46)$$

which we have normalized according to Eq. (10.16). The covariant and contravariant metrics are given by

$$g_{\mu\nu} = \begin{pmatrix} 1 + (\partial_x z)^2 & \partial_x z \partial_y z \\ \partial_x z \partial_y z & 1 + (\partial_y z)^2 \end{pmatrix}_{\mu\nu}, \quad g^{\mu\nu} = \frac{1}{g} \begin{pmatrix} 1 + (\partial_y z)^2 & -\partial_x z \partial_y z \\ -\partial_x z \partial_y z & 1 + (\partial_x z)^2 \end{pmatrix}^{\mu\nu}, \quad (10.47)$$

where g is the determinant of the covariant metric

$$g = \det g_{\mu\nu} = 1 + (\partial_x z)^2 + (\partial_y z)^2. \quad (10.48)$$

For the curvature tensor we obtain

$$h_{\mu\nu} = \frac{1}{\sqrt{g}} \begin{pmatrix} \partial_x^2 z & \partial_x \partial_y z \\ \partial_x \partial_y z & \partial_y^2 z \end{pmatrix}_{\mu\nu}, \quad (10.49)$$

or in the form we need it for calculating the mean and the Gaussian curvature:

$$h_{\mu}{}^{\nu} = g^{\rho\nu} h_{\mu\rho} = \frac{1}{g^{3/2}} \begin{pmatrix} [1 + (\partial_y z)^2] \partial_x^2 z - \partial_x z \partial_y z \partial_x \partial_y z & [1 + (\partial_y z)^2] \partial_x \partial_y z - \partial_x z \partial_y z \partial_y^2 z \\ [1 + (\partial_x z)^2] \partial_x \partial_y z - \partial_x z \partial_y z \partial_x^2 z & [1 + (\partial_x z)^2] \partial_y^2 z - \partial_x z \partial_y z \partial_x \partial_y z \end{pmatrix}_{\mu}{}^{\nu}. \quad (10.50)$$

The mean curvature (10.40) of a Monge parameterized surface in the point $(x, y, z(x, y))$ is half the trace of the tensor (10.50). Thus it is given by

$$H = \frac{1}{2} \frac{1}{[1 + (\partial_x z)^2 + (\partial_y z)^2]^{3/2}} \{ [1 + (\partial_x z)^2] \partial_y^2 z + [1 + (\partial_y z)^2] \partial_x^2 z - 2\partial_x z \partial_y z \partial_x \partial_y z \} \quad (10.51)$$

$$\approx \frac{1}{2} \Delta z [1 + \mathcal{O}((\nabla z)^2)], \quad (10.52)$$

where Δ is the Laplace operator $\partial_x^2 + \partial_y^2$ and ∇ the gradient (∂_x, ∂_y) in two dimensions. The Gaussian curvature (10.39) is obtained from the determinant of $h_{\mu}{}^{\nu}$:

$$K = \frac{1}{[1 + (\partial_x z)^2 + (\partial_y z)^2]^2} [\partial_x^2 z \partial_y^2 z - (\partial_x \partial_y z)^2]. \quad (10.53)$$

The simplest form of the curvature energy (10.43) for a membrane, which can be parameterized with the Monge representation is given by the expression

$$E_C = \frac{\kappa}{2} \int dx dy [\Delta z(x, y)]^2, \quad (10.54)$$

which we will use in the sequel to describe thermal fluctuations of membranes between walls.

Strong-Coupling Calculation of Fluctuation Pressure of a Membrane Between Walls

We calculate analytically the proportionality constant in the pressure law of a membrane thermally fluctuating between parallel walls from the strong-coupling limit of variational perturbation theory up to third order. Extrapolating these approximants to infinite order yields the pressure constant $\alpha = 0.0797149$ [48]. This result lies well within the error bounds of the most accurate available Monte Carlo result $\alpha_{\text{GK}}^{\text{MC}} = 0.0798 \pm 0.0003$ [88].

11.1 Membrane Between Walls

The violent thermal out-of-plane fluctuations of a membrane between parallel walls generate a pressure p following the law

$$p = \alpha \frac{k_B^2 T^2}{\kappa (d/2)^3}, \quad (11.1)$$

whose form was first derived by Helfrich [50] using dimensionality arguments. Here, κ denotes the elasticity constant of the membrane, and d the distance between the walls. The exact value of the prefactor α is unknown, but estimates have been derived from crude theoretical approximations by Helfrich [50] and by Janke and Kleinert [85], which yielded

$$\alpha_{\text{H}}^{\text{th}} \approx 0.0242, \quad \alpha_{\text{JK}}^{\text{th}} \approx 0.0625. \quad (11.2)$$

More precise values were found from Monte Carlo simulations by Janke and Kleinert [85] and by Gompper and Kroll [88], which gave

$$\alpha_{\text{JK}}^{\text{MC}} \approx 0.079 \pm 0.002, \quad \alpha_{\text{GK}}^{\text{MC}} \approx 0.0798 \pm 0.0003. \quad (11.3)$$

In a previous work [89], a systematic method was developed for calculating α with any desired high accuracy. Basis for this method is the strong-coupling version of variational perturbation theory [4]. The application of this method to the fluctuation pressure of the membrane is similar to that for the particle in a box developed in Ref. [95]. In that theory, the free energy of the membrane is expanded into

a sum of connected loop diagrams, which is eventually taken to infinite coupling strength to account for the hard walls. As a first approximation, an infinite set of diagrams was calculated, others were estimated by invoking a mathematical analogy with a similar one-dimensional system of a quantum mechanical particle between walls. The result of this procedure was a pressure constant

$$\alpha_K^{\text{th}} = \frac{\pi^2}{128} = 0.0771063\dots, \quad (11.4)$$

very close to (11.3).

It is the purpose of this paper to go beyond this estimate by calculating all diagrams up to four loops exactly. In this way, we improve the analytic approximation (11.4) and obtain a value

$$\alpha^{\text{th}} \approx 0.0797149, \quad (11.5)$$

which is in excellent agreement with the precise MC value $\alpha_{\text{GK}}^{\text{MC}}$ in Eq. (11.3).

11.2 Smooth Potential Model of Membrane Between Walls

To set up the theory, we let the membrane lie in the \mathbf{x} -plane and fluctuate in the z -direction with vertical displacements $\varphi(\mathbf{x})$. The walls at $z = \pm d/2$ restrict the displacements to the interval $\varphi(\mathbf{x}) \in (-d/2, d/2)$. Near zero temperature, the thermal fluctuations are small, $\varphi(\mathbf{x}) \approx 0$. The curvature energy E_C of the membrane has the harmonic approximation (10.54)

$$E_C = \frac{1}{2}\kappa \int d^2x [\partial^2\varphi(\mathbf{x})]^2. \quad (11.6)$$

The thermodynamic partition function Z of the membrane is given by the sum over all Boltzmann factors of field configurations $\varphi(\mathbf{x})$

$$Z = \prod_{\mathbf{x}} \left[\int_{-d/2}^{+d/2} \frac{d\varphi(\mathbf{x})}{\sqrt{2\pi k_B T / \kappa}} \right] \exp \left\{ -\frac{\kappa}{2k_B T} \int d^2x [\partial^2\varphi(\mathbf{x})]^2 \right\}. \quad (11.7)$$

This simple harmonic functional integral poses the problem of dealing with a finite range of fluctuations. This problem is solved by the strong-coupling theory of Ref. [89] as follows.

If the area of the membrane is denoted by A , the partition function (11.11) determines the free energy per area as

$$f = -\frac{1}{A} \ln Z. \quad (11.8)$$

By differentiating f with respect to the distance d of the walls, we obtain the pressure $p = -\partial f / \partial d$.

11.2.1 Smooth Potential Adapting Walls

We introduce some smooth potential restricting the fluctuations $\varphi(\mathbf{x})$ to the interval $(-d/2, d/2)$, for instance

$$V(\varphi(\mathbf{x})) = m^4 \frac{d^2}{\pi^2} \tan^2 \frac{\pi}{d} \varphi(\mathbf{x}) \equiv m^4 \varphi^2(\mathbf{x}) + \frac{\pi^2}{d^2} V_{\text{int}}(\varphi(\mathbf{x})), \quad (11.9)$$

where we have split the potential into a harmonic and an interacting part

$$V_{\text{int}}(\varphi(\mathbf{x})) = m^4 \left[\varepsilon_4 \varphi^4(\mathbf{x}) + \varepsilon_6 \left(\frac{\pi}{d} \right)^2 \varphi^6(\mathbf{x}) + \varepsilon_8 \left(\frac{\pi}{d} \right)^4 \varphi^8(\mathbf{x}) + \dots \right] \quad (11.10)$$

with $\varepsilon_4 = 2/3, \varepsilon_6 = 17/45, \varepsilon_8 = 62/315, \dots$. Thus we are left with the functional integral

$$Z = \oint \mathcal{D}\varphi(\mathbf{x}) \exp \left(-\frac{1}{2} \int d^2x \left\{ [\partial^2\varphi(\mathbf{x})]^2 + m^4 \varphi^2(\mathbf{x}) + \frac{\pi^2}{d^2} V_{\text{int}}(\varphi(\mathbf{x})) \right\} \right), \quad (11.11)$$

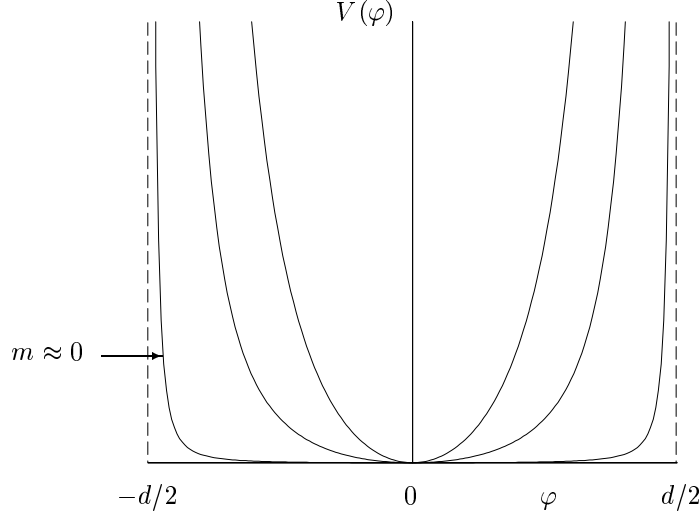


FIGURE 11.1: Smooth potential $V(\varphi)$ for different values of the parameter m . In the limit $m \rightarrow 0$ the hard walls at $\varphi = \pm d/2$ are adapted.

where we have set $\kappa = k_B T = 1$. After truncating the Taylor expansion around the origin, the periodicity of the trigonometric function is lost and the integrals over $\varphi(\mathbf{x})$ in (11.7) can be taken from $-\infty$ to $+\infty$. The interacting part is treated perturbatively. Then, the harmonic part of $V(\varphi(\mathbf{x}))$ leads to an exactly integrable partition function Z_{m^2} . The mass parameter m is arbitrary at the moment, but will eventually be taken to zero, in which case the potential $V(\varphi(\mathbf{x}))$ describes two hard walls at $\varphi = \pm d/2$. Figure 11.1 illustrates this behavior of the potential.

We shall now calculate a perturbation expansion for Z up to four loops. This will serve as a basis for the limit $m \rightarrow 0$, which will require the strong-coupling theory of Ref. [89].

11.2.2 Perturbation Expansion for Free Energy

The perturbation expansion proceeds from the harmonic part of Eq. (11.11):

$$Z_{m^2} = \oint \mathcal{D}\varphi(\mathbf{x}) e^{-\mathcal{A}_{m^2}[\varphi]} = e^{-\mathcal{A}f_{m^2}} \quad (11.12)$$

with

$$\mathcal{A}_{m^2}[\varphi] = \frac{1}{2} \int d^2x \{ [\partial^2 \varphi(\mathbf{x})]^2 + m^4 \varphi^2(\mathbf{x}) \}. \quad (11.13)$$

From Refs. [85,89], the harmonic free energy per unit area f_{m^2} is known as

$$f_{m^2} = \frac{1}{8} m^2. \quad (11.14)$$

The harmonic correlation functions associated with (11.12) are

$$\langle O_1(\varphi(\mathbf{x}_1)) O_2(\varphi(\mathbf{x}_2)) \cdots \rangle_{m^2} = \frac{1}{Z_{m^2}} \oint \mathcal{D}\varphi(\mathbf{x}) O_1(\varphi(\mathbf{x}_1)) O_2(\varphi(\mathbf{x}_2)) \cdots e^{-\mathcal{A}_{m^2}[\varphi]}, \quad (11.15)$$

where the functions $O_i(\varphi(\mathbf{x}_j))$ may be arbitrary polynomials of $\varphi(\mathbf{x}_j)$. The basic harmonic correlation function

$$G_{m^2}(\mathbf{x}_1, \mathbf{x}_2) = \langle \varphi(\mathbf{x}_1) \varphi(\mathbf{x}_2) \rangle_{m^2} \quad (11.16)$$

determines, by Wick's rule, all correlation functions (11.15) as sums of products of (11.16):

$$\langle \varphi(\mathbf{x}_1) \cdots \varphi(\mathbf{x}_n) \rangle_{m^2} = \sum_{\text{pairs}} G_{m^2}(\mathbf{x}_{P(1)}, \mathbf{x}_{P(2)}) \cdots G_{m^2}(\mathbf{x}_{P(n-1)}, \mathbf{x}_{P(n)}), \quad (11.17)$$

where the sum runs over all pair contractions, and P denotes the associated index permutations. The harmonic correlation function (11.16) reads in momentum space

$$G_{m^2}(\mathbf{k}) = \frac{1}{k^4 + m^4} = \frac{i}{2m^2} \left[\frac{1}{k^2 + im^2} - \frac{1}{k^2 - im^2} \right], \quad (11.18)$$

thus being proportional to the difference of two ordinary correlation functions $(p^2 - \mu^2)^{-1}$ with an imaginary square mass $\mu^2 = \pm im^2$. From their known \mathbf{x} -space form we have immediately

$$G_{m^2}(\mathbf{x}_1, \mathbf{x}_2) = G_{m^2}(\mathbf{x}_1 - \mathbf{x}_2) = \frac{i}{4\pi m^2} \left[K_0(\sqrt{im}|\mathbf{x}_1 - \mathbf{x}_2|) - K_0(\sqrt{-im}|\mathbf{x}_1 - \mathbf{x}_2|) \right], \quad (11.19)$$

where $K_0(z)$ is a modified Bessel function [96, Section 8.432]. At zero distance, the ordinary harmonic correlations are logarithmically divergent, but the difference is finite yielding $G_{m^2}(0) = 1/8m^2$.

We now expand the partition function (11.11) in powers of $gV_{\text{int}}(\phi(\mathbf{x}))$, where $g \equiv \pi^2/d^2$, and use the expectation values (11.15) to obtain a perturbation series for Z . Going over to the cumulants, we find the free energy per unit area

$$f = f_{m^2} + \frac{g}{2A} \int d^2x \langle V_{\text{int}}(\varphi(\mathbf{x})) \rangle_{m^2, c} - \frac{g^2}{2!} \frac{1}{4A} \int d^2x_1 d^2x_2 \langle V_{\text{int}}(\varphi(\mathbf{x}_1)) V_{\text{int}}(\varphi(\mathbf{x}_2)) \rangle_{m^2, c} + \dots, \quad (11.20)$$

where the subscript c indicates the cumulants. Inserting the expansion (11.10) and using (11.15) as well as (11.17), the series can be written as

$$f = m^2 \left[a_0 + \sum_{n=1}^{\infty} a_n \left(\frac{g}{m^2} \right)^n \right], \quad (11.21)$$

where the coefficients a_n are dimensionless real numbers, starting with $a_0 = 1/8$ from Eq. (11.14). The higher expansion coefficients a_n are combinations of integrals over the connected correlation functions:

$$a_1 = \varepsilon_4 \frac{m^4}{2A} \int d^2x \langle \varphi^4(\mathbf{x}) \rangle_{m^2, c}, \quad (11.22)$$

$$a_2 = \varepsilon_6 \frac{m^6}{2A} \int d^2x \langle \varphi^6(\mathbf{x}) \rangle_{m^2, c} - \varepsilon_4^2 \frac{m^{10}}{8A} \int d^2x_1 d^2x_2 \langle \varphi^4(\mathbf{x}_1) \varphi^4(\mathbf{x}_2) \rangle_{m^2, c}, \quad (11.23)$$

$$a_3 = \varepsilon_8 \frac{m^8}{2A} \int d^2x \langle \varphi^8(\mathbf{x}) \rangle_{m^2, c} - \varepsilon_4 \varepsilon_6 \frac{m^{12}}{4A} \int d^2x_1 d^2x_2 \langle \varphi^6(\mathbf{x}_1) \varphi^4(\mathbf{x}_2) \rangle_{m^2, c} \\ + \varepsilon_4^3 \frac{m^{16}}{48A} \int d^2x_1 d^2x_2 d^2x_3 \langle \varphi^4(\mathbf{x}_1) \varphi^4(\mathbf{x}_2) \varphi^4(\mathbf{x}_3) \rangle_{m^2, c}. \quad (11.24)$$

To find the free energy (11.21) between walls, we must go to the limit $m^2 \rightarrow 0$. Following [4,89], we substitute m^2 by the variational parameter M^2 , which is introduced via the trivial identity

$$m^2 \equiv \sqrt{M^4 - gr} \quad (11.25)$$

with

$$r = \frac{1}{g} (M^4 - m^4), \quad (11.26)$$

and expand the r.h.s. of Eq. (11.25) in powers of g up to the order g^N . In the limit $m^2 \rightarrow 0$, this expansion reads

$$m^2(M^2) = M^2 - \frac{1}{2} \frac{r}{M^2} g - \frac{1}{8} \frac{r^2}{M^6} g^2 - \frac{1}{16} \frac{r^3}{M^{10}} g^3 - \dots \quad (11.27)$$

Inserting this into (11.21), re-expanding in powers of g , re-substituting r from Eq. (11.26), and truncating after the N th term, we arrive at the free energy per unit area

$$f_N(M^2, d) = M^2 a_0 b_0 + \sum_{n=1}^N a_n g^n M^{2(1-n)} b_n, \quad (11.28)$$

with

$$b_n = \sum_{k=0}^{N-n} (-1)^k \binom{(1-n)/2}{k} \quad (11.29)$$

being the binomial expansion of $(1-1)^{(1-n)/2}$ truncated after the $(N-n)$ th term [89]. The optimization of (11.28) is done as usual [4] by determining the minimum of $f_N(M^2, d)$ with respect to the variational parameter M^2 , i.e. by the condition

$$\frac{\partial f_N(M^2, d)}{\partial M^2} \stackrel{!}{=} 0, \quad (11.30)$$

whose solution gives the optimal value $M_N^2(d)$. Re-substituting this result into Eq. (11.28) produces the optimized free energy $f_N(d) = f_N(M_N^2(d), d)$, which only depends on the distance as $f_N(d) = 4\alpha_N/d^2$. Its derivative with respect to d yields the desired pressure law with the N th-order approximation for the constant α_N :

$$p_N = \alpha_N \left(\frac{d}{2}\right)^{-3}. \quad (11.31)$$

We must now calculate the cumulants occurring in the expansion (11.21).

11.3 Evaluation of the Fluctuation Pressure up to Four-Loop Order

The correlation functions appearing in (11.22)–(11.24) are conveniently represented by Feynman graphs. Green functions are pictured as solid lines and local interactions as dots, whose coordinates are integrated over:

$$\mathbf{x}_1 \text{ — } \mathbf{x}_2 \equiv G_{m^2}(\mathbf{x}_1, \mathbf{x}_2), \quad (11.32)$$



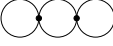
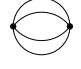
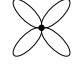
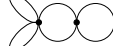
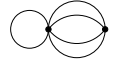

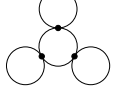
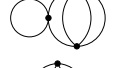

$$\bullet \equiv \int d^2 x. \quad (11.33)$$

These rules can be taken over to momentum space in the usual way. One easily verifies that the integrals over the connected correlation functions in (11.22)–(11.24) have a dimension $A/m^{2(l+V-1)}$, where V is the number of the vertices and l denotes the number of lines of the associated Feynman diagrams. Thus we parameterize each Feynman diagram by $vA/m^{2(l+V-1)}$, with a dimensionless number v , which includes the multiplicity. In Table 11.1, we have listed the values v for all diagrams up to four loops. No divergences are encountered. Exact results are stated as fractional numbers. The other numbers are obtained by numerical integration, which are reliable up to the last written digit. The right-hand column shows numbers v_K obtained by the earlier approximation [89], where all the Feynman diagrams were estimated by an analogy to the the problem of a particle in a box. In Ref. [89], it was shown that the value v of a large class of diagrams of the membrane problem can be obtained by simply dividing the value of the corresponding particle-in-a-box-diagram v_{PB} by a factor $1/4^L$, where L is the number of loops in the diagrams.

Inserting the numbers in Table 11.1 into (11.22)–(11.24), we obtain the coefficients a_1, a_2, a_3 of the free energy per area (11.28), which is then extremized in M^2 . To see how the results evolve from order to order, we start with the first order

$$f_1(M^2, d) = \frac{1}{2} a_0 M^2 + a_1 \frac{\pi^2}{d^2} \quad (11.34)$$

TABLE 11.1: Feynman diagrams with loops L , multiplicities s , and their dimensionless values v . The last column shows the values $v_K = v_{PB}/4^L$ used in Ref. [89].

L	Graph	s	v	v_K
2		3	$\frac{3}{64}$	$\frac{3}{64}$
			$a_1 = a_1^K$	$a_1^K = 1/64$
3		15	$\frac{15}{512}$	$\frac{15}{512}$
		72	$\frac{9}{128}$	$\frac{9}{128}$
		24	$0.828571 \times \frac{3}{256}$	$\frac{3}{256}$
		$a_2 = 1.114286 a_2^K$		$a_2^K = 1/1024$
4		105	$\frac{105}{4096}$	$\frac{105}{4096}$
		540	$\frac{135}{2048}$	$\frac{135}{2048}$
		360	$0.828571 \times \frac{45}{2048}$	$\frac{45}{2048}$
		2592	$\frac{81}{512}$	$\frac{81}{512}$
		1728	$\frac{81}{512}$	$\frac{81}{512}$
		3456	$0.828571 \times \frac{135}{1024}$	$\frac{135}{1024}$
		1728	$0.713194 \times \frac{81}{2048}$	$\frac{81}{2048}$
		$a_3 = 2.763097 \cdot 10^{-5}$		$a_3^K = 0$

with $a_0 = 1/8$ and $a_1 = 1/64$. Here, an optimal value of M^2 does not exist. Thus we simply use the perturbative result for $m = 0$, which is equal to (11.34) for $M = 0$. Differentiating $f_1(0, d)$ with respect to d yields the pressure constant in (11.31):

$$\alpha_1 = \frac{1}{4} a_1 \frac{\pi^2}{d^2} = \frac{\pi^2}{256} \approx 0.038553. \quad (11.35)$$

This value is about half as big as the Monte Carlo estimates (11.3) and agrees with the value found in [89]. To second order, the re-expansion (11.28) reads

$$f_2(M^2, d) = \frac{3}{8} a_0 M^2 + a_1 \frac{\pi^2}{d^2} + a_2 \frac{\pi^4}{d^4} \frac{1}{M^2} \quad (11.36)$$

with $a_2 \approx 1.0882 \cdot 10^{-3}$ from Table 11.1. Minimizing this free energy in M^2 yields an optimal value

$$M_2^2(d) = \sqrt{\frac{8 a_2 \pi^2}{3 a_0 d^2}} \approx 0.152362 \frac{\pi^2}{d^2}, \quad (11.37)$$

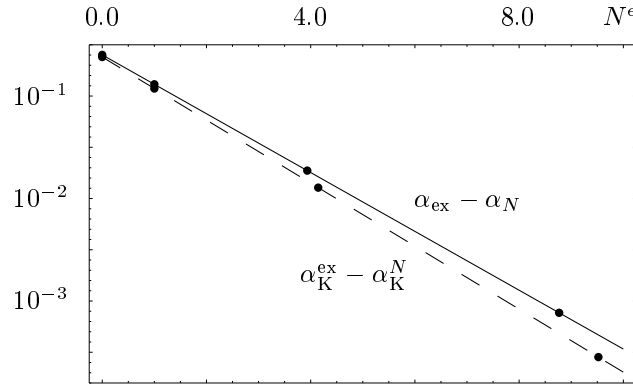


FIGURE 11.2: Difference between the extrapolated pressure constant α_{ex} and the optimized N -th order value α_N obtained from variational perturbation theory for the method presented in this chapter (solid line) and the first four values of the approximation scheme introduced in Ref. [89] (dashed line). Dots represent the values to order N in these approximations.

and

$$f_2(d) = \frac{\pi^2}{d^2} \left(a_1 + \sqrt{\frac{3}{2} a_0 a_2} \right). \quad (11.38)$$

Inserting $a_0 = 1/8$ and a_1, a_2 from Table 11.1, we obtain

$$\alpha_2 \approx 0.073797, \quad (11.39)$$

thus improving drastically the first-order estimate (11.35). This value is by a factor 1.026 larger than that obtained in the approximation of Ref. [89].

Continuing this proceeding to third order, we must minimize

$$f_3(M^2, d) = \frac{5}{16} a_0 M^2 + a_1 \frac{\pi^2}{d^2} + \frac{3}{2} a_2 \frac{\pi^4}{d^4} \frac{1}{M^2} + a_3 \frac{\pi^6}{d^6} \frac{1}{M^4} \quad (11.40)$$

with $a_3 \approx 2.7631 \cdot 10^{-5}$. The optimal value of M^2 is

$$M_3^2(d) = \sqrt{\frac{32 a_2}{5 a_0}} \cos \left[\frac{1}{3} \arccos \sqrt{\frac{5 a_0 a_3^2}{2 a_2^3}} \right] \frac{\pi^2}{d^2} \approx 0.219608 \frac{\pi^2}{d^2}. \quad (11.41)$$

Inserted into (11.40), we find the four-loop approximation for the proportionality constant α :

$$\alpha_3 \approx 0.079472. \quad (11.42)$$

This result is in very good agreement with the Monte Carlo results in (11.3) and should be a lower bound for the exact value since the successive approximations increase monotonously with the order of the approximation. It differs from the approximate value of the method presented in Ref. [89] by a factor 1.047.

An even better result will now be obtained by extrapolating the sequence $\alpha_1, \alpha_2, \alpha_3$ to infinite order.

11.4 Extrapolation Towards the Exact Constant

Variational perturbation theory exhibits typically an exponentially fast convergence. This was exactly proven for the anharmonic oscillator [4]. Other systems treated by variational perturbation theory

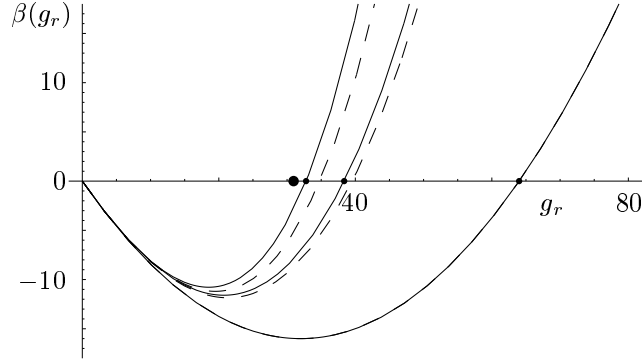


FIGURE 11.3: Plot of successive β -like functions associated with expansion (11.46) to orders $N = 1, 2, 3$ (solid curves). For comparison, we also plot the corresponding functions obtained from the approximate expansion coefficients a_n^K (dashed curves). The curves coincide for $N = 1$. The zeros $g_{r,N}^*$ of the N th approximation are from right to left: $g_{r,1}^* = 64$ (64), $g_{r,2}^* = 38.369$ (39.554), and $g_{r,3}^* = 32.783$ (34.796). The zeros approach rapidly the value $g_r^* = 30.953$ (fat dot) associated with the pressure constant (11.45).

show a similar behavior [53]. Assuming that an exponential convergence exists also here, we may extrapolate the sequence of values $\alpha_1, \alpha_2, \alpha_3$ calculated above to infinite order. It is useful to extend this sequence by one more value at the lower end, $\alpha_0 = 0$, which follows from the one-loop energy (11.14) at $m^2 = 0$. This sequence is now extrapolated towards a hypothetical exact value α_{ex} by parameterizing the approach as

$$\alpha_{\text{ex}} - \alpha_N = \exp(-\eta - \xi N^\epsilon). \quad (11.43)$$

The parameters η, ξ, ϵ , and the unknown value of α_{ex} are determined from the four values $\alpha_0, \dots, \alpha_3$, with the result

$$\eta = 2.529298, \quad \xi = 0.660946, \quad \epsilon = 1.976207, \quad (11.44)$$

and the extrapolated value for the exact constant:

$$\alpha_{\text{ex}} = 0.0797149. \quad (11.45)$$

This is now in perfect agreement with the Monte Carlo values (11.3).

The approach is graphically shown in Fig. 11.2, where the optimized values $\alpha_0, \dots, \alpha_3$ all lie on a straight line (solid line). For comparison, we have also extrapolated the first four values $\alpha_K^0, \dots, \alpha_K^3$ in the approach of Ref. [89] yielding a value $\alpha_{\text{ex K}} \approx 0.0759786$, which is 4.9% smaller than (11.45).

11.5 Comparison with the Renormalization Group Approach

Rewriting the perturbation series (11.21) as $f = [g_r(\tilde{g})]^{-1} \pi^2 / d^2$ with the dimensionless function

$$g_r(\tilde{g}) = \tilde{g}(a_0 + a_1 \tilde{g} + a_2 \tilde{g}^2 + a_3 \tilde{g}^3 + \dots)^{-1} = \frac{1}{a_0} \left[\tilde{g} - \frac{a_1}{a_0} \tilde{g}^2 + \left(\frac{a_1^2}{a_0^2} - \frac{a_2}{a_0} \right) \tilde{g}^3 + \dots \right] \quad (11.46)$$

of the reduced coupling constant $\tilde{g} = g/m^2$, its logarithmic derivative $s(\tilde{g}) = \partial \log g_r(\tilde{g}) / \partial \log \tilde{g}$ vanishes at infinitively strong coupling since $g_r(\tilde{g} \rightarrow \infty) = g_r^* = \text{const.}$ This constant determines the pressure constant as

$$\alpha = \frac{\pi^2}{4} [g_r^*]^{-1}. \quad (11.47)$$

In analogy to the renormalization group method in field theory, we may now define a β -like function by $\beta(\tilde{g}) = -g_r(\tilde{g})s(\tilde{g})$, as done in Ref. [97]. Since this function vanishes in the limit of infinitely strong

coupling $\tilde{g} \rightarrow \infty$, we invert the series (11.46) for $\tilde{g}(g_r)$ and re-expand the β -like function in powers of g_r obtaining $\beta(g_r)$. This function vanishes at the value g_r^* determining once more the pressure constant via Eq. (11.47). The terms in Eq. (11.46) yield successively the values $\alpha_1 = 0.038553$, $\alpha_2 = 0.064308$, $\alpha_3 = 0.075265$, which approach the estimate (11.45). Figure 11.3 shows the first three β -like functions for different orders and their zeros together with the zero corresponding to our value (11.45).

Fluctuation Pressure of a Stack of Membranes

We calculate the universal constants α_N in Helfrich's pressure law for a stack of N membranes between walls by strong-coupling theory [49]. Using the close analogy between this system and a stack of strings, where the universal constants are exactly known, we construct a smooth potential that keeps the membranes apart. The strong-coupling limit of the perturbative treatment of the free energy yields pressure constants for an arbitrary number of membranes, which are in very good agreement with values from Monte Carlo simulations.

12.1 Introduction

The tension of membranes vanishes in equilibrium with a reservoir of molecules. Its shape is governed by the extrinsic curvature energy E_C . If a stack of membranes is placed between two parallel walls, violent thermal out-of-plane fluctuations of the membranes exert a pressure p upon the walls. The pressure law is given by Eq. (10.1). The pressure constant for a single membrane, α_1 , was roughly estimated by theoretical [50] and Monte Carlo methods [85–88]. The most precise theoretical result was obtained by strong-coupling theory [48] (see also Chapter 11 of this thesis), yielding $\alpha_1^{\text{th}} = 0.0797149$, which lies well within the error bounds of the latest Monte Carlo estimate $\alpha_1^{\text{MC}} = 0.0798 \pm 0.0003$ [88].

For more than one membrane between the walls, the strong-coupling calculation of Refs. [48,89] must be modified in a nontrivial way. We must find a different potential that keeps the membranes apart and whose strong-coupling limit ensures non-interpenetration. For this, we take advantage of the fact that membranes between walls have similar properties to a stack of nearly parallel strings fluctuating in a plane between line-like walls [98,99], in particular the same type of pressure law (10.1) with κ substituted by the string tension σ . The characteristic universal constants of the latter system were *exactly* calculated in Refs. [88,98] from an analogy to a gas of fermions in $1 + 1$ dimensions [100–102]. We use these exact values to determine a potential that, when applied to the stack of membranes, yields a perturbation expansion for the pressure constants for an *arbitrary* number of membranes to be evaluated in the strong-coupling limit of complete repulsion.

Our results are in excellent agreement with all available Monte Carlo estimates [86–88] for $N = 1, 3, 5$. Extrapolating to $N \rightarrow \infty$, we estimate the pressure constant α_∞ for infinitely many membranes.

12.2 Stack of Strings

We begin by studying the exactly solvable statistical properties of a stack of N almost parallel strings in a plane, which are not allowed to cross each other and whose average spacing at low temperature is a . The system is enclosed between parallel line-like walls with a separation L as illustrated in Fig. 12.1. In the Monge parameterization, the vertical position of a point of the n th string is $z_n = z_n(x)$. Since the vertical positions of the n th string are fluctuating around the low-temperature equilibrium position at na , it is useful to introduce the displacement fields

$$\varphi_n(x) \equiv z_n(x) - na. \quad (12.1)$$

The thermodynamic partition function is given by the functional integral

$$Z^s = \prod_{n=1}^N \prod_x \left[\int_{\varphi_{n-1}(x)-a}^{\varphi_{n+1}(x)+a} \frac{d\varphi_n(x)}{\sqrt{2\pi k_B T/\sigma}} \right] \exp \left\{ -\frac{\sigma}{2k_B T} \sum_{n=1}^N \int_{-\infty}^{\infty} dx \left[\frac{d\varphi_n(x)}{dx} \right]^2 \right\}, \quad (12.2)$$

where σ is the string tension, T is the temperature, and k_B is the Boltzmann factor. We are interested in the free energy per unit length

$$f_N^s \equiv -\frac{k_B T}{A} \ln Z^s, \quad (12.3)$$

with $A = \int_{-\infty}^{\infty} dx$. Since the strings may not pass through each other, the fluctuations $\varphi_n(x)$ of the n th string are restricted to the interval

$$\varphi_n(x) \in \{\varphi_{n-1}(x) - a, \varphi_{n+1}(x) + a\}. \quad (12.4)$$

12.2.1 Free Fermion Model

The restriction (12.4) makes it difficult to solve the functional integral (12.2) explicitly. It is, however, possible to find a solution by identifying the system with a $(1+1)$ -dimensional Fermi gas, as done by de Gennes [100]. Using this analogy, Gompper and Kroll [88] determined the $1/a^2$ contribution to Δf_N^s relevant for the pressure law (10.1) as

$$\Delta f_N^s = \alpha_N^s \frac{(k_B T)^2}{\sigma a^2}, \quad (12.5)$$

with the pressure constants

$$\alpha_N^s = \frac{\pi^2}{12} \frac{2N+1}{N+1}. \quad (12.6)$$

For $N \rightarrow \infty$, this constant has the finite limit $\alpha_\infty^s = \pi^2/6$. The analogy with fermions cannot be used to calculate the free energy of a stack of membranes, where only approximate methods are available. We will tackle this problem by making use of a strong-coupling theory as in Refs. [48,89]. As a preparation, we apply this theory to the exactly solvable system of a stack of strings.

12.2.2 Perturbative Approach

The difficulty in solving the functional integral (12.2) arises from the restriction (12.4) of the fluctuations by the neighboring strings. To deal with this strong repulsion, we introduce into the action of the functional integral (12.2) a smooth potential that keeps the strings apart in such a way that the integration interval for the fluctuations can be extended to $\varphi_n(x) \in \{-\infty, \infty\}$. At the end, we take a strong-coupling limit, which ensures (12.4). In Refs. [48,89], such a method was used to evaluate the pressure constant for one membrane between walls. The smooth potential for the analogous case of one string is $V(\varphi(x)) = (2a\mu/\pi)^2 \tan^2[\pi\varphi(x)/2a]$, which describes the hard walls *exactly* for $\mu \rightarrow 0$. This potential is symmetric and possesses a minimum at $\varphi(x) = 0$. Thus its Taylor expansion around this minimum is a series in even powers of $\varphi(x)$.

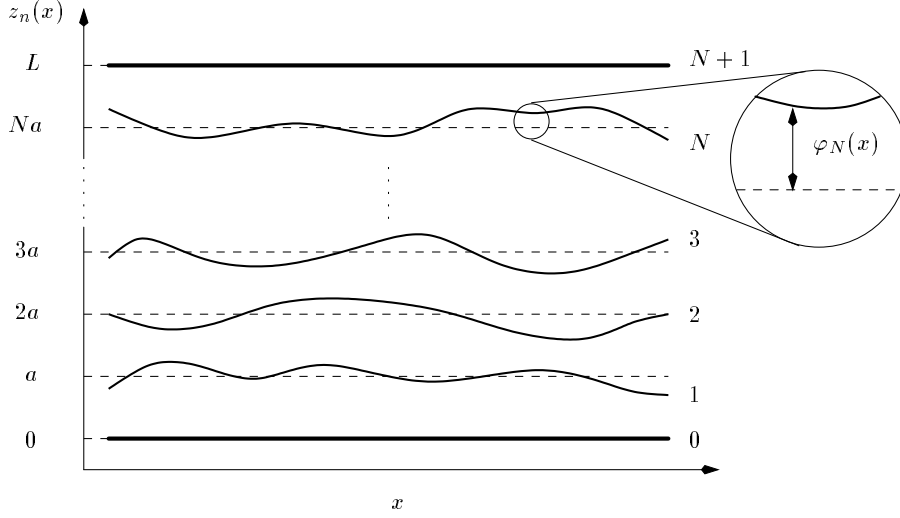


FIGURE 12.1: Stack of N strings with equilibrium spacing a between two walls of distance L . The magnifier shows the local displacement field $\varphi_N(x)$ as the distance from the position Na . The walls are labeled by 0 and $N+1$ and treated as non-fluctuating strings with $\varphi_0(x) \equiv \varphi_{N+1}(x) \equiv 0$.

In the case of N strings, the minima of the repulsion potential should lie at the equilibrium positions of the strings. The Taylor expansion of such a potential will also have terms with odd powers. Unlike the one-string system, where fluctuations are limited by fixed walls, the range of the displacements $\varphi_n(x)$ of the n th string in an N -string system depends on the positions $z_{n-1}(x)$ and $z_{n+1}(x)$ of the neighboring strings. Thus the potential will be taken as a sum,

$$V_{\text{eff}}(z_0(x), z_1(x), \dots, z_N(x), z_{N+1}(x)) = \frac{\sigma}{2} \sum_{n=1}^{N+1} V_{\mu}(\bar{\nabla}_n z_n(x)), \quad (12.7)$$

where $\bar{\nabla}_n z_n(x)$ denotes the prepoint lattice gradient $z_n(x) - z_{n-1}(x)$. This potential includes the interaction of the first and last strings with the walls as non-fluctuating strings at $z_0 = 0$ and $z_{N+1} = (N+1)a = L$:

$$\varphi_0(x) = \varphi_{N+1}(x) = 0. \quad (12.8)$$

In the limit $\mu \rightarrow 0$, the potential $V_{\mu}(\bar{\nabla}_n z_n(x))$ should again yield an infinitely strong repulsion of two neighboring strings for $z_n(x)$ close to $z_{n-1}(x)$. For $z_n(x) > z_{n-1}(x)$, the limiting potential should be zero. As a matter of choice, we let the potential between two strings $V_{\mu}(\bar{\nabla}_n z_n(x))$ be minimal and zero at the positions $z_n^{\text{eq}} = na$ and $z_{n-1}^{\text{eq}} = a(n-1)$: $dV_{\mu}(a)/d\bar{\nabla}_n z_n(x) = 0$ and $V_{\mu}(z_n^{\text{eq}} - z_{n-1}^{\text{eq}}) = V_{\mu}(a) = 0$ (see Fig. 12.2).

The Taylor expansion around the minimum is, in terms of the variables (12.1),

$$V_{\mu}(\bar{\nabla}_n \varphi_n(x)) = \frac{\mu^2}{2} [\bar{\nabla}_n \varphi_n(x)]^2 + \mu^2 \sum_{k=1}^{\infty} c_k g^k [\bar{\nabla}_n \varphi_n(x)]^{k+2}. \quad (12.9)$$

The parameter μ governs the harmonic term, whereas higher-order terms scale with the coupling constant $g = 1/a$, which makes the coefficients c_k dimensionless.

An example for a potential showing qualitatively the behavior in Fig. 12.2 with a Taylor expansion of the type (12.9) is $V_{\mu}(\bar{\nabla}_n z_n(x)) = \mu^2 (a/[\bar{\nabla}_n z_n(x)]^2 - 2/\bar{\nabla}_n z_n(x) + 1/a) / 2$, which vanishes everywhere for infinitesimal μ , except at $\bar{\nabla}_n z_n(x) = 0$. The strong-coupling limit of the perturbative expansion of order g^2 presented in this chapter cannot yield, however, reasonable results for such an arbitrary choice of the potential. The calculation of higher-order perturbative coefficients requires high numerical power, which would make this procedure of calculating the universal constants inefficient.

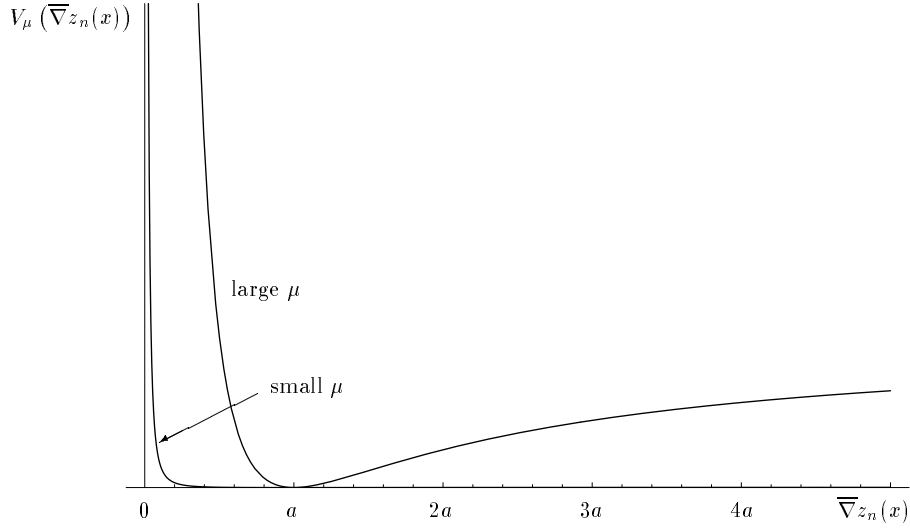


FIGURE 12.2: Potential $V_\mu(\overline{\nabla}_n z_n(x))$ of string-string interaction for finite μ and small μ as a function of $\overline{\nabla}_n z_n(x) = z_n(x) - z_{n-1}(x)$. The strings repel each other strongly for $\overline{\nabla}_n z_n(x) \rightarrow 0$, while the potential has a minimum at the equilibrium separation $\overline{\nabla}_n z_n(x) = a$, and we choose to normalize it to zero at that point.

Thus, we continue with the Taylor expansion (12.9), and the partition function (12.2) becomes

$$Z^s = \lim_{\mu \rightarrow 0} \oint \mathcal{D}^N \varphi(x) \exp \left\{ -\frac{\sigma}{2k_B T} \sum_{n=1}^{N+1} \int_{-\infty}^{\infty} dx \left(\left[\frac{d\varphi_n(x)}{dx} \right]^2 + \frac{1}{2} \mu^2 [\overline{\nabla}_n \varphi_n(x)]^2 \right) \right\} \\ \times \exp \left\{ -\frac{\sigma}{2k_B T} \mu^2 \sum_{k=1}^{\infty} c_k g^k \sum_{n=1}^{N+1} \int_{-\infty}^{\infty} dx [\overline{\nabla}_n \varphi_n(x)]^{k+2} \right\} \quad (12.10)$$

with the integral measure

$$\oint \mathcal{D}^N \varphi(x) = \prod_{n=1}^N \prod_x \left[\int_{-\infty}^{\infty} \frac{d\varphi_n(x)}{\sqrt{2\pi k_B T / \sigma}} \right]. \quad (12.11)$$

The harmonic part of the partition function can be written as

$$Z_\mu^s = \oint \mathcal{D}^N \varphi(x) \exp \left\{ -\frac{1}{2} \sum_{n=1}^{N+1} \sum_{n'=1}^{N+1} \int_{-\infty}^{\infty} dx \int_{-\infty}^{\infty} dx' \varphi_n(x) [G_{nn'}^s(x, x')]^{-1} \varphi_{n'}(x') \right\} \quad (12.12)$$

with the functional matrix

$$[G_{nn'}^s(x, x')]^{-1} = -\frac{\sigma}{k_B T} \left(\frac{d^2}{dx^2} + \frac{1}{2} \mu^2 \overline{\nabla}_n \nabla_n \right) \delta(x - x') \delta_{nn'}. \quad (12.13)$$

Here $\nabla_n \varphi_n(x) = \varphi_{n+1}(x) - \varphi_n(x)$ denotes the postpoint lattice gradient in the z direction, and $\overline{\nabla}_n \nabla_n$ is the lattice version of the Laplace operator [4].

Let us now impose the vanishing of the fluctuations of the walls (12.8), corresponding to Dirichlet boundary conditions. For a finite number N of strings, the Kronecker symbol $\delta_{nn'}$ in Eq. (12.13) has the Fourier representation

$$\delta_{nn'} = \frac{2}{N+1} \sum_{m=1}^N \sin \nu_m n a \sin \nu_m n' a \quad (12.14)$$

with wave numbers $\nu_m = \pi m/(N+1)a$. Thus the kernel $[G_{nn'}^s(x, x')]^{-1}$ may be written in Fourier space as

$$[G_{nn'}^s(x, x')]^{-1} = \frac{2}{N+1} \sum_{m=1}^N \sin \nu_m n a \sin \nu_m n' a \int_{-\infty}^{\infty} \frac{dk}{2\pi} [G_m^s(k)]^{-1} e^{-ik(x-x')} \quad (12.15)$$

with the Fourier components

$$[G_m^s(k)]^{-1} = \frac{\sigma}{k_B T} [k^2 + 2\mu^2 \sin^2(\nu_m a/2)]. \quad (12.16)$$

Integrating over k in the spectral representation (12.15) leads immediately to the correlation function in configuration space,

$$G_{nn'}^s(x, x') = \frac{1}{\sqrt{2}(N+1)} \frac{k_B T}{\mu\sigma} \sum_{m=1}^N \frac{\sin \nu_m n a \sin \nu_m n' a}{\sin(\nu_m a/2)} e^{-\sqrt{2}\mu|x-x'|\sin(\nu_m a/2)}, \quad (12.17)$$

and to the harmonic partition function (12.12),

$$Z_\mu^s = \exp \left\{ -\frac{1}{2} \text{Tr} \ln [G^s]^{-1} \right\} = e^{-A f_{N,\mu}^s / k_B T}, \quad (12.18)$$

the exponent giving the free energy per length,

$$f_{N,\mu}^s = \mu \frac{k_B T \sin[\pi N/4(N+1)]}{2 \sin[\pi/4(N+1)]}, \quad (12.19)$$

which vanishes for $\mu = 0$.

The full partition function Z^s in Eq. (12.10) is now calculated perturbatively. We introduce harmonic expectation values

$$\langle \cdots \rangle_\mu^s = [Z_\mu^s]^{-1} \oint \mathcal{D}^N \varphi(x) \cdots \exp \left\{ -\frac{1}{2} \sum_{n=1}^{N+1} \sum_{n'=1}^{N+1} \int_{-\infty}^{\infty} dx \int_{-\infty}^{\infty} dx' \varphi_n(x) [G_{nn'}^s(x, x')]^{-1} \varphi_{n'}(x') \right\} \quad (12.20)$$

in terms of which the correlation function is given by

$$G_{nn'}^s(x, x') = \langle \varphi_n(x) \varphi_{n'}(x') \rangle_\mu^s. \quad (12.21)$$

The perturbation expansion contains the two-point correlation function of $\bar{\nabla}_n \varphi_n(x)$, which is given by

$$\langle \bar{\nabla}_n \varphi_n(x) \bar{\nabla}_{n'} \varphi_{n'}(x') \rangle_\mu^s = \bar{\nabla}_n \bar{\nabla}_{n'} G_{nn'}^s(x, x'). \quad (12.22)$$

We now expand the second exponential in Eq. (12.10) in powers of the coupling constant g . Harmonic expectation values with odd powers of $\bar{\nabla}_n \varphi_n(x)$ do not contribute, and the expansion reads

$$Z^s = \lim_{\mu \rightarrow 0} Z_\mu^s \left[1 - g^2 \left(\frac{\sigma}{2k_B T} \mu^2 c_2 \sum_{n=1}^{N+1} \int_{-\infty}^{\infty} dx \langle [\bar{\nabla}_n \varphi_n(x)]^4 \rangle_\mu^s \right. \right. \\ \left. \left. - \frac{1}{2!} \frac{\sigma^2}{4k_B^2 T^2} \mu^4 c_1^2 \sum_{n,n'=1}^{N+1} \int_{-\infty}^{\infty} dx \int_{-\infty}^{\infty} dx' \langle [\bar{\nabla}_n \varphi_n(x)]^3 [\bar{\nabla}_{n'} \varphi_{n'}(x')]^3 \rangle_\mu^s \right) + \dots \right]. \quad (12.23)$$

In the sequel, we restrict ourselves to the terms of second order in $g = 1/a$, which contribute directly to the pressure law as in Eq. (12.5). The higher powers diverge for $\mu \rightarrow 0$, and in Refs. [48,89] it was shown how to calculate from them a finite strong-coupling limit. Here we shall ignore these terms for

reasons to be explained shortly. Re-expressing the right-hand side of Eq. (12.23) as an exponential of a cumulant expansion, we obtain the free energy per length,

$$f_N^s = \lim_{\mu \rightarrow 0} g^2 \left(\frac{\sigma}{2k_B T} \mu^2 c_2 \sum_{n=1}^{N+1} \int_{-\infty}^{\infty} dx \langle [\bar{\nabla}_n \varphi_n(x)]^4 \rangle_{\mu, c}^s - \frac{1}{2!} \frac{\sigma^2}{4k_B^2 T^2} \mu^4 c_1^2 \sum_{n, n'=1}^{N+1} \int_{-\infty}^{\infty} dx \int_{-\infty}^{\infty} dx' \langle [\bar{\nabla}_n \varphi_n(x)]^3 [\bar{\nabla}_{n'} \varphi_{n'}(x')]^3 \rangle_{\mu, c}^s \right) + \dots \quad (12.24)$$

We have used that the free energy $f_{N, \mu}^s$ of the harmonic system (12.19) vanishes in the limit $\mu \rightarrow 0$. The first cumulants are the expectations

$$\begin{aligned} \langle O_1(\bar{\nabla} \varphi_{n_1}(x_1)) \rangle_{\mu, c}^s &= \langle O_1(\bar{\nabla} \varphi_{n_1}(x_1)) \rangle_{\mu}^s \\ \langle O_1(\bar{\nabla} \varphi_{n_1}(x_1)) O_2(\bar{\nabla} \varphi_{n_2}(x_2)) \rangle_{\mu, c}^s &= \langle O_1(\bar{\nabla} \varphi_{n_1}(x_1)) O_2(\bar{\nabla} \varphi_{n_2}(x_2)) \rangle_{\mu}^s \\ &\quad - \langle O_1(\bar{\nabla} \varphi_{n_1}(x_1)) \rangle_{\mu}^s \langle O_2(\bar{\nabla} \varphi_{n_2}(x_2)) \rangle_{\mu}^s, \\ &\quad \vdots \end{aligned} \quad (12.25)$$

defined for any polynomial function $O_i(\bar{\nabla} \varphi_{n_i}(x_i))$ of $\bar{\nabla} \varphi_{n_i}(x_i)$. Following Wick's rule, we expand the expectations into products of two-point correlation functions (12.22). The different terms are displayed with the help of Feynman diagrams, in which lines and vertices represent the correlation functions and interactions:

$$x_1, n_1 \text{ --- } x_2, n_2 \quad \longrightarrow \quad \langle \bar{\nabla}_{n_1} \varphi_{n_1}(x_1) \bar{\nabla}_{n_2} \varphi_{n_2}(x_2) \rangle_{\mu}^s, \quad (12.26)$$

$$\bullet \quad \longrightarrow \quad \sum_{n=1}^{N+1} \int_{-\infty}^{\infty} dx. \quad (12.27)$$

In what follows, we assume that the potential parameters c_k with $k \geq 3$ are chosen in such a way that they make all terms of order g^3 and higher vanish. Dividing the free energy (12.24) by N , we obtain the following expression for the free energy per length and string, which can be compared with Eq. (12.5):

$$\Delta f_N^s = \lim_{\mu \rightarrow 0} \left\{ \frac{3}{2} \frac{\sigma \mu^2}{A a^2} c_2 \text{ (diagram)} - \frac{1}{8} \frac{\sigma^2 \mu^4}{k_B T A a^2} c_1^2 \left(6 \text{ (diagram)} + 9 \text{ (diagram)} \right) \right\}. \quad (12.28)$$

The calculation of the Feynman diagrams is straightforward using Eq. (12.17). The evaluation is only complicated by the Dirichlet boundary conditions, which destroy momentum conservation. This makes the numeric calculation quite time-consuming for an increasing number N of strings. As an explicit example, consider the sunset diagram, which requires the evaluation of the multiple sum

$$\begin{aligned} \text{(diagram)} &\equiv A \frac{k_B^3 T^3}{\mu^4} \frac{1}{2(N+1)^3} \sum_{n_1, n_2=1}^{N+1} \sum_{\substack{m_1, m_2, \\ m_3=1}}^N h_{n_1 n_2}^{m_1} h_{n_1 n_2}^{m_2} h_{n_1 n_2}^{m_3} \\ &\quad \times \frac{1}{\sin(\nu_{m_1} a/2) \sin(\nu_{m_2} a/2) \sin(\nu_{m_3} a/2) [\sin(\nu_{m_1} a/2) + \sin(\nu_{m_2} a/2) + \sin(\nu_{m_3} a/2)]}, \end{aligned} \quad (12.29)$$


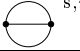

with the abbreviation

$$\begin{aligned} h_{n_1 n_2}^m &= \sin \nu_m n_1 a \sin \nu_m n_2 a - \sin \nu_m n_1 a \sin \nu_m (n_2 - 1) a \\ &\quad - \sin \nu_m (n_1 - 1) a \sin \nu_m n_2 a + \sin \nu_m (n_1 - 1) a \sin \nu_m (n_2 - 1) a. \end{aligned} \quad (12.30)$$

It is useful to factor out the physical dimension of the diagram. Any Feynman integral W^s with l lines and v vertices can be expressed in terms of a reduced dimensionless Feynman integral $W^{s,r}$ as

$$W^s = A \left(\frac{k_B T}{\sigma} \right)^l \mu^{-(l+v-1)} W^{s,r}. \quad (12.31)$$

TABLE 12.1: Reduced numeric values $W^{s,r}$ of the two-loop diagrams for the free energy for a stack of N strings.

N			
1	1/2	0	0
2	1.288675	0.398717	0.089316
3	2.100656	0.832299	0.146447
4	2.915827	1.270787	0.184463
5	3.730993	1.709326	0.211325
6	4.545586	2.147034	0.231245
7	5.359574	2.583849	0.246583

This brings Eq. (12.28) to the form

$$\Delta f_N^s = \alpha_N^s \frac{k_B^2 T^2}{\sigma a^2}, \quad (12.32)$$

$$\alpha_N^s = \frac{1}{N} \left[\frac{3}{2} c_2 \text{ (two circles connected by two arcs)} - c_1^2 \left(\frac{3}{4} \text{ (circle with horizontal line)} + \frac{9}{8} \text{ (two circles connected by a horizontal line)} \right) \right], \quad (12.33)$$

where the diagrams indicate the reduced Feynman integrals. Their values are listed in Table 12.1 for different string numbers N . Note that the $1/a^2$ contributions to the free energy per length and string in Eq. (12.28) are independent of μ since the μ prefactors are canceled by the μ dependence of the diagrams. Thus the limit $\mu \rightarrow 0$ becomes trivial for these contributions.

With the knowledge of the exact values of the constants α_N^s from Eq. (12.6), we are now in a position to determine the potential parameters c_1 and c_2 from Eq. (12.33) to obtain the exact result from the two-loop expansion Eq. (12.33). Comparing Eqs. (12.33) and (12.6) for $N = 1$ and $N = 2$, we obtain

$$c_1 = \frac{\pi}{3}, \quad c_2 = \frac{\pi^2}{6}. \quad (12.34)$$

Note that (12.33) consists of more equations than necessary to compute c_1 and c_2 . It turns out, however, that all of them give the same parameters c_1 and c_2 , such that the same potential (12.9) can be used for any N . This is the essential basis for applying this procedure to a stack of membranes.

We now justify the neglect of the higher g powers that would in principle give further contributions to the pressure constant α_N^s in the strong-coupling limit. We simply observe that it is possible to choose the higher expansion coefficients c_k to make all higher g^n contributions vanish [103].

12.3 Stack of Membranes

Having determined the parameters c_1 and c_2 of the Taylor expansion (12.9) of the smooth potential applicable for any number of strings, we shall now use the same potential for a perturbative expansion in a stack of N membranes displayed in Fig. 12.3. The equilibrium spacing at low temperature between the membranes is again a . Denoting the vectors in the plane by $\mathbf{x} = (x, y)$, the vertical displacements of the membranes from the positions na are $\varphi_n(\mathbf{x})$, with Dirichlet boundary conditions at z_0 and z_{N+1} ,

$$\varphi_0(\mathbf{x}) = \varphi_{N+1}(\mathbf{x}) = 0. \quad (12.35)$$

For membranes without tension, the energy has the harmonic approximation

$$E_{C,n} = \frac{\kappa}{2} \int d^2x [\partial^2 \varphi_n(\mathbf{x})]^2, \quad (12.36)$$

where κ is the bending stiffness and $\partial^2 = \partial_x^2 + \partial_y^2$ is the Laplacian in the plane parallel to the walls. By analogy with the preceding section, the kernel of the harmonic stack now reads

$$[G_{n_1 n_2}(\mathbf{x}_1, \mathbf{x}_2)]^{-1} = -\frac{\kappa}{k_B T} \left([\partial_{\mathbf{x}_1}^2]^2 + \frac{1}{2} \mu^4 \bar{\nabla}_{n_1} \nabla_{n_1} \right) \delta(\mathbf{x}_1 - \mathbf{x}_2) \delta_{n_1 n_2}, \quad (12.37)$$

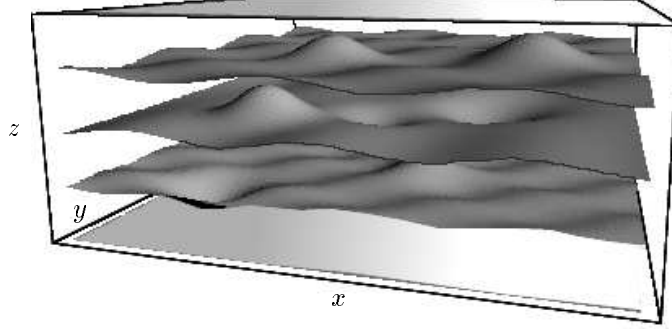


FIGURE 12.3: Stack of self-avoiding fluid membranes fluctuating in the z direction between two walls. As for the previous stack of strings, the walls are treated as non-fluctuating membranes.

where we have used a mass parameter μ^4 instead of μ^2 , for dimensional reasons. The partition function for the stack of membranes is then written up to order $g^2 = 1/a^2$ by

$$\begin{aligned}
Z = & \lim_{\mu \rightarrow 0} \oint \mathcal{D}^N \varphi(\mathbf{x}) \exp \left\{ -\frac{1}{2} \sum_{n_1, n_2=1}^{N+1} \int d^2 x_1 \int d^2 x_2 \varphi_{n_1}(\mathbf{x}_1) [G_{n_1 n_2}(\mathbf{x}_1, \mathbf{x}_2)]^{-1} \varphi_{n_2}(\mathbf{x}_2) \right\} \\
& \times \left[1 - g^2 \left(\frac{\kappa}{2k_B T} \mu^4 c_2 \sum_{n=1}^{N+1} \int d^2 x [\nabla \varphi_n(\mathbf{x})]^4 - \frac{\kappa^2}{8k_B^2 T^2} \mu^8 c_1^2 \sum_{n_1, n_2=1}^{N+1} \int d^2 x_1 \int d^2 x_2 \right. \right. \\
& \left. \left. \times [\nabla \varphi_{n_1}(\mathbf{x}_1)]^3 [\nabla \varphi_{n_2}(\mathbf{x}_2)]^3 \right) \right], \tag{12.38}
\end{aligned}$$

with the same parameters c_1 and c_2 of the Taylor expansion (12.9) as in the string system, determined in Eq. (12.34). We neglect terms of order g^3 , which certainly contribute in the strong-coupling limit, and which vanish only for the strings, where the partition function (12.23) with the choice (12.34) for the parameters c_1, c_2 is exact in second order. An evaluation of the neglected terms by variational perturbation theory is expected to give only a negligible contribution to our final result.

Inverting the kernel (12.37) yields the correlation function

$$G_{n_1 n_2}(\mathbf{x}_1, \mathbf{x}_2) = \frac{2}{N+1} \frac{k_B T}{\kappa} \sum_{m=1}^N \sin \nu_m n_1 a \sin \nu_m n_2 a \int \frac{d^2 k}{(2\pi)^2} \frac{1}{k^4 + 2\mu^4 \sin^2(\nu_m a/2)} e^{-i\mathbf{k}(\mathbf{x}_1 - \mathbf{x}_2)}. \tag{12.39}$$

The explicit calculation of the Fourier integral leads to a difference of modified Bessel functions $K_0(x)$ as in Ref. [48]:

$$\begin{aligned}
G_{n_1 n_2}(\mathbf{x}_1, \mathbf{x}_2) = & \frac{i}{\sqrt{8\pi(N+1)\mu^2}} \frac{k_B T}{\kappa} \sum_{m=1}^N \frac{\sin \nu_m n_1 a \sin \nu_m n_2 a}{\sin(\nu_m a/2)} \\
& \times \left[K_0 \left(2^{1/4} \sqrt{i \sin(\nu_m a/2)} \mu |\mathbf{x}_1 - \mathbf{x}_2| \right) - K_0 \left(2^{1/4} \sqrt{-i \sin(\nu_m a/2)} \mu |\mathbf{x}_1 - \mathbf{x}_2| \right) \right]. \tag{12.40}
\end{aligned}$$

For $\mathbf{x}_1 = \mathbf{x}_2 \equiv \mathbf{x}$ and $n_1 = n_2 \equiv n$, this reduces to

$$G_{nn}(\mathbf{x}, \mathbf{x}) = \frac{1}{\sqrt{32(N+1)\mu^2}} \frac{k_B T}{\kappa} \sum_{m=1}^N \frac{\sin^2 \nu_m n a}{\sin(\nu_m a/2)}, \tag{12.41}$$

leading to the partition function of the harmonic system,

$$Z_\mu = \exp \left\{ -\frac{1}{2} \text{Tr} \ln G^{-1} \right\} = \exp \left\{ -\mu^2 \frac{A \sin[\pi N/4(N+1)]}{8 \sin[\pi/4(N+1)]} \right\}, \tag{12.42}$$

where $A = \int d^2x$ is the area of the projected plane of the membranes. The free energy per area $f_{N,\mu} = -(k_B T/A) \ln Z_\mu$ vanishes again for $\mu = 0$.

As for the calculation of the free energy of the stack of strings, we introduce harmonic expectation values

$$\langle \cdots \rangle_\mu = [Z_\mu]^{-1} \oint \mathcal{D}^N \varphi(\mathbf{x}) \cdots \exp \left\{ -\frac{1}{2} \sum_{n=1}^{N+1} \sum_{n'=-\infty}^{N+1} \int d^2x \int_{-\infty}^{\infty} d^2x' \varphi_n(\mathbf{x}) [G_{nn'}(\mathbf{x}, \mathbf{x}')]^{-1} \varphi_{n'}(\mathbf{x}') \right\}, \quad (12.43)$$

which appear in the perturbation expansion of Eq. (12.38), the cumulants yielding a perturbative expansion for the free energy per area $f_N = -(k_B T/A) \ln Z$. The lines and vertices in the Feynman diagrams now stand for

$$\mathbf{x}_1, n_1 \text{ --- } \mathbf{x}_2, n_2 \longrightarrow \langle \bar{\nabla}_{n_1} \varphi_{n_1}(\mathbf{x}_1) \bar{\nabla}_{n_2} \varphi_{n_2}(\mathbf{x}_2) \rangle_\mu \quad (12.44)$$

$$\bullet \longrightarrow \sum_{n=1}^{N+1} \int d^2x, \quad (12.45)$$

and the two-loop approximation to the free energy per area and membrane in order $1/a^2$ reads

$$\Delta f_N = \lim_{\mu \rightarrow 0} \left\{ \frac{\pi^2 \kappa \mu^4}{4 A a^2} \text{ (two-loop diagram) } - \frac{\pi^2 \kappa^2 \mu^8}{k_B T A a^2} \left(\frac{1}{12} \text{ (circle with line) } + \frac{1}{8} \text{ (two circles with line) } \right) \right\}. \quad (12.46)$$

Going over to reduced Feynman integrals as in Eq. (12.31),

$$W = A \left(\frac{k_B T}{\kappa} \right)^l \mu^{-2(l+v-1)} W^r, \quad (12.47)$$

where v is the number of vertices and l the number of lines of the diagram, we obtain

$$\Delta f_N = \alpha_N \frac{k_B^2 T^2}{\kappa a^2}, \quad (12.48)$$

$$\alpha_N = \frac{\pi^2}{N} \left(\frac{1}{4} \text{ (two-loop diagram) }^r - \frac{1}{12} \text{ (circle with line) }^r - \frac{1}{8} \text{ (two circles with line) }^r \right). \quad (12.49)$$

The pressure exerted by the membranes upon the walls is obtained by differentiating the free energy $f_N = N \Delta f_N$ with respect to the distance of the walls $L = a(N+1)$:

$$p_N = -N \frac{\partial \Delta f_N}{\partial L} = \frac{2N}{N+1} \alpha_N \frac{k_B^2 T^2}{\kappa a^3}. \quad (12.50)$$

The first and the last Feynman integrals in Eq. (12.49) are the simplest:

$$\text{ (two-loop diagram) }^r \equiv \frac{1}{32(N+1)^2} \sum_{n=1}^{N+1} \left[\sum_{m=1}^N \frac{h_{nn}^m}{\sin(\nu_m a/2)} \right]^2, \quad (12.51)$$

$$\text{ (two circles with line) }^r \equiv \frac{1}{32(N+1)^3} \sum_{n_1, n_2=1}^{N+1} \sum_{\substack{m_1, m_2, \\ m_3=1}}^N \frac{h_{n_1 n_1}^{m_1} h_{n_1 n_2}^{m_2} h_{n_2 n_2}^{m_3}}{\sin(\nu_{m_1} a/2) \sin^2(\nu_{m_2} a/2) \sin(\nu_{m_3} a/2)}, \quad (12.52)$$

where we have used the abbreviation $h_{n_1 n_2}^m$ defined in Eq. (12.30). The evaluation of the second diagram in Eq. (12.49) is much more involved. The Fourier integrals can be done exactly, except for one, which must be treated numerically. This calculation is deferred to Appendix 12A. The values of the three diagrams are listed in Table 12.2 for various numbers of membranes. With these numbers, the evaluation of the pressure constants yields the results given in Table 12.3. Except for $N = 1$ and $N \rightarrow \infty$, no analytical values were found in the literature. We also compare with pressure constants

TABLE 12.2: Numeric values W^r of the reduced two-loop Feynman integrals contributing to the pressure constants of a stack of N membranes in Eq. (12.49).

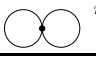
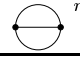
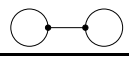
N			
1	1/32	0	0
2	0.080542	0.022446	0.005582
3	0.131291	0.046992	0.009153
4	0.182239	0.071866	0.011529
5	0.233187	0.096762	0.013208
6	0.284099	0.121619	0.014453
7	0.334973	0.146428	0.015411
8	0.385815	0.171195	0.016172
9	0.436630	0.195925	0.016789
10	0.487422	0.220624	0.017300
11	0.538197	0.245300	0.017730
12	0.588958	0.269954	0.018097
13	0.639706	0.294592	0.018414
14	0.690444	0.319215	0.018690
15	0.741174	0.343827	0.018933

TABLE 12.3: Pressure constants α_N for different numbers N of membranes in the stack, calculated from Eq. (12.49), with the numerical values of the two-loop diagrams given in Table 12.2. We compare with results from Monte Carlo simulations and earlier analytic results.

N	α_N	Monte Carlo results	earlier analytic values
1	$\pi^2/128 \approx 0.07711$	0.060 [85], 0.078 ± 0.001 [86], 0.0798 ± 0.0003 [88], 0.080 [86]	$\pi^2/128$ [87,89], 0.079715 [48]
2	0.08669		
3	0.09134	0.093 ± 0.004 [88], 0.1002 ± 0.0006 [86]	
4	0.09408		
5	0.09590	0.0966 [88], 0.1022 ± 0.0006 [86]	
6	0.09719		
7	0.09815	0.1009 ± 0.0007 [86]	
8	0.09890		
9	0.09950		
10	0.09999		
11	0.10039		
12	0.10074		
13	0.10103		
14	0.10129		
15	0.10151		
∞	0.10409	0.074 [104], 0.101 ± 0.002 [86], 0.106 [88]	$3\pi^2/128 \approx 0.23$ [50]

obtained by Monte Carlo simulations and find a good agreement [86,88]. The values of the Monte Carlo simulations for $N = 3, 5, 7$ from Ref. [86] show an independence of the number N of membranes. This arises by the simulation technique, where the free energy of the central membrane was determined. In contrast to that, we have calculated the pressure constant from the free energy of the complete system averaged over all membranes. Thus these Monte Carlo values cannot directly be compared with ours.

Table 12.3 contains also a value α_∞ for an infinite number $N \rightarrow \infty$ of membranes in the stack. This pressure constant is obtained by the following extrapolation procedure. We assume that the pressure constants determined for $N = 12, 13, 14, 15$ are of higher accuracy than those for lower numbers of membranes. This assumption is justified by comparing our values for $N = 1, 3, 5$ with the latest Monte Carlo results [88]. For $N = 1$, the deviation is about 3.4%. Considering $N = 3$, the deviation reduces to 1.8% and further to 1.1% for five membranes. Since the pressure constants are approximated increasingly fast with an increasing number N of membranes, we make the following exponential ansatz for determining the approach to infinite N :

$$\alpha_N = \alpha_\infty [1 - \eta \exp(-\xi N^\varepsilon)]. \quad (12.53)$$

The unknown four parameters in this equation are then determined by solving the system of equations with the pressure constants α_{12} , α_{13} , α_{14} , and α_{15} listed in Table 12.3. We obtain $\eta \approx 1.1712$, $\xi \approx 1.6417$, $\varepsilon \approx 0.3154$, and thus the limiting pressure constant for an infinite stack of membranes,

$$\alpha_\infty \approx 0.1041. \quad (12.54)$$

This value is in very good agreement with the Monte Carlo result [88] (see the last row of Table 12.3). It differs by a factor close to 9/4 from the initial result by Helfrich [50,105].

12A Evaluation of the Sunset Diagram

The second diagram in Eq. (12.49) requires some simplification before the numerical calculation. We write the reduced Feynman integral as

$$\textcircled{\text{---}}^r \equiv \frac{8}{A(N+1)^3} \sum_{n_1, n_2=1}^{N+1} \sum_{\substack{m_1, m_2, \\ m_3=1}}^N h_{n_1 n_2}^{m_1} h_{n_1 n_2}^{m_1} h_{n_1 n_2}^{m_1} K_{m_1 m_2 m_3} \quad (12A.1)$$

with the integral

$$K_{m_1 m_2 m_3} = \int d^2 x_1 d^2 x_2 \int \frac{d^2 k_1}{(2\pi)^2} \frac{d^2 k_2}{(2\pi)^2} \frac{d^2 k_3}{(2\pi)^2} \frac{e^{-i(\mathbf{k}_1 + \mathbf{k}_2 + \mathbf{k}_3)(\mathbf{x}_1 - \mathbf{x}_2)}}{(\mathbf{k}_1^4 + 2 \sin^2 \nu_{m_1} a)(\mathbf{k}_2^4 + 2 \sin^2 \nu_{m_2} a)(\mathbf{k}_3^4 + 2 \sin^2 \nu_{m_3} a)}. \quad (12A.2)$$

All integrals are easily calculated, except for one. If we introduce abbreviations

$$M_l^2 = 2 \sin^2 \nu_{m_l} a, \quad l = 1, 2, 3, \quad (12A.3)$$

we find

$$K_{m_1 m_2 m_3} = \frac{A}{2\pi} \int_0^\infty dk \frac{k}{\mathbf{k}^4 + M_3^2} J(\mathbf{k}, M_1^2, M_2^2) \quad (12A.4)$$

with

$$J(\mathbf{k}, M_1^2, M_2^2) = \int \frac{d^2 p}{(2\pi)^2} \frac{1}{(\mathbf{p} - \mathbf{k})^4 + M_1^2} \frac{1}{\mathbf{p}^4 + M_2^2}. \quad (12A.5)$$

Decomposing the integrand into partial fractions

$$J(\mathbf{k}, M_1^2, M_2^2) = -\frac{1}{4M_1 M_2} \int \frac{d^2 p}{(2\pi)^2} \left[\frac{1}{(\mathbf{p} - \mathbf{k})^2 + iM_1} - \frac{1}{(\mathbf{p} - \mathbf{k})^2 - iM_1} \right] \left[\frac{1}{\mathbf{p}^2 + iM_2} - \frac{1}{\mathbf{p}^2 - iM_2} \right]$$

$$= -\frac{1}{4M_1M_2} [I(\mathbf{k}, M_1, M_2) - I(\mathbf{k}, M_1, -M_2) - I(\mathbf{k}, -M_1, M_2) + I(\mathbf{k}, -M_1, -M_2)], \quad (12A.6)$$

we are left with integrals of the type

$$I(\mathbf{k}, \gamma_1, \gamma_2) = \int \frac{d^2p}{(2\pi)^2} \frac{1}{(\mathbf{p} - \mathbf{k})^2 + i\gamma_1} \frac{1}{\mathbf{p}^2 + i\gamma_2}, \quad (12A.7)$$

where $\gamma_{1,2} = \pm M_{1,2}$ are real numbers. Employing Feynman's parameterization, these integrals become

$$I(\mathbf{k}, \gamma_1, \gamma_2) = \frac{1}{4\pi} \int_0^1 dx \frac{1}{-x^2k^2 + x(k^2 + i\gamma_1 - i\gamma_2) + i\gamma_2}, \quad (12A.8)$$

taking the general form

$$\int dx \frac{1}{ax^2 + bx + c} = \frac{2}{\sqrt{\Delta}} \arctan z(x) \quad (12A.9)$$

with

$$\Delta = 4ac - b^2, \quad z(x) = \frac{b + 2ax}{\sqrt{\Delta}}, \quad a = -k^2, \quad b = k^2 + i(\gamma_1 - \gamma_2), \quad c = i\gamma_2. \quad (12A.10)$$

Since b is a complex number, $\text{Re} \arctan z$ is discontinuous, if $\text{Re} z$ changes sign and $|\text{Im} z| > 1$. Thus the right-hand side of Eq. (12A.9) is discontinuous at a certain point x_0 within the interval $[0, 1]$. As will be seen subsequently, $J(\mathbf{k}, M_1^2, M_2^2)$ from Eq. (12A.5) must be real and thus all imaginary contributions in the decomposed form (12A.6) cancel each other.

We determine the point of discontinuity x_0 to obtain the solution of the integral (12A.8) by investigating the zero of the real parts of $z(x)$. Decomposing $z(x_0)$ into real and imaginary part, we obtain

$$\text{Re} z(x) = |\Delta|^{-1/2} \left[k^2(1 - 2x) \cos \left(\frac{1}{2} \arctan \frac{\text{Re} \Delta}{\text{Im} \Delta} \right) + (\gamma_1 - \gamma_2) \sin \left(\frac{1}{2} \arctan \frac{\text{Re} \Delta}{\text{Im} \Delta} \right) \right], \quad (12A.11)$$

$$\text{Im} z(x) = |\Delta|^{-1/2} \left[(\gamma_1 - \gamma_2) \cos \left(\frac{1}{2} \arctan \frac{\text{Re} \Delta}{\text{Im} \Delta} \right) - k^2(1 - 2x) \sin \left(\frac{1}{2} \arctan \frac{\text{Re} \Delta}{\text{Im} \Delta} \right) \right], \quad (12A.12)$$

where

$$\text{Re} \Delta = (\gamma_1 - \gamma_2)^2 - k^4, \quad \text{Im} \Delta = -2k^2(\gamma_1 + \gamma_2). \quad (12A.13)$$

Thus, the zero of $\text{Re} z(x)$ is found at

$$x_0 = \frac{1}{2} \left\{ 1 + \frac{\gamma_1 - \gamma_2}{k^2} \tan \left[\frac{1}{2} \arctan \frac{2k^2(\gamma_1 + \gamma_2)}{k^4 - (\gamma_1 - \gamma_2)^2} \right] \right\}. \quad (12A.14)$$

From the bounds of integration in Eq. (12A.8), it follows that we must include the discontinuities of Eq. (12A.9) for $x_0 \in [0, 1]$. This occurs if $k < |\gamma_1 - \gamma_2|$ and $\text{sign} \gamma_1 \neq \text{sign} \gamma_2$. Thus the solution of the integral (12A.8) reads

$$I(\mathbf{k}, \gamma_1, \gamma_2) = \begin{cases} S(\mathbf{k}, \gamma_1, \gamma_2, x) \Big|_{x=0}^{x=1}, & \text{sign} \gamma_1 = \text{sign} \gamma_2 \vee (\text{sign} \gamma_1 \neq \text{sign} \gamma_2 \wedge k \geq \sqrt{|\gamma_1 - \gamma_2|}), \\ \lim_{\varepsilon \rightarrow 0} \left[S(\mathbf{k}, \gamma_1, \gamma_2, x) \Big|_{x=0}^{x=x_0-\varepsilon} + S(\mathbf{k}, \gamma_1, \gamma_2, x) \Big|_{x=x_0+\varepsilon}^{x=1} \right], & \text{sign} \gamma_1 \neq \text{sign} \gamma_2 \wedge k < \sqrt{|\gamma_1 - \gamma_2|}, \end{cases} \quad (12A.15)$$

where $S(\mathbf{k}, \gamma_1, \gamma_2, x)$ is the explicit right-hand side of Eq. (12A.9):

$$S(\mathbf{k}, \gamma_1, \gamma_2, x) = \frac{1}{2\pi \sqrt{(\gamma_1 - \gamma_2)^2 - k^4 - 2ik^2(\gamma_1 + \gamma_2)}} \arctan \frac{k^2(1 - 2x) + i(\gamma_1 - \gamma_2)}{\sqrt{(\gamma_1 - \gamma_2)^2 - k^4 - 2ik^2(\gamma_1 + \gamma_2)}}. \quad (12A.16)$$

The function $I(\mathbf{k}, \gamma_1, \gamma_2)$ possesses the properties

$$I(\mathbf{k}, \gamma_1, -\gamma_2) + I(\mathbf{k}, -\gamma_1, \gamma_2) = 2\operatorname{Re} I(\mathbf{k}, \pm\gamma_1, \mp\gamma_2), \quad (12A.17)$$

$$I(\mathbf{k}, \gamma_1, \gamma_2) + I(\mathbf{k}, -\gamma_1, -\gamma_2) = 2\operatorname{Re} I(\mathbf{k}, \pm\gamma_1, \pm\gamma_2). \quad (12A.18)$$

Inserting Eq. (12A.15) into Eq. (12A.6), the remaining integral in Eq. (12A.4) together with the sums in expression (12A.1) for the sunset diagram can be calculated numerically. The values are listed for $N = 1, \dots, 15$ in the third column of Table 12.2.

Concluding Remarks

Summary

The main aspect of this thesis was to extend the range of applicability for functional integrals in quantum statistics and quantum field theory. Distributed over four parts, this thesis combines the formal justification of dealing with continuous path integrals from a perturbative point of view and a general solution for Gaussian path integrals in phase space with variational perturbation theory as a powerful resummation method which is also applicable for strongly coupled systems, where perturbative methods fail. The perturbative column on the one hand and the nonperturbative one on the other hand are bridged by a recursive graphical construction method which permits a systematic generation of all topologically different Feynman diagrams contributing to any order of perturbation with their correct multiplicities. As an interesting detail, the applicability of this method in quantum field theory is demonstrated for quantum electrodynamical scattering processes.

Motivated by the partial nonexistence of analytic results we have applied variational perturbation theory for atomic systems at arbitrary temperature and thermodynamical properties of fluctuating membranes. To this end, we have extended and generalized variational perturbation theory in a manifold way. For calculating density matrices, we generalized the smearing formula which accounts for the effects of thermal and quantum fluctuations. This was essential for the treatment of nonpolynomial interactions. We applied the theory to calculate the particle density in the double-well potential, and the electron density in the Coulomb potential, the latter as an example for nonpolynomial application. In both cases, the approximations were satisfactory.

We have also calculated the effective classical potential for the hydrogen atom in a magnetic field. For this we have extended variational perturbation theory to phase space to make it applicable to physical systems with uniform external magnetic field. The effective classical potential containing the complete quantum statistical information of the system was determined in first-order variational perturbation theory. For zero-temperature, it gave the binding energy of the system. Our result consists of a single analytic expression which is quite accurate at all temperatures and magnetic field strengths. The different asymptotic behavior of the perturbation series for the binding energy for weak and strong magnetic fields has been investigated in detail. In the weak-field case, we confirmed the power series character of the expansion, while for strong magnetic field strengths a deeply structured logarithmic behavior occurs.

As an application for strong-coupling theory in membrane physics, we have calculated the universal constant α occurring in the pressure law of a membrane fluctuating between two walls. This has been done by replacing the walls by a smooth potential with a parameter m^2 . This potential approaches the wall potential in the limit $m^2 \rightarrow 0$. The anharmonic part of the smooth potential was treated perturbatively. The limit $m^2 \rightarrow 0$ corresponds to a strong-coupling limit of the power series, and was

calculated by variational perturbation theory. Extrapolating the lowest four approximations to infinity yields a pressure constant, which is in very good agreement with Monte Carlo values.

We have also calculated the pressure constants for a stack of different numbers of membranes between two walls in excellent agreement with results from Monte Carlo simulations. The requirement that the membranes cannot penetrate each other was accounted for by introducing a repulsive potential and going to the strong-coupling limit of hard repulsion. We have used the similarity of the membrane system to a stack of strings enclosed by line-like walls, which is exactly solvable, to determine the potential parameters in such a way that the two-loop result is exact. This minimizes the neglected terms in the variational perturbation expansion, when applying the same potential to membranes.

It was shown in this thesis that variational perturbation theory can successfully be applied to a large variety of problems in quantum statistics and membrane physics. The results obtained for fluctuating strings and membranes open the gate to a large field of applications to be harvested with the help of this strong-coupling theory.

Acknowledgments

I am deeply thankful to **Professor H. Kleinert** for giving me the opportunity to participate in his broad and fine-structured spectrum of knowledge that covers almost all fields of physics. It was a pleasure to be guided safely through the jungle of theoretical physics by his expert advice, brilliant ideas, and what I would call his *ingenious* moments, whenever he already foresaw the solution of a problem before I calculated it. Nevertheless, I had enough free space to develop my own ideas which we fairly discussed. Following his example, he motivated me to gain insight into different fields of physical research, ranging from atomic physics and quantum statistics over quantum field theory to membrane physics. It was just the mixture of his advice and my independent work that made this cooperation so successful and pleasurable.

I am also highly indebted to **Dr. A. Pelster**, who kindly integrated me into the work group and strongly helped me to setup a Ph.D. research program. He initiated our first project which made it quite easy for me to continue my research without delay. From him I learned innumerable mathematical tricks being extremely valuable for the daily work with path integrals. We continued our successful cooperation over the past years, culminating in numerous research projects from several areas in physics. His motivating kind made it also possible for me to survive times of rather low progress.

It is also a pleasure to thank **Dr. H.-J. Schmidt** for our joint project in quantum cosmology¹ and for his support. It was he who introduced me to general relativity and cosmology.

I would also like to thank all members of our research group I enjoyed to learn to know in discussions and talks. In particular, I thank **Dr. B. Kastening** for sharing the interest in the systematic graphical construction of Feynman diagrams and **Dr. A. Chervyakov** for the interchange of experiences in establishing a perturbative definition of path integrals.

I am grateful to the other editors of our book *Fluctuating Paths and Fields* (World Scientific, Singapore, 2001), **Professor W. Janke**, **Dr. A. Pelster**, and **Dr. H.-J. Schmidt** for giving me the possibility to participate in this project.

The calculations for the determination of the quantum statistical properties of hydrogen in the presence of an external magnetic field were very exhaustive and thus I appreciate the correspondence with **Professor J. Čížek** and **Dr. E. J. Weniger**, who supported me with valuable hints and references to the perturbative treatment of the ground-state properties of hydrogen in magnetic field. I also thank my esteemed M.S. thesis adviser **Professor W. Ebeling** as well as my former colleagues at the Humboldt University, **Dr. J. Ortner** and **Dr. M. Steinberg**, for discussions on the finite-temperature behavior of the system. We had also interesting discussions on this subject with **Professor J. T. Devreese** and **Professor G. Wunner**, whom I would also like to thank.

I am indebted to **Professor R. Lipowsky** for interesting discussions about membrane and polymer physics in the mountains of Molveno in the Dolomites. Hints and references as well as the preparation of the talk I held there about membranes and vesicles influenced my own work in this subject. I also thank **Professor W. Janke** for comments about the Monte Carlo simulation procedure he used to calculate the pressure constants for a stack of membranes.

I deeply appreciate support by the Studienstiftung des deutschen Volkes, in particular I thank

¹We adiabatically solved the Wheeler-DeWitt equation for the minisuperspace of a strongly anisotropic cosmological Bianchi type-I model with a minimally coupled massive scalar field. As a main result, we found a period-doubling bifurcation of the ψ function near the cosmological quantum boundary [106].

the official for Ph.D. furtherance, **Dr. N. Weidtmann**. Attending three summer academies in La Rochelle, Bradfield, and Molveno, and participating in the meeting of Ph.D. students at Jerusalem, this foundation enabled me to enlarge my scientific horizon and to get into contact with like-minded students and renowned scientists.

A special thank is dedicated to my family for their patience, comprehension, and support over the past years of physics study and Ph.D. research. In any situation I was welcome, even though I neglected my domestic duties, whenever a new problem captured my mind . . .

Bibliography

- [1] R. P. Feynman, *Rev. Mod. Phys.* **20**, 367 (1948).
- [2] R. P. Feynman and A. R. Hibbs, *Quantum Mechanics and Path Integrals* (McGraw-Hill, New York, 1965).
- [3] R. P. Feynman, *Statistical Mechanics* (Benjamin, Reading MA, 1972).
- [4] H. Kleinert, *Path Integrals in Quantum Mechanics, Statistics, and Polymer Physics*, 2nd ed. (World Scientific, Singapore, 1995).
- [5] H. Kleinert and V. Schulte-Frohlinde, *Critical Properties of ϕ^4 -Theories* (World Scientific, Singapore, 2001).
- [6] M. E. Peskin and D. V. Schroeder, *Introduction to Quantum Field Theory* (Addison-Wesley, Redwood City, CA, 1995).
- [7] J. Polchinski, *String Theory*, 2 vols. (Cambridge University Press, 1998).
- [8] R. P. Feynman and H. Kleinert, *Phys. Rev. A* **34**, 5080 (1986).
- [9] R. Giachetti and V. Tognetti, *Phys. Rev. Lett.* **55**, 912 (1985).
- [10] H. Kleinert, *Phys. Rev. D* **57**, 2264 (1998).
- [11] H. Kleinert, *Phys. Lett. B* **434**, 74 (1998).
- [12] M. Bachmann, *Perturbatively Defined Path Integral in Phase Space*, in *Fluctuating Paths and Fields*, Eds. W. Janke, A. Pelster, H.-J. Schmidt, and M. Bachmann (World Scientific, Singapore, 2001), p. 57.
- [13] J. de Boer, B. Peeters, K. Skenderis, and P. van Nieuwenhuizen, *Nucl. Phys. B* **446**, 211 (1995); **459**, 631 (1996); F. Bastianielli, K. Schalm, and P. van Nieuwenhuizen, *Phys. Rev. D* **58**, 44002 (1998).
- [14] H. Kleinert and A. Chervyakov, *Phys. Lett. A* **273**, 1 (2000); *Phys. Lett. B* **464**, 257 (1999); **477**, 373 (2000).
- [15] G. 't Hooft and M. Veltman, *Nucl. Phys. B* **44**, 189 (1972).
- [16] H. Kleinert and A. Chervyakov, eprint: quant-ph/000206.
- [17] H. Kleinert, A. Pelster, and M. Bachmann, *Phys. Rev. E* **60**, 2510 (1999), eprint: quant-ph/9902051.
- [18] M. Bachmann, H. Kleinert, and A. Pelster, *Phys. Rev. A* **62**, 52509 (2000), eprint: quant-ph/0005074.

-
- [19] M. Bachmann, H. Kleinert, and A. Pelster, Phys. Lett. A **279**, 23 (2001), eprint: quant-ph/0005100.
- [20] M. Bachmann, H. Kleinert, and A. Pelster, Phys. Rev. A **60**, 3429 (1999), eprint: quant-ph/9812063. See also *Smearing Formulas for Density Matrices*, in Proceedings to the 6th Conference on *Path Integrals from peV to TeV* at Florence, Eds. R. Casalbuoni, R. Giachetti, V. Tognetti, R. Vaia, and P. Verucchi (World Scientific, Singapore, 1999), p. 489.
- [21] H. Kleinert, Fortschr. Phys. **30**, 187 (1982).
- [22] H. Kleinert, Fortschr. Phys. **30**, 351 (1982).
- [23] H. Kleinert, A. Pelster, B. Kastening, and M. Bachmann, Phys. Rev. E **62**, 1537 (2000), eprint: hep-th/9907168.
- [24] J. Külbeck, M. Böhm, and A. Denner, Comp. Phys. Comm. **60**, 165 (1991).
- [25] T. Hahn, hep-ph/9905354.
- [26] P. Nogueira, J. Comput. Phys. **105**, 279 (1993).
- [27] J. Neu, MS Thesis (in German), FU-Berlin (1990).
- [28] B. Kastening, Phys. Rev. D **54**, 3965 (1996).
- [29] B. Kastening, Phys. Rev. D **57**, 3567 (1998).
- [30] S. A. Larin, M. Mönnigmann, M. Strösser, and V. Dohm, Phys. Rev. B **58**, 3394 (1998).
- [31] H. Kleinert, *Gauge Fields in Condensed Matter*, Vol. I: *Superflow and Vortex Lines* (World Scientific, Singapore, 1989).
- [32] M. Bachmann, H. Kleinert, and A. Pelster, Phys. Rev. D **61**, 085017 (2000), eprint: hep-th/9907044.
- [33] R. F. Streater and A. S. Wightman, *PCT, Spin and Statistics, and All That* (Benjamin, New York, 1964).
- [34] J. Schwinger, *Particles, Sources, and Fields*, Vols. I and II (Addison-Wesley, Redwood City, 1973).
- [35] B. Kastening, Phys. Rev. E **61**, 3501 (2000).
- [36] A. Pelster and H. Kleinert, eprint: hep-th/0006153.
- [37] J. D. Bjorken and S. D. Drell, Vol. I: *Relativistic Quantum Mechanics*, Vol. II: *Relativistic Quantum Fields* (McGraw-Hill, New York, 1965).
- [38] D. J. Amit, *Field Theory, the Renormalization Group, and Critical Phenomena* (McGraw-Hill, New York, 1978).
- [39] C. Itzykson and J.-B. Zuber, *Quantum Field Theory* (McGraw-Hill, New York, 1985).
- [40] M. Le Bellac, *Quantum and Statistical Field Theory* (Oxford Science Publications, New York, 1991).
- [41] J. Zinn-Justin, *Quantum Field Theory and Critical Phenomena*, 3rd ed. (Oxford Science Publications, New York, 1996).
- [42] F. J. Dyson, Phys. Rev. **85**, 631 (1952).

-
- [43] C. M. Bender and S. A. Orszag, *Advanced Mathematical Methods for Scientists and Engineers* (McGraw-Hill, New York, 1978).
- [44] E. J. Weniger, *Comput. Phys. Rep.* **10**, 189 (1989); *Comput. Phys. Commun.* **92**, 1 (1991).
- [45] R. P. Feynman, *Phys. Rev.* **97**, 660 (1955).
- [46] H. Kleinert, *Phys. Lett. A* **173**, 332 (1993).
- [47] H. Kleinert and H. Meyer, *Phys. Lett. A* **184**, 319 (1994).
- [48] M. Bachmann, H. Kleinert, and A. Pelster, *Phys. Lett. A* **261**, 127 (1999), eprint: cond-mat/9905397.
- [49] M. Bachmann, H. Kleinert, and A. Pelster, *Phys. Rev. E* **63** 51709 (2001), eprint: cond-mat/0011281.
- [50] W. Helfrich, *Z. Naturforsch. A* **33**, 305 (1978); W. Helfrich and R.M. Servuss, *Nuovo Cimento D* **3**, 137 (1984).
- [51] P.M. Stevenson, *Phys. Rev. D* **23**, 2916 (1981).
- [52] W. Janke and H. Kleinert, *Phys. Rev. Lett.* **75**, 2787 (1995); *Phys. Lett. A* **206**, 283 (1995); R. Guida, K. Konishi, and H. Suzuki, *Ann. Phys.* **249**, 109 (1996).
- [53] H. Kleinert, W. Kürzinger, and A. Pelster, *J. Phys. A: Math. Gen.* **31**, 8307 (1998).
- [54] H. Kleinert, *Phys. Lett. A* **118**, 267 (1986).
- [55] W. Janke and H. Kleinert, *Phys. Lett. A* **118**, 371 (1986).
- [56] A. Cuccoli, V. Tognetti, P. Verrucchi, and R. Vaia, *Phys. Rev. A* **45**, 8418 (1992). See also the treatment of dissipation in: A. Cuccoli, A. Rossi, V. Tognetti, and R. Vaia, *Phys. Rev. E* **55**, 4849 (1997).
- [57] R. Jackiw, *Physica A* **159**, 269 (1989).
- [58] A. Okopińska, *Phys. Lett. A* **249**, 259 (1998).
- [59] This quantity should not be confused with the standard *effective potential* in quantum field theory in which the path average x_0 is not separated out. The effective classical potential always leads to a *convex* effective potential, due to the extra x_0 -integral in Z . See H. Kleinert, *Phys. Lett. B* **181**, 324 (1986).
- [60] G. C. Rossi and M. Testa, *Ann. Phys.* **148**, 144 (1983).
- [61] T. Kunihiro, *Phys. Rev. Lett.* **78**, 3229 (1997).
- [62] A. P. Prudnikov, Yu. A. Brychkov, and O. I. Marichev, *Integrals and Series*, Vol. 2 (Gordon and Breach, New York, 1986).
- [63] R. G. Storer, *J. Math. Phys.* **9**, 964 (1968).
- [64] J. C. Le Guillou and J. Zinn-Justin, *Ann. Phys. (N.Y.)* **147**, 57 (1983).
- [65] J. E. Avron, B. G. Adams, J. Čížek, M. Clay, M. L. Glasser, P. Otto, J. Paldus, and E. Vrscay, *Phys. Rev. Lett.* **43**, 691 (1979).
- [66] B. G. Adams, J. E. Avron, J. Čížek, P. Otto, J. Paldus, R. K. Moats, and H. J. Silverstone, *Phys. Rev. A* **21**, 1914 (1980).
- [67] V. A. Gani, A. E. Kudryavtsev, and V. M. Weinberg, eprint: physics/9708005 (1997).

-
- [68] I. D. Feranchuk and L. I. Komarov, *J. Phys. A: Math. Gen.* **17**, 3111 (1984).
- [69] L. D. Landau and E. M. Lifschitz, *Quantenmechanik*, 6. Auflage (Akademie-Verlag Berlin, 1979).
- [70] R. Loudon, *Am. J. Phys.* **27**, 649 (1959).
- [71] L. K. Haines and D. H. Roberts, *Am. J. Phys.* **37**, 1145 (1969).
- [72] R. Cohen, J. Lodenquai, and M. Ruderman, *Phys. Rev. Lett.* **25** (1970).
- [73] M. V. Ivanov and P. Schmelcher, *Phys. Rev. A* **61**, 022505 (2000).
- [74] P. Schmelcher and W. Schweizer (Eds.), *Atoms and Molecules in Strong External Fields* (Plenum Press, New York, 1998).
- [75] J. S. Heyl and L. Hernquist, *Phys. Rev. A* **58**, 3567 (1998).
- [76] H. Ruder, G. Wunner, H. Herold, and F. Geyer, *Atoms in Strong Magnetic Fields* (Springer-Verlag, Berlin, 1994).
- [77] J. T. Devreese and F. Brosens, in *Elementary Excitations in Solids*, Eds. J. L. Birman, C. Sébenne, and R. F. Wallis (Elsevier, Amsterdam, 1992), p. 283.
- [78] J. T. Devreese and F. Brosens, *Solid State Comm.* **79**, 819 (1991).
- [79] J. T. Devreese and F. Brosens, *Phys. Rev. B* **45**, 6459 (1992).
- [80] M. Steinberg, J. Ortner, and W. Ebeling, *Phys. Rev. E* **58**, 3806 (1998).
- [81] M. Steinberg, J. Ortner, and W. Ebeling, *Phys. Rev. E* **61**, 2290 (2000).
- [82] W. Ebeling, M. Steinberg, and J. Ortner, *Eur. Phys. J. D* **12**, 513 (2000).
- [83] C. Kouveliotou, S. Dieters, T. Strohmayer, J. van Paradijs, G. J. Fishman, C. A. Meegan, K. Hurley, J. Kommers, I. Smith, D. Frail, and T. Murakami, *Nature* **393**, 235 (1998); K. Hurley, P. Li, C. Kouveliotou, T. Murakami, M. Ando, T. Strohmayer, J. van Paradijs, F. Vrba, C. Luginbuhl, A. Yoshida, and I. Smith, *Astrophys. Journal*, **510**, L111 (1998); C. Kouveliotou, T. Strohmayer, K. Hurley, J. van Paradijs, M. H. Finger, S. Dieters, P. Woods, C. Thompson, and R. C. Duncan, *Astrophys. Journal*, **510**, L115 (1998).
- [84] T. O. Klaassen, J. L. Dunn, and C. A. Bates, in *Atoms and Molecules in Strong External Fields*, Eds. P. Schmelcher and W. Schweizer (Plenum Press, New York, 1998), p. 291.
- [85] W. Janke and H. Kleinert, *Phys. Lett. A* **117**, 353 (1986).
- [86] W. Janke, H. Kleinert, and M. Meinert, *Phys. Lett. B* **217**, 525 (1989).
- [87] W. Janke, *Int. J. Mod. Phys. B* **4**, 1763 (1990).
- [88] G. Gompper and D. M. Kroll, *Europhys. Lett.* **9**, 59 (1989).
- [89] H. Kleinert, *Phys. Lett. A* **257**, 269 (1999).
- [90] U. Seifert, *Adv. in Physics* **46**, 13 (1997).
- [91] M. P. do Carmo, *Differentialgeometrie von Kurven und Flächen*, 3. Auflage (Vieweg, Braunschweig, 1998).
- [92] E. Kreyszig, *Differential Geometry* (Dover Publications, New York, 1991).
- [93] W. Helfrich, *Z. Naturforsch. C* **28**, 693 (1973).

-
- [94] R. Lipowsky, in *Statistical Mechanics of Biocomplexity*, Vol. 527 of Lecture Notes in Physics, Eds. D. Reguera, J. M. G. Vilar, and J. M. Rubi (Springer-Verlag, Berlin, 1999).
- [95] H. Kleinert, A. Chervyakov, and B. Hamprecht, *Phys. Lett. A* **260**, 182 (1999).
- [96] I. S. Gradstein and I. M. Ryshik, *Tables of Series, Products, and Integrals*, Vol. 2 (Verlag Harry Deutsch, Thun, 1981).
- [97] H. Kleinert, *Phys. Lett. B* **463**, 69 (1999).
- [98] R. Lipowsky, *Z. Phys. B* **97**, 193 (1995).
- [99] C. Hiergeist and R. Lipowsky, *Physica A* **244**, 164 (1997).
- [100] P.-G. De Gennes, *J. Chem. Phys.* **48**, 2257 (1968).
- [101] V. Pokrovski and A. Talapov, *Sov. Phys. JETP* **51**, 267 (1980).
- [102] H. B. Thacker, *Rev. Mod. Phys.* **53**, 253 (1981).
- [103] This technique was developed by H. Kleinert and A. Chervyakov in a perturbative calculation of the energy of a particle in a box (to be published).
- [104] W. Janke and H. Kleinert, *Phys. Rev. Lett.* **58**, 144 (1987).
- [105] An analogous estimate for a stack of strings [87] with Helfrich's method [50] is also too large by a factor $9/4$.
- [106] M. Bachmann and H.-J. Schmidt, *Phys. Rev. D* **62**, 043515 (2000), eprint: gr-qc/9912068.

Zusammenfassung

Ein wesentlicher Aspekt dieser Dissertationsschrift ist die Erweiterung der Anwendbarkeit von Funktionalintegralen in Quantenstatistik und Quantenfeldtheorie. Im ersten Teil wird die Definition kontinuierlicher statistischer Pfadintegrale von einem störungstheoretischen Standpunkt aus diskutiert, der automatisch auf eine Hochtemperamentwicklung führt. Anschließend werden allgemeine Gaußsche Phasenraum-Pfadintegrale behandelt, wobei die harmonischen Korrelationsfunktionen dazu dienen, die Variationsstörungstheorie als Resummationsmethode für divergente Störungsreihen in den Teilen drei und vier weiterzuentwickeln. Der störungstheoretische Teil auf der einen Seite und die nichtperturbative Berechnung von Pfadintegralen auf der anderen wird überbrückt mit der Entwicklung einer rekursiven graphischen Konstruktionsmethode für Feynman-Diagramme in Teil zwei. Damit lassen sich systematisch alle topologisch verschiedenen Diagramme und ihre Multiplizitäten generieren, die zu einer bestimmten Ordnung der Störungsentwicklung beitragen. Entwickelt für die Erzeugung der Vakuumdiagramme für die freie Energie des anharmonischen Oszillators in hohen störungstheoretischen Ordnungen, lassen sich die grundlegenden graphischen Manipulationstechniken wie Aufschneiden und Amputieren von Linien und Vertizes auch auf n -Punkt-Korrelationsfunktionen anwenden. Damit können auch Graphen für Streuprozesse in Quantenfeldtheorien systematisch generiert werden, wie an verschiedenen Beispielen aus der Quantenelektrodynamik demonstriert wird.

Motiviert durch zum Teil nicht existierende analytische Resultate wenden wir die Variationsstörungstheorie auf atomare Systeme bei beliebigen Temperaturen und zur Bestimmung thermodynamischer Eigenschaften fluktuierender Membranen an. Um dies zu ermöglichen, wird das Resummationsverfahren in vielfältiger Weise erweitert. Die Berechnung von Dichtematrizen macht z.B. eine Verallgemeinerung der Verschmierungsformel erforderlich, bei der eine Gaußsche Faltung des klassischen Potentials die Berücksichtigung von thermischen und Quantenfluktuationen ermöglicht. Diese Verschmierungsformel ist ein wesentliches Hilfsmittel insbesondere bei nichtpolynomialen Potentialen, wo die übliche Wick-Regel zur Zerlegung der Korrelationsfunktionen einer Verallgemeinerung bedarf. Diese Theorie wird auf die Berechnung der Teilchendichte im Doppelmulden-Potential und die Elektronendichte im Coulomb-Potential angewendet, wobei letzteres als nichtpolynomiales Beispiel dient. In beiden Fällen liefert das Näherungsverfahren gute Ergebnisse.

Eine weitere wichtige Anwendung ist die Berechnung des effektiven klassischen Potentials für das Wasserstoffatom im Magnetfeld. Hierfür wird die Variationsstörungstheorie im Phasenraum formuliert, so daß sie jetzt auch für Systeme mit verallgemeinerten Impulsen benutzt werden kann. Das effektive klassische Potential, das die gesamte quantenstatistische Information eines Systems enthält, wurde in erster Ordnung Variationsstörungstheorie bestimmt. Im Grenzfall verschwindender Temperatur liefert das Minimum des effektiven klassischen Potentials die Grundzustandsenergie des Systems. Wir erhalten einen analytischen Ausdruck, der automatisch die Grenzfälle schwacher und starker Magnetfelder interpoliert und für alle Feldstärken genaue Ergebnisse liefert. Das für schwache und starke Felder sehr unterschiedliche asymptotische Verhalten der Bindungsenergie läßt sich mit Hilfe unseres Ausdruckes detailliert untersuchen. Im Schwachfeldfall wird das Potenzreihenverhalten der Entwicklung bestätigt, während für starke Felder ein kompliziert strukturiertes logarithmisches Verhalten auftritt.

Als Anwendung der Starkkopplungstheorie in der Membranphysik berechnen wir die universelle Druckkonstante, die im Druckgesetz von Helfrich für eine Membran auftritt, die zwischen zwei Wänden fluktuiert. Dabei werden die Wände durch ein parameterbehaftetes Potential simuliert, das so konstru-

iert ist, das es für verschwindenden Parameter die Wände exakt reproduziert. Der nichtharmonische Anteil des Potentials kann störungstheoretisch behandelt und die Störungsreihe mit Hilfe der Variationsstörungstheorie näherungsweise aufsummiert werden. Die erhaltenen Näherungen in verschiedenen Ordnungen der Variationsstörungstheorie lassen sich ins Unendliche extrapolieren. Die so erhaltene Druckkonstante ist in exzellenter Übereinstimmung mit früheren Monte-Carlo-Ergebnissen.

Ein ähnliches Verfahren dient dazu, die Druckkonstanten für einen Stapel von mehreren Membranen zwischen zwei Wänden zu berechnen. Wiederum stimmen die Ergebnisse sehr gut mit aus Monte-Carlo-Simulationen gewonnenen Werten überein. Der Notwendigkeit, daß sich die Membranen nicht gegenseitig durchdringen dürfen, wird durch die Betrachtung des Starkkopplungs-Grenzwertes eines künstlich eingeführten Abstoßungspotentials Rechnung getragen. Dabei wird die Ähnlichkeit zwischen dem Membranstapel und einem System von Strings ausgenutzt, die sich zwischen zwei linienartigen Wänden befinden. Dieses Vergleichssystem ist exakt behandelbar und dient der Bestimmung von Potentialparametern, die sich dann unmittelbar für das Membranproblem verwenden lassen.

In dieser Arbeit wird gezeigt, daß sich die Variationsstörungstheorie erfolgreich auf eine Reihe von Problemen aus verschiedenen Gebieten der Quantenstatistik und Membranphysik anwenden läßt. Die für fluktuierende Strings und Membranen gewonnenen Ergebnisse öffnen das Tor zu einem großen Feld von Anwendungen, das sich mit Hilfe der Starkkopplungstheorie bearbeiten läßt.

Curriculum Vitae

Universitätsadresse

Michael Bachmann
Institut für Theoretische Physik
Freie Universität Berlin
Arnimallee 14
14195 Berlin

Telefon: (030) 8385 3041

E-mail: mbach@physik.fu-berlin.de

Homepage: <http://www.physik.fu-berlin.de/~mbach>

Eltern:	Gerhard Bachmann, Diplom-Chemiker Bärbel Bachmann, geb. Nuck, Industriekauffrau
14. Feb. 1973	Geburt in Berlin-Mitte
Sept. 1979–Juli 1989	Polytechnische Oberschule Berlin-Mitte
Aug. 1989–Juli 1992	Berufsausbildung (Elektronik) mit Abitur in Berlin
Okt. 1992–Sept. 1997	Physikstudium an der Humboldt-Universität Berlin
Okt. 1996–Sept. 1997	Diplomarbeit <i>Dynamik von Quantensystemen mit effektiven Pfaddarstellungen</i> am Institut für Statistische Physik und Nicht-lineare Dynamik der Humboldt-Universität Berlin bei Prof. Dr. W. Ebeling
18. Dez. 1997	Verleihung des Wilhelm- und Else-Heraeus-Preises
Okt. 1997	Beginn der Promotion am Institut für Theoretische Physik der Freien Universität Berlin bei Prof. Dr. H. Kleinert
Juli 1998–Juni 2001	Promotionsstipendium der Studienstiftung des deutschen Volkes